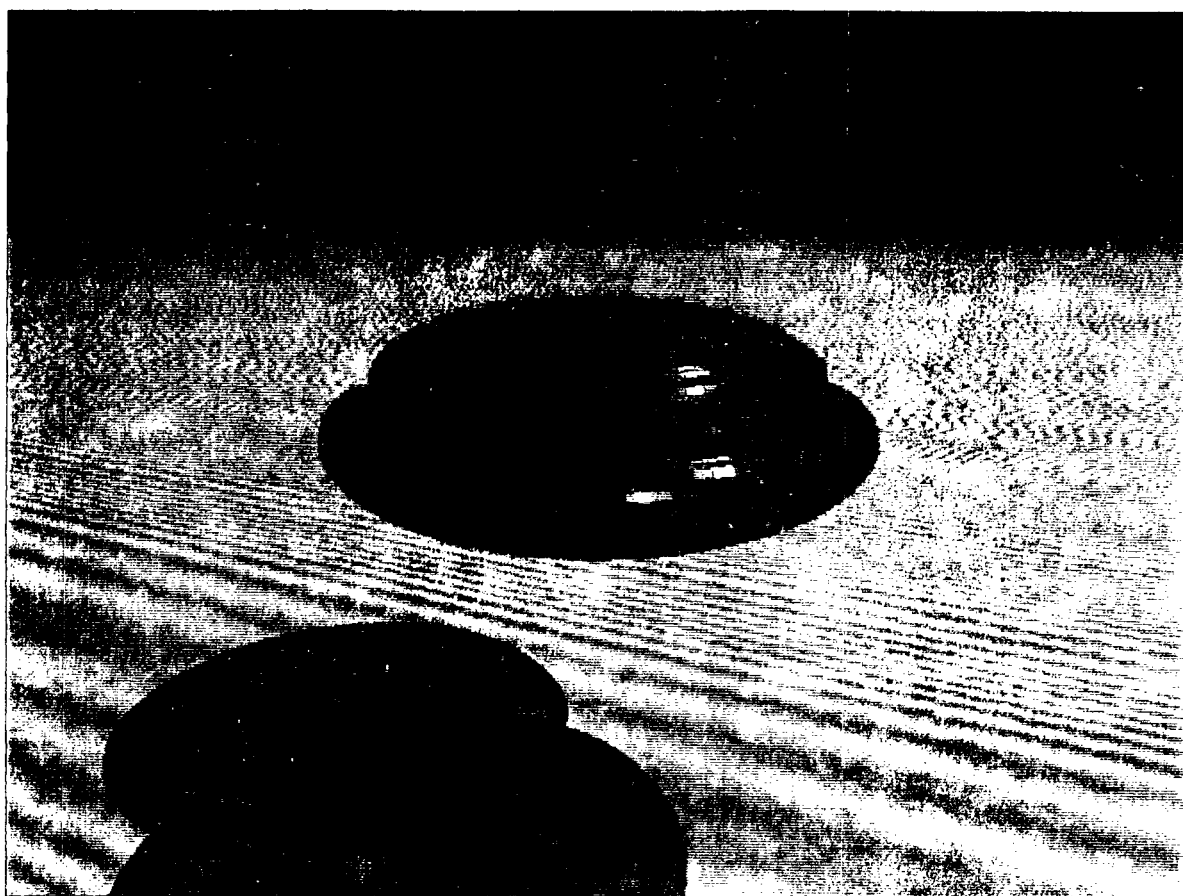


2000 Atomic, Molecular and Optical Physics Research Meeting



Sponsored by:
U.S. Department of Energy
Office of Basic Energy Sciences
Chemical Sciences, Geosciences & Biosciences Division

Front Cover:

Theoretically calculated isodensity surfaces for a two-component Bose-Einstein condensate in a magnetic “TOP” trap. The red surface represents 100,000 ^{87}Rb atoms in their $F=1$, $M=-1$ hyperfine substate, while the blue surface represents an equal number of ^{87}Rb atoms in their $F=2$, $M=2$ substate. These calculations require solution of the coupled Gross-Pitaevskii equations for the ground state of the double condensate. The theoretical description is discussed by Esry, Greene, Burke, and Bohn in *Phys. Rev. Lett.* **78**, 3594 (1997). The first experimental observation of such a double condensate was carried out by Myatt, Burt, Ghrist, Cornell, and Wieman, *Phys. Rev. Lett.* **78**, 586 (1997). (Courtesy of Chris Greene, JILA, University of Colorado)

Foreword

This volume summarizes the technical content of the 2000 meeting of the Atomic, Molecular and Optical Physics (AMOP) Program sponsored by the U. S. Department of Energy (DOE), Office of Basic Energy Sciences (BES). This meeting is held annually for the DOE laboratory and university principal investigators within the BES AMOP Program in order to facilitate scientific interchange among the PIs and to promote interaction with DOE management. For the past three years, the meeting has included significant participation from scientists outside of the BES AMOP Program and has had a specific topical focus. Each of these topics can be directly traced to a 1997 DOE/BES workshop that identified a number of exciting areas in AMO science of interest to BES. The 1998 topic was *The Interactions of Novel Electromagnetic Fields with Matter* and the topic in 1999 was *Molecular Ions, Nanostructures and Surfaces*. This year's meeting is organized around the theme of *Ultracold Atoms and Molecules*, and includes sessions on quantum condensates of atoms and coherent atom waves, formation and trapping of ultracold molecules and the collisional interactions of atoms and molecules at ultracold temperatures.

The BES AMOP Program has evolved in recent years. In the past, it was largely an atomic physics program directed at the fundamental properties and complete quantum mechanical description of atoms and the interactions of atoms or ions with electrons or photons. That role continues through support of AMO science at the DOE synchrotron facilities and via ongoing projects examining the physics of highly charged ions, which is relevant to understanding fusion plasmas. New directions in the program include the interactions of intense electromagnetic fields (from lasers or highly-charged ion collisions) with atoms and molecules, coherent control of quantum processes, development and application of novel x-ray light sources and ultracold interactions and quantum condensates. This is a logical broadening of the program to include topics of current interest to the AMOP community that also fit well with the BES mission in the context of utilization of next-generation light sources and control of materials on the nanoscale. The BES AMOP Program is characterized by the close coupling between experiment and theory; approximately 70% of the PIs in the program are experimentalists and 30% are theorists.

The AMOP Program is viewed within BES as one that provides fundamental physical insight and is thus "underpinning" in relation to more obviously energy-relevant programs in BES or the Office of Fusion Energy Sciences, in relation to current and future BES facilities that probe matter with photons, electrons or heavy ions, and in relation to more applied efforts in high- and low-temperature plasma modeling. However, we encourage a proactive version of this underpinning role, in which the AMOP PIs understand the important research issues in other areas of science and engineering and communicate effectively with scientists in other fields. The BES AMOP Program will continue to evolve in response to changes in the landscape of AMO science while maintaining solid, justifiable connections to the BES mission.

We gratefully acknowledge the speakers, particularly those not supported by the BES AMOP program, for their investment of time and effort and for their willingness to share their ideas with the meeting participants. We also thank the staff of the Oak Ridge Institute of Science and Education and the Airlie Conference Center for assisting with logistical aspects and Chris Greene (JILA, Univ. of Colorado) and Phil Gould (Univ. of Connecticut) for their assistance in developing the technical program.

Eric Rohlfig, Program Manager
Atomic, Molecular and Optical Physics
Chemical Sciences, Geosciences and Biosciences Division
Office of Basic Energy Sciences
U. S. Department of Energy

August, 2000

Agenda

U. S. Department of Energy
Office of Basic Energy Sciences

2000 Meeting of the Atomic, Molecular and Optical Physics Program
Ultracold Atoms and Molecules

Tuesday, Sept. 26

3:00-6:00 pm **** Registration ****
6:00 pm **** Reception (No Host) ****
7:00 pm **** Dinner ****

Wednesday, Sept. 27

7:00 am **** Breakfast ****

8:00 am Introductory Remarks
Eric Rohlfing, U.S. Dept. of Energy

Session I Chair: **Eric Rohlfing**

8:15 am *Collective Enhancement and Suppression of Bose-Einstein Condensates*
Wolfgang Ketterle, MIT

9:15 am *Ultra-cold Interactions and Entanglement in Bose-Einstein Condensed Gases*
Keith Burnett, University of Oxford

9:45 am *Studies of Ultracold and Bose-Einstein Condensed Hydrogen*
Dan Kleppner, MIT

10:15 am **** Break ****

10:30 am *Creation of Ultra-long-range Rydberg Molecules in a Cold Quantum Gas*
Chris Greene, JILA

11:00 am *Toward Cooper Pairing of Fermionic Atoms*
Debbie Jin, JILA

11:30 am *Atom Trap Trace Analysis*
Linda Young, Argonne National Laboratory

12:00 pm **** Lunch ****

5:00 pm **** Reception (No Host) ****
6:00 pm **** Dinner ****

Session II Chair: **Chris Greene**

7:30 pm *Coherent Atom Optics with Bose-Einstein Condensates*
Bill Phillips, NIST

8:30 pm *Quantum Theory of Collective Effects in the Atom Laser*
Murray Holland, JILA

9:00 pm *Recent Progress and Future Opportunities for the Application of Ab Initio
Relativistic-Correlation Methods to Complicated Atomic States*
Donald Beck, Michigan Technical University

Thursday, Sept. 28

7:00 am **** Breakfast ****

Session III Chair: **Phil Gould**

8:00 am *Overview of the Formation of Cold Molecules*
Bill Stwalley, University of Connecticut

9:00 am *Deceleration and Trapping of Neutral Dipolar Molecules*
Gerard Meijer, University of Nijmegen

9:30 am *Buffer-gas Loaded Magnetic Traps for Atoms and Molecules*
John Doyle, Harvard University

10:00 am **** Break ****

10:15 am *Slowing, Storing and Cooling Neutral Molecules with Synchrotrons*
Harvey Gould, Lawrence Berkeley National Laboratory

10:45 am *Molecules in a Dilute Gas Bose-Einstein Condensate*
Dan Heinzen, University of Texas

11:15 am *Determination of Atom/Molecule-Wall Interactions and Molecular Bond Distances
via Diffraction from Nanostructures*
Peter Toennies, MPI Göttingen

11:45 am *Spectroscopy and Dynamics in ⁴He Nanodroplets*
Kevin Lehmann, Princeton University

12:15 pm **** Lunch ****

Session IV Chair: **Harvey Gould**

4:00 pm *Cold and Dense Rydberg Gases*
Georg Raithel, University of Michigan

4:30 pm *MOTRIMS: Ion-Atom Collisions with a Laser-Cooled Target*
Brett DePaola, Kansas State University

5:00 pm *Experimental Studies of Resonant Charge Transfer from Rydberg States by
Highly-Charged Ions*
Steve Lundeen, Colorado State University

5:30 pm *Probing Structure and Dynamics of Atoms and Molecules using the Advanced
Light Source*
Nora Berrah, Western Michigan University

6:00 pm **** Reception (No Host) ****

7:00 pm **** Dinner ****

Friday, Sept. 29

7:00 am **** Breakfast ****

Session V Chair: **Steve Lundeen**

8:00 am *Ultracold Atom-Molecule Collisions*

Alex Dalgarno, Harvard University

9:00 am *Experiments in Ultracold Collisions*

Phil Gould, University of Connecticut

9:30 am *Threshold Resonances: A Key to Cold Collision Phenomena*

Paul Julienne, NIST

10:00 am **** Break ****

10:15 am *Ultracold Three-Body Collisions*

Brett Esry, Kansas State University

10:45 am *Recent Results from Rochester on Homo- and Heteronuclear Ultracold Molecules*

Nick Bigelow, University of Rochester

11:15 am *Theoretical Studies of Atomic Transitions*

Charlotte Froese Fischer, Vanderbilt University

11:45 am *Dynamics of Three Body Dissociative Recombination in Collisions of Vibrationally*

Cold H_2O^+ with Electrons at ~ 1 meV (10 K)

Sheldon Datz, Oak Ridge National Laboratory

12:15 pm *Closing Remarks*

Eric Rohlfing, U.S. Dept. of Energy

12:20 pm **** Lunch ****

Table of Contents

Table of Contents

Invited Presentations

Collective Enhancement and Suppression in Bose-Einstein Condensates	1
Ultra-cold Interactions and Entanglement in Bose-Einstein Condensed Gases.....	2
Studies of Ultracold and Bose-Einstein Condensed Hydrogen.....	3
Physics of Correlated Systems	4
Toward Cooper Pairing of Fermionic Atoms.....	7
Atom Trap Trace Analysis	9
Coherent Atom Optics with Bose-Einstein Condensates.....	10
Quantum Theory of Collective Effects in the Atom Laser	11
Recent Progress and Future Opportunities for the Application of Ab Initio Relativistic-Correlation Methods to Complicated Atomic States.....	15
Overview of the Formation of Cold Molecules	19
Deceleration and Trapping of Neutral Dipolar Molecules.....	20
Buffer-gas Loaded Magnetic Traps for Atoms and Molecules.....	21
Slowing, Storing and Cooling Neutral Molecules with Synchrotrons.....	22
Molecules in a Dilute Gas Bose-Einstein Condensate	24
Determination of Atom/Molecule-Wall Interactions and Molecular Bond Distances via Diffraction from Nanostructures.....	25
Spectroscopy and Dynamics in ^4He Nanodroplets.....	26
High-Angular-Momentum Rydberg Atoms in Magnetic Plasma Environment	27
MOTRIMS: Ion-Atom Collisions with a Laser-Cooled Target.....	31
Ion/Excited-Atom Collision Studies with a Rydberg Target and a CO_2 Laser	32
Probing Structure and Dynamics of Atoms and Molecules Using the Advanced Light Source.....	36
Theoretical Investigations of Atomic Collision Physics.....	40
Experiments in Ultracold Collisions.....	42
Threshold Resonances: A Key to Cold Collision Phenomena.....	46
Ultracold Three-Body Collisions	47
Recent Results from Rochester on Homo- and Heteronuclear Ultracold Molecules	48
Theoretical Studies of Atomic Transitions	50

Research Summaries (Multi-PI Programs, Alphabetical by Institution)

Structure and Collisions with Few-Electron Ions	54
X-Ray Interactions with Atoms and Molecules	58
Double K Photoionization of Heavy Atoms	59
Atomic Physics with Highly Charged Ions: Low Velocity.....	62
Atomic Physics with Highly Charged Ions: High Velocity	66
Charge Transfer and Elastic Scattering in Very Slow $\text{H}^+ + \text{D} (1s)$ "Half" Collisions	67

Research Summaries (Multi-PI Programs, continued)	
Elastic Scattering of Electrons from Metastable Ions – Formation of Triply Excited States	68
Theory of Structure and Dynamics of Atoms, Ions and Surfaces.....	70
Atomic, Molecular, and Optical Sciences of LBNL	74
Photon and Heavy Particle Collisions with Aligned Molecules	78
Atomic Physics at the LLNL EBIT.....	82
Atomic and Molecular Physics at Oak Ridge National Laboratory.....	86
High-Energy Atomic Collisions.....	87
Research Summaries (Single-PI Grants, Alphabetical by PI)	
Molecular Structure and Collisional Dissociation and Ionization	94
Low-Energy Ion-Surface and Ion-Molecule Collisions.....	98
Amplitude Modulation of Atomic Wavefunctions	102
Semiempirical Studies of Atomic Structure.....	105
High Intensity Laser Interactions with Atomic Clusters.....	109
Collective Few Body Coulomb Excitations.....	113
Studies of Autoionizing States Relevant to Dielectronic Recombination	117
Experiments in Molecular Optics.....	120
Quantum Control of Time-Dependent Electron Correlation	124
Nonperturbative Laser-Atom Interactions for Nonlinear Optics	127
High Resolution Spectroscopy of Cluster Ions in Discharges, Clusters in Jets, and Nanoparticles.....	131
Spectroscopic Studies of Hydrogen Atom and Molecule Collisions.....	135
Nonclassical Spectroscopy with Localized Atoms	139
Experimental Study of Interactions of Highly Charged Ions with Atoms at keV Energies	143
Dynamics of Multielectron Systems Interacting with Light and Matter.....	146
Project: Electron Collisions in Processing Plasmas	150
Electron/Photon Interactions with Atoms/Ions	153
The Structure and Dynamics of Negative Ions	157
Energetic Photon and Electron Interactions with Positive Ions	159
X-ray Spectroscopy of $n=3 \rightarrow 4 \rightarrow 5 \rightarrow 1$ Transitions in Heliumlike Ar, Ti, and Cr	163
Dynamics of Few-Body Atomic Processes.....	167
Correlated Charge-Changing Ion-Atom Collisions	170
Precision Measurements of Atomic Lifetimes in Alkali-Like Systems.....	174
Laser-Produced Coherent X-Ray Sources	178

**Invited
Presentations**
(ordered by agenda)

Collective Enhancement and Suppression in Bose-Einstein Condensates

Wolfgang Ketterle

Department of Physics and Research Laboratory of Electronics
Massachusetts Institute of Technology, Cambridge, MA 02139, USA

The coherent and collective nature of Bose-Einstein condensate can enhance or suppress physical processes. We have observed the suppression and enhancement of elastic collisions of impurity atoms [1], the suppression of dissipation due to superfluidity [2, 3], and the suppression [4] and enhancement of light scattering [5]. Bosonically enhanced Rayleigh scattering was used to amplify either atoms [6] or light [7] in a condensate dressed by laser light. The talk will review these experiments and discuss common roots and differences of these phenomena.

1. A.P. Chikkatur, A. Görlitz, D.M. Stamper-Kurn, S. Inouye, S. Gupta, and W. Ketterle, *Suppression and enhancement of impurity scattering in a Bose-Einstein condensate*, cond-mat/0003387; Phys. Rev. Lett., in print.
2. C. Raman, M. Köhl, R. Onofrio, D.S. Durfee, C.E. Kuklewicz, Z. Hadzibabic, and W. Ketterle, *Evidence for a critical velocity in a Bose-Einstein condensed gas*, Phys. Rev. Lett. **83**, 2502-2505 (1999).
3. R. Onofrio, C. Raman, J.M. Vogels, J. Abo-Shaeer, A.P. Chikkatur, and W. Ketterle, *Observation of Superfluid Flow in a Bose-Einstein Condensed Gas*, cond-mat/0006111; Phys. Rev. Lett., submitted.
4. D.M. Stamper-Kurn, A.P. Chikkatur, A. Görlitz, S. Inouye, S. Gupta, D.E. Pritchard, and W. Ketterle, *Excitation of phonons in a Bose-Einstein condensate by light scattering*, Phys. Rev. Lett. **83**, 2876-2879 (1999).
5. S. Inouye, A.P. Chikkatur, D.M. Stamper-Kurn, J. Stenger, D.E. Pritchard, and W. Ketterle, *Superradiant Rayleigh scattering from a Bose-Einstein condensate*, Science **285**, 571-574 (1999).
6. S. Inouye, T. Pfau, S. Gupta, A.P. Chikkatur, A. Görlitz, D.E. Pritchard, and W. Ketterle, *Observation of phase-coherent amplification of atomic matter waves*, Nature **402**, 641-644 (1999).
7. S. Inouye, R.F. Löw, S. Gupta, T. Pfau, A. Görlitz, T.L. Gustavson, D.E. Pritchard, and W. Ketterle, *Amplification of light and atoms in a Bose-Einstein condensate*, cond-mat/0006455; Phys. Rev. Lett., submitted.

Ultra-cold Interactions and Entanglement in Bose-Einstein Condensed Gases

Keith Burnett

Department of Physics
University of Oxford
Oxford OX1 3PU
United Kingdom

The nature of the interactions between atoms in Bose-Einstein condensed gases are now accessible to direct experimental investigation and manipulation. These interactions modify the shapes and evolution of condensates as described by the Gross-Pitaevskii equation. They also produce correlations between atoms that may be thought of in terms of correlations, quantum fluctuations or entanglements depending on your point of view. I will review briefly the way one puts the description of ultra-cold collisions into the field theory of condensed gases, and discuss how one goes beyond the simplest mean field theory of these systems. This involves the specific inclusion of the effects of correlations in the effective interactions between particles. I shall then discuss the prospects for using the interactions as sources of entangled atoms, through the extraction of entangled pairs of atoms from a condensate. These entangled pairs may well be useful in the new types of quantum limited atomic interferometry.

STUDIES OF ULTRACOLD AND BOSE-EINSTEIN CONDENSED HYDROGEN

Daniel Kleppner
Research Laboratory of Electronics
Massachusetts Institute of Technology

The dynamics of Bose-Einstein Condensation in atomic hydrogen differ from other BEC atomic gases because of the slow thermalization rate. The condensate achieves a quasi-steady state in which heating due to dipolar decay cooling is balanced by cooling through replenishment by the normal gas. This process has been investigated both experimentally and theoretically. Ultracold hydrogen provides an attractive testing ground for elementary atomic elastic and inelastic scattering processes. Recent studies will be discussed.

Research supported by the National Science Foundation and the Office of Naval Research.

Physics of Correlated Systems
Chris H. Greene
JILA
University of Colorado
Boulder, Colorado 80309-0440
Chris.Greene@Colorado.EDU

1. Program Scope

This project is a multifaceted theoretical attack on problems in atomic and molecular physics in which two or more degrees of freedom are strongly coupled or correlated. We are developing innovations, extensions, and improvements to existing theoretical methods, which can handle a broad class of physical systems. The studies focus on developing a quantitative understanding of the quantum mechanical behavior of systems, in regimes where standard approximations like the independent particle approximation constitute a poor starting point. Two specific problems will receive the greatest amount of attention in the coming year: photoabsorption processes in complex atoms in the presence of a static external field, and the ionization and high-harmonic generation that occurs in a two-electron atom subjected to an intense laser pulse.

2. Interpreting coarse-grained photoabsorption spectra as simple time-domain physics

A major accomplishment during the past year has been a complete reformulation of semiclassical photoabsorption theory and scattering theory in a form that connects these methods with powerful multichannel quantum defect techniques. Our first study, published earlier this year[1], derives a new general expression for the exact total photoabsorption cross section in a “preconvolved form”. This extends a formulation developed by F. Robicheaux in the early 1990s when he was a postdoctoral associate supported by this grant. The extension is important because scattering and photoionization calculations increasingly probe energy ranges and atomic species whose spectra consist of extremely high level densities. For instance, it is not unusual to treat autoionizing states in systems that require 10^5 or even 10^6 energy mesh points in order to trace out the full resonance profiles of all resonances adequately. Yet the resolution in such experiments is typically limited, to the extent that two or three orders of magnitude fewer mesh points are needed to describe an actual measured spectrum.

Prior to Robicheaux’s introduction of preconvolution techniques, there was no alternative except to calculate the full spectrum on the ultrafine energy mesh, and then “smear out” that information upon convolving the theoretical spectrum to mimic experimental resolution. Preconvolution permits the “smeared-out” spectrum to be calculated at the outset, without requiring the expensive intermediate step of 10^6 energy mesh points. Whereas Robicheaux’s work was restricted to zero-field Rydberg states of atoms and molecules, in which an escaping electron experiences a pure Coulomb field, our generalized form yields the same gains more generally, such as when an external static field is present. Our first application treats an atom in an external magnetic field [1], in the richly complicated energy range near the ionization threshold, where quasi-Landau diamagnetic physics dominates the spectrum. The accurate quantum mechanical calculations were obtained using a newly-implemented basis-spline R-matrix calculation that determines the “outer-field scattering matrix” S^{LR} at a complex energy whose imaginary part is half of the preconvolution width. A second, more extensive investigation of the strengths and limitations of the semiclassical formulation of the long-range physics is currently being prepared for publication.

A key reason for conducting a “coarse-grained” analysis of a complex spectrum is that the Fourier transformed time-domain spectrum frequently possesses far more simplicity than does the raw high resolution energy domain spectrum. The simpler time-domain spectra are readily interpreted using a semiclassical approximation to the long range scattering matrix S^{LR} , of the type developed extensively by W. Miller, J. M. Rost, and others. That approximation correlates each peak in the time-domain spectrum with a single trajectory (or more precisely, with a family of very similar trajectories).

In the coming year, Brian Granger’s efforts will apply the reformulated theory to a broader class of systems that have not been accessible to closed-orbit theory in its existing forms. A prime example is atomic

photoabsorption in the presence of an external field, in an atom possessing a complex, multichannel ionic core. For instance, the barium atom has several low-lying ionic thresholds $6s$, $5d_{3/2}$, $5d_{5/2}$, $6p_{1/2}$, $6p_{3/2}$. These cause even the zero field photoabsorption spectrum of barium to display rich complexity.

3. Correlations between the electronic and nuclear motions in an electron-molecule collision

When an incident electron strikes a diatomic molecule, one frequently views the nuclei as being effectively frozen during the collision. In resonant ion-pair formation, however, this is manifestly not the case. The process $e + HD^+ \rightarrow H^+ + D^-$ has recently been studied in a storage-ring experiment at Stockholm. Such resonant ion-pair formation events proceed through an intermediate doubly-excited resonant state of HD, which then proceeds to dissociate after the initial electronic excitation. Essentially, the temporary trapping of the incident electron in an autoionizing state gives it leverage to dissociate the nuclei efficiently. The experiment showed around a dozen sharp peaks in the cross section for D^- formation. In a collaboration with both experimentalists and theorists at Stockholm, and with the JILA experimental group of G. Dunn and N. Djuric, the P.I. has developed a Landau-Zener-Stueckelberg description that semiquantitatively explains the observed peaks as resulting from a quantum mechanical interference between competing dissociation pathways.[2]

4. Joint motions of doubly-excited atomic electrons

Some continuing progress has been made toward the goal of being able to describe the rich multichannel photoabsorption spectra that arise when a helium atom or H- ion absorbs a photon that brings the system near but slightly below the two-electron escape threshold. A two-electron B-spline R-matrix description developed by Hugo van der Hart before he left to assume a position at Queen's University has already provided some insights into the underlying regularities in the spectrum. Further work has also been carried out toward understanding the photoionization-produced alignment and orientation of Ar^+ ions, and a paper should be finished on this subject during the coming year.

5. Atoms in an intense laser field

A new postdoctoral associate, Mark Baertschy, has begun to study the theoretical description of two-electron ejection induced by the strong fields present in an ultra-short laser pulse. In the initial exploratory phases of this effort, we have implemented some popular time-dependent propagation algorithms that have been successful in other contexts. Our first calculations utilize finite elements written in hyperspherical coordinates, which will permit us to assess the efficiency of an expansion in adiabatic channel functions. We anticipate that we will be able to carry out quantitative calculations of single ionization, double ionization, and high-harmonic generation processes in atomic helium, in the very near future.

6. Bose-Einstein condensation studies

While the BEC-related portion of this project ended when the present year of funding started, there has been some continued effort in this area as studies started in the preceding years have been either finished or brought closer to completion. One of these is a study of the behavior of a condensate with a negative or attractive scattering length as it grows up to its maximum possible size, and then collapses. A condensate of 7Li atoms, for instance, is the most prominent example since it has been studied extensively by the group of R. Hulet. Its maximum size has been measured to consist of approximately 1400 atoms, in agreement with theoretical expectations. After the condensate grows to contain this many atoms, calculations by H. van der Hart show how it undergoes a rapid collapse to a very small but nonzero number of atoms remaining in the condensate.[3]

Recent Papers

[1] *Extending closed-orbit theory using quantum defect ideas, I: Basic concepts and derivations*, B. E. Granger and C. H. Greene, Phys. Rev. A. **62**, 012511-[1-17] (2000).

[2] *Resonant ion-pair formation in electron collisions with HD+ and OH+*, A. Larson, N. Djuric, W. Zong, C. H. Greene, A. E. Orel, A. Al-Khalili, A. M. Derkatch, A. Le Padellec, A. Neau, S. Rosen, W. Shi, L. Viktor, H. Danared, M. Af Ugglas, M. Larsson, and G. H. Dunn, in press, Phys. Rev. A.

[3] *Collapse versus growth for a Bose-Einstein condensate with attractive interactions*, H. W. van der Hart, Phys. Rev. A **62**, 013601-[1-8] (2000).

Other published journal articles supported at least partially by this grant during 1998-2000

[4] *Validity of the shape-independent approximation for Bose-Einstein condensates*, B. D. Esry and C. H. Greene, Phys. Rev. A **60**, 1451-1462 (1999).

[5] *Spin-orbit effects on photoionization-produced alignment of the Ar+ 3p⁴(³P) 4p levels*, H. van der Hart and C. H. Greene, J. Phys. B **32**, 4029-4037 (1999).

[6] *Spontaneous spatial symmetry breaking in two-component Bose-Einstein condensates*, B. D. Esry and C. H. Greene, Phys. Rev. A **59**, 1457-1460 (1999).

[7] *Multichannel photoionization spectroscopy of Ar: Total cross section and threshold photoelectrons*, H. W. van der Hart and C. H. Greene, Phys. Rev. A **58**, 2097-2105 (1998).

[8] *Double and triple photoionization of ground-state lithium*, H. W. van der Hart and C. H. Greene, Phys. Rev. Lett. **81**, 4333-4336 (1998).

[9] *Superfluids mixing it up*, B. D. Esry and C. H. Greene, Nature **392**, 434-435 (1998). [This was a "News and Views" article, which means that we were not allowed to cite our DOE support for this work under Nature's policies.]

[10] *Effective potentials for dilute Bose-Einstein condensates*, J.L. Bohn, B.D. Esry and C.H. Greene, Phys. Rev. A **58**, 584-597 (1998).

[11] *Double photoionization and ionization of the metastable helium S-states*, H.W. van der Hart, K. W. Meyer and C.H. Greene, Phys. Rev. A **57**, 3641-3645 (1998).

[12] *Low-lying excitations of double Bose-Einstein condensates*, B.D. Esry and C.H. Greene, Phys. Rev. A **57**, 1265-1271 (1998).

Abstract for the AMOP Research Meeting, 2000

Toward Cooper Pairing of Fermionic Atoms

Deborah S. Jin
JILA
Campus Box 440
University of Colorado
Boulder, CO 80309
Email: jin@jilau1.colorado.edu

The long-term goal of this program is to explore the possibility of Cooper pairing of fermionic atoms. In analogy with the physics of superconductors, an ultracold trapped gas of fermionic atoms can in principle undergo a phase transition to a Cooper-paired state. This new phase of the Fermi gas would then provide a unique system in which to investigate the underlying physics of superconductivity. Cooper pairing requires attractive interactions between the atoms in a quantum degenerate Fermi gas. A combination of relatively strong interactions (although still weak in the sense of having a dilute gas system) and high quantum degeneracy (low temperature) will be required for Cooper pairing. To this end, one goal of the research program is to produce mixtures of bosonic and fermionic atoms and study the possibility of reaching higher degeneracy using sympathetic cooling. Another goal is to explore the effects of interactions, both in a mixture of bosons and fermions as well as between fermionic atoms in different spin-states.

Recent progress has concentrated on the development of the necessary technology for a two species magneto-optical trap (MOT), which is the first step toward sympathetic cooling using a mixture of bosonic and fermionic atoms. The existing apparatus that produces a quantum degenerate gas of ^{40}K includes a Rb atom source but lacks the necessary lasers for a Rb MOT. For this purpose we are developing a high power ($\cong 0.5$ W) laser diode system based on a broad area diode¹. Producing the laser light necessary for the Rb MOT with a robust diode laser system is essential for minimizing the additional complexity of the experiment. This laser system has been built and currently produces 0.4 W of light at 780 nm. After some final tests (to secure a decent output spatial mode and to measure the linewidth) this laser system will be used for a Rb/K two-species MOT. We also plan to attempt a current modulation scheme² with this laser in order to produce the second light frequency (for repumping) required for the ^{87}Rb MOT.

Initial studies of the Rb/K MOT will be conducted in a simple test vacuum chamber before incorporation into the existing apparatus. The components of this vacuum chamber, including a JILA-made enriched ^{40}K atom source and a glass MOT cell, will be ready for assembly in the coming weeks. With this setup our goal is to produce overlapping MOT's with roughly a billion ^{87}Rb atoms and a few million ^{40}K atoms. We will explore issues such as how to achieve good spatial overlap of the trapped Rb and K gases, what will be the limit on number due to collisional losses³, and what are the optimum laser detunings and intensities of the four laser frequencies required for the two-species MOT.

We have also made progress toward the goal of studying the interactions in a mixture of two-spin states of fermionic atoms. These studies will be conducted in the existing apparatus, where we have recently added the capability to simultaneously image the two spin-states gases. A magnetic field with a large spatial gradient is applied after the ultracold Fermi gas is released from the magnetic trap. This field separates the two spin-states through the Stern-Gerlach effect so that the two separated clouds can be imaged simultaneously. This tool will assist us in controlling and monitoring the spin composition of the gas.

Because Cooper pairing will require a relatively strong, effectively attractive interaction, we intend to search for a magnetic-field Feshbach resonance between two spin-states of ^{40}K . Such a collisional resonance will allow experimental control over both the sign and relative strength of the atom-atom interactions. The most promising theoretically predicted Feshbach resonance for ^{40}K occurs between two spin-states which cannot be confined in our current magnetic trap. Therefore we are developing a far-off resonant optical trap (FORT) for the Fermi gas. We now have a 5 W Nd:YAG laser for this purpose and are implementing the necessary optics and intensity stabilization for the optical trap.

Future plans for this project include continuing the development of the two-species MOT for boson-fermion mixtures as well as the FORT for two spin-state studies. With these two new capabilities and our existing quantum degenerate Fermi gas we will explore interactions in the Fermi gas.

1. I. Shvarchuck, K. Dieckmann, M. Zielonkowski and J. T. M. Walraven, to be published in *Appl. Phys. B*, available online (2000).
2. C. J. Myatt, N. R. Newbury and C. E. Wieman, *Opt. Lett.* **18**, 649 (1993).
3. G. D. Telles, L. G. Marcassa, S. R. Muniz, M. S. Santos, A. Antunes and V. S. Bagnato, *Laser Physics* **10**, 21-25 (2000).

Atom Trap Trace Analysis

Z.-T. Lu, K. Bailey, C.-Y. Chen, X. Du, Y.-M. Li, T. P. O'Connor, L. Young
Argonne National Laboratory, Argonne, IL 60439

lu@anl.gov, young@anl.gov

Ultrasensitive isotope trace analysis has been an important tool in modern science, with applications ranging from radioisotope dating, studies of transport processes in the ocean, atmosphere and groundwater to medicine. Two well-developed methods, low-level counting (LLC) [1] and accelerator mass spectrometry [2] have been widely used at the part-per-trillion level. Recent careful implementations of resonance ionization mass spectrometry approach this level [3].

We have recently developed a new method for ultrasensitive trace isotope analysis based upon laser manipulation of neutral atoms, atom trap trace analysis (ATTA)[4]. In this method, individual atoms are counted while residing in a magneto-optical trap (MOT), which affords extremely high isotopic selectivity. We have demonstrated a selectivity of 10^{-11} to 10^{-13} for ($^{85}\text{Kr}/\text{Kr}$) and ($^{81}\text{Kr}/\text{Kr}$) by counting these rare atoms in a natural atmospheric krypton sample. With no observed contamination from neighboring isotopes, the selectivity appears to be limited only by the number of atoms that can be sorted during a finite operation time. Key technical features are an efficient capture rate and the ability to detect a single atom in the MOT. These two requirements are independently optimized with separate capture and detection phases. Current overall efficiency of the system is 10^{-7} , where 10^{-4} arises from the need to produce metastable krypton atoms for the trapping process. Methods to improve the overall efficiency, by gas recirculation and optical excitation of the metastable state, are presently under investigation.

While many applications are envisioned, two involving ^{85}Kr and ^{81}Kr should be of particular interest to the Department of Energy. ^{85}Kr (half-life 10.5 years) atoms are produced in nuclear fission processes. Trace detection of ^{85}Kr can be used to monitor environmental contamination around nuclear-waste storage areas, to monitor nuclear-fuel reprocessing activities around the world, and to provide advanced warning of reactor leakage problems. ^{81}Kr is a cosmogenic nuclide with a half-life of 210,000 years. Due to its gaseous and inert nature, it is homogeneously distributed over the earth. In addition, its concentration is unaltered by human activities with nuclear fission because stable ^{81}Br shields ^{81}Kr from the neutron-rich isotopes that are produced in nuclear fission. Thus, ^{81}Kr is an ideal tracer for dating polar ice and groundwater in the 100,000 year range, and may be useful for characterizing nuclear waste repository sites.

References:

- [1] J. R. Arnold and W. F. Libby, *Science* **113**, 111 (1951).
- [2] R. A. Muller, *Science* **196**, 489 (1977).
- [3] K. Wendt *et al.*, *Fresenius J. Anal. Chem.* **364**, 471 (1999).
- [4] C.-Y. Chen, Y. M. Li, K. Bailey, T.P. O'Connor, L. Young and Z.-T. Lu, *Science* **286**, 1139 (1999).

Coherent Atom Optics with Bose-Einstein Condensates

William D. Phillips
Laser Cooling and Trapping Group
Atomic Physics Division, Physics Laboratory
NIST, Gaithersburg, MD

A Bose-Einstein condensate represents a source of coherent deBroglie waves, analogous to the laser as a source of coherent photons. We have demonstrated the coherent manipulation of condensates by normal diffraction and Bragg diffraction from optical fields. We have applied these techniques to interferometric studies of the condensate coherence and of the effects of interatomic, mean-field interactions. Atom-atom interactions also enable non-linear atom optical effects such as four-wave mixing and soliton generation

Quantum Theory of Collective Effects in the Atom Laser

Murray J. Holland

JILA, Campus Box 440, University of Colorado, Boulder, CO 80309-0440
Murray.Holland@Colorado.EDU

I. Program scope

The main goal of this research program has been the theoretical formulation of a quantum description of the atom laser. This would allow quantitative examination of strong collective effects typically present in Bose-Einstein condensed atomic gases. Efforts have been focussed on developing the relevant quantum kinetic equations for weakly interacting bosonic systems, and on treating the complementary problem in weakly interacting fermionic systems. On a number of occasions, these efforts have been strengthened by significant collaborative interactions with experiments at JILA.

II. Recent results

One of the core prerequisites for developing a theory of the atom laser is the understanding of the reversible and irreversible evolution of a condensed gas immersed in a non-condensed thermal background. In detail, this forms a challenging problem in which sophisticated analytical and numerical methods must be employed in order to make the dynamical equations solvable. Our first task was therefore to develop the relevant quantum kinetic theory for the trapped gas—a non-equilibrium and non-uniform system—and to incorporate all relevant dynamical quantities in the analytic and numerical solution.

Starting from a fundamental two-particle Hamiltonian which describes binary collisions in the gas, the energy and number conserving kinetic equations for the condensate and the normal and anomalous fluctuations were derived. The condensate, represented as the mean value of the atomic field, is associated in the usual way with spontaneous symmetry breaking in the phenomenon of Bose-Einstein condensation. In order to provide a complete description of the kinetic evolution, it is necessary to expand the set of relevant observables to treat also the correlation functions. These are described by the classical-like normal densities which represent the non-condensed particles, and carry information such as the thermal de Broglie wavelength. In addition, it is necessary to include the effects of the anomalous densities which describe the quantum mechanical two-particle correlations in the gas.

Within this framework, explicit and quantitative results were presented for the evolution of these kinetic equations in an isotropic situation [1]. Numerical and analytic solutions were investigated at the level of the Hartree-Fock-Bogoliubov equations, evolving self-consistently the mean-field along with the non-condensed gas. An analysis was made of the evolution of an ergodic distribution toward equilibrium in the presence of collisions.

Studying the collective behavior of atomic Bose-Einstein condensates in the nano-Kelvin temperature scale is typically made easy by the characteristic regime of low density and weak interactions. The collective dynamics of the condensate are often found by application of the Gross-Pitaevskii equation. The Gross-Pitaevskii equation represents the solution of

the mean-field theory, and is analogous to the use of classical fields in optics.

However, coexisting condensates of atoms and molecules may be generated by tuning a Bose-Einstein condensate near a Feshbach resonance, or by using Raman lasers to induce a photoassociative coupling. In this case the atom-molecule composite system is more complex and more interesting. The quantum statistical properties are modified due to the development of intrinsic pairing fields. Pairing-fields are created because molecules may spontaneously break-up into pairs of atoms located at the same coordinate. The thermal cloud which is thereby generated does not satisfy the usual classical equilibrium statistics, and for example, can contain only even numbers of atoms. This situation is reminiscent of a squeezed vacuum state of light which may be generated when photons are produced in pairs in a parametric nonlinear crystal.

We recently incorporated these ideas into a quantum kinetic theory of the atom-molecule system [2]. The calculations resolved some serious conceptual difficulties which had arisen in previous theoretical studies examining the solely mean-field equations. The solely mean-field equations had drawn a lot of criticism based on physical arguments such as time-scales. Our approach rectified this issue by going beyond mean-field theory. A comparison of the mean-field predictions against the kinetic theory is shown in Fig. 1.

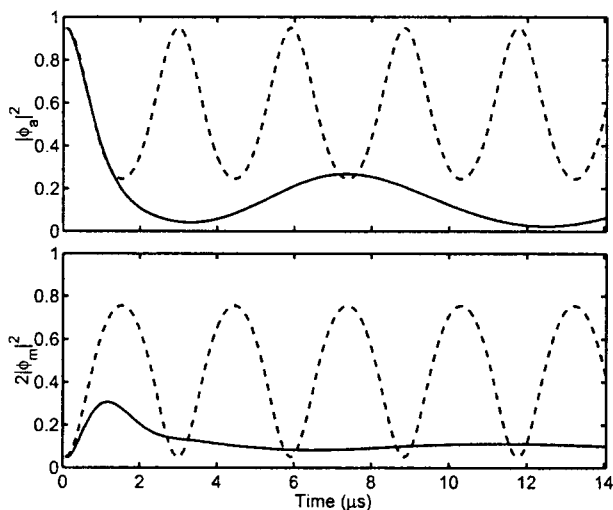


Figure 1: Time evolution of the atomic condensate $|\phi_a|^2$ and molecular condensate $2|\phi_m|^2$ for solely mean-field theory (dashed) and for the quantum kinetic theory (solid). The discrepancy is due to the formation of correlations and pairing-fields which are not accounted for in the solely mean-field theory.

These results have significant implications because they open up the study of quantum statistical fluctuations in the atom laser scenario. Connections are made with quantum optics, where extensive studies have been made of fluctuations in the radiation field.

We recently proposed a scheme for loading an atom laser operating in a continuous-wave mode [3]. The schematic diagram is illustrated in Fig. 2. To date, no continuous-wave atom laser has been demonstrated in which there is replenishing of the reservoir in direct analogy with a continuous-wave optical laser. Replenishing of the reservoir is required in steady state to compensate for the loss due to output coupling as well as to compensate for various

intrinsic loss mechanisms such as collisions with hot atoms from the background vapor and inelastic two-body and three-body collisions between trapped atoms.

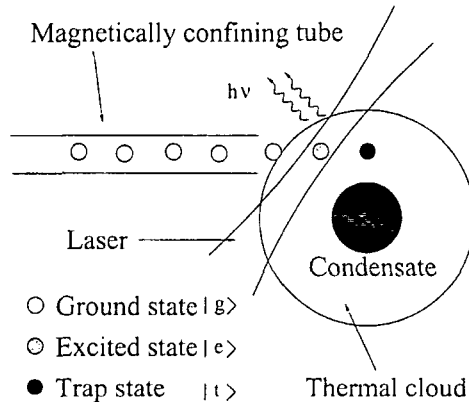


Figure 2: Schematic diagram showing the proposed loading scheme for obtaining a steady state Bose-Einstein condensation and a continuous-wave atom laser. Atoms entering the laser field from the confining tube are in the ground state. As the atoms pass through the laser field, the population is continuously transferred to the trap state by a sequence of coherent pumping and spontaneous emission.

A dissipative process is required in order to load the atoms into a conservative magnetic trap which is typically used to form the confining potential. A three level scheme was proposed to avoid the enormous heating effects usually associated with the reabsorption of spontaneously emitted photons required by the dissipative process. The proposed scheme allowed reabsorption of photons only in the tiny region of the pumping laser beam which is used to transfer the atomic internal state to the trapped state.

Although research into the atom laser has primarily focussed on bosonic systems, the possibility for demonstrating thermodynamic phase transitions in Fermi gases through Cooper-pairing makes this system also a potential candidate as a coherent atomic source. The quantum theory of Fermi gases undergoing evaporative cooling and collisional relaxation through binary interactions is itself interesting. At temperatures higher than the pairing transition, the condensate (or mean-value of the atomic field) is zero. We recently carried out a quantitative study of evaporation and thermodynamic relaxation in the two-component Fermi gas in order to elucidate the effects of Fermi-blocking, and other quantum statistical features [4]. An optimized evaporation trajectory was considered and compared with the data taken in the laboratory of Professor Jin at JILA. Reasonable agreement was found as illustrated in Fig. 3. The optimized trajectory showed that there is no fundamental reason why significantly lower temperatures could not be reached, and that the current limits are technical in nature.

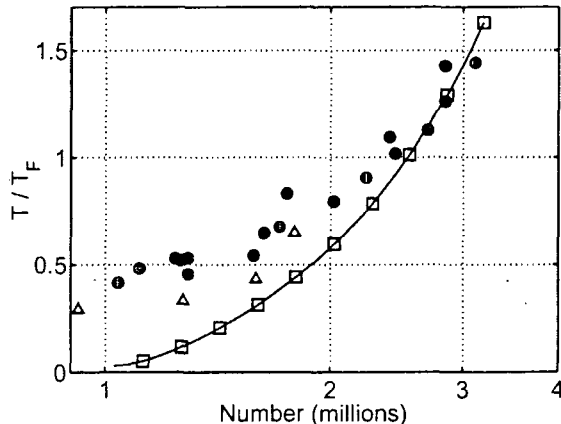


Figure 3: Optimum evaporation trajectory. The \square symbols show points on the theoretical evaporation trajectory at time intervals of 5 s. For comparison, the \bullet symbols show experimental data points giving a typical evaporation trajectory. The \triangle symbols show the lowest T/T_F achieved in the experiment (where T is the temperature and T_F is the Fermi temperature).

III. Future plans

These initial publications describe our foundation work in the theoretical description of the atom laser. Now that most of the necessary theoretical elements have been derived, future research will focus on applying the quantum kinetic theory to the atom laser model system. Observables which we intend to consider are the phase properties of the macroscopic condensate wave function and the squeezing and pairing statistics in steady-state.

In parallel to the usual kinetic description of mean-field and normal and anomalous densities we intend to examine the feasibility for unraveling the single particle density matrix evolution into simultaneously evolving wave function trajectories. This approach is in analogy with the quantum Monte Carlo methods used in quantum optics.

IV. References to DOE sponsored research

- [1] R. Walser, J. Cooper, and M. Holland, *Reversible and irreversible evolution of a condensed bosonic gas*, accepted for Phys. Rev. A, (2000).
- [2] M. Holland, J. Park, and R. Walser, *Formation of Pairing Fields in Resonantly Coupled Atomic and Molecular Bose-Einstein Condensates*, preprint (2000).
- [3] Satyan Bhongale and Murray Holland, *Loading a continuous-wave atom laser by optical pumping techniques*, accepted for Phys. Rev. A, (2000).
- [4] M. Holland, B. DeMarco, and D. S. Jin, *Evaporative cooling of a two-component degenerate Fermi gas*, Phys. Rev. A **61**, 053610 (2000).

Recent Progress and Future Opportunities for the Application of Ab Initio Relativistic-Correlation Methods to Complicated Atomic States

Donald R. Beck
Physics Department
Michigan Technological University
Houghton, MI 49931
e-mail: donald@mtu.edu

Introduction

Complex atoms (e.g., transition metals and rare earths) are of considerable technological importance for plasmas, astrophysics, catalysis, semiconductors, high-temperature superconductors, nuclear waste, time and frequency standards, novel lighting sources, and alternative energy sources. Yet, due to the open d and/or f subshell electrons, they are challenging to treat with ab initio methods which include both relativity and a thorough treatment of electron correlation effects. The purpose and scope of this work is to develop and apply advanced relativistic-correlation methods to properties of transition metal atoms and ions.

Methodology

Our calculations employ a Relativistic Configuration Interaction (RCI) methodology, which begins with a limited Dirac-Fock calculation [1] for the spectroscopic manifold(s) [2] of the occupied radial functions. The correlation radials are represented by relativistic screened hydrogenic functions, whose effective charge is determined as part of the RCI process. These virtuals have the merit of both representing the Rydberg and continuum series (for bound states), and avoiding variational collapse.

Until very recently, our attention was focused solely on properties (e.g., hyperfine structure, f-values, Landè g-values, electron affinities) of bound states; all computer codes, unless otherwise noted, were written by the PI [3]. However, an ultimate goal is to develop and apply a set of codes capable of obtaining most properties (bound or continuum) of complicated atoms to competitive accuracy (e.g., for bound states, currently: $\sim 200 \text{ cm}^{-1}$ for energy differences, 10% for hyperfine structure constants, 5-10% for f-values).

During this last year, a computer program essential to the treatment of properties involving the continuum was made [4] robust enough to be used for complex atomic states. This program produces a relativistic frozen core radial continuum function with proper normalization, orthogonality, and treatment of exchange. It was originally developed by Perger [5] at the PI's suggestion, and applied [6] to Hg resonances. It has now been made [4] into a stand-alone program, obtaining its atomic structure externally [7], making it very general. It has also been given a more stable starting estimate, and evaluates magnetic Breit integrals. Initial application has been to the lifetime of a metastable state in Ba^- [8].

Applications

Our original DOE project was to systematically and accurately account for hyperfine structure (hfs) in transition metal atoms; in particular to predict and remove the discrepancies between Dirac-Fock results and experiment [9]. It was found that proper positioning of the $d^n s$ configuration (with its large contact hfs contribution) relative to d^{n+1} (or $d^{n-1} s^2$), followed by the usual core polarization effects, was essential.

With hfs constants properly accounted for in these species [$n < 5$], attention was turned to another property associated with them—oscillator strengths and lifetimes of the relatively unknown $d^n p$ states. Among other things, we wished to see whether there were any systematic discrepancies between Dirac-Fock and RCI values (or experiment), and if so to understand what causes them. The presence of the extra p electron serves to further complicate the treatment. Additionally, Landè g -values were needed for some of these states [10].

Work began on two lifetimes in Nb II [11], for which there was an experimental result, and wavefunctions for the even parity states existed [12]. Despite a relatively crude treatment of the odd parity states, due to their complexity, a 20% agreement between RCI and experimental lifetime results was achieved, though individual oscillator strength errors could be larger, due to cancellation effects. Next, we chose to take two simpler systems, Cs II and Ba III, initially because their electric quadrupole constants (B) were thought [13] to be in need of improvement, and because two conflicting sets of lifetime measurements were available. Our hfs results [14] suggest B needs remeasurement, and favor [15] one set of lifetime measurements over the other (agreement to 6% for two of the three lifetimes, with f -value errors likely larger). This was our first calculation of Landè g -values: for thirteen levels we differed from experiment by 2.3%, which was the same size as the experimental uncertainty itself. Landè g -values, which included the anomalous g -factor, were predicted for nine additional levels.

In 1991 Feldman et al [16] computationally found an unusual magnetic dipole (M1) transition between the $J=2$ and $J=3$ levels of the $3d^4$ configuration. This had an unusually constant wavelength along the isoelectronic sequence in a region [$> 2500 \text{ \AA}$] where transmission optics could be used, and is thought to offer a very convenient line for plasma diagnostics. In 1995 and 1996 [17] Morgan, Serpa et al measured the wavelength for the Ba^{34+} , Xe^{32+} , Nd^{38+} , and Gd^{42+} members of this sequence and found it to differ from Dirac-Fock results by about 5%. Because of our DOE experience with this type of configuration, we were asked to see if we could reduce this error. A reduction to about 1% was achieved [18] by including an adequate amount of correlation. Later, we predicted [19] wavelengths and M1 rates for the W^{52+} and Bi^{61+} members of this sequence. W^{52+} has now been measured [20] and is in excellent agreement with our prediction.

Dr. Avgoustoglou was a member of our group during 1997-8, bringing with him the ability to do Relativistic Many-Body Perturbation Theory (RMBPT) calculations. In seeking a suitable problem to tackle with RMBPT, our attention was brought [13] to the discrepancy between Dirac-Fock and experimental f -values for the resonance transition in Kr I. RMBPT calculations on Kr I, Ar I, and Xe I resolved this problem [21], and in the process of writing up this work, we realized that a number of experimenters had underestimated their errors (i.e., experimental ranges did not overlap). Thus, these transitions are still in need of precise measurement.

Most lifetimes in highly ionized high- Z ions which decay by an electric dipole process are too short to be measured currently, but there are some intercombination ones such as $3s 3p^2 \ ^4P \rightarrow 3s^2 3p \ ^2P$ with lifetimes a few tens of ps [Au^{66+}] or longer, which have been measured [22], thus opening up an isoelectronic sequence for study. For the Au^{66+} and Br^{22+} members of the sequence, there were significant discrepancies between length gauge limited MCDF results and experiment. We did RCI calculations with both length and velocity

gauges [23], with the result that for three of the four transitions, there are no significant discrepancies. For the $J=5/2$ lifetime in Au^{66+} , the lifetime still differs by 13% and the wavelength by 2.5 eV. While the origin of the difference is more likely experimental than computational, the large radiative contribution (5.9 eV) to the energy differences makes one wish that QED effects in many-electron atoms could be treated more accurately.

We have just completed work on $d^4 J=0 \rightarrow d^3 p J=1$ transitions in Fe V with RCI. These have been the subject of a very recent large-scale (over 1 million transitions) Breit-Pauli R-Matrix study [24]. We have done careful RCI calculations on thirty of the largest, energetically lowest transitions in Fe V [25], and are in substantial disagreement with their [24] results. Our conclusion is that it is too early to expect accurate computational results from calculations undertaking to do vast numbers of transitions at one time. We find cases where the proper location (within 100 cm^{-1}) of energy levels is essential, and for which the total oscillator strength for the group of levels is nearly constant [26]. A similar study of the $(d+s)^4 J=1 \rightarrow (d+s)^3 p J=1$ levels in Ta II, which are of astrophysical interest, is under way. Unlike Fe V, here there is interpenetration among $d^3 p$ and $d^2 s p$ levels, which means a greater variety of electron correlation needs to be included, making substantial use of REDUCE [3] necessary. Nonetheless, the study on this system is nearly complete [27].

Future Plans

With our enlarged RCI code [3], and by updating REDUCE [3] to make it more user-friendly and capable of dealing larger problems (more determinants and parents), we can look at some more difficult transitions, such as the Yb II $6s \rightarrow 6p$ transition. This is difficult to treat [28] because of the interpenetration of $4f^{14} 6p$ and $4f^{13} 5d 6s$, which requires the inclusion of much core- $4f$ correlation [29], i.e. very large N -electron basis sets.

An even more exciting direction to follow is to apply the Tews-Perger radial continuum code [6] (within the context of a larger code, to be developed by the PI) to obtain Auger widths of states involving significant correlation effects (e.g., those having significant Coster-Kronig effects). A longer-term objective is to work with the Nicolaides group to develop a RCI approach to photoionization of high- Z atoms in intense laser fields [30].

Recent Publications Supported by DOE

Publications 15, 19, 21, and 23 (reference list) were published in 1998-2000 and report work sponsored by DOE (Grant No. DE-FG02-92ER14282).

References

- [1] J. P. Desclaux, *Comp. Phys. Commun.* **9**, 31 (1975)
- [2] e.g., C. E. Moore, *Atomic Energy Levels*, Volume III, NBS Circular 467, U.S. GPO, Washington, D.C. (1958)
- [3] There are three major codes for bound states: program RCI calculates the RCI wavefunctions, then obtains hfs constants and Landè g -values; program RFE uses the RCI wavefunctions to obtain E1, E2, and M1 f -values, including the effects of non-orthonormality; program REDUCE (provides RCI input) rotates large groups of eigenvectors to maximize the number of zero interactions with the reference vectors (the zero interactions are then discarded). This can reduce the number of vectors that must be kept by factors of 3-100, depending on the degree

of complexity of the configurations of the reference function(s).

The size limit of the RCI matrix has been increased recently from 7000 to 20 000 vectors, as the result of memory that was added courtesy of DOE. Because of the power of REDUCE, our matrices can be equivalent to conventional matrices of order 200 000 or more.

- [4] M. Tews and W. F. Perger, to be submitted to *Comp. Phys. Commun.* Tews received his M.S. this spring under my supervision, and was supported by DOE.
- [5] W. F. Perger and V. Karighattam, *Comp. Phys. Commun.* **66**, 392 (1991)
- [6] Z. Cai, D. R. Beck, and W. F. Perger, *Phys. Rev. A* **43**, 4660 (1991)
- [7] In particular, the RCI program [3] supplies the structure
- [8] M. Tews, P. L. Norquist, and D. R. Beck, unpublished
- [9] L. Young, W. J. Childs, T. Dinneen, C. Kurtz, H. G. Berry, L. Engstrom, and K. T. Cheng, *Phys. Rev. A* **37**, 4213 (1988); N. Berrah Mansour, T. Dineen, L. Young, and K. T. Cheng, *Phys. Rev. A* **39**, 5762 (1989); T. P. Dinneen, N. Berrah Mansour, C. Kurtz, and L. Young, *Phys. Rev. A* **43**, 4824 (1991)
- [10] Bill Martin, NIST (retired), private communication.
- [11] D. R. Beck and D. Datta, *Phys. Rev. A* **52**, 2436 (1995)
- [12] L. Young, S. Hasegawa, C. Kurtz, D. Datta, and D. R. Beck, *Phys. Rev. A* **51**, 3534 (1995)
- [13] Gordon Berry, private communication
- [14] S. M. O'Malley and D. R. Beck, *Phys. Rev. A* **54**, 3894 (1996)
- [15] D. R. Beck, *Phys. Rev. A* **57**, 4240 (1998)
- [16] U. Feldman, P. Indelicato, and J. Sugar, *J. Opt. Soc. Am.* **B8**, 3 (1991)
- [17] C. A. Morgan, F. G. Serpa, E. Takacs, E. S. Meyer, J. D. Gillaspay, J. Sugar, J. R. Roberts, C. M. Brown, and U. Feldman, *Phys. Rev. Lett.*, **74**, 1716 (1995); F. G. Serpa, E. S. Meyer, C. A. Morgan, J. D. Gillaspay, J. Sugar, J. R. Roberts, C. M. Brown, and U. Feldman, *Phys. Rev. A* **53**, 2320 (1996)
- [18] D. R. Beck, *Phys. Rev. A* **56**, 2429 (1997)
- [19] D. R. Beck, *Phys. Rev. A* **60**, 3304 (1999)
- [20] J. V. Porto, I. Kink, and J. D. Gillaspay, *Phys. Rev. A* **61**, 054501 (2000)
- [21] E. N. Avgoustoglou and D. R. Beck, *Phys. Rev. A* **57**, 4286 (1998)
- [22] E. Träbert, U. Staude, P. Bosselmann, K. H. Schartner, P. H. Molder, and X. Todor, *Eur. Phys. J. D* **2**, 117 (1998)
- [23] D. R. Beck and P. L. Norquist, *Phys. Rev. A* **61**, 044504 (2000)
- [24] S. N. Nahar and A. K. Pradhan, *Phys. Scr.* **61**, 675 (2000)
- [25] S. M. O'Malley, D. R. Beck, and D. P. Oros, submitted for publication
- [26] C. A. Nicolaidis and D. R. Beck, *Chem. Phys. Lett.* **53**, 87 (1978); D. R. Beck and C. A. Nicolaidis, *Chem. Phys. Lett.* **53**, 91 (1978)
- [27] D. R. Beck and P. L. Norquist, to be submitted for publication
- [28] E. H. Pinnington, G. Rieger, and J. A. Kernahan, *Phys. Rev. A* **56**, 2421 (1997)
- [29] The PI has already done moderately-sized calculations for this f-value (unpublished)
- [30] Th. Mercouris, Y. Komninos, S. Dionissopoulos, and C. A. Nicolaidis, *Phys. Rev. A* **50**, 4109 (1994); S. Dionissopoulos, Th. Mercouris, A. Lyras, Y. Komninos, and C. A. Nicolaidis, *Phys. Rev. A* **51**, 3104 (1995)

Overview of the Formation of Cold Molecules*

William C. Stwalley, Department of Physics
University of Connecticut, Storrs, CT 06269-3046

The cooling and trapping of atoms and atomic ions is a rapidly advancing field of fundamental science (e.g. Bose-Einstein condensation {recently reviewed in [1]}). We at the University of Connecticut and many others are attempting to extend the field to molecules (recently reviewed in [2]), including many presenting results at this meeting.

The coldest molecules formed in terms of translational temperature (< 1 mK) are diatomic alkali molecules formed by photoassociative techniques (recently reviewed in [3]), including one- and two-color photoassociation followed by spontaneous emission, and state-selective stimulated Raman photoassociation.

Molecules with mK translational temperatures have also been formed by several other techniques, e.g. helium buffer gas cooling, deceleration of molecular beams, and evaporation from large helium clusters.

The current status of these approaches will be summarized and some speculations concerning their future prospects and potential applications will be presented.

*Support received from the National Science foundation is gratefully acknowledged.

- [1] J. Weiner, V. S. Bagnato, S. C. Zilio and P. S. Julienne, *Rev. Mod. Phys.* **71**, 1 (1999).
- [2] J. T. Bahns, P. L. Gould and W. C. Stwalley, *Advan. At. Mol. Opt. Phys.* **42**, 171 (1999).
- [3] W. C. Stwalley and H. Wang, *J. Mol. Spectrosc.* **195**, 194 (1999).

DECELERATION AND TRAPPING OF NEUTRAL DIPOLAR MOLECULES

Gerard Meijer

FOM Institute for Plasma Physics 'Rijnhuizen'
Edisonbaan 14, NL-3439 MN Nieuwegein, The Netherlands,
and
Dept. of Molecular and Laser Physics, University of Nijmegen,
Toernooiveld 1, NL-6525 ED Nijmegen, The Netherlands

In a pulsed supersonic expansion high densities of molecules can be obtained at low translational temperatures. Typically, densities of 10^{12} molecules/cm³ per quantum state can be reached at a temperature of only a few K. These high phase-space densities can be transferred from the moving frame of the molecular beam to the lab-frame using deceleration in a series of synchronously switched electric fields (1). When molecules are in a quantum-state that gains Stark energy ('potential' energy) with increasing electric field, they will lose kinetic energy when moving into a region of high electric field. If the electric field is greatly reduced before the molecules have left this region they will not regain the lost kinetic energy. When this process is repeated by letting the molecules pass through a series of electric field stages that are switched synchronously with the arrival of the package of decelerating molecules in these stages, a sample of neutral molecules can be decelerated while maintaining the initial phase-space density (2), much like is done in charged particle accelerators. The intense pulsed beams of slow molecules that are thus obtained hold great promise for a variety of molecular beam experiments. In addition, the slow molecules can be trapped in an electrostatic trap that is rapidly switched on once the molecules have 'climbed' into it (3) or they can be injected in a storage ring.

(1) H.L. Bethlem, G. Berden, and G. Meijer, *Phys. Rev. Lett.* 83 (1999) 1558.

(2) H.L. Bethlem, G. Berden, A.J.A. van Roij, F.M.H. Cromptoets, and G. Meijer, *Phys. Rev. Lett.* 84 (2000) 5744.

(3) H.L. Bethlem, G. Berden, F.M.H. Cromptoets, R.T. Jongma, A.J.A. van Roij, and G. Meijer, *Nature* (submitted).

Buffer-gas Loaded Magnetic Traps for Atoms and Molecules

John Doyle
Department of Physics
Harvard University

Over the past three years we have developed the technique of buffer-gas cooling and loading of atoms and molecules into magnetic traps. Buffer-gas cooling relies solely on elastic collisions (thermalization) of the species-to-be-trapped with a cryogenically cooled helium gas and so is independent of any particular energy level pattern. This makes the cooling technique general and potentially applicable to any species trappable at the temperature of the buffer gas (as low as 240 mK). Using buffer-gas loading, paramagnetic atoms (europium and chromium) as well as a molecule (calcium monohydride) were trapped at temperatures around 300 mK. The numbers of the trapped species (about 10^{12} atoms and 10^8 molecules) were limited by the production method, which was laser ablation of suitable solid precursors. About 50% of the atoms or molecules introduced into the trapping region were trapped. In conjunction with evaporative cooling, buffer-gas loaded magnetic traps offer the means to further lower the temperature and increase the density of the trapped ensemble to study a large variety of both static (spectra) and dynamic (collisional cross sections) properties of many atoms and molecules at ultra-low temperatures. The method and main results will be presented in this talk.

Slowing, Storing and Cooling Neutral Molecules with Synchrotrons

Harvey Gould

MS: 71-259, Lawrence Berkeley National Laboratory,
Berkeley, California, 94720

Charged particles can be accelerated, slowed, deflected, focused, bunched, cooled, and stored for hours - by the application of static and time-varying magnetic and electric fields. Neutral polar molecules are not charged, but they do have an intrinsic separation of charge. In an electric field gradient they will experience a force. Polar molecules [1-3], and neutral atoms through polarizability [3], can be slowed, deflected, focused, and bunched using static and time-varying electric field gradients.

A standard technology for accelerating and storing charged particles (as in a synchrotron light source) is a synchrotron storage ring, fed by a booster synchrotron that accelerates the particles. The booster synchrotron is in turn injected from a particle source and small linear accelerator. The two-synchrotron approach is advantageous because the design requirements for acceleration (where the particles are held for only a few seconds) and storage, are significantly different. Following this approach I have considered the application of the two-synchrotron technique to slowing, storing and cooling neutral polar molecules.

A possible system, shown in Fig. 1, uses a pulsed jet source to produce a series of pulses of molecules that are directly loaded into a molecular synchrotron slowing ring. In a few seconds the molecules are slowed to an energy of 10 K or lower. After slowing, the pulse of molecules is transferred to the synchrotron storage ring. The slow molecules are much easier to deflect and the synchrotron storage ring can be quite small - possibly even laptop size.

If the density of molecules is high enough it will be possible to evaporatively cool them in the synchrotron storage ring. The focusing and bunching elements compress the bunch of molecules which allows them to thermalize by intrabeam elastic scattering. Then, as the bunch spreads, the hottest molecules spread furthest, allowing them to be picked off. The bunch is then refocused and rebunched, and the process repeated. Focusing and bunching are integral parts of the storage process in particle storage rings. In this situation we would create a high local density by setting all three foci to coincide.

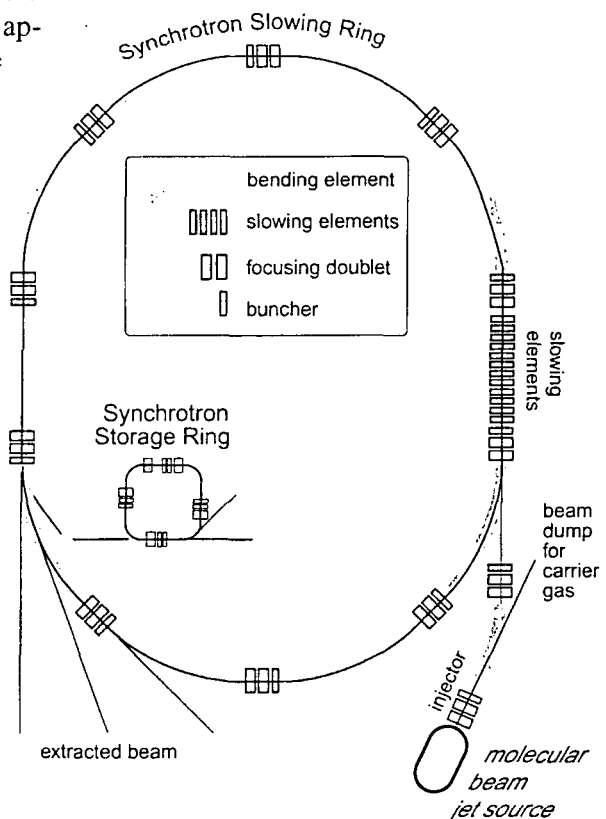


Figure 1. Schematic diagram of a molecular synchrotron slowing ring and a synchrotron storage ring. Deflecting, bunching, and focusing elements are shown but actual number and placement will be determined from lattice calculations. The layout of the elements and the size of the ring - from 1/2 - m radius to 3 m radius - is based on the methyl fluoride example (see text) with electric field gradients from a maximum electric field of 1×10^7 V/m.

As an example, consider a beam of methyl fluoride, produced by the pulsed jet source, using argon carrier gas, at a reservoir temperature of 300 K. The methyl fluoride will have a velocity of 560 m/s corresponding to a kinetic energy of 640 K. If the maximum electric field is kept to a modest 1×10^7 V/m, the synchrotron slowing ring will have a 3-meter bending radius. (This is a rather extreme example. A synchrotron with a 1/2-meter bending radius would be sufficient if the reservoir were cooled and a heavier carrier gas used. However the intensities would be much lower).

Even with the narrow velocity distribution of a jet source, the synchrotron can accept less than 0.1 percent of the available beam, and a pulse of about 0.1 ms duration. The resulting intensity of the slowed molecules will be close to 10^{12} molecules/pulse with an average density of $>10^{12}$ molecules/cm³ at an energy of 10 K and average temperature of ≤ 0.5 K. One may obtain much lower temperatures (and energies) in the slowing synchrotron at some sacrifice of intensity and density.

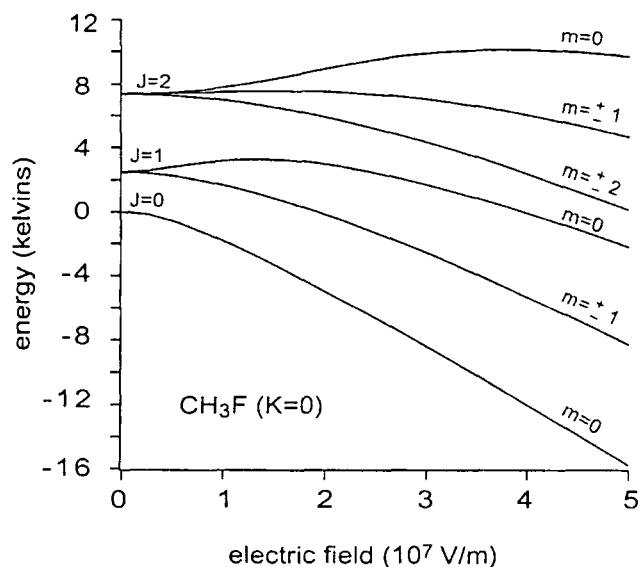


Figure 2. Energy levels of the low rotation levels of methyl fluoride (CH_3F) in electric fields (Stark effect). The energy is in units of kelvins ($1 \text{ K} = 0.69 \text{ cm}^{-1}$). CH_3F has an electric dipole moment of $d_e = 1.86$ Debye and a rotational constant of $B = 0.85 \text{ cm}^{-1}$ (1.23 K). The $J = 0$ state has the largest Stark shift and hence the largest deflection, focusing, and slowing effects of any state. It is also the only rotational level that is not degenerate at zero field. Levels whose energy decreases with increasing electric field are "strong field seeking."

The 10^{12} molecules of methyl fluoride, transferred to the synchrotron storage ring would then be evaporatively cooled. The major impediment to evaporative cooling is loss of the molecules by elastic and inelastic collisions. In this example, methyl fluoride is in the lowest vibrational and rotational ($J = 0$) state, so that once its temperature is below the $J = 0 \leftrightarrow J = 1$ transition (about 2.4 K), there should be little excitation out of the $J = 0$ state (Fig. 2). Dimer formation should be less of a problem than for alkali atoms, as methyl fluoride has a much lower boiling point. Finally, a vacuum in the 10^{-11} Torr range would minimize the losses due to scattering by hot background gasses. With the large number of molecules, the high initial density and limited collisional losses *in this example, it may be possible to reach quantum condensates in a molecular synchrotron storage ring.*

The major impediment to evaporative cooling is loss of the molecules by elastic and inelastic collisions. In this example, methyl fluoride is in the lowest vibrational and rotational ($J = 0$) state, so that once its temperature is below the $J = 0 \leftrightarrow J = 1$ transition (about 2.4 K), there should be little excitation out of the $J = 0$ state (Fig. 2). Dimer formation should be less of a problem than for alkali atoms, as methyl fluoride has a much lower boiling point. Finally, a vacuum in the 10^{-11} Torr range would minimize the losses due to scattering by hot background gasses. With the large number of molecules, the high initial density and limited collisional losses *in this example, it may be possible to reach quantum condensates in a molecular synchrotron storage ring.*

I thank Jason Maddi and Daniel Schwan for their many contributions to this work. This work was supported by the U.S. Department of Energy under Contract No. DE-AC03-76SF00098.

1. H.L. Bethlem, G. Berden, and G. Meijer, "Decelerating neutral dipolar molecules," *Phys. Rev. Lett.* **83**, 1558 (1999); H. Bethlem, G. Berden, A.J.A. van Roij, F.M.H. Crompvoets and G. Meijer, "Trapping Neutral Molecules in a Traveling Potential Well," *Phys. Rev. Lett.* **84**, 5744 (2000).
2. J.A. Maddi, T.P. Dinneen, and H. Gould, "Slowing and cooling molecules and neutral atoms by time-varying electric field gradients," *Phys. Rev. A* **60**, 3882 (1999).
3. See, for example, D. Auerbach, E.E.A. Bromberg, and L. Wharton, "Alternate-Gradient Focusing of Molecular Beams" *J. Chem. Phys.* **45**, 2160 (1966); A. Lübbert, F. Günther, and K. Schügerl, "Focusing of Polar Molecules in an Alternate Gradient Focusing System," *Chem. Phys. Lett.* **35**, 210 (1975).

"Molecules in a Dilute Gas Bose-Einstein Condensate"

Daniel J. Heinzen, The University of Texas at Austin

Recently, several groups including ours have produced a dilute gas Bose-Einstein condensate. Dilute gas Bose condensates are similar in certain respects to other quantum collective systems such as lasers or superfluid helium, but there are important differences as well. One such difference is that atoms in a dilute gas can combine into molecules. We have studied the coherent conversion of Bose-condensed ^{87}Rb atoms into $^{87}\text{Rb}_2$ molecules. The conversion was accomplished through stimulated Raman free-to-bound transitions induced by two laser fields. We observed extremely narrow transition lineshapes, and found that these lineshapes were shifted and broadened by interactions between the molecules and the atomic condensate. With further work, it should be possible to reversibly convert an atomic Bose-Einstein condensate into a molecular condensate through this mechanism. The process we have studied is a natural matter wave analog to optical frequency doubling and parametric down conversion in nonlinear optics.

Determination of Atom/Molecule-Wall Interactions and Molecular Bond Distances via Diffraction from Nanostructures

J. Peter Toennies
Max-Planck-Institut, Göttingen, Germany

Diffraction of atoms and molecules from nanostructure gratings have provided beautiful textbook examples of matter-wave phenomena. Recently we have shown that small deviations from the diffraction intensities predicted by traditional optics are related to the internal structures of the particles. This phenomenon has been used to measure the long range particle-surface potentials for a number of atoms and molecules and the geometrical sizes of small He clusters [1]. Other applications of nanostructures will be briefly mentioned.

[1] R.E. Grisenti, W. Schöllkopf, J.P. Toennies, G.C. Hegerfeldt and T. Köhler, Phys.Rev. Lett. 83, 1755 (1999) and Phys. Rev. Lett., in print (2000)

Spectroscopy and Dynamics in ^4He Nanodroplets

Kevin Lehmann
Department of Chemistry
Princeton University

Helium nanodroplet isolation (HENDI) spectroscopy combines many of the most attractive features of gas phase spectroscopy and traditional rare gas matrix isolation spectroscopy. Rotational resolved ro-vibrational spectroscopy has been observed even for heavy and highly anisotropic molecules and it has been demonstrated that novel metastable chemical species and complexes can be synthesized in this environment. Sharp (< 1 GHz) ro-vibrational transitions are usually observed, and even these are often dominated by inhomogeneous broadening whose origin is likely related to a distribution of center of mass translational states of the molecules in the superfluid, though a quantitative theory of the observed lineshapes has not yet been developed. In this talk, the work of the Princeton group will be discussed with particular focus on our attempts to characterize molecular dynamics in this highly unusual environment.

High-Angular-Momentum Rydberg Atoms in Magnetic Plasma Environment

G. Raithel, University of Michigan, 4223 Randall Laboratory, Ann Arbor, MI 48109-1120, e-mail: graithel@umich.edu

1 Physical system under investigation and research goals

We study the atomic properties, the excitation and the decay mechanisms of high-angular-momentum (high- m_l) Rydberg states in clouds of cold Rydberg atoms in strong magnetic fields, and the role these states play in magnetized cold plasmas.

For large enough magnetic field B and large m_l , the classical motion of a Rydberg electron is regular, comprising a rapid gyromotion in the B -field, and slower bounce and drift(=magnetron) motions in the Coulomb field of the atom [1]. An optional weak electric field E distorts the drift motion without destroying the drift character of the trajectories. Fig. 1 shows examples of bound and free drift orbits of Rydberg electrons in crossed electric and magnetic fields.

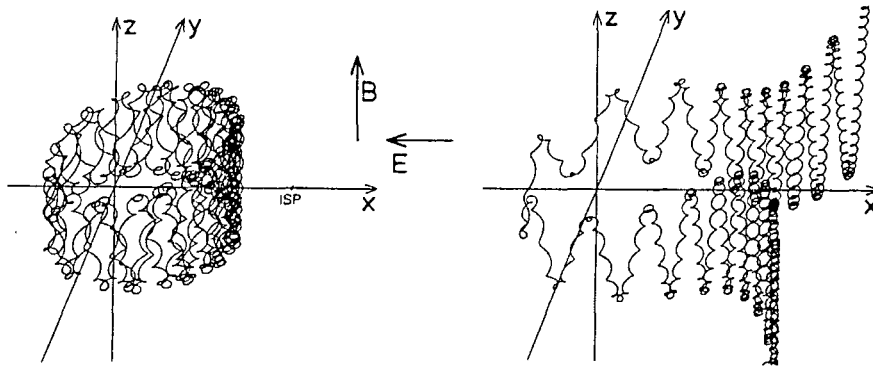


Figure 1: Bound (left) and free (right) high- m_l orbits (= drift orbits) of Rydberg electrons for $B = 5.63\text{T}$, $E = 58\text{V/cm}$, and an excitation energy of 41.2cm^{-1} below the field-free photo-ionization threshold of the atom.

A semiclassical quantization of the drift orbits can be performed using the Born-Oppenheimer approximation (BOA) [1]. The gyromotion gives rise to a cyclotron quantum number n_c with associated cyclotron energy $W = B(n_c + 1/2)$; the cyclotron energy splitting is 28GHz/T . The bouncing motion generates a bounce quantum number n_z . The associated energy levels are anharmonic; the typical energy splitting of the bounce energy levels is roughly one-tenth of the cyclotron energy splitting. The magnetron motion induces a magnetron quantum number n_m with an associated magnetron frequency of order one-hundredth of the cyclotron frequency. The density of high- m_l states is larger than the density of low- m_l states, and the wavefunctions of the high- m_l states do not overlap with the atomic core region. Because of the latter property, the lifetimes of the high- m_l states must be longer than the lifetimes of low- m_l states. All these properties indicate that in dense Rydberg-atom clouds and in plasmas in high magnetic fields the high- m_l drift-type Rydberg states should be more important than low- m_l states.

It is planned to investigate the RF and microwave spectra of high- m_l Rydberg states in strong magnetic fields. The spectra should reflect the above discussed three types of oscillatory and rotation frequencies. RF and microwave spectra will also yield information on the validity of the Born-Oppenheimer approximation (BOA), which has been invoked for the quantization of the drift motion [1]. The degree to which the BOA is valid can be varied by the magnetic-field strength and/or the excitation energy.

The lifetimes of the high- m_l Rydberg states will be determined by measuring the loss of Rydberg population versus time. Lifetime data will be an important input for the determination of the steady-state population

of high- m_l Rydberg states in plasmas.

In previous low- B experiments we have observed that a few slow electrons can efficiently populate high- m_l states [2]. We expect that in a high- B environment slow electrons and ions also lead to an efficient production of high- m_l states of the above discussed exotic nature. To measure the collision-induced production rates of high- m_l states in a quantitative way, we plan on collision experiments where a known and independently variable amount of ions and/or electrons is immersed into the Rydberg gas. The subsequent collision-induced dynamics of the gas will depend on the initial fractions of ions, electrons and Rydberg atoms.

It is intended to study recombination rates in cold, magnetized plasmas. Three-body and radiative recombination, which are known to play a role in non-magnetic plasmas [3], are expected to also populate Rydberg levels in high- B environment.

2 Methods

Laser-cooling and trapping techniques now make it possible to investigate cold, magnetized Rydberg gases and cold plasmas in small-scale experiments. To obtain a plasma-like state of high-density, magnetized Rydberg gas, we will laser-cool and trap dense samples of cold ground-state atoms in a high- B atom trap generated by a set of superconducting coils. This trap, which will generate $\sim 6T$ field strength, requires significant new development. We currently have three possible designs of high- B atom traps under consideration, for which we have calculated the fields and the coil forces (see Sec. 3). Our final choice of the design will depend on the quotations that we have received / will receive from the three companies that are willing to manufacture our proposed custom magnet designs.

To load the trap with laser-cooled atoms, we intend to use an “LVIS” [4] magneto-optic trap, magnetic guiding and focusing, and optical pumping techniques. Since we use rubidium atoms, the LVIS lasers are diode lasers with 780nm wavelength and a couple of mW power, which are stabilized to about 1MHz linewidth using saturation spectroscopy in small auxiliary vapor cells. The LVIS output velocity is tuned to about 30m/s. As the atoms enter the superconducting high- B trap, they are further slowed down to about zero velocity, because they have to climb against the magnetic-dipole potential created by the B -field and the spin of the atoms. Atoms will be accumulated and cooled in the high- B trap minimum using six optical-molasses beams [5]. Because the high magnetic field decouples the nuclear spin and lifts the degeneracy of the remaining magnetic substates of the relevant $5S_{1/2}$ and $5P_{3/2}$ -levels, the molasses practically operates on a two-level system. Thus, according to the theory of Doppler cooling [6], the trapped atoms should reach a temperature of $\sim 150\mu K$.

An important issue is the loading efficiency of the trap. The loading efficiency can be influenced by the direction from which the pre-cooled atoms enter the high- B -atom trap, and by the shape of the fringe field the atoms pass as they move into the trap center. Varying the geometry of the trap coils and the position of the LVIS source of incoming slow atoms, it is possible to minimize de-focusing effects, i.e. excessive transverse deflection of atoms that approach the trap slightly off the ideal loading trajectory. Depending on what field geometries can be technically realized, it may even be possible to achieve a focusing effect. We also consider a number of optical-pumping strategies to improve the loading efficiency.

The trapped atoms will be excited into Rydberg states using an existing pulsed dye laser. The excitation of high- m_l Rydberg states in strong magnetic fields requires a weak crossed electric field or, more elegantly, collisions between low- m_l Rydberg atoms and slow electrons. Slow electrons can be efficiently provided by a number of mechanisms, including the photoionization of trapped atoms or - employing the thermo-electric effect - by the injection of electrons emitted by a warm wire.

The analysis of the high- B Rydberg gas includes studies of its response to electromagnetic radiation, its collision-induced dynamics, and its decay patterns. The experimental tools we intend to employ include RF and microwave spectroscopy, state-selective field ionization [7, 8], time-resolved counting of free electrons and Rydberg atoms, and electron-beam injection into the atom trap. We have used some of these tools in

our recent low- B work [2, 9].

3 High- B atom trap

Since the emphasis of this project is on the study of Rydberg atoms and cold plasmas in high- B , where Rydberg states of the type shown in Fig. 1 become dominant, we want to realize an atom trap with a three-dimensional B -field minimum of order 6T. All designs we consider use a main split dipole magnet that provides most of the field at the trap center. The dipole coils also define the primary axis of the trap. Auxiliary quadrupole coils create a local minimum of the B -field, which then acts as a magnetic trap for the neutral atoms [10] as well as a magnetic bottle for ions and electrons. The final system will therefore have two independently controllable superconducting coil systems, namely a dipole bias field and a trapping (quadrupole) field.

To achieve an atom trap with 6T center field, it is necessary to efficiently fill the bore of the main dipole magnet with superconducting quadrupole coils. Sufficient trap volume and six-way optical access to the trap location must remain. When the desired field value at the trap center and the desired trap depth are reached, the maximum field strength throughout the coil package must not exceed a value of 9 to 10T.

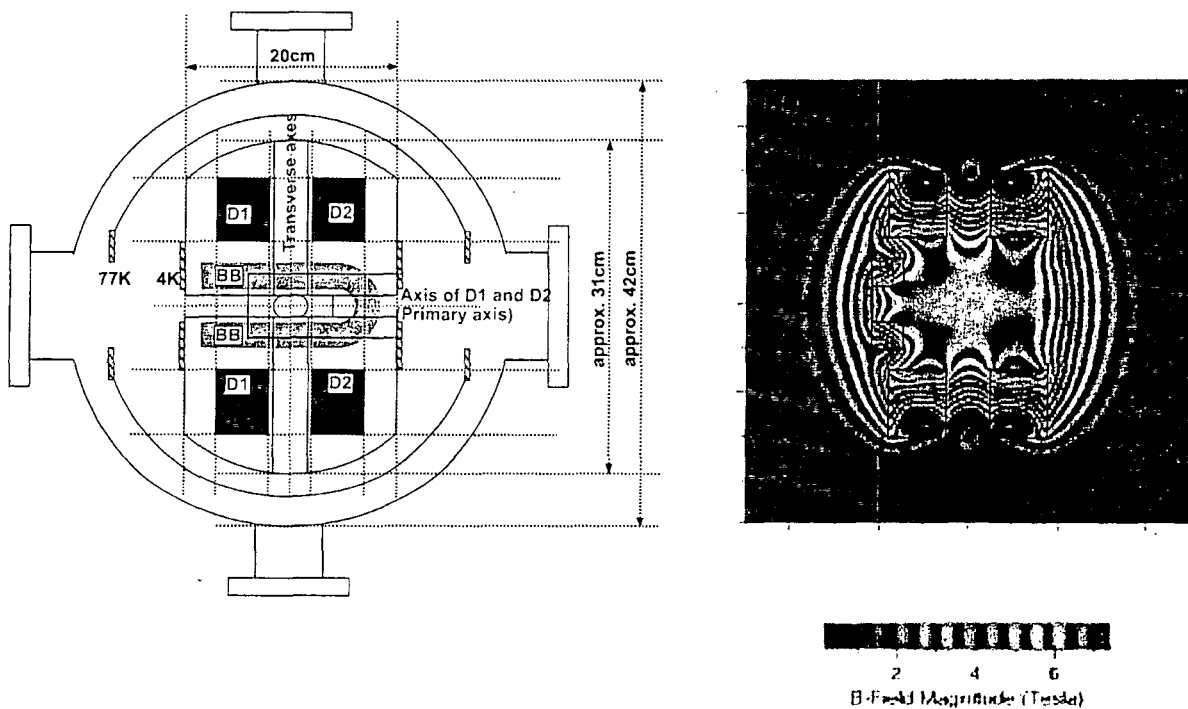


Figure 2: Left: Cryostat containing a high- B atom trap formed by split-dipole (D1 and D2) and baseball (BB) coils. Right: Cut through B -profile produced by the coils shown in the drawing on the left at a current density of $20000\text{A}/\text{cm}^2$. The rectangles show the coil cross sections.

The design shown in Fig. 2 has two large access cones along the primary axis. The cones will accommodate numerous laser beams and detector instrumentation. The primary axis is horizontal, because this allows one to use a horizontal atomic beam, which is easier to handle than a vertical one. A direct optical observation of the atom trap fluorescence through the large access cones from outside the vacuum will be possible, allowing us to optimize the trap. The pulsed lasers for the Rydberg atom excitation will also be brought in through

the large access cones.

Planar 4K and 77K radiation baffles located in the large access cones provide removable and modifiable mounting platforms for the instrumentation to be used for the analysis and the manipulation of the Rydberg gas. Tubular radiation baffles with inner diameters of order 1/2" will be inserted into these platforms to allow the mentioned laser beams to pass.

Four small access channels transverse to the primary axis are provided for the introduction of transverse laser-cooling beams. These beams cool the atoms in the degrees of freedom transverse to the primary axis.

4 Progress report and plans

Staffing: A post-doctorial researcher works full-time on the project since June 2000. A graduate student has been supported from this grant during summer 2000.

Equipment purchase: In 2000, a high- B atom trap as outlined in Sec. 3 will be purchased. It has become possible to buy this essential piece of equipment through a DoE equipment upgrade grant. While we have found three companies that are willing to manufacture a 6T atom trap according to our specifications, the trap is a highly custom piece of equipment that is new to all manufacturers. Therefore, the input that is required from our side includes extensive field calculations, calculations of forces and torques on the coils, and calculations of the trap loading efficiency. To make sure that the system will operate in a satisfactory way, we will spend a minimum four more weeks (from now) to numerically check the relevant aspects before we will make a final order. If needed, the preparation and designing phase will be extended.

Laser systems: A complete pulsed YAG and PDL laser system, which has been provided by a retiring faculty, has been modified such that it can be used for the project. Stabilized diode laser systems for the LVIS and the high- B molasses are under construction using standard techniques.

LVIS source: An LVIS-MOT [4] to be used as a loading tool for the high- B atom trap is under construction.

References

- [1] G. Raithel, H. Walther, Phys. Rev. A **49**, 1646 (1994), G. Raithel, M. Fauth, J. Phys. B **28**, 1687 (1995).
- [2] "The ZEKE-effect in Cold Rydberg Gases", S. K. Dutta, D. Feldbaum, G. Raithel, submitted, posted on the LANL preprint server (2000).
- [3] for a review of this field, see Y. Hahn, Rep. Prog. Phys. **60**, 691 (1997).
- [4] Z. T. Lu, K. L. Corwin, M. J. Renn, M. H. Anderson, E. A. Cornell, C. E. Wieman, Phys. Rev. Lett **77**, 3331 (1996).
- [5] S. Chu, L. Hollberg, J. E. Bjorkholm, A. Cable, A. Ashkin, Phys. Rev. Lett. **55**, 48 (1985).
- [6] D. Wineland, W. Itano, Phys. Rev. A **20**, 1521 (1979).
- [7] *Rydberg States of Atoms and Molecules*, eds. R. F. Stebbings, F. B. Dunning, Cambridge University Press, Cambridge 1983.
- [8] T. F. Gallagher, *Rydberg Atoms*, Cambridge University Press, Cambridge 1994.
- [9] "Spectroscopic electric-field measurement in laser-excited plasmas", S. K. Dutta, D. Feldbaum, G. Raithel, submitted, posted on the LANL preprint server (2000).
- [10] A. L. Migdall, J. V. Prodan, W. D. Phillips, T. H. Bergeman, H. J. Metcalf, Phys. Rev. Lett. **54**, 2596 (1985), T. Bergman, G. Erez, H. J. Metcalf, Phys. Rev. A **35**, 1535 (1987).

MOTRIMS: Ion-Atom Collisions with a Laser-Cooled Target

B. D. DePaola
James R. Macdonald Laboratory
Department of Physics
Kansas State University
Manhattan, KS 66506
Email: depaola@phys.ksu.edu

In recent years the study of kinematic details in ion-atom collisions through the measurement of the momentum vectors of the recoiling target ions has proven itself to be an extremely powerful technique. The experimental arrangement, referred to as COLTRIMS (cold target recoil ion momentum spectroscopy) generally makes use of a supersonically cooled target, and a time-of-flight spectrometer for the measurement of the recoil ions. Much of the usefulness of recoil-momentum spectroscopy comes from the fact that the target is cold. If it were not, the experiments would not work. For example, a room temperature helium atom has 4 a.u. of momentum and, since a typical momentum transfer in an ion-atom collision can be 1-2 a.u., the target temperature would render impossible a meaningful measurement of the recoil ion momentum without special provisions. Using a pre-cooled, supersonically expanded jet of helium, one can produce a target having an internal temperature below 0.2 K, or a momentum spread below 0.1 a.u.

Nevertheless, the COLTRIMS technique, though incredibly useful, still suffers on two accounts: (1) the target species is restricted to those gases or vapors that can be sufficiently cooled through supersonic expansion. For example, lithium would be a problematic target due to both nozzle clogging and dimer production. (2) Even with 0.2 K helium, COLTRIMS resolution is still limited by target temperature. A possible solution to these limitations is the use of a laser-cooled and trapped target, instead of a supersonic jet. Although limited to target species which may be laser-excited in a cycling transition, trapping restrictions for atomic targets are nevertheless less severe than those of supersonic cooling. Furthermore, with the three orders of magnitude lower temperature expected from laser-cooling, the resolution of the technique should be limited only by the position-sensitive detectors and timing electronics. We have therefore constructed a magneto-optical trap (MOT) to cool and trap rubidium atoms. The MOT is in working order, providing a target having a density of about 10^{10} atoms per cm^3 , at a temperature of roughly 200 μK . A novel recoil spectrometer has been designed and installed. This combination of technologies is referred to as MOTRIMS. In the first series of collision experiments we will explore charge transfer in $\text{Na}^+ + \text{Rb}$, where the rubidium is in either the 5s or 5p state. At this meeting, progress on the MOTRIMS project will be reported.

Program Title:

"Ion/Excited-Atom Collision Studies with a Rydberg Target and a CO₂ Laser"

Principal Investigator:

Stephen R. Lundeen,
Dept. of Physics
Colorado State University
Ft. Collins, CO 80523
Lundeen@Lamar.colostate.edu

Program Scope:

The program involves three related projects, all involving the interaction of multiply-charged ion beams with a Rydberg target.

1) Continued studies of charge transfer, aiming to reveal details about the L-distributions formed in the collisions.

2) Studies of X-rays emitted from the highly-excited Rydberg ions formed in these collisions.

3) Studies of the fine structure of high-L Rydberg ions, in order to extract measurements of dipole polarizabilities and quadrupole moments of the positive ion cores.

Recent Progress:

The final report of the completed study of energy distributions in charge transfer by slow ions on Rydberg states is nearing completion. This work constitutes the PhD thesis of Daniel Fisher, at Colorado State University, submitted in August, 2000. A paper for publication is in preparation.

Projects 1) and 3) above require much higher beam intensities than can be obtained on the CYREBIS ion source at KSU, and so we have moved our Rydberg target/CO₂ laser apparatus to a beamline on the 5 GHz ECR source there. This was a major effort. Once this apparatus was completely assembled, we carried out studies to optimize the S/N ratio in the RESIS studies of moderately charged ions. We discovered one major background source which degrades the S/N for some ions. This is tied to the existence of metastable excited states of the ions which lead to long-lived auto-ionizing Rydberg ions and produce background in our Rydberg detector. This problem was particularly severe for the Ar³⁺ beam which we had selected for initial tests. Fortunately, for alkali-like beams, such as Si³⁺ or Th³⁺, it should be much less of a difficulty. We have confirmed this with Si³⁺, obtaining the spectrum in Fig. 1 for excitation of Silicon III from 29-90. In this spectrum, we obtained a S/N of about 10 in 30 seconds for excitation of a single L state, such as the n=29, L=9 line at an angle of 7.4 degrees in the figure. This should be adequate to allow microwave spectroscopy of fine structure intervals in the n=29 state of SiIII, which we plan to begin soon. This will be a useful intermediate step prior to attempting to study Th³⁺. In the meantime, we are making plans to obtain a Th³⁺ beam, and to make the modifications of the ECR beamline that are required to launch it into the RESIS/RT apparatus.

Using the same spectrum of 29-90 transitions in SiliconIII shown in Fig. 1, we carried out an initial study relating to the L-distributions formed in Ion/Rydberg charge transfer. For this study, we measured the ratio between the well-resolved moderate L excitation peaks, e.g. the L=9 peak at 7.4 degrees, and the large high-L peak at 6.1 degrees. According to CTMC, when the n=29 state is produced by collisions with an 8F target, far fewer high-L states will be formed than when it is produced from a 14F target. Our measurements confirmed this expected contrast. Fig. 2 shows the measured ratio between the L=9 peak and the high-L peak, as a function of the target binding energy. As predicted by CTMC, formation from the 8F target ($E=-.212$ eV) gives a relatively large ratio because of the low population of the high-L levels. A short paper describing these observations is in preparation.

Progress on the second project (X-ray emission) required the design and construction of a new apparatus, incorporating a translatable X-ray detector, and a new Rydberg target allowing for close access by the X-ray detector. This device was completed in June, 2000 and installed on the CRYEBIS beamline. Initial tests confirmed the operation of the X-ray detector, but indicated the need for further work on the Rydberg target laser system in the new geometry. In particular, a new approach to monitoring the target brightness and locking the pump lasers is necessary that will continue to work even when the X-ray detector is looking directly at the target position. This work is still in progress.

Immediate Future Plans:

On the EBIS beamline, we plan to

- 1) continue to improve the operation and diagnostics of the new Rydberg target.
- 2) obtain further X-ray spectra following capture by bare Silicon.

Our initial goal with this experiment is to obtain an estimate of the average lifetime of the highly-excited states populated in the collisions. This will be a measure of the average L state formed.

On the ECR beamline, we plan to

- 1) Complete the analysis of the initial L-distribution experiment and explore further L-distribution studies.
- 2) Initiate microwave fine structure studies in the n=29 state of SiliconIII, based on the optical spectrum of Fig. 1. This experiment will allow us to test most aspects of the apparatus to be used for the Th^{3+} experiment, and should yield valuable results in its own right.
- 3) Design, construct, and install the beam transport hardware necessary in order to launch a Th^{3+} beam into the RESIS/RT beamline presently mounted at the ECR.

Recent Publications:

- 1) "Experimental Studies of Resonant Charge Transfer from Rydberg States by Highly-Charged Ions", S.R. Lundeen, D.S. Fisher, C.W. Fehrenbach, and B.D. DePaola (to be published in *Physica Scripta*)
- 2) "Energy Transfer in charge exchange collisions between slow ions and Rydberg atoms", D.S. Fisher, C.W. Fehrenbach, S.R. Lundeen, E.A. Hessels, and B.D. DePaola, *Phys. Rev. Lett.* 81, 1817 (1998)

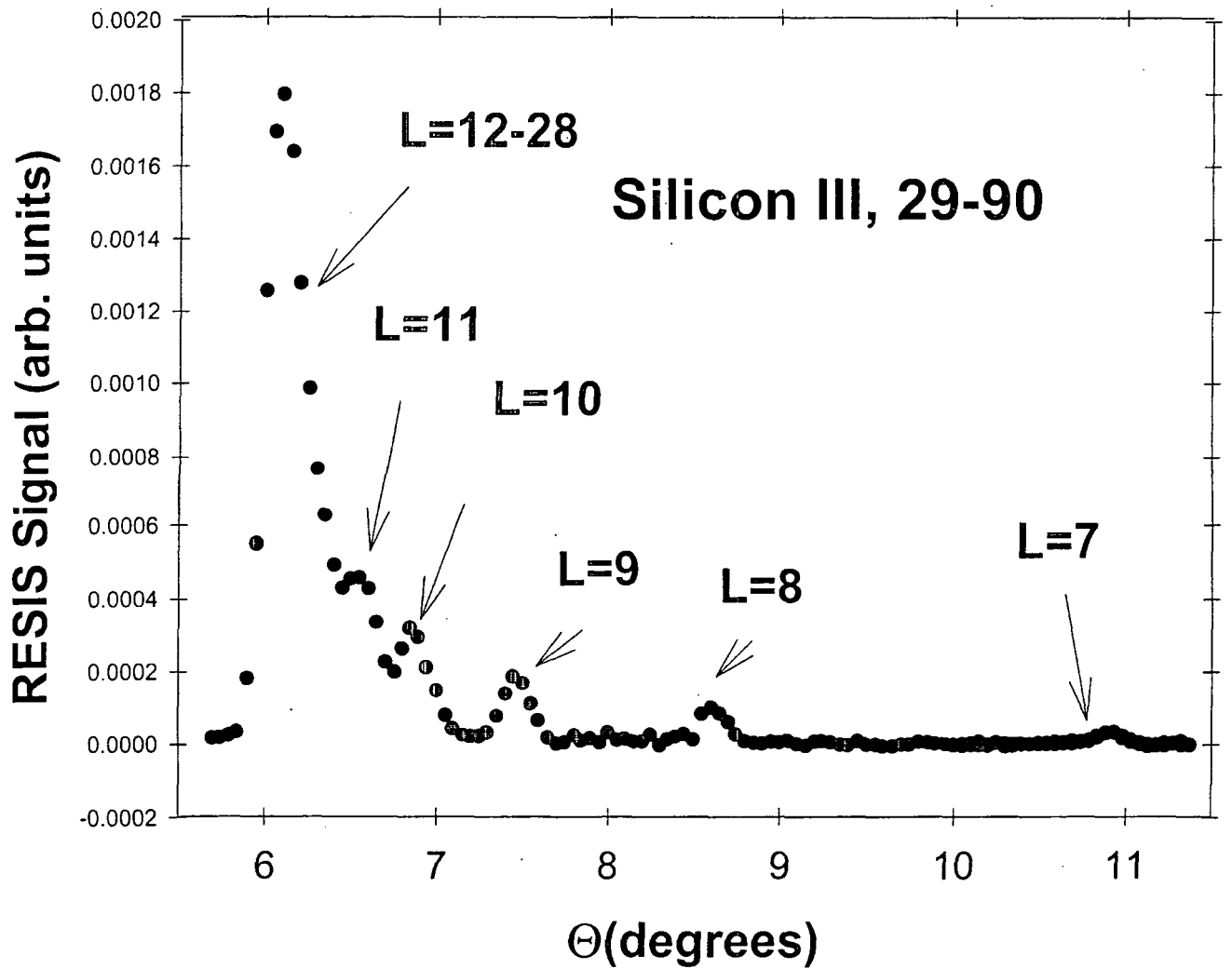


Fig. 1. RESIS excitation signal of Si²⁺ from n=29 to n=90, showing well-resolved contributions from L=7-11 states in n=29. For this data, a Si³⁺ beam with v=0.130 a.u. captured a single electron from a 10F/11D target prior to RESIS excitation.

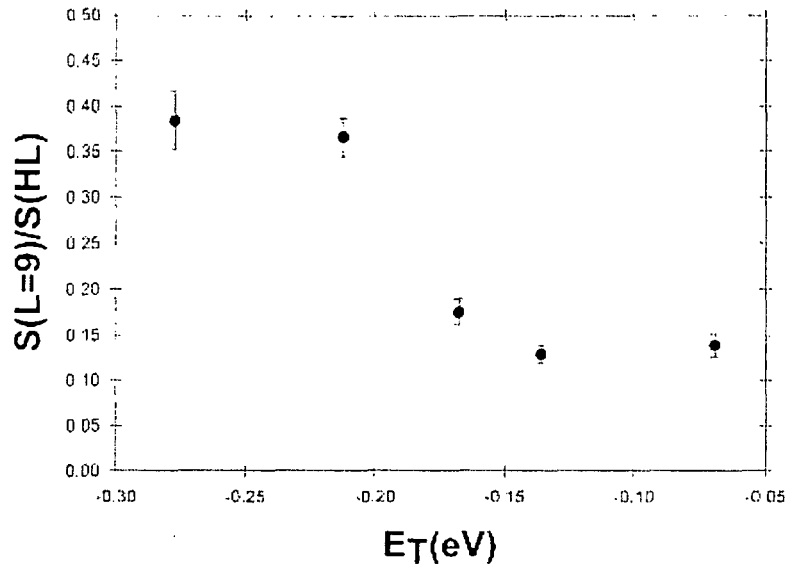


Fig. 2. Measured ratio between the $n=29$, $L=9$ RESIS excitation peak and the $n=29$ high- L peak, as a function of the binding energy of the Rydberg target used to product the $n=29$ population. The initial ion was Si^{3+} at 0.130 a.u., as in Fig. 1.

PROBING STRUCTURE AND DYNAMICS OF ATOMS AND MOLECULES USING THE ADVANCED LIGHT SOURCE

Nora Berrah

Physics Department, Western Michigan University, Kalamazoo, MI 49008

e-mail: Berrah@wmich.edu

Program scope

The objective of the research program is to advance fundamental understanding of the electronic structure and dynamics of atom and molecules through gas phase-vuv/soft x-ray interaction. The goal of the program is to understand, at the atomic and molecular level, detailed processes important to the understanding of the properties of complex materials. We use photons from the Advanced Light Source as our probes because they allow detailed knowledge and an impressive degree of precision. We have also developed and improved experimental techniques to achieve high detection efficiency and high precision measurements. We present here results completed and underway this past year and plans for the immediate future.

Recent Progress

1) Mirroring Doubly-Excited Resonances in Argon.

The early measurements of the low-energy photoionization spectrum in Ar were able to delineate window-like resonances due to the singly-excited $3s^{-1}(np)(^1P_1)$ Rydberg series, and later were also able to identify two low-lying, doubly-excited resonances, $3s^2 3p^4 4s(^2P_{1/2,3/2}) 4p(^1P_1)[1]$. Despite more than three decades of subsequent investigations, however, there has been no evidence of any other photoionization resonances in the energy region below the $Ar^+ 3s^{-1}$ threshold.

We recently used high resolution, differential measurements to carry out detailed study of the low-lying resonances in the $Ar 3p^{-1}_{3/2,1/2}$ continua in the spectral range $26.4 \leq h\nu \leq 29.4$ eV. Two new doubly-excited, predominantly triplet resonances were observed for the first time. They belong to a class of *mirroring* resonances, described recently by Liu and Starace [2], giving equal and opposite resonant contributions to the individual partial cross sections. As a result, their net contribution to the total cross section vanishes, which is why they are not observable in photoabsorption experiments.

These resonances have not been detected in previous measurements of partial cross sections since the achievable resolution was insufficient for resolving the rather narrow features (< 3 meV FWHM) that can now be observed using the ALS.

Although we focused on photoionization of atomic argon, this phenomenon can apply to general collisional processes in atoms, ions, molecules and solids.

2) Angular distribution of molecular-field- and spin-orbit-split sulfur 2p photoemission in OCS: a sensitive probe of the molecular environment.

To date, only experiments on spatially oriented diatomic molecules have been able to probe the molecular (body-frame) environment in angle-resolved photoemission studies. In such experiments, the photoelectrons are detected in coincidence with ionic fragments of the molecule detected at selected angles, furnishing information on the direction of the molecular axis and providing an internal frame in which to reference the angular distribution [3]. It is very difficult,

however, to obtain sufficiently high count rates together with high energy resolution in such coincidence experiments.

Since angular distributions of photoemitted electrons are sensitive probes of the potential field encountered by the departing electrons, and since a single anisotropy parameter still characterizes the angular distribution of photoelectrons emitted from an ensemble of randomly oriented molecules [4], non-coincidence PES measurements of angular distributions, with their high count rates and high energy resolution, can provide a possible alternative to coincidence techniques by fully resolving the effects of spin-orbit and molecular-field splitting.

We decided to learn about the molecular environment by utilizing high resolution angle resolved measurement, hoping to establish a simpler and complementary method to coincidence measurements. The experiment was carried out at the AMO undulator beamline 10.0.1 of the ALS. Electron spectra were measured using an end station designed for gas-phase angle-resolved studies and based on the Scienta SES-200 hemispherical analyzer. The measurement consisted of angle-resolved sulfur 2p photoelectron spectra from the OCS molecule with very high electron and photon energy resolution. The measurements revealed completely resolved spin-orbit with significant differences in the angular distributions of ejected electrons associated with different core-level ionic multiplet states. In addition, vibrational and molecular-field splitting were resolved, providing supporting theoretical interpretation of the measured values. A concomitant theoretical analysis relates these data to the perturbing effects of spin-orbit and molecular-field splitting, indicated that the measured angular distributions in high resolution provide a new and sensitive probe of the molecular body-frame environment in the absence of explicit sample alignment. Our work showed that spin-orbit and molecular-field perturbations of the angular distributions of inner-shell electrons photoejected from molecules can be observed under conditions of sufficiently high energy resolution. Accordingly, the measurements provide a sensitive probe of the influence of the molecular environment on the wavefunctions describing the ionized core electrons and, consequently, a new method for obtaining molecular body-frame information in the absence of explicit sample alignment.

3) Angular distribution measurements of the xenon $N_{4,5}O_{2,3}O_{2,3}$ Auger electrons: determination of alignment and intrinsic parameters

The investigation of Auger processes beyond relative yield measurements can give information about the dynamics of the underlying processes. In particular, angular distribution and spin polarization measurements of Auger electrons give valuable insight into the primary photoionization process, which is governed by the dipole interaction, and the successive decay process governed by the Coulomb interaction.

The transition from a single-hole to a double-hole state is described by the scalar Coulomb operator. This means, that Auger electrons from an isotropic initial state can only have an isotropic angular distribution and no spin polarization. The photoionization process usually leaves the singly charged photoion in a polarized state, i.e. with an uneven population of the magnetic sublevels. Thus, decay of a polarized photoion may lead to an anisotropic angular distribution and also to spin polarization of the Auger electrons [5].

The Xe 4d photoionization process, which leads to the emission of the $N_{4,5}O_{2,3}O_{2,3}$ Auger electrons, has been very well examined in a broad photon energy range [6]. In contrast, a thorough investigation of the angular distribution of the Auger decay process, which follows the 4d photoionization, was done only at select energies due to the relatively low 4d photoionization cross section (<1 Mb).

The aim of our work, was to obtain quantitative information about the alignment parameter of the Xe $4d^1$ hole states using angular distribution measurements of the Xe $N_{4,5}O_{2,3}O_{2,3}$ Auger electrons in a broad photon energy range including the important region of the Cooper minimum. In addition, our measurements allow the determination of the Auger anisotropy parameters for all the lines of the $N_{4,5}O_{2,3}O_{2,3}$ Auger group.

We measured the angular distribution of the Xe $N_{4,5}O_{2,3}O_{2,3}$ Auger electrons over a wide photon energy range, covering the Cooper minimum of the $4d$ ionization. Using the framework of the two-step model of Auger decay:

i) The alignment A_{20} of the $4d^1 \ ^2D_{3/2}$ and $\ ^2D_{5/2}$ ionic states was determined at different excitation energies including the region of the $4d$ photoionization Cooper minimum around 180 eV. The pronounced minimum in our data experimentally proves for the first time the vanishing of the \mathcal{E} component of the outgoing electron wave. This is in good agreement with theoretical predictions of an RPAE calculation [7], taking into account a small deviation in the position of the predicted minimum.

ii) The Auger anisotropy parameter α_2 for all lines of the $N_{4,5}O_{2,3}O_{2,3}$ Auger group was determined. A very good agreement with a previous experiment was found for all but one line. The calculations of Chen [8] agree well with the experimental data with the exception of the $N_4 \ ^3P_2$ line, for which all existing theories fail to predict the correct α_2 value. Interestingly, the inclusion of the exchange interaction and relaxation effects in the MMCDF calculation of Tulkki *et al.*[9] does not improve the agreement with experiment.

4) Microsphere plate detectors used with a compact Mott polarimeter for time of flight studies.

Compact retarding-potential Mott polarimeters are now widely used to measure electron spin polarizations [10]. The emphasis in their continuing development has centered on maximizing their overall figure of merit (efficiency). However, a number of potential applications call for a polarimeter capable of spin-resolved high-resolution time-of-flight measurements. A time-of-flight electron energy analyzer combined with a retarding-potential Mott polarimeter allows very effective data acquisition, because all electron lines are energy- and spin-analyzed simultaneously with a high signal to noise ratio

We built a compact retarding-potential Mott polarimeter combined with microsphere plates (MSP) as electron detectors to perform spin-resolved time-of-flight electron spectroscopy. The comparison of the performance of MSP and channeltron detectors shows that the MSP detector has a better time resolution but a lower efficiency. The overall time resolution of the system was determined to be 350 ps using synchrotron radiation pulses.

We have recently tested this apparatus and used it to conduct spin-resolved experiments in photoexcitation and photoionization of the Xe $4d$ lines.

Future Plans

The principal areas of investigation planned for the coming year are: (1) Continue our spin resolved studies in Xe and extend them to Ba, (2) continue our coincidence measurement in double photoionization, (3) continue our high resolution measurements in atoms and molecules.

References:

- [1] R. P. Madden, D. L. Ederer, and K. Codling, Phys. Rev. Lett. **10**, 516 (1963); R. P. Madden, D. L. Ederer, and K. Codling, Phys. Rev. **177**, 136 (1969).
- [2] C. N. Liu, and A. Starace, Phys. Rev. A **59**, R1731 (1999).
- [3] D. Hanson, Advances in Chemical Physics vol 77, ed. S. A. Rice and I. Prigogine (New York: Wiley), 1990.
- [4] J. Berkowitz, Photoabsorption, Photoionization and Photoelectron Spectroscopy (New York: Academic) ch. VII., 1979.
- [5] E. G. Berezhko and N. M. Kabachnik, J. Phys. B **10**, 2467 (1977); H. Klar, J. Phys. B **13**, 4741 (1980).
- [6] U. Becker, D. Szostak, H. G. Kerkhoff, M. Kupsch, B. Langer, R. Wehlitz, A. Yagishita, and T. Hayaishi, Phys. Rev. A **39**, 3902 (1989); D. W. Lindle, T. A. Ferrett, P. A. Heimann, and D. A. Shirley, Phys. Rev. A **37**, 3808 (1988).
- [7] N. A. Cherepkov, J. Phys. B **12**, 1279 (1979); N. A. Cherepkov and B. Zimmermann 9 (private communication).
- [8] M. H. Chen, Phys. Rev. A **45**, 1684 (1992).
- [9] J. Tulkki, N. M. Kabachnik, and H. Aksela, Phys. Rev. A **48**, 1277 (1993).
- [10] T. J. Gay and F. B. Dunning, Rev. Sci. Instrum. **63**, 1635 (1992); F. B. Dunning, Nucl. Instrum. and Methods in Phys. Res. A **347**, 152 (1994).

Publications from DOE sponsored research.

- 1) A.A. Wills, N. Berrah, T. W. Gorczyca, B. Langer, Z. Felfi, M. Alsherhi, O. Nayandin, and J. D. Bozek "Breakdown of LS coupling for a parity unfavored transition in Ne: Angle Resolved 2D Imaging of Two Electron Processes" Phys. Rev.Lett. **80**, (1998).
- 2) A. Farhat, A. A. Wills, B. Langer and N. Berrah, "Resonant Auger Decay Studies in Kr $3d_{3/2,5/2}^{-1} np$ states using angle-resolved electron spectroscopy", Phys. Rev. A **59**, 320 (1999).
- 3) T. X. Carroll, N. Berrah, J. D. Bozek, J. Hahne, E. Kukk, L. J. Saethre and D. T. Thomas, "High-Resolution Carbon 1s Photoelectron Spectrum of Methane:Vibrational Excitation and Core-Hole Lifetime", Phys. Rev. A. **59**, 3386 (1999).
- 4) Yench, G. C. King, M. C. Lopes, J. D. Bozek and N. Berrah "Photo-Double Ionization of Deuterium Chloride Studies by Threshold Photoelectrons Coincidence Spectroscopy", Chem. Phys. Lett. **315**, 37 (1999).
- 5) G. Snell, E. Kukk, B. Langer, and N. Berrah, "Angular distribution measurements of the xenon $N_{4,5}O_{2,3}O_{2,3}$ Auger electrons:determination of alignment and intrinsic parameters. Phys. Rev. A **61**, 42709 (2000).
- 6) E. Kukk, J. D. Bozek and N. Berrah, "Angular Distribution of the Sulphur 2p Photoemission in OCS:Variations Revealed by Molecular Field Splitting", J. Phys. B. Lett. **51**, 51 (2000).
- 7) G. Snell, J. Viehhaus, F. B. Dunning, and N. Berrah, "Compact retarding-potential Mott polarimeter for high-resolution time-of-flight studies" Rev. Scien. Instrum. **71**, 2608 (2000).

June 2000

Theoretical Investigations of Atomic Collision Physics

A. Dalgarno

Harvard-Smithsonian Center for Astrophysics
Cambridge, MA 02138
adalgarno@cfa.harvard.edu

We are exploring a diverse range of atomic and molecular collision phenomena with some emphasis on the behavior of scattering processes at ultralow temperatures.

We have extended our study of the collisions of atoms with molecules in excited rotational and vibrational levels to collisions involving heteronuclear molecules. We have explicit results for the scattering of ^4He with CO. The van der Waals well supports shape resonances which control the relaxation cross sections at very low energies. Feshbach resonances occur near channel thresholds. There are discrepancies in the predicted and measured line shifts and widths that we are exploring. Calculations are in progress on collisions of ^3He with CO.

A study of ultracold ion atom collisions has been completed. The cross sections for charge transfer of Na^+ in Na are very large.

The possibility of enhanced or accelerated cooling of hydrogen atoms by an admixture of lithium atoms has been explored. Accurate potential energy curves were constructed and the scattering lengths were determined. The calculations show that for triplet scattering the $^7\text{Li-H}$ rate coefficient is one thousand times the H-H rate coefficient. Similar calculations are in progress for Na-H and K-H.

We continue our development of methods for calculating molecular properties at large internuclear distances. We have presented a method for the determination of expectation values of operators and applied it to obtain the relativistic corrections to the energies of the H_2 molecule.

We have used a combination of approaches to predict the long range interactions of pairs of metastable inert gas atoms and we are now investigating the interactions between alkaline earth atoms.

The collisions of a pair of metastable hydrogen $\text{H}(2s)$ atoms have been studied. We have shown that at thermal energies, the most

probable result is the production of a pair of H(2p) atoms which then radiate. The more complex situation that occurs at ultralow temperatures is being considered. Various aspects of the collision of hydrogen with anti-hydrogen are being explored, including the possibility of cooling of H by $\bar{\text{H}}$ and the possibility of radiative association to form H $\bar{\text{H}}$.

References

- J. M. Taylor, J. F. Babb and A. Dalgarno, The Dipole Polarizability of the Hydrogen Molecular Ion, *Phys. Rev. A* 60, R2630, 1999.
- R.C. Forrey, A. Dalgarno and J. Schmiedmayer, Determining the Electron Forward Scattering Amplitude Using Electron Interferometry, *Phys. Rev. A* 59, R942, 1999.
- M.J. Jamieson, B. Zygelman, A. Dalgarno, P.S. Krstic and D. Schultz, Collisions of Ground-state Hydrogen Atoms, *Phys. Rev. A* 61, 014701.
- M.J. Jamieson, L. Wolniewicz and A. Dalgarno, The Calculation of Properties of Two-Center Systems *Phys. Rev. A* 61, 042705-1, 2000.
- R. Côté, M. J. Jamieson, Z-C. Yan, N. Geum, G.-H. Jeung and A. Dalgarno, Enhanced Cooling of Hydrogen Atoms by Lithium Atoms, *Phys. Rev. Lett.* 84, 2807, 2000
- P. Froelich, S. Jonsel, A. Saenz, B. Zygelman and A. Dalgarno, Hydrogen-Antihydrogen Collisions, *Phys. Rev. Lett.* 84, 4577, 2000.
- R. Côté and A. Dalgarno, Ultracold Atom-ion Collisions, *Phys. Rev. A* in press 2000.
- N. Balakrishna, A. Dalgarno and R. C. Forrey, Vibrational Relaxation of CO by Collisions with ^4He at Ultracold Temperatures, *J. Chem. Phys.* in press 2000.
- A. Derevianko and A. Dalgarno, Long-range Interaction of Two Metastable Rare-gas Atoms, *Phys. Rev. A* submitted.
- B. Zygelman, A. Saenz, P. Froelich, S. Jonsel and A. Dalgarno, Radiative Association of Atomic Hydrogen with Antihydrogen at Subkelvin Temperatures, *Phys. Rev. A* submitted.
- R. C. Forrey, R. Cote, A. Dalgarno, S. Jonsell, A. Saenz and P. Froelich, Collisions between Metastable Hydrogen Atoms at Thermal Energies, *Phys. Rev. Lett.* submitted.

Experiments in Ultracold Collisions

Phillip L. Gould
Department of Physics U-46
University of Connecticut
2152 Hillside Road
Storrs, CT 06269-3046
<gould@uconnvm.uconn.edu>

Program Scope:

The techniques of laser cooling and trapping have enabled many new and exciting research directions in atomic, molecular, and optical physics. Samples of ultracold (e.g., $T < 100 \mu\text{K}$) atoms at high density (e.g., $n > 10^{11} \text{ cm}^{-3}$) are the starting point for many investigations, including Bose-Einstein condensation and atom lasers, improved atomic clocks, photoassociative spectroscopy, ultracold molecule production, optical lattices, ultracold Rydberg atoms and plasmas, and fundamental atomic and nuclear physics experiments with radioactive isotopes. In most of these applications, ultracold collisions play a important role. Inelastic processes can limit density and temperature, so improved knowledge and control of these interactions is necessary for continued progress. Our program is focused on experimental investigations of collisions between ultracold atoms, especially those which occur in a typical laser trap environment.

In addition to their relevance to the many applications of laser-cooled atoms, ultracold collisions exhibit several fascinating features. Although various collisional channels may exist, the collision energy is so low (e.g., $\sim 10^{-8} \text{ eV}$) that only exoergic processes are possible. Since the collisions generally involve low angular momentum, quantum effects are usually important. In contrast to higher energy collisions, the long-range ($R \sim 100 \text{ nm}$) potentials can be dominant, i.e., the colliding atoms “feel” each other at extremely long range. This allows control of the collision dynamics with laser light. Finally, the combination of the long range of the potential and the low collisional velocity yields a collisional time scale many orders of magnitude longer than for room-temperature collisions. In fact, atomic excitation can spontaneously decay during the course of a slow collision, dramatically affecting the outcome.

All of our experiments utilize 780 nm diode lasers to cool and confine rubidium atoms in a magneto-optical trap (MOT). Atoms are loaded into the MOT from either a laser-slowed beam or a room-temperature vapor. Measurements of inelastic collisions are carried out by monitoring the loss rate of atoms from the trap. Specific trap-loss processes include: radiative escape (RE), where the excited-atom pair emits a less energetic photon than it absorbed; fine-structure-changing (ΔJ) collisions; and hyperfine-changing (ΔF) collisions.

Recent Progress:

During the past year, we have performed two major experiments in the area of laser cooling and ultracold collisions: demonstration of the dramatic effects of laser light on ground-state hyperfine-changing collisions between ^{87}Rb atoms; and the use of trap-loss to measure the wavelength dependence of photoionization of the highly-excited Rb 5D level. In addition, we have made two major technical advances: the realization of a new double MOT and the demonstration of frequency modulation of injection-locked diode lasers. We briefly describe each of these below.

Previously, we measured the rate of ground-state hyperfine-changing (ΔF) collisions in a ^{87}Rb MOT at temperatures of $\sim 100\ \mu\text{K}$. Meanwhile, experiments with a ^{87}Rb two-state Bose-Einstein condensate (BEC) determined the rate of spin-exchange collisions at a much lower temperature of $\sim 1\ \mu\text{K}$. Since ΔF collisions and spin-exchange collisions are closely related, we expected the two measurements, accounting for the temperature dependence, to be consistent. In fact, there was a rather large discrepancy. One important difference between the two experiments is that the MOT measurements took place in the presence of trapping light, while the BEC measurements were performed in the dark. We therefore developed a population switching technique which allowed us to measure the ΔF collision rate in the dark. We found that even at our low trap laser intensities, the laser light has a dramatic effect on the rate of ground-state collisions. This may be related to the flux enhancement effect which we have previously observed to be important in excited-state collisions. In any event, when rates in the dark are compared, the discrepancy largely disappears.

Recent experiments on the highly-excited 5D level in Rb have focused on photoionization. This is a loss process which competes with ultracold 5D collisions, so its cross section must be measured. To efficiently prepare cold atoms in the 5D level, we use two-photon diode-laser excitation from the ground state: $5S \rightarrow 5P \rightarrow 5D$, with pulses applied in the “counterintuitive” order, i.e., $5P \rightarrow 5D$ followed by $5S \rightarrow 5P$. The photoionization cross section is determined by measuring the increased loss rate of atoms from the trap when photoionizing light is applied. In addition, by using intense pulsed laser light, we can completely ionize all 5D atoms, which gives a direct measure of the 5D excitation efficiency. We have measured the absolute photoionization cross section over a range of photon energies as shown in Fig. 1. Agreement with theoretical calculations performed by H.R. Sadeghpour (ITAMP) are excellent.

A major technical advance in our lab has been the development of a double MOT for use in our ultracold collision experiments. Previously, we loaded our MOT from a laser-slowed atomic beam. However, this apparatus was rather cumbersome and subject to vibration. We have replaced this atomic beam source with a “source” MOT which captures large numbers of atoms from a room temperature vapor. Cold atoms from the source MOT are ejected with a laser beam, forming a slow atomic beam which propagates into a separate vacuum chamber and loads a second MOT. The background pressure in this second chamber can be very low, allowing a very long MOT lifetime

(e.g., 100 s) which is necessary for measuring ultracold trap loss collisions. Another improvement is that the second MOT is operated in a configuration which is phase stable, i.e., the relative time phase between its six laser beams is fixed. This greatly improves the temporal stability of the trapped cloud.

Another technical advance in our lab involves the modulation of diode lasers at microwave frequencies. Cooling and trapping of rubidium atoms requires laser light at two frequencies separated by 2.9 GHz for ^{85}Rb (6.6 GHz for ^{87}Rb). We have previously used two separate external-cavity diode lasers to generate these trapping and repumping beams. A simpler scheme is to stabilize one external-cavity laser at the trapping frequency and inject the light from this “master” laser into a free-running “slave” laser. The frequency of the slave laser is thereby injection-locked to that of the master. We then modulate the current in the slave laser at 2.9 GHz, which generates the desired sideband for repumping. There are two advantages to this scheme. The slave laser provides a higher power than the master, and only one laser needs to be locked to an atomic resonance.

Future Plans:

We have several experiments in ultracold collisions planned for the coming year. First, we would like to expand the temperature range of our recent measurements of ^{87}Rb ground-state hyperfine-changing collisions. We would also like to make measurements on the other isotope, ^{85}Rb , to see if the effects of near-resonant laser light are as dramatic as they are in ^{87}Rb . More extensive measurements may allow us to determine the origin of the light-induced effect and also place tighter constraints on the ground state potentials.

We previously observed ultracold collisions in real time by using two pulses in a pump-probe configuration. The first pulse, tuned close to the atomic resonance, excites the colliding atom pair at very long range. The atoms accelerate towards each other on the attractive excited-state potential, decaying back to the ground-state as they approach short range. A second pulse, detuned significantly below the atomic resonance, re-excites this enhanced collisional flux, causing an observable inelastic process at short range. The magnitude of the flux enhancement effect is limited by the fact that an atom pair excited at long range, where the potential is very flat, decays before significant deflection of its trajectory takes place. We are attempting to optimize the collisional flux enhancement by rapidly chirping the laser frequency in order to maintain resonance during the course of the collision. This type of active control may prove useful in enhancing the rate of cold molecule formation via photoassociation, a process which occurs at relatively short range. Preliminary results of these experiments are promising.

Finally, we will study ultracold collisions which involve the highly-excited Rb 5D level. In contrast to the more commonly studied collisions involving the first excited level (5P), 5D collisions will be strongly influenced by the long radiative lifetime and the shorter range of the potential. The rate of trap loss collisions will be measured as a function of detuning from the two-photon (5S \rightarrow 5P \rightarrow 5D) resonance.

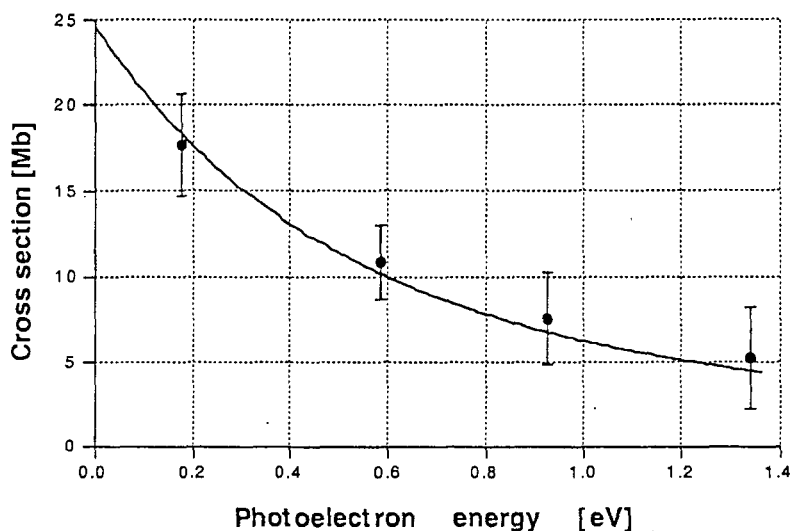


Fig. 1 Plot of the $5D_{5/2}$ photoionization cross section as a function of photon energy above threshold (photoelectron energy). The data points correspond to wavelengths (left to right) of 1064 nm, 788 nm, 647 nm, and 532 nm. The solid line is the theoretical prediction.

Recent Publications:

“Efficient 5D Excitation of Trapped Rb Atoms Using Pulses of Diode-Laser Light in the Counterintuitive Order”, W. Süptitz, B.C. Duncan, and P.L. Gould, *J. Opt. Soc. Am. B* **14**, 1001 (1997).

“Trap-Loss Collisions of ^{85}Rb and ^{87}Rb : Dependence on Trap Parameters”, S.D. Gensemer, V. Sanchez-Villicana, K.Y.N. Tan, T.T. Grove, and P.L. Gould, *Phys. Rev. A* **56**, 4055 (1997).

“Ultracold Collisions Observed in Real Time”, S.D. Gensemer and P.L. Gould, *Phys. Rev. Lett.* **80**, 936 (1998).

“Ultracold ^{87}Rb Ground-State Hyperfine-Changing Collisions in the Presence and Absence of Laser Light”, S.D. Gensemer, P.L. Gould, P.J. Leo, E. Tiesinga, and C.J. Williams, *Phys. Rev. A* (Rapid Communication), in press.

“Measurement of the $\text{Rb}(5D_{5/2})$ Photoionization Cross Section Using Trapped Atoms”, B.C. Duncan, V. Sanchez-Villicana, P.L. Gould, and H.R. Sadeghpour, submitted for publication.

Threshold resonances: a key to cold collision phenomena

Paul S. Julienne

*Physics Laboratory, National Institute of Standards and Technology, 100 Bureau Drive Stop
8423, Gaithersburg, MD 20899-8423 USA*

Collisions play a crucial role in the fundamental physics and applications of cold, trapped atoms, and we may expect them to be just as important for cold, trapped molecules. Scattering resonances, where two colliding species form a transient quasibound complex, have provided one of the most fruitful avenues for probing and utilizing cold collisions of trapped atoms. Resonances have the advantage of being tunable by varying some external field. Photoassociation resonances are selected by tuning a laser frequency, whereas magnetic fields can move near-threshold bound states into resonance with threshold collisions. These are examples of optically-tunable and magnetically tunable Feshbach resonances. Double (or multiple) resonance experiments are also possible by tuning two (or more) lasers, or by combining optical and magnetic tuning. Collisional stabilization of transient resonances provides a route for three-body recombination. Resonance scattering theory provides a unified approach for describing a variety of single and multiple resonance phenomena.

Much of what we know quantitatively about cold atom collisions is derived from interpreting such resonance spectroscopy. The sign and magnitude of the scattering lengths for alkali ground state collisions has been derived from several joint experimental-theoretical investigations. For example, we have recently analyzed data from the Stanford group [1] to obtain definitive scattering lengths for collisions of ground state Cs atoms [2]. In interpreting such experiments it is important to take into account the full spin structure of the alkali dimer Hamiltonian matrix, as well as the molecular interaction potentials. It is also necessary to take into account the specific threshold properties of the particular systems being studied in order to properly interpret experiments. When scattering lengths are large, the standard threshold laws only apply over a very narrow collision energy range above threshold.

We may expect threshold resonance spectroscopy to be important for probing collisions of new species that may come to be cooled and trapped. Some possibilities for such future applications are Group II atoms and molecular species.

Thanks are expressed to the Office of Naval Research and the Army Research Office for partial support.

1. C. Chin, V. Vuletic, A. J. Kerman, and S. Chu, "High Resolution Feshbach Spectroscopy of Cesium," *Phys. Rev. Lett.*, in press (2000).
2. P. J. Leo, C. J. Williams, and P. S. Julienne, "The collision properties of ultracold ^{133}Cs atoms," *Phys. Rev. Lett.*, in press (2000).

Ultracold three-body collisions

B.D. Esry

Department of Physics, Kansas State University

Chris H. Greene

Department of Physics and JILA, University of Colorado

James P. Burke, Jr.

NIST Gaithersburg

Bose-Einstein condensates are increasingly being studied in regimes in which three-body collisions can play an important role. For instance, as the density is pushed higher, the importance of three-body recombination grows. Three-body recombination can also be important for condensates whose two-body scattering length is being manipulated by external magnetic fields. The typical scenario is to scan the magnetic field such that the two-body elastic collision cross section is swept through a Feshbach resonance which, in turn, changes the two-body scattering length. Three-body recombination has been shown to scale roughly with the fourth power of the scattering length and can thus be significantly enhanced around a Feshbach resonance. I will present the results of extensive nonperturbative calculations of the three-body recombination rate carried out within the hyperspherical formalism. It is found that the overall scaling of the recombination rate follows the power law mentioned above, but is modulated by multichannel interference effects for positive scattering lengths and by three-body shape resonances for negative scattering lengths. These phenomena and their connection to the Efimov effect will be discussed. The role of the Efimov effect in atom-molecule collisions will also be addressed.

Recent Results from Rochester on Homo- and Heteronuclear Ultracold Molecules

N. P. Bigelow
Department of Physics and Astronomy
The University of Rochester
Rochester, NY 14627 USA

In this talk I will describe studies of the formation of ultracold molecules via photoassociation of laser cooled and trapped atoms and on the application of these molecules to precision spectroscopy and to the formation of novel degenerate quantum gasses.

In the first part of the talk, I will describe the spectroscopy of highly excited states of ultracold Na_2 molecules using a new photoassociative approach based on resonantly enhanced multiphoton ionization (REMPI). Using near resonant light to photoassociate colliding ultra-cold atoms in a magneto-optical trap, we excite a remarkable number of Na_2 rotational states providing a rich rovibrational REMPI spectrum. We find that rotational states with quantum numbers up to $J = 22$ are excited and show that the measured population distribution can be well described using a local equilibrium model. By careful analysis of the REMPI spectrum, we extract not only the first order quadrupole-quadrupole (C-5) and the VanderWaals constants (C-6) but also sensitive atom-atom interaction parameters such as spin-spin, spin-orbit and perturbative constants.

I will then describe our work which has followed pioneering work of the groups at Orsay, the University of Connecticut, Pisa and elsewhere: we have observed that both ultracold Cs_2 and Rb_2 molecules are spontaneously formed in a magneto-optical trap (MOT). We have uniquely detected the production of ground-state homonuclear molecules using resonantly enhanced multi-photon ionization via nsec laser pulses. Quite recently we have also demonstrated the ability to detect and probe these molecules using ultra-fast (femtosecond) laser pulses and I will describe our efforts to extend these results to studies of wavepacket dynamics and to the coherent control of ultracold molecule formation. In the last part of the talk, I will describe our concurrent experimental results on the formation of cold ground-state *heteronuclear* molecules in a multi-species MOT. Absolute production rates of heteronuclear molecules will be discussed in terms of the difference between homo- and heteronuclear pair-

potentials and relevant Frank-Condon overlap. Progress towards the realization of novel polar-molecular traps will also be mentioned as well as theoretical predictions on the nature of Bose-Einstein condensates (BEC) of polar molecules.

Theoretical Studies of Atomic Transitions

Charlotte Froese Fischer

Department of Electrical Engineering and Computer Science, Box 1679B

Vanderbilt University

Nashville, TN 37235

The atomic structure project is concerned with the accurate determination of wave functions from which a number of atomic properties can be predicted. Of particular importance are properties associated with energy transfer mechanisms such as transition probabilities, where relativistic effects are essential, and photoionization. Light elements have been investigated primarily in the Breit-Pauli approximation, but for heavier elements our methodology is shifting towards those based on Dirac theory.

Recent Progress

1. Transition probability studies for light atoms

We have developed methods suitable for "spectrum" calculations where all the energy levels up to a certain excitation level are computed along with all transitions between these levels. As a result, lifetimes of levels may be determined which often can be compared more directly with experiment. These are based on the Breit-Pauli approximation which includes low-order relativistic corrections, but judicious choice of terms controls the size of the computational problem and, relative to MCDHF, more correlation can be included. The results are being made available for ready access on the internet :

(See http://www.vuse.vanderbilt.edu/~cff/mchf_collection).

We have completed the evaluation of both beryllium-like[1] and boron-like[2] sequences, and the calculation of carbon-like and nitrogen-like are completed but not yet evaluated. Our computational method is systematic allowing for an estimation of the uncertainty in the transition rates, many of which are accurate to 1% or better, though exceptional cases, where the line strengths are small due to cancellation, will always be less accurate. This was clearly evident in the study of the $3s^2S_{1/2} - 4p^3P_{1/2,3/2}$ transition in Mg^+ [3]. Unlike other collections, all these results include the effects of the low-order relativistic corrections and include many weak intercombination lines. Already for the $2s^22p^23d$ levels, it was necessary to revise our Breit-Pauli codes to separate the angular and radial integrations since the former needs to be done only once per iso-electronic sequence. This significantly reduced the time required on the T3E at NERSC. The codes have also been modified to determine the g_J factor that enters into the Zeeman effect. This property is often used by experimentalists for line identification. Similarly, the isotope parameter is automatically computed, but for reliable values the latter often requires a different correlation model, since the isotope parameter depends more on correlation with the core. This was shown in the study of the isotope effect on the electron affinity of oxygen [4].

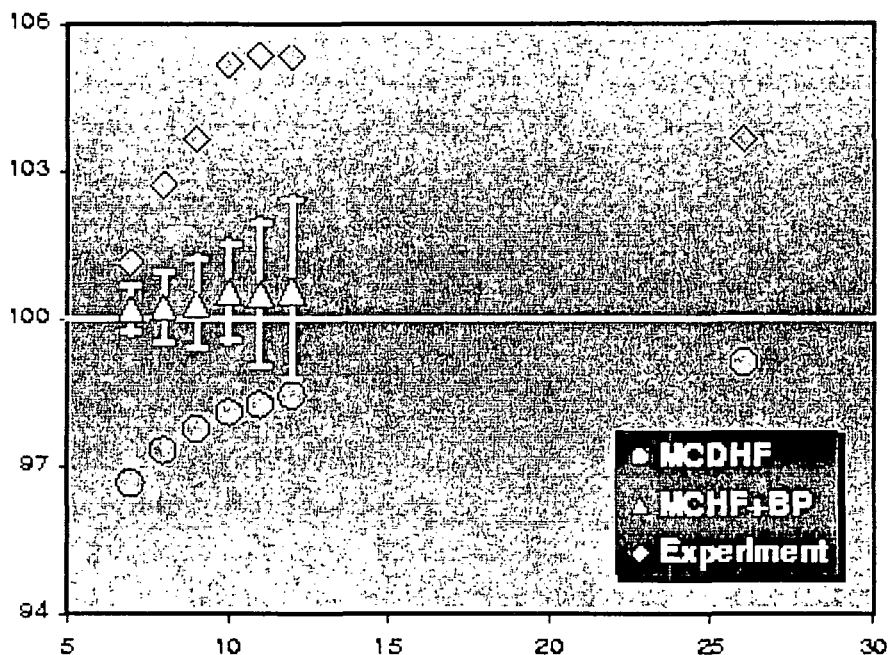


Figure 1: Comparison of previous MCDHF, MCHF+BP, and semi-empirical results with revised MCDHF values. Plotted is $100 \times \text{Previous}/\text{New}$ as a function of nuclear charge Z .

2. Relativistic Multiconfiguration Dirac-Hartree-Fock Calculations

An intercombination transition arises from relativistic-spin effects. At first sight, it might appear that starting with Dirac theory and including correlation, would be the best course to follow, but this has not been the case. We observed that earlier MCDHF calculations for Be-like[5] were all outside the uncertainty estimates of our carefully computed Breit-Pauli results. An idea was investigated in order to understand this phenomenon [6]. Both the multiconfiguration Hartree-Fock (MCHF) and the multiconfiguration Dirac-Hartree-Fock (MCDHF) are variational methods. This implies that orbitals and wave function expansions are optimized solely on the basis of energy. Though MCDHF calculations are done in jj -coupling, it is possible to transform to LSJ. Thus any jj -expansion for Be-like $2s2p\ ^3P_1$ will have both a 3P and a 1P component. The variational method based on the energy will favor the former and neglect the latter to some extent, thereby predicting too low a transition rate from $2s^2\ ^1S_0$. The idea we explored was simultaneous optimization on all the levels of $^3P_{0,1,2}$ and 1P_1 . With this change in methodology, the revised MCDHF results are in excellent agreement with the Breit-Pauli values and definitely within the uncertainty estimates of the latter which increase rapidly with the nuclear charge. This is shown in Figure 1 above. The basis of comparison are the new results and triangles represent MCHF+BP. The agreement is excellent. It also is clear the uncertainty estimates for the MCHF+BP grow too rapidly with nuclear charge. The circles are the earlier results.

A similar intercombination line can be found in the Mg-like sequence, namely $3s^2\ ^1S_0 - 3s3p\ ^3P_1$. Unlike the Be-like sequence where $2s3d$ is a minor correlation player, in Mg-like $3p3d$ is in the same complex as $3s3p$ and hence an accurate core-polarization calculation would also consider this as a reference configuration state. In earlier investigations, this effect was included in an

Table 1: Relativistic and non-relativistic transition energies (in cm^{-1}), radiative dipole elements (in a.u.) and transition rates (in s^{-1}) for the $3s^2\ ^1S_0 - 3s3p\ ^3P_1$ intercombination of Al^+ ion. Column A represents the rates from MCDHF, A' with the NR offset subtracted and A'' with the normalization. Expansions included orbitals up to $n = 7$ but with $l \leq 4$ (g-orbitals). The optimization strategy is defined by the eigenstates and corresponding weights.

	ΔE^R	ΔE^{NR}	Matrix Element		Transition Rate (s^{-1})			Optimization Parameters	
			M^R	M^{NR}	A	A'	A''	Eigenstate	Weight
I	37452	37240	-1.5770(-5)	1.9821(-7)	2845	2917	3083	$^3P_{0,1,2}^o$	2J+1
II	37511	37302	-1.6124(-5)	3.5391(-8)	2979	2992	3076	$^3P_{0,1,2}^o, ^1P_1^o$	2J+1
III	37514	37300	-1.6898(-5)	-7.4711(-7)	3272	2987	3071	$^3P_{0,1,2}^o, ^1P_1^o$	1
IV	37454	37244	-1.6495(-5)	-3.2778(-7)	3113	2990	3061	$^3P_1^o, ^1P_1^o$	1
V	37543	37329	-1.6452(-5)	-2.4333(-7)	3104	3012	3067	$^3P_1^o, ^1P_1^o$	1

approximate manner. Since codes have been refined and computers are more powerful, we decided to re-investigate the sequence. There also were major discrepancies with experiment. In this case, various optimization schemes were investigated. In particular, the idea proposed by Kim *et al*[7] that calculations should be corrected for an incorrect non-relativistic limit, was incorporated along with adjustments for deviations of the 3P_1 and 1P_1 separation. With these adjustments, the different strategies predicted transition rates that differed by only 0.7% whereas the *ab initio* data differed by 7%. The most reliable, unadjusted strategy was then applied for other members of the sequence. These results are shown in Table 1. The strategy with the smallest non-relativistic offset is strategy II which simultaneously optimizes on four levels and hence is CPU intensive. The strategy with the smallest overall correction (the offset cancels with normalization) is V which also requires the least amount of computation.

3. Basis splines and non-orthogonal orbitals in R-matrix calculations

Non-orthogonal spline methods have been applied to the R-matrix method. One of the main innovations of this approach is that non-orthogonal orbitals place more flexibility at our disposal so that target states can be represented more accurately. The continuum orbitals in the inner region are described in terms of B-splines, because of their excellent numerical properties. Using a Bloch operator, for which an analytic expression in the B-spline basis, is known, a good description of the electron flux through the boundary is obtained while maintaining the Hermiticity of the inner region. The completeness of the B-spline basis ensures that no Buttle correction to the R-matrix elements is required and a lot of computational time may be saved.

In general, the introduction of the non-orthogonal technique into the scattering calculations leads to more time-consuming calculations in comparison with orthogonal orbitals. On the other hand, the non-orthogonal approach allows us to use more compact expansions for target wave functions with the same accuracy. Another advantage is that the correlation of the $N + 1$ electron bound configurations, describing short range interactions, can be introduced naturally with great flexibility in their choice. The present approach is totally free of the problem of pseudo-resonances which arise from an inconsistent description of the scattering and bound parts of the wave function, plaguing many close-coupling calculations in the case of complex atoms.

The effectiveness of the present approach has been demonstrated by exploring the resonance

structure in Li photoionization cross sections [8]. The availability of accurate experimental results enabled the theoretical methods to be evaluated.

Future Plans

We want to continue the spectrum calculation up to at least F-like. In the latter, problems already have been identified in experimental identifications in Ne II which are worse in Na III. The problem lies with the $2p^33d$ levels where the relativistic effects of the various terms of $2p^3$ become stronger and correlation with terms is large.

The `graspVU` codes need to be improved. MCDHF calculations grow rapidly in size and current methods produce large amounts of data that are stored on disk. In order to be able to deal efficiently with complex, heavy ions, we plan to investigate a revision of the algorithms. At the same time, we will continue to improve our understanding of the factors that are important for accurate MCDHF calculations by performing detailed studies including heavier atoms.

Since the spline approach has been shown to be so effective in scattering calculations and earlier in Rydberg series, we plan to incorporate our latest algorithms to the study of Rydberg series.

References and Recent Publications (* DOE supported research)

1. **Breit-Pauli energy levels, lifetimes and transition data: beryllium-like spectra*, G. Tachiev and C. Froese Fischer, J. Phys. B: Atom. Molec. Phys. **32**, 5805 (1999).
2. **Breit-Pauli energy levels, lifetimes and transition data: boron-like spectra*, G. Tachiev and C. Froese Fischer, J. Phys. B: Atom. Molec. Phys. **33**, 2419 (2000).
3. **The $Mg^+ a 3s \ ^2S_{1/2} - 4p \ ^2P_{3/2,1/2}$ weak transitions revisited*, M. Godefroid and C. Froese Fischer, J. Phys. B: Atom. Molec. Phys. **32** 4467 (1999).
4. **Isotope shift in the oxygen electron affinity*, M. Godefroid and C. Froese Fischer, Phys. Rev. A **60**, R2637 (1999).
5. **On the status and perspectives of MCDF calculations and measurements of transition data in the Be isoelectronic sequence*, P. Jönsson, C. Froese Fischer, and M. Godefroid, J. Phys. B: Atom. Molec. Phys. **31** 3497 (1998).
6. **Multiconfiguration Dirac-hartree-Fock calculations for Be-like intercombination lines revisited*, C. Froese Fischer, Physica Scripta (accepted).
7. *Failure of multiconfiguration Dirac-Fock wave functions in the nonrelativistic limit*, Y.-K. Kim, F. Parente, J.P. Marques, P. Indelicato, J.P. Desclaux, Phys. Rev. A **58**, 1885 (1998).
8. **The use of basis splines and non-orthogonal orbitals in R-matrix calculations: application to Li photoionization* O. Zatsarinny and C. Froese Fischer, J. Phys. B: Atom. Molec. Phys. **33**, 3113 (2000).

Research Summaries

**(multi-PI programs,
alphabetical by institution)**

Structure and Collisions with Few-Electron Ions

R. W. Dunford and E. P. Kanter
Argonne National Laboratory, Argonne, Illinois 60439

Dunford@anl.gov , Kanter@anl.gov

Program Scope:

This is an experimental program focused on understanding the atomic physics of highly charged ions. Experiments on atomic structure are done to provide tests of QED and relativistic many-body theory in a regime where both electron correlations and relativistic effects are simultaneously important. In addition, atomic collision experiments are carried out to provide data, which are needed, for applications to laboratory and astrophysical plasmas. This work is done in collaboration with scientists in the US, Germany and Poland. Experiments utilize both the ATLAS heavy-ion accelerator at Argonne and the heavy-ion synchrotron SIS at the GSI laboratory in Germany. Recently, the Lamb Shifts in Ar^{17+} and U^{91+} have been measured and a study has been made of two-photon decay in He-like ions at both intermediate and high nuclear charge. We have also studied excitation of highly stripped ions in ion-atom collisions and made a comparison of excitation mechanisms.

I. K-shell Excitation of He-like Ions

R. W. Dunford, E. P. Kanter, Th. Stöhlker^b, H. G. Berry^c, S. Cheng^a, L. J. Curtis^a, A. E. Livingston^c, and P. H. Mokler^b

Progress and Future Plans:

Coulomb excitation is an important mechanism leading to the production of characteristic projectile photons in collisions of fast charged particles with atomic targets. This has been a neglected area of the field of atomic collision physics. In particular, little information is available for state-specific excitation in the intermediate energy regime where the orbital velocity of the projectile electron is similar to the velocity of the ion. We are studying projectile excitation at intermediate energies at ATLAS using both foil and gas targets.

Initial measurements of the cross sections for excitation from the ground state of He-like Ni ions to the $n=2$ excited states have recently been completed. Identification of final states produced in the collisions was done by a combination of low-resolution x-ray spectroscopy using Si(Li) detectors and measurements of the lifetimes of the excited states. The results show that direct excitation to the triplet He-like states is important in excitation by both gas and foil targets. This is significant since excitation to this level from the $1s2s\ ^1S_0$ ground state requires a spin flip and is forbidden in the lowest order theories currently available.

In the future we plan to study excitation in both ^{61}Ni and ^{58}Ni in order to resolve an ambiguity between the 3P_0 and the 3S_1 states which have indistinguishable lifetimes in ^{58}Ni . The isotope ^{61}Ni has a nuclear spin and the lifetime of the He-like $1s2p\ ^3P_0$ state in this system is shortened by the hyperfine interaction. By comparing data taken with the

two isotopes, information about Coulomb excitation may be obtained for both the $1s2p\ ^3P_0$ and the $1s2s\ ^3S_1$ states.

II. Measurement of the $1s$ Lamb shift in Hydrogenlike U^{91+} using Cooled, Decelerated Ions

Th. Stöhlker^b, P. H. Mokler^b, F. Bosch^b, R. W. Dunford, F. Franzke^b, O. Klepper^b, C. Kozhuharov^b, T. Ludziejewski^b, Z. Stachura^f, P. Swiat^g, and A. Warczak^g

Progress and Future Plans:

One of the frontiers in testing quantum electrodynamics (QED) is the study of electrons in intense electromagnetic fields. The important experiment is the measurement of the $1s$ Lamb shift in the most highly-charged, one-electron ion available in the laboratory U^{91+} . This is a relativistic system containing high momentum components and the electric field strength begins to approach the critical value for the spontaneous emission of electron-positron pairs. All of this makes it ideal for testing the limits of our understanding of bound state QED. Although QED has had tremendous success in describing electrons in weak fields, it has not been as well tested in the limit of high field strengths [1].

Experiments have been done at the gas jet of the storage ring ESR at GSI Darmstadt to measure the energies of the Lyman- α lines resulting from electron capture by bare ions. These measurements directly determine the $1s$ Lamb. The high circulating currents of cooled ions available at the storage ring provides the optimum conditions for precision spectroscopy. The main limitation in previous experiments was the uncertainty in the correction for the Doppler effect. The correction is large because the ions are stripped at relatively high energy (e.g. 360 MeV/u) in order to obtain the bare charge state. A significant reduction in the Doppler correction is possible if the ions are decelerated after stripping. We have completed the first Lamb shift measurement to utilize the deceleration capability of the ESR storage ring. The experiment achieved an uncertainty of 13 eV. The significance of this measurement is that it demonstrates a procedure for handling the Doppler problem which will ultimately allow experiments with a precision at the 1 eV level. This is comparable to the uncertainty in the theoretical results for U^{91+} due to uncalculated terms in the two-loop self-energy contribution [2]. Note that the theoretical uncertainty from the finite nuclear size correction for uranium (about 0.1 eV [2]) is insignificant at this level of precision. The future goal of this work is to perform experiments which combine use of the deceleration capability and high resolution devices such as crystal spectrometers or bolometers.

[1] P. J. Mohr, G. Plunien, and G. Soff, Phys. Rep. **293**, 227 (1998).

[2] T. Beier, P. J. Mohr, H. Persson, G. Plunien, M. Greiner, and G. Soff, Phys. Lett. A **236**, 329 (1997).

III. Two-photon decay

R. W. Dunford, E. P. Kanter, H. G. Berry^d, A. E. Livingston^d, S. Cheng^b, and L. Curtis^b

Progress and Future Plans:

A measurement of the exact shape of the continuum spectrum from two-photon decay of H- or He-like ions tests our understanding of the entire structure of these ions since the theory requires a sum over a complete set of intermediate states and both energy levels and wavefunctions must be understood. Fully relativistic calculations for two-photon decay in He-like ions have recently been performed by Derevianko and Johnson which show a marked dependence of the continuum shape on nuclear charge. We are studying this change by comparing the shapes of two-photon decay at intermediate nuclear charge Z in He-like Ni ($Z=28$) and at high- Z in the region of He-like Au and U. The Ni experiments have been carried out at the ATLAS accelerator and the high- Z experiments have been done using the SIS facility at GSI in Germany.

In the ATLAS experiment, two-photon decays were measured in both H-like and He-like nickel during the same run, switching between the two ions several times during the experiment. Since the continuum shape in the two-photon decay of the $2^2S_{1/2}$ level in H-like Ni is known precisely, this served as an on-line calibration of the spectral efficiency of the detection system used. The nickel experiment has demonstrated that high precision measurements of two-photon spectral shapes at intermediate Z are possible using the technique of comparing the shapes of H-like and He-like two-photon decays but we have not yet achieved our goal of obtaining sensitivity to the relativistic corrections at medium- Z . In the future we will make an improved measurement of the Ni two-photon continuum using improved detectors and electronics which will provide sensitivity down to lower x-ray energies.

At GSI, preliminary results have been obtained in for the two-photon decay of He-like Au ions using the SIS facility. In the future, we plan an improved version of this experiment which would run for a significantly longer time, provide an increase in the sensitivity for low energy photons, and provide better characterization of the detector efficiencies. We will also investigate two-photon decay of the 2^3P_0 level in He-like Uranium. This work aims to provide the first measurement of the E1M1 decay mode of the 2^3P_0 level in He-like ions.

^aUniversity of Toledo, ^bGSI, Darmstadt, Germany, ^cUniversity of Notre Dame, ^dSoltan Institute, Swierk, Poland, ^eInstitute for Nuclear Research, Debrecen, Hungary, ^fInstitute for Nuclear Physics, Cracow, Poland, ^gJagiellonian University, Cracow, Poland

Publications 1998 - 2000

Interference Between Electric and Magnetic Amplitudes for K-Shell Excitation of High- Z H-like Projectiles

T. Stöhlker, D. C. Ionescu, P. Rymuza, F. Bosch, H. Geissel, C. Kozhuharov, T. Zudziejewski, P. H. Mokler, C. Scheidenberger, Z. Stachura, A. Warczak, and R. W. Dunford
Phys. Lett. A **238**, 43-48, (1998).

K-shell Excitation Studied for H- and He-like Bismuth Ions in Collisions with Low- Z Target Atoms

T. Stöhlker, D. C. Ionescu, P. Rymuza, F. Bosch, H. Geissel, C. Kozhuharov, T. Ludziejewski, P. H. Mokler, C. Scheidenberger, Z. Stachura, A. Warczak, and R. W. Dunford
Phys. Rev. A **57**, 845-854, (1998).

Charge-Exchange Cross Sections and Beam Lifetimes for Stored and Decelerated Bare Uranium Ions

- T. Stöhlker, T. Ludziejewski, H. Reich, F. Bosch, R. W. Dunford, J. Eichler, B. Franzke, C. Kozhuharov, G. Menzel, P. Mokler, F. Nolden, P. Rymuza, Z. Stachura, M. Steck, P. Swiat, A. Warczak, and T. Winkler
Phys. Rev. A **58**, 2043-2050, (1998).
- Electron Bremsstrahlung in Collisions of 223 MeV/u He-like Uranium Ions with Gaseous Targets
 T. Ludziejewski, T. Stöhlker, S. Keller, H. Beyer, F. Bosch, O. Brinzaescu, R. W. Dunford, B. Franzke, C. Kozhuharov, D. Liesen, A. E. Livingston, G. Menzel, J. Meier, P. H. Mokler, H. Reich, P. Rymuza, Z. Stachura, M. Steck, L. Stenner, P. Swiat, and A. Warczak
J. Phys. B **31**, 2601-2609, (1998).
- Lifetime of the $3p^2P_{3/2}$ Level in Sodiumlike Bromine (Br XXV)
 A. Vasilyev, E. Jasper, H. G. Berry, A. E. Livingston, L. J. Curtis, S. Cheng, and R. W. Dunford
Phys. Rev. A **58**, 732-735, (1998).
- The Two-Photon Decay in Helium-Like Gold
 H. W. Schäffer, R. W. Dunford, C. Kozhuharov, A. Krämer, T. Ludziejewski, P. H. Mokler, H.-T. Prinz, P. Rymuza, L. Sarkadi, T. Stöhlker, P. Swiat, and A. Warczak
Hyperfine Interactions **114**, 49-53, (1998).
- Higher Order Photon Transitions in H-like and He-like Ions
 R. W. Dunford, E. P. Kanter, H. W. Schäffer, P. H. Mokler, H. B. Berry, A. E. Livingston, S. Cheng, and L. J. Curtis
Physica Scripta **T80**, 143-144, (1999).
- Measurement of the Two-Photon Spectral Distribution from Decay of the $1s2s^1S_0$ level in Heliumlike Nickel
 H. W. Schäffer, R. W. Dunford, E. P. Kanter, S. Cheng, L. J. Curtis, A. E. Livingston, and P. H. Mokler
Phys. Rev. A **59**, 245-250, (1999).
- Angular Distribution Studies for the Time-Reversed Photoionization Process in Hydrogenlike Uranium: The Identification of Spin-Flip Transitions
 T. Stöhlker, T. Ludziejewski, F. Bosch, R. W. Dunford, C. Kozhuharov, P. H. Mokler, H. F. Beyer, O. Brinzaescu, B. Franzke, J. Eichler, A. Griegal, S. Hagmann, A. Ichihara, A. Krämer, J. Lekki, D. Liesen, F. Nolden, H. Reich, P. Rymuza, Z. Stachura, M. Steck, P. Swiat, and A. Warczak
Phys. Rev. Lett. **82**, 3232-3235, (1999).
- Two-Photon Decay in Strong Central Fields Observed for the Case of He-Like Gold
 H. W. Schäffer, P. H. Mokler, R. W. Dunford, C. Kozhuharov, A. Krämer, A. E. Livingston, T. Ludziejewski, H.-T. Prinz, P. Rymuza, L. Sarkadi, Z. Stachura, T. Stöhlker, P. Swiat, and A. Warczak
Phys. Lett. A **260**, 489-494, (1999).
- Evolution of Beam-Foil-Excited Rydberg States at Femtosecond Time Scales
 E. P. Kanter, R. W. Dunford, D. S. Gemmell, M. Jung, T. LeBrun, K. E. Rehm, and L. Young
Phys. Rev. A **61**, 042708, 1-5 (2000).
- Simultaneous Excitation and Ionization of He-like Uranium Ions in Relativistic Collisions with Gaseous Targets
 T. Ludziejewski, T. Stöhlker, D. C. Ionescu, P. Rymuza, H. Beyer, F. Bosch, C. Kozhuharov, A. Krämer, D. Liesen, P. H. Mokler, Z. Stachura, P. Swiat, A. Warczak, and R. W. Dunford
Phys Rev A **61**, 052706, 1-9 (2000).

X-ray Interactions with Atoms and Molecules

R. W. Dunford, E. P. Kanter, B. Krässig, S. H. Southworth, L. Young
Argonne National Laboratory, Argonne, IL 60439

dunford@anl.gov, kanter@anl.gov, kraessig@anl.gov, southworth@anl.gov, young@anl.gov

Program Scope: We seek to establish a fundamental and quantitative understanding of x-ray interactions with free atoms and molecules. We have explored the broad energy range where the dominant interaction evolves from photoabsorption to scattering, with careful attention to regions near resonances and thresholds. The focus has been on understanding the limitations of theory, in particular the validity of the independent particle approximation and the role of multipole effects. In these studies, we have found significant uncertainties (up to 10%) in basic quantities such as Rayleigh scattering and photoabsorption cross sections even at photon energies far from thresholds and resonances. Armed with a basic understanding of weak-field x-ray atom interactions, we are now planning to move into the strong-field regime and are developing laser-prepared targets for such studies.

Forward-Backward Photoelectron Asymmetries of Atoms and Molecules

B. Krässig, S. H. Southworth, R. W. Dunford, E. P. Kanter, and L. Young

Photoionization transition amplitudes due to electric-quadrupole (E2) and higher-order photon-atom interactions beyond electric-dipole (E1) are manifested in photoelectron angular distributions through interference terms such as E1·E2. The interference terms give rise to angular distributions which are forward-backward asymmetric with respect to the photon propagation vector \mathbf{k} . Forward-backward asymmetries were observed in early x-ray photoionization experiments and understood to vary simply with photoelectron velocity v as v/c according to Born-approximation calculations. In modern theoretical treatments, transition amplitudes for E1, E2, ... interactions are calculated explicitly, and forward-backward asymmetries are predicted to exhibit interesting variations with atomic number and subshell which persist at threshold. To confirm these predictions, we measured forward-backward asymmetries of rare gases using 2-5 keV x-rays at Brookhaven's NSLS [1]. Other groups have recently studied atoms and molecules using soft x-rays, valence-shell autoionizing resonances, and atoms adsorbed on crystalline surfaces.

We have extended our measurements on rare gases to deeper subshells using 4-19 keV x-rays at Argonne's APS. The new experiments have focused on variations near threshold and the search for interchannel-coupling effects. We have also developed an advanced version of our spectrometer system in which four parallel-plate analyzers are positioned at "double-magic" angles with respect to \mathbf{k} and the x-ray polarization vector $\boldsymbol{\epsilon}$. Forward-backward asymmetries can be determined from the photoelectron intensities recorded simultaneously at the four angles, greatly increasing detection efficiency and reducing systematic errors.

Ionization of helium with keV x-rays

B. Krässig

The ionization of helium by x-rays with energies above a few keV can proceed either by photoabsorption or by Compton (inelastic) scattering. To date there are no direct experimental determinations of the cross sections of either one of these two processes. The existing measurements refer to the attenuation cross section, which is the *sum* of these two contributions plus the contribution of Rayleigh (elastic) scattering. We extracted the *ratio* of cross sections for Compton scattering and photoabsorption from the data of a COLTRIMS experiment originally designed to study double ionization in Compton scattering [cf. Pub 5]. The extraction of the photoabsorption contribution involved careful analysis of the distortions in the imaging of the COLTRIMS instrument in order to identify the nondipolar angular distributions in the ion recoil momenta. Results for the cross section ratio of Compton scattering to photoabsorption were obtained for 7, 8, 10, 13, and 16 keV with 5% uncertainty margins. The comparison with published theoretical results reveals discrepancies with some works greater than this margin, particularly for the photoabsorption cross section. For the Compton cross section the discrepancies are smaller. Even at the lower end of our energy range no indication is to be seen that would point to a failing of the impulse approximation used in some of the Compton calculations. A continuation of these measurements down to 2-3 keV x ray energy is therefore highly desirable.

Double K photoionization of heavy atoms

R. W. Dunford, D.S. Gemmell, E. P. Kanter, B. Krässig, S. H. Southworth, L. Young

The most basic multielectron process is the complete emptying of an atomic K shell in photoabsorption. We recently demonstrated a relatively simple method to investigate such processes in heavy atoms by the creation of double-K-vacancy states in X-ray photoionization and subsequent detection through the observation of the K-hypersatellite transitions as those states relax. Using hard x-rays provided by the Advanced Photon Source, we unambiguously detected the double K-ionization molybdenum. The presence of these double-hole states is signaled by the observation of $K_{\alpha,\beta}$ hypersatellite fluorescence detected in coincidence with the subsequent satellite transition filling the second vacancy. From these data we deduced the relative probabilities for production of double and single K vacancies by photon impact at 50 keV and reported the most precise measure of that quantity in a heavy atom [cf. Pub 7].

That ratio has been shown to provide an important probe of electron-electron correlations in high-Z atoms where theoretical descriptions must consider those correlations simultaneously with relativity and our results suggest the failure of present theoretical treatments to properly deal with such systems. In order to provide a more definitive test however, it is important to separate the contributions of shake processes from the double ionization yield. Recently, we extended these measurements to Ag ($Z=47$). Because of extensive previous studies of this system produced by the electron capture (EC) decay of ^{109}Cd , the shakeoff contribution is well-known experimentally for the single-electron final state produced in EC. Thus, our photoionization measurements will isolate the effects of the dynamic electron-electron scattering (TS1) term. Measurements were carried out at several energies from the double K-ionization threshold to the region of the expected maximum (from 50-90 keV) in the cross-section and analysis is currently underway. With the higher-energy beams soon available at the BESSRC wiggler, we expect to extend these measurements to much heavier atoms such as Au ($Z=79$) and Pb ($Z=82$) which can provide a new probe of the effects of relativity on inner-shell wave functions and can be compared directly with the time-reversed double K-REC (Radiative Electron Capture) experiments.

Nuclear Excitation by Electronic Transition in ^{189}Os

I. Ahmad, R. W. Dunford, H. Esbensen, D. S. Gemmell, E. P. Kanter,
U. Rütt and S. H. Southworth

Nuclear excitation by electronic transition (NEET) is a rare but fundamental mode of decay of an excited atomic state. It is a process by which the energy of an excited atomic state is transferred via the exchange of a virtual photon into excitation of the atom's nucleus. It can only occur when the atomic and nuclear states have closely matching transition energies and also involve the same changes in spin and parity. The NEET process is characterized by the probability P_{NEET} of the atomic vacancy state decaying by nuclear excitation. A candidate system for the NEET process is ^{189}Os , in which an atomic transition between an initially-excited K-vacancy state and a final M-vacancy state can couple to an excited nuclear state at 69.5 keV. A decay branch of the 69.5 keV state involves a 30.8-keV metastable state with 6-hr half-life which can be counted off-line with low-background Ge detectors.

Various methods have been used to measure P_{NEET} in ^{189}Os by generating K-vacancies and counting the metastable decays. K-vacancies have been produced non-selectively, e.g., by electron impact or bremsstrahlung, and have resulted in a wide range of values of P_{NEET} , over the 10^{-9} to 10^{-6} range. A similar wide range of theoretical values of P_{NEET} has been calculated. We have performed a series of experiments at the Advanced Photon Source using both broad-band and narrow-band xrays to generate K-vacancies in ^{189}Os as well as to produce the 69.5-keV nuclear state by direct photoexcitation. We conclude that all previously reported observations of nuclear excitation in ^{189}Os have been due to direct photoexcitation and that NEET has in fact not been observed [cf. Pub 8]. Our measurements give an upper limit of $P_{\text{NEET}} < 3 \times 10^{-10}$, which is consistent with our own theoretical calculation and that of Tkalya [2].

Development of a Terawatt Laser Facility for Ultrafast Electron Pulses and Xrays

R. A. Crowell, R. W. Dunford, D. J. Gosztola, C. D. Jonah, S. H. Southworth,
A. D. Trifunac, and L. Young

We are developing a terawatt laser facility to be used for ultrafast electron-pulse chemical radiolysis and x-ray physics. For pulsed radiolysis applications, an MeV electron bunch with ≈ 1 nC charge and ≈ 1 ps duration can be produced by focusing the output of a terawatt laser into a He gas jet, as demonstrated by Umstadter *et al.* [3]. The terawatt laser system at the University of Michigan was used to demonstrate that this method is capable of generating sufficient charge to produce a measureable amount of hydrated electrons in liquid water [4]. Since the

electron pulses are synchronized with the laser pulses, ultrafast pump-probe techniques can be applied to the study of the physical and chemical processes induced by ionizing radiation. The terawatt laser system being assembled at Argonne uses three stages of amplification in a configuration similar to those developed in other laboratories [5] to produce an estimated output of ≈ 1 J, 25 fs, 10 Hz, at 800 nm. We also plan to use the laser pulses produced at the second stage of amplification (≈ 75 mJ, 25 fs, 60 Hz, 800 nm) to produce ultrafast soft x-ray pulses by the phase-matched high-harmonic-generation method [6]. These ultrafast x-ray pulses will be used for pump-probe experiments and, if estimated intensities are realized, the study of nonlinear processes at short wavelengths.

Development of a Li MOT for ionization studies

M.T. Huang, L. Zhang, S. Hasegawa, S.H. Southworth, L. Young

The use of laser-cooled atomic targets to investigate ionization dynamics promises unprecedented resolution in kinematically complete experiments involving recoil ions and electrons in coincidence [7]. Photon and charged particle ionization processes have been extensively studied using the COLTRIMS technique with supersonic gas jet targets, particularly He, to elucidate dynamical electron correlation effects. We chose to focus on Li to develop the techniques because the potential of theory to address multielectron effects in complex ionization processes in this three-electron system [8]. Considerable progress has been made in the past year. Direct loading from an atomic beam results in trapped ${}^7\text{Li}$ atoms at a density of $10^{10}/\text{cm}^3$ and temperature of 1 mK. The rapid ballistic expansion of the MOT, as measured by imaging LIF from a probe beam, limits the interaction time for ionization projectiles to a few ns before recapture or reloading is required. Initial studies will be on low energy electron impact ionization cross sections where 80% differences between recent theories [Bray95, Chang95] are not distinguished by earlier measurements. In the future, we plan to use the Li MOT target and recoil ion imaging technique to investigate high-field effects with short wavelength radiation.

Production of Polarized Rare Gas Atoms

R. W. Dunford, D. Yang, L. Young

Rare gases with high nuclear polarization are termed "hyperpolarized" gases. They are important in tests of fundamental symmetries, production of polarized targets, studies of surface interactions and NMR imaging of materials. They are also the basis for a new method of medical imaging of lungs and other organs of the body. Both ${}^3\text{He}$ and ${}^{129}\text{Xe}$ gases are currently used in these applications, but although two methods are used for production of hyperpolarized ${}^3\text{He}$ gas, only one method has been developed so far for ${}^{129}\text{Xe}$: spin exchange with optically-pumped alkali vapors. We are developing a second method for polarizing ${}^{129}\text{Xe}$, which may be more suitable for some of the applications. This technique can also be used to polarize radon gas. The scheme involves two steps, the first is a two-photon excitation to a $5p^56p$ excited state followed by decay to the metastable $5p^56s[3/2]_2$ state. Nuclei of metastable atoms can be efficiently polarized by optical pumping with 882 nm light. Polarization is transferred to ground state atoms via metastability exchange collisions, which conserve the nuclear spin.

As a first step in this project we have been studying methods for producing metastable rare gas atoms. An efficient method of metastable production is important for many applications, but of particular interest at Argonne is the vast enhancement in the overall efficiency of atom trap trace analysis for Kr isotopes. We recently produced metastable Kr atoms using a combination of a Kr resonance lamp and a Ti-sapphire laser to excite the atoms to the metastable ($J=2$) first excited state. The transition sequence is $4p^6\ {}^1S_0 \rightarrow 4p^55s[3/2]_1 \rightarrow 4p^55p[3/2]_2 \rightarrow 4p^55s[3/2]_2$. The first two transitions are driven by the lamp and the laser, respectively, while the third involves spontaneous decay into the metastable state ($5s[3/2]_2$). In the near future we will set up the apparatus required to polarize ${}^{83}\text{Kr}$. We will also develop new methods for measuring the polarization of the atoms using direct optical probes. After developing the methods for Kr gas we will turn attention to polarization of Xe and Rn which are of most interest for the applications.

References:

- [1] M. Jung, B. Krässig, D. S. Gemmell, E. P. Kanter, T. LeBrun, S. H. Southworth, and L. Young, *Phys. Rev. A* **54**, 2127 (1996).
- [2] E. Tkalya, *Nucl. Phys.* **A539**, 209 (1992).
- [3] D. Umstadter, S.-Y. Chen, A. Maksimchuk, G. Mourou, and R. Wagner, *Science* **273**, 472 (1996).
- [4] N. Saleh, K. Flippo, K. Nemoto, D. Umstadter, R. A. Crowell, C. D. Jonah, and A. D. Trifunac, *Rev. Sci. Instrum.* **71**, 2305 (2000).
- [5] S. Backus, C. G. Durfee III, M. M. Murnane, and H. C. Kapteyn, *Rev. Sci. Instrum.* **69**, 1207 (1998).
- [6] A. Rundquist, C. G. Durfee III, Z. Chang, C. Herne, S. Backus, M. M. Murnane, and H. C. Kapteyn, *Science* **280**, 1412 (1998).

- [7] R. Dörner *et al*, Phys. Rep. **330**, 95 (2000).
[8] H. van der Hart and C. Greene, Phys. Rev. Lett. **81**, 4333 (1998).

Publications 1998 - 2000

- [1] Manifestations of Nonlocal Exchange, Correlation, and Dynamic Effects in X-Ray Scattering
M. Jung, R. W. Dunford, D. S. Gemmell, E. P. Kanter, B. Kraessig, T. W. LeBrun, S. H. Southworth, L. Young, J. P. J. Carney, L. LaJohn, R. H. Pratt, and P. M. Bergstrom, Jr.
Phys. Rev. Lett. **81**, 1596-1599 (1998).
- [2] Sulfur K β x-ray emission from carbonyl sulfide: Variations with polarization and excitation energy at the S K threshold
K. E. Miyano, U. Arp, S.H. Southworth, T. E. Meehan, T. R. Walsh, F.P. Larkins
Phys. Rev. A. **57**, 2430-2435 (1998).
- [3] Argon KM photoelectron satellites
S.H. Southworth, T. LeBrun, Y. Azuma, K.G. Dyll
J. Elect. Spec. **94**, 33-38 (1998).
- [4] Absolute triple differential cross sections for photo double ionization of helium - experiment and theory
H. Bräuning, R. Dörner, C.L. Cocke, M.H. Prior, B. Krässig, A.S. Kheifets, I. Bray, A. Bräuning-Demian, K. Carnes, S. Dreuil, V. Mergel, P. Richard, J. Ullrich and H. Schmidt-Böcking
J. Phys. B: At. Mol. Opt. Phys **31**, 5149 (1998).
- [5] Compton double ionization of helium in the region of the cross-section maximum
B. Krässig, R.W. Dunford, D. S. Gemmell, S. Hasegawa, E.P. Kanter, H. Schmidt-Böcking, W. Schmitt, S.H. Southworth, Th. Weber, and L. Young
Phys. Rev. Lett. **83**, 53-56 (1999).
- [6] Radiationless resonant Raman scattering at the Ar K edge
T. LeBrun, S. H. Southworth, G. B. Armen, M. A. MacDonald, and Y. Azuma
Phys. Rev. A **60**, 4667-4672 (1999).
- [7] Double K-vacancy production in molybdenum by x-ray photoionization
E. P. Kanter, R. W. Dunford, B. Krässig, S. H. Southworth
Phys. Rev. Lett. **83**, 508-511 (1999).
- [8] Nuclear Excitation by Electronic Transition in ^{189}Os
I. Ahmad, R. W. Dunford, H. Esbensen, D. S. Gemmell, E. P. Kanter, U. Rütt and S. H. Southworth
Phys. Rev. C **61**, 051304 (2000).
- [9] X-ray Scattering and Fluorescence from Atoms and Molecules
S. H. Southworth, L. Young, E. P. Kanter, and T. LeBrun
In Photoionization and Photodetachment, Advanced Series in Physical Chemistry, Vols. 10A and 10B, Ed. C.-Y. Ng (World Scientific, Singapore 2000).

Atomic Physics with Highly Charged Ions : Low Velocity
J.R.Macdonald Laboratory, Kansas State University, Manhattan, KS 66506
cocke@phys.ksu.edu

The purpose of this program is to investigate the interaction of very slow singly and multiply charged ions with atomic, ionic and molecular targets and with surfaces. The work is carried out using the KSU CRYEBIS, ECR and Ion-Ion facilities. Some, but not all, current projects are described here.

Charge Transfer in Very Slow Collisions between Highly Charged Ions and He (*B. D. DePaola, C. W. Fehrenbach, K. Okuno**, *M. P. Stockli and H. Tawara***) Electron capture processes involving very slow, multiply charged silicon ions are known to play a key role in determining the balance of ions and their abundance in some extraterrestrial plasmas as well as in material science applications. To date, very few experimental and theoretical studies of Si^{q+} collision systems have been reported. Indeed, in the few cases reported in the literature, there are significant discrepancies (two orders of magnitude) between the experimental and theoretical results at thermal energies. In an effort to address this situation, we have measured the one- and two-electron capture cross sections for Si^{q+} ($q = 3, 4$ and 5) ions colliding with He atoms over a few 100 to a few 1000 eV collision energies. We have then used our results to test recent quantum mechanical calculations. The experiment was performed using the recently developed octopole ion beam guide (OPIG) technique which is virtually a copy of the one developed at Tokyo Metropolitan University and brought to the Macdonald Lab through the TMU K-State collaboration. The entire OPIG is floated at the decelerating potential, and the ion-atom collisions take place inside a differentially pumped cell in the interior of the OPIG. An octopole electric field serves to confine the decelerated primary ions as well as the product ions. Initial data have been obtained and experimental improvements to the system are currently under construction.

* Tokyo Metropolitan University, Japan; ** National Institute for Fusion Science, Japan.

Rydberg Targets

Our work with Rydberg atoms is largely motivated by their nearly classical nature. In the limit of very high n , one might expect a Rydberg atom to behave very much like a classical system, both in its interaction with external fields and highly charged projectile ions. The interest is partially in determining just how well one can describe these interactions using classical models. This is important not only on epistemological grounds, but for the very practical reason that while the classical study of these systems is relatively simple, the quantum mechanical treatment is extremely challenging. Thus, experimental results are needed both to validate classical approaches and to provide test cases against which quantum mechanical results may be tested.

1. Collisions of Slow, Highly Charged Ions with Coherent Elliptical State (CES) Rydberg Atoms: Electron Capture as a Function of Principal Quantum Number (*B.D. DePaola, E. Horsdal-Pedersen**) Classically, at low collision velocity total capture cross sections are known to scale with target principal quantum number, n , as $\sigma \propto n^4$. One may arrive at this result *via* many different models, for example, CTMC calculations, the Bohr-Lindhard model, or the classical over-barrier model. However, all these approaches suffer from making simplifying assumptions with respect to the

classical orbits which the transferred electron is presumed to follow. Using CES of lithium, total electron capture cross sections have been measured over a range of principal quantum number from $n = 20$ to 35, while varying the generalized eccentricity and the angle between the projectile beam and the normal to the plane containing the CES. The results indicate that at a scaled projectile velocity of 1.20, the n^4 dependence of the cross section is correct. However, at the higher scaled projectile velocity of 1.68, the scaling with n is closer to n^3 , while existing CTMC calculations at this velocity indicate powers ranging from 3.5 to 4. These results have been submitted for publication.

*Univ. Aarhus; work performed at Univ. of Aarhus.

2. Ion-Rydberg Atom Collisions: Energy Transfer in Charge Exchange (*B. D. DePaola, C. W. Fehrenbach, and S. L. Lundeen**) Charge transfer collisions between an ion of charge q and a highly excited atom having principal quantum number n occur with quite large cross sections approximately $qn^4a_0^2$ for sufficiently low collision velocity. Such collisions are believed to result in a narrow distribution of final states, with the captured electron being bound by approximately the same energy as in the original excited atom. No satisfactory quantum mechanical calculations exist for this process, the most satisfying treatment being CTMC calculations. On the other hand, CTMC is not expected to be valid at very low velocities, and may not accurately predict final n and l distributions on the projectile following charge capture. In order to more severely test theoretical models in ion-Rydberg collisions, it is therefore desirable to make measurements which are differential in as many parameters as possible, including initial and final n and l . In the case of charge transfer cross sections, we have extended previous measurements to include collisions with multiply charged ions, having $q = 1 - 4$. In the case of these investigations, final l quantum numbers were not resolved. However, the distribution of initial target n was expanded to include $n_i = 7 - 18$. Using the same RESIS technique to unambiguously identify the final n_p of the projectile, the focus of this study was to concentrate on the relationship between n_i and n_p , over a range of collision velocities ($v = 0.031, 0.057$ and 0.100 a.u.) and charge states. In general, the data show a clear resonance in the capture cross section to a particular energy state as the binding energy of the Rydberg target is varied. The resonance position differs significantly from the predictions of the classical over-barrier model, and its width becomes very small (0.025 eV) at the lowest velocities studied.

*Colorado State University, Ft. Collins, Colorado

COLTRIMS Measurements of Electron Spectra from Low Energy Ionization of Light Targets (*H. Wolf, W. Wolff, M. Abdallah, E. Edgu and C. L. Cocke*) The purpose of this project is to identify and characterize as cleanly as possible the process whereby a slow charged projectile promotes into the continuum an electron from a neutral target. The projectile velocity is sufficiently low that direct kinematic ionization is forbidden. The experiments are carried out using Cold-Target Recoil Momentum Spectroscopy (COLTRIMS) and done in such a way that full electron momentum images are recorded for experimentally determined vector impact parameters. Our most recent results, reported in publication (1), show that evidence for ionization via a $2p\pi$ - $2p\sigma$ rotational coupling followed by a saddle-like promotion to the continuum, seen previously for a He target, is present even for a molecular hydrogen target. Because theoretical calculations for this process are available only for a true one-electron target, we are attempting to

extend the experimental technique to accommodate an atomic hydrogen target. A Slevin type atomic hydrogen source has been mounted on the COLTRIMS apparatus and initial measurements have been made. It has not yet been possible to isolate the signal from the atomic target, however, due to large backgrounds, work on this problem is in progress.

Non-Coulombic Effects in the Fragmentation of N₂ in Collision with 100 kV/q C⁴⁺

(*I. Ali, R. D. DuBois*, S. Hagmann, C. L. Cocke.*) We have measured the kinetic energy release of the fragments emitted from the dissociation of N₂ in collision with 100 kV/q C⁴⁺. The energy of the fragments is calculated from the measured momentum vectors of both fragments emitted in the dissociation of the diatomic molecule (N₂) using a three dimensional momentum imaging multi-hit detector system. The energy is measured separately for the ion pairs from the dissociation of the molecule into different dissociation channels. For the ion pairs with higher charge states, the position of maxima for the measured energy distributions is higher than the Coulomb energies calculated from the product of the fragment charges divided by the bond length. This behavior contradicts the expectation that the Coulomb-explosion model should work better for more highly stripped molecular fragments as well as quantum chemical *ab initio* calculations.

*Univ. of Missouri-Rolla.

Low-Energy, Highly-Charged Ions Interacting with Surfaces

The interaction of low-energy, charged particles with surfaces plays an important role in many technologies. Highly charged ions can carry a substantial amount of electronic energy which is released in the vicinity of the surface. The area over which this energy is released depends on the recombination processes of the ions especially as to whether the vacancies are filled by X-ray or Auger transitions. These processes can be studied by measuring the X-rays and electrons that are emitted when charged ions impact on different surfaces. Most of the present work has been carried out in a new chamber which allows one to measure absolute emission yields from surfaces that can be cleaned with low-energy Ar ions in a vacuum environment in the range of 0.1 nTorr.

1. X-ray Emission from Highly Charged Ne Ions Striking an Aluminum Surface (*H. Tawara, C. Fehrenbach and M. P. Stockli*) Bare, hydrogen-like, helium-like and Li-like ²²Ne ions were directed onto an Al surface with energies in the range between 0.1 and 1.5 MeV. At these low impact energies one observes a significant X-ray yield only if the impacting ions carry an inner shell vacancy, such as are present in the hydrogen-like and bare Ne ions. The X-ray emission is normally completely dominated by the projectile K-X-rays emitted whenever the inner shell is filled when the ion reaches the surface. However, with increasing impact energy one can clearly observe a small, but growing fraction of K-X-rays from the Al target. As the probability for direct impact ionization is negligible at this energy, the target X-rays are produced after a projectile vacancy is transferred to the target during a close collision. The transfer is caused by the radial coupling between 1sσ and the 2pσ orbitals that form transiently in close collisions from the K-shells of both collision partners. In addition one also observes a continuous band of X-rays which extends well beyond the energies of the characteristic X-rays but with an intensity which decreases approximately exponentially with increasing X-ray energy. This band is caused when vacancies in the transient 2pσ orbital are filled during close

collisions. The rapidly changing binding energies during close collisions induce a collision broadening which allows for the emission of X-rays way beyond the static transition energies. The exponential slope of the observed band scales as expected for collision broadening. A manuscript is in preparation.

2. Emission of Secondary Electrons from a Gold Surface (*J. Krasa^{*}, L. Laska^{*}, D. Fry and M. P. Stockli*) Highly charged ions impacting on surfaces can emit an incredibly large number of secondary electrons. The number of secondary electrons and its dependence on charge state, potential energy, impact-velocity and angle can reveal important information regarding the neutralization- and energy-loss processes, but are also of great importance for the calibration of unsuppressed current measuring devices. The number of secondary electrons emitted from below the surface has to be proportional to the number of secondary electrons generated at a certain depth below the surface and therefore is indirectly proportional to the cosine of the impact angle. The number of electrons emitted above the surface should depend only on the projectile velocity normal to the surface, and therefore depends only weakly on the impact angle as the secondary electron emission depends only weakly on impact velocity. In this experiment the number of emitted electrons per incident ion has been measured for Ta¹¹⁺ through Ta⁴¹⁺ with energies per charge in the range between 15 and 150 keV striking a clean polycrystalline gold surface with impact angle between 0 (normal incidence) and 70 degrees. Fitting the measured data with a two component model allowed the deduction that the majority of electrons (between 50 and 85%) originate from above the surface. The ratio between the electron yield from above the surface and the electron yield from below the surface increases with charge state but decreases with increasing velocity. A manuscript has been submitted for publication. ^{*}Czech Scientific Academy

FIVE RECENT PUBLICATIONS

1. "Observation of a 'Quasi-Molecular' Ionization Window in Low to Intermediate Impact Velocity Collisions of He⁺ Ions with H₂ and He," M. A. Abdallah, W. Wolff, H. E. Wolf, L.F.S. Coelho, C. L. Cocke, and M. Stockli, *Phys. Rev. A* **62**, 012711 (2000).
2. "Gain of Windowless Electron Multipliers 226EM and EMI9643/2B for Highly Charged Ta Ions," J. Krasa, E. Woryna, M.P. Stockli, S. Winecki, and B.P. Walch, *Rev. Sci. Instrum.* **69**, 95-100 (1998).
3. "State-Selective Electron Capture in (0.5-50)-keV/u C⁵⁺-He Collisions Studied by Cold-Target Recoil-Ion Momentum Spectroscopy," E. Y. Kamber, M. A. Abdallah, C. L. Cocke, and M. Stöckli, *Phys. Rev. A* **60**, 2907 (1999).
4. "Micro Channel Plate Gains for Ta¹⁰⁺ - Ta⁴⁴⁺ Ions, Measured in the Energy Range from 3.7 keV/q up to 150.7 keV/q," W. Mróz, D. Fry, M. P. Stöckli, and S. Winecki, *Nucl. Instrum. and Methods* **A437**, 335 (1999).
5. "Capture and Ionization Processes Studied with COLTRIMS," M. A. Abdallah, A. Landers, M. Singh, W. Wolff, H. E. Wolf, E. Y. Kamber, M. Stöckli, and C. L. Cocke, *Nucl. Instruments and Methods in Physics Research B* **154**, 73 (1999).

ATOMIC PHYSICS WITH HIGHLY CHARGED IONS: HIGH VELOCITY
J. R. Macdonald Laboratory, Kansas State University, Manhattan, KS 66506
richard@phys.ksu.edu

The purpose of this program is to investigate the interaction of high velocity multiply charged ions with atomic, and molecular targets. The work is carried out using the tandem Van de Graaff and LINAC accelerators. Some, but not all, current projects are described here.

Superelastic Scattering of Electrons from Metastable Ions

*Patrick Richard, C. P. Bhalla, Peter Zavodszky, *H. Aliabadi, G. Toth, + and J. Tanis#*

*Michigan State University, Ann Arbor, +Kla-Tencor, Bedford, MA, #Western Michigan University, Kalamazoo.

We recently performed an experiment where the superelastic scattering of electrons from ions has been observed by the use of the ion-atom collision technique. Superelastic scattering of electrons can occur by scattering target electrons from a metastable ion beam. This process is the inverse of inelastic scattering [Pub.#1] and gets its name from the fact that the outgoing electron has more energy than the incoming electron. Direct electron superelastic scattering has been observed for atoms and ions with very low states of excitation,¹ but it had not been observed previously for inner shell excitation of highly charged ions. Figure 1 shows the results of our experiment for $F^{7+} + H_2$. The superelastic scattering is from the $1s2s\ ^3S$ metastable component of the F^{7+} beam. The observed superelastic scattering peak is obtained by subtracting the F^{6+} DDCS, modified by the F^{6+} to F^{7+} DDCS enhancement factor, from the F^{7+} DDCS. The continuous background is the tail of the binary encounter peak due to elastic scattering of the target electrons. This observation gives another example of the power of the ion-atom collision method in the study of electron-ion collision processes that are not yet feasible to perform by direct electron-ion collision techniques.

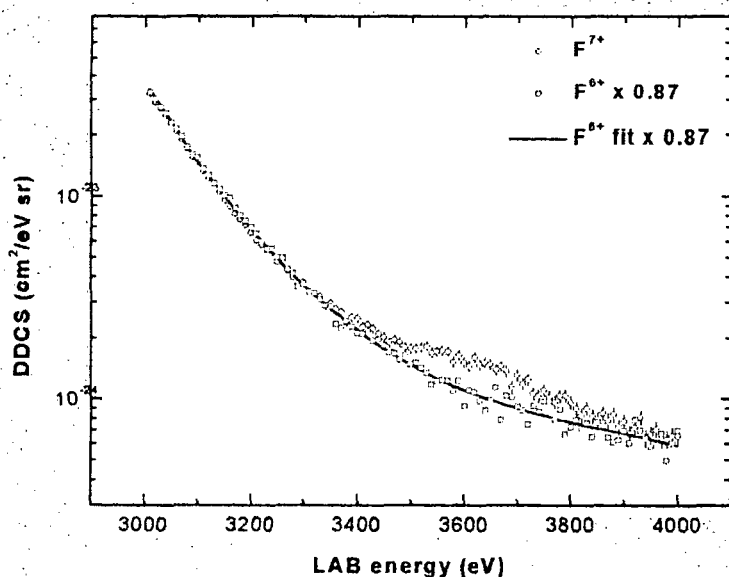


Figure 1. Superelastic scattering of quasi-free electrons in $F^{7+} + H_2$ collisions. DDCS for F^{6+} and $F^{7+} + H_2$ are given with respect to the electron laboratory energy. The difference in the DDCS for the two cases is the superelastic scattering cross section.

¹I. D. Williams, *Physica Scripta T* 73, 121 (1997).

Charge Transfer and Elastic Scattering in Very Slow $H^+ + D(1s)$ “Half” Collisions

*Itzik Ben-Itzhak, Eric Wells, Kevin D. Carnes, Brett D. Esry, Hossein Sadeghpour**

*Harvard Smithsonian, Cambridge

We have studied charge transfer and elastic scattering in the $H^+ + D(1s)$ collision system. This system provides an interesting case study for theorists, since scattering calculations for this system depend on correctly accounting for the difference in nuclear mass in the HD^+ structure calculations. Our aim was to study the collision at energies from about 1 eV down to the charge transfer threshold at 3.7 meV, and below for the elastic channel. So far we have measured down to about 10 meV, much lower in energy than previous charge transfer measurements, and we are working on improving our experiment to meet our original goal. The half collisions are induced by high velocity ions.

To accomplish this goal we are using ground state dissociation (GSD) of HD^+ to measure electron transfer from the $1s\sigma$ to the $2p\sigma$ state. GSD is the process in which a vertical ionization of HD populates the vibrational continuum of $HD^+(1s\sigma)$, which then dissociates into either the $H^+ + D(1s)$ or $D^+ + H(1s)$ final state [Pub.#2]. The latter is populated if charge transfer occurs at an internuclear separation of about 12 a.u., around the avoided crossing. The energy of the resulting H^+ or D^+ fragment is typically less than 300 meV, and is determined for each fragment by imaging its momentum vector using a COLTRIMS-style apparatus.

The measured relative yields of H^+ and D^+ fragments as a function of kinetic energy in the HD^+ center-of-mass frame provide a direct measure of the electron transfer probability from the initial $1s\sigma$ to the final $2p\sigma$ state. This experimental approach provides a probe of very slow collisions. It is important to note, however, that during the GSD process the “avoided crossing” is traversed only once in contrast to twice in a “full” collision. As a result of the “half collision” nature of our experiment, we cannot compare directly to theoretical results available for full collisions. Therefore, we performed coupled channels calculations of the transition probability for both half and full collisions. The experimental results, shown in figure 1, are in good agreement with the half collision calculations except near the charge transfer threshold where better resolution is needed.

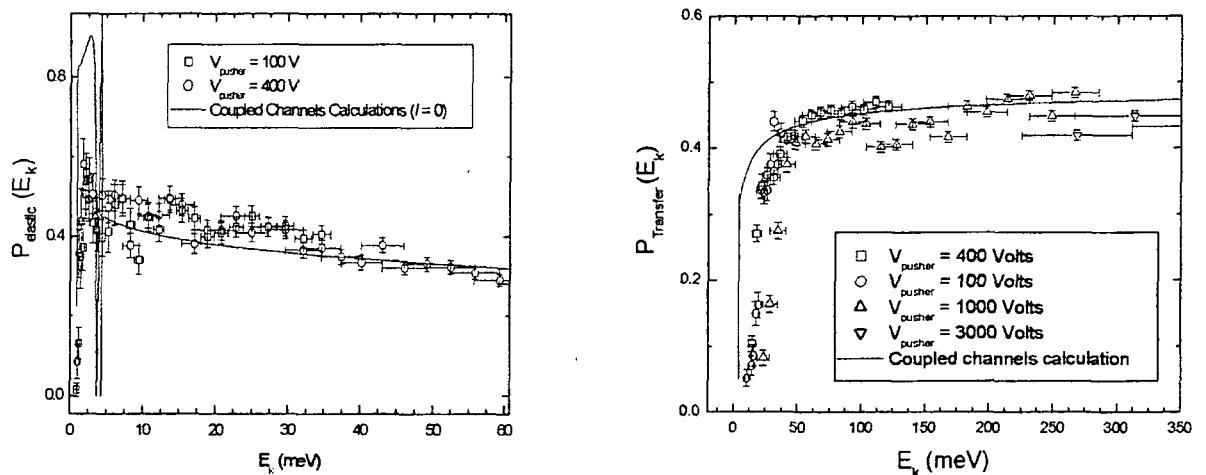
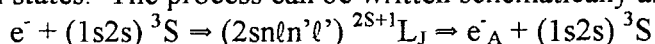


Figure 1: Right: Charge Transfer and Left: Elastic Scattering in $H^+ + D(1s)$ “half” collision.

Elastic Scattering of Electrons from Metastable Ions — Formation of Triply Excited States-Patrick Richard, Chander Bhalla, P. A. Zavodszky,* Tom J. Gray, H. Aliabadi, E. P. Benis,[†] and T.J.M. Zouros[†]

*Western Michigan University, Kalamazoo; [†]University of Crete, Greece

The collision of a $(1s2s) \ ^3S$ metastable ion with a quasi-free target electron can lead to the capture of the electron into an excited state $n\ell$ ($n \geq 2$) while a $1s$ projectile electron can be excited into an $n'\ell'$ ($n' \geq 2$) state, producing a double vacancy in the K-shell, i.e., a hollow ion. The experimental signature of the production of triply excited ionic projectile states is the detection of the electrons resulting from the decay by autoionization of such states. The process can be written schematically as



which can be referred to as resonance elastic scattering or dielectronic excitation plus decay. We have observed $2s \ 2p^2 \ ^2D$ triply excited hollow ionic states in $F^{7+} + e^-$ [1] and $B^{3+} + e^-$ [2] systems.

In the process of this research we have discovered a method of producing ion beams with and without a metastable component. The metastable fraction in an ion beam depends on the ion beam energy at which the stripping of the ion occurs. It is possible to produce a beam of a given energy by stripping the ion either in the terminal of a tandem Van de Graaff accelerator or after acceleration, resulting in beams with different metastable fractions. For a given beam energy, ion stripping in the terminal of the tandem occurs at a lower energy than ion stripping after acceleration and can lead to ion beams with a small metastable component. We came to this interpretation of the metastable components based on the observation that the Auger electron spectra from the beams produced by terminal stripping and post-acceleration stripping are different. This difference in spectra provides us with a unique way of identifying triply excited resonance states formed by the interaction of quasi-free target electrons with metastable ions.

¹"Evidence for Triply Excited Hollow Ionic States," by Zavodszky, *et al.*, DAMOP 1999, Atlanta, GA

²"Production of Triply Excited in Li-like Boron," by Benis, *et al.*, ICPEAC 1999, Sendai, Japan.

The Dynamics of Double Ionization of D_2 by High Velocity Charged Ions: 1 MeV/u Protons and F^{9+}

I. Ali, A. Landers,* J. Tanis,* H. Tawara, P. Richard, S. Hagmann, I. Reiser, E. Wells, T. Osipov, I. Ben-Itzhak, and C. L. Cocke

*Western Michigan University, Kalamazoo

In this work we performed an experiment to study the dynamics of the double ionization process of D_2 in collision with energetic ions ($\geq 1 \text{ MeV/u}$ protons and F^{9+}). The interaction of energetic charged particles and photons with atoms and molecules in collision processes has a common nature. The time and impact parameter dependent equivalent electromagnetic field of the projectile $E(b,t)$ results from the superposition of two pulses propagating along and transversal to the projectile direction. Depending on the charge and velocity of the projectile, these electromagnetic pulses are quantized to one or more virtual photons with particular frequencies. In the collision process of an atom or a molecule (D_2) with high energy charged ions, the virtual photons equivalent to the projectile electromagnetic field can be absorbed or scattered leading to single or multiple

ionization of the target. Combining the momentum recoil ion spectroscopy and multi-hit detection techniques, the full momentum vectors of four particles: both charged fragments and both electrons emitted after the break-up of the molecule are measured. This experiment provides a kinematically complete measurement of the dynamics of the double ionization of the diatomic molecule (D_2) in collision with energetic charged particles.

Orientation Effects of the Fragments Emitted from the Dissociation of N_2 in Collision with 1 MeV/u F^{9+}

S. Hagmann, I. Ali, C. L. Cocke, H. Tawara and P. Richard

The collision process of a fast highly charged projectile (1MeV/u F^{9+}) with a diatomic molecule can lead to the breakup of the molecule and the ejection of energetic fragments. The breakup of the molecule results from double and multiple ionization of the molecule in collision with the projectile leading to the dissociation of the molecule into different dissociation channels with charged fragments that are dependent on the number of electrons lost in the ionization process. The different dissociation channels result from different molecular dissociative states. Detection of the ejected electrons or fragments provides a method to investigate these molecular dissociative states and the dynamics of the dissociation process. In this experiment both fragments emitted from the dissociation of the diatomic molecule are detected, and the full momentum vector of each fragment is measured using a fast position sensitive multi hit detector. The emission angle of the emitted fragments is calculated from the measured momentum vectors for the fragments from the different dissociation channels with different charge states. Orientation effects of the emitted fragments provides an approach to investigate the molecular dissociative states and the dynamics of the dissociation process

Five Recent Publications:

1. "Forward-Backward Asymmetry in the Inelastic Scattering of Electrons from Highly Charged Ions," P. A. Zavodszky, G. Toth, S. R. Grabbe, T.J.M. Zouros, P. Richard, C. P. Bhalla, and J. A. Tanis, *J. Phys. B* **32**, 4425 (1999).
2. "Symmetry Breakdown in Ground State Dissociation of HD^+ ," I. Ben-Itzhak, E. Wells, K. D. Carnes, Vidhya Krishnamurthi, O. L. Weaver, and B. D. Esry, *Phys.Rev. Lett.* **85**, 58 (2000).
3. "Differential Electron-Cu $^{5+}$ Elastic Scattering Cross Sections Extracted from Electron Emission in Ion-Atom Collisions," C. Liao, S. Hagmann, C. P. Bhalla, S. R. Grabbe, C. L. Cocke, and P. Richard, *Phys. Rev. A* **59**, 2773 (1999).
4. "Effect of the Projectile Charge on the Ionization and Excitation of Hydrogen Molecules by Fast Ion Impact," E. Wells, I. Ben-Itzhak, K. D. Carnes, and Vidhya Krishnamurthi, *Phys. Rev. A* **60**, 3734 (1999).
5. "Energy Dependence of Binary Encounter Electron Emission in Collisions of Screened Heavy Bi^{26+} Ions with He Gas Targets," U. Ramm, U. Bechthold, O. Jagutzki, M. Damrau, S. Hagmann, G. Kraft, H. Böttcher, and H. Schmidt-Böcking, *Physica Scripta* **T80**, 341 (1999).

Theory of Structure and Dynamics of Atoms, Ions and Surfaces

J. R. Macdonald Laboratory, Kansas State University, Manhattan, KS 66506

A. Ion-atom collisions Theory

(i) *Ionization (E. Sidky, Clara Illescas and C. D. Lin)*

We have developed a new numerical method of solving the time-dependent Schrödinger equation in momentum space. This method allows us to extract the momentum distributions of the ejected electrons which can be compared directly with measurements carried out using the COLTRIM apparatus. Of particular interest is the so-called saddle point mechanism for ionization at low impact energies. We have obtained the ejected momentum distributions for the ionized electrons in proton-hydrogen atom collisions in the 10-100 keV energy region. In view of the lack of experimental data for this system we have also carried out calculations using the classical trajectory Monte Carlo method. The two results agree fairly well. Thus, the latter was used to analyze the mechanism of ionization at low energies, in particular, the relative importance of saddle point mechanism for ionization and direct ionization where the electrons are ejected to the continuum at small internuclear separations. We demonstrated that the saddle point mechanism plays no role for ionization for collisions above matching velocity. We also showed that it is not possible to deduce the importance of saddle point mechanism based on the measured structure in the longitudinal velocity distribution alone. A report of this work has been accepted by the Physical Review Letters. We comment that an experiment is in progress for measuring the ejected electron spectra for proton-hydrogen collisions at the JRM laboratory.

In the coming year we expect to continue this project, first working on the asymmetric He^{++} on H collisions. Preliminary results indicate that the transverse momentum distributions oscillate with collision energies similar to what was observed in proton-helium collisions [Dormer et al, Phys. Rev. Let. 77,4520 (1996)]. Classical calculations also will be carried out to analyze the role of saddle point mechanism for this system.

(ii) *Ionization cross sections at low energies for antiproton collisions with He (Teck Lee and C. D. Lin)*

We have calculated the ionization cross sections for antiproton collisions with He at low energies using the close-coupling method. By performing a careful calculation we have been able to resolve the earlier discrepancy between experiment and theory. It appears that the experimental data are too large at low energies. Our new results have been confirmed by a few other recent calculations. New experiments are expected to be carried out at CERN when the new antiproton ring becomes available.

(iii) *Charge transfer and other ion-atom collision processes (H. C. Tseng and C. D. Lin)*

We continue to investigate selective ion-atom collisions based on the close-coupling method. The calculations are performed when new experimental data show discrepancy with other calculations. Recent calculations include $\text{C}^{3+}+\text{H}$, $\text{N}^{4+}+\text{H}$ and $\text{B}^{4+}+\text{H}$ collisions where charge transfer cross sections were investigated. In the coming year we will investigate the quenching of $\text{He}^+(2s)$ in collisions with H and He. This system is of interest since the quenching can be due to the collisional excitation of He^+ from 2s to 2p which decays radiatively. It can also occur through electron capture process where doubly excited states are formed and then

autoionize. These two processes have not been investigated theoretically so far, even though experiments are underway.

(iv) *Ion-atom collisions at thermal energies (Teck Lee, A. Igarashi, B.D. Esry and C. D. Lin)*

Recent developments in laser cooling and ion trapping makes it possible to perform ion-atom collisions at subthermal energies in the near future. The traditional approach for treating ion-atom collision is based on the so-called molecular approach or the perturbed stationary state approximation. This approach has fundamental difficulties in that the scattering boundary conditions are not satisfied. Recently we have shown that the hyperspherical approach can be used to perform such calculations for a prototype ion-atom collision without the inherent difficulties of the molecular approach. We have performed the calculation for $D^+ + H(1s)$ charge transfer reaction and showed that it is a practical method for obtaining benchmark results for these elementary reactions. We are currently working on implementing the program to deal with multichannel collisions and to extend the method to include many partial waves such that the calculations can be carried out at higher energies.

B. Atomic Structure and the De-excitation of multiply excited states and of hollow atoms

(i) *Classification of triply excited states of atoms (Toru Morishita and C. D. Lin)*

We have analyzed the angular correlation of the $3l3l'3l''$ triply excited states of a model atom with three electrons confined to the surface of a sphere. By examining the density distribution of the three electrons in the body-frame of the atom, we have partially succeeded in grouping the 64 intrashell $3l3l'3l''$ triply excited states into different groups where within each group the energy levels of the states have the pattern of the rotational multiplet structure of a symmetric top. It is found that mode mixing is not small for the higher excited states in the manifold, but the main features of electron correlation can still be identified. The analysis provides a partial classification of these triply excited states.

(ii) *Radiative and Auger decays of hollow atoms (K. Karim and C. P. Bhalla)*

The Hartree-Fock atomic model has been used to calculate radiative and Auger rates and the X-ray energies for hollow atoms of Ca and Ar with configurations $1s\ 2s^0 2p^n$, $1s2s^1 2p^n$, $1s2s^2 2p^n$ with $n=1-6$. These data are important for understanding the decay of hollow atoms which are formed in ion-surface collisions.

C. Interactions of ions with surfaces, thin films and clusters

(i) *Close-coupling method (B. Bahrim, and U. Thumm)*

For a detailed description of one-electron charge exchange and level hybridization near metal surfaces and thin films, two-center close-coupling calculations were performed. The dynamics of the active electron is spanned by a basis of hydrogenic projectile states in parabolic coordinates and discretized conduction band states. Calculations have been performed to study the hybridization of He^{++} , Li^{3+} and Be^{4+} levels and the formation of surface resonances induced by interactions with an Al surface. The hybridization has also been investigated for the interaction of ions with thin films.

(ii) *Interactions of highly charged ions with surfaces (Jens Ducree, Uwe Thumm)*

The classical over-barrier model (COM) for slow highly charged ion--surface interactions has been very successful for the case of metal surfaces. We have written a new and extended COM code which applies to metal and insulating (ionic crystal) surfaces and found good agreement of our simulated projectile energy gains with experiments on LiF and KI surfaces. For insulator-specific effects, we included local charge accumulations and work function changes at the surface.

(iii) *Soft collisions between highly charged ions and C_{60} (Lotten Hägg and Uwe Thumm)*

With respect to interactions with clusters, we investigated the generation and decay of hollow ions, the simulation of Auger electron and X-ray spectra due to the relaxation of the collisionally produced multiply excited projectiles, the projectile kinetic energy gain, and angular distributions.

D. Hyperspherical approach to few-body systems (Teck Lee, Brett Esry and C. D. Lin)

(i) *Weakly bound molecules*

We have been investigating weakly bound triatomic molecules using hyperspherical coordinates. By employing pair interactions, we solved the three-atom system in hyperspherical coordinates within the adiabatic approximation. From the nature of the hyperspherical potential curve for each system the existence of bound Van der Waals molecules has been investigated. In the last year we have examined several systems such as HeHeH, HeHH, He₂H⁺. These systems have binding energies of the order of degrees Kelvin or less. In our most recent work we searched for the existence of excited states of helium trimers with nonzero total angular momentum. It is known that there are two bound states for ⁴He₃ for J=0 and thus it has been speculated that there are possible J > 0 excited states. We have carried out the hyperspherical calculations recently to show that there are no J > 0 excited states for the helium trimer.

(ii) *Asymmetric three-body systems*

This is a new initiative to be undertaken by Brett Esry if he is admitted into this program. One example of an asymmetric three-body system is the antiproton plus H system. Calculating the protonium formation cross section in this system is a challenging theoretical problem. The formation is expected to occur at high Rydberg states with principal quantum numbers on the order of 30. A quantum solution of such a problem has not been addressed adequately. While it is possible to obtain thousands of potential curves, extracting the collision dynamics from the coupling of these curves is a daunting task. Some diabatization procedures for selected curves have been proposed and procedures for obtaining selected diabatic curves have been envisioned. The goal of this project is to find a general method for attacking the class of problems where high-lying levels are involved.

E. New Time-dependent treatment of continuum phenomena (B. D. Esry, Z. Zhao and C. D. Lin)

The direct solution of the time-dependent Schrödinger equation has become very popular in recent years, from the ionization of atoms by ions to ionization of atoms in a laser field. Practically all of the approaches perform the calculation inside a box since discretization of the

basis set is often used. These methods make accurate treatment of continuum electrons difficult since a quantum mechanical wavepacket spreads and acquires a rapidly oscillating phase as time increases. In a new development, Esry and Sidky have found that most of this "kinetic phase" can be factored out by introducing a scaled coordinate. Moreover, the wavefunction in the scaled coordinate is localized, adding to its appeal for numerical calculations. This approach is now being implemented to study atoms in intense laser fields. We expect to extend the method to ion-atom collisions as well in order to extract the ejected electron momentum distributions. The numerical method discussed in Section A cannot be extended to large internuclear separation because of the problem of representing the fast phase oscillations, and it is hoped that this new approach can be useful for treating ionization in ion-atom collisions as well.

E. Other projects

We expect to continue our close collaboration with our JRM colleagues on problems of their interest where they fall within the domain of our specialty. In particular, electron-ion scattering cross sections will be calculated by Bhalla for collision systems studied by Richard's group. State-selective electron capture cross sections for collisions at low energies with laser-cooled atomic targets will be investigated in conjunction with the experimental effort of DePaola. Similarly, transfer ionization and single electron capture cross sections by multiply charged ions on He will be calculated in conjunction with the improved precise data from Richard's group. The phase-amplitude method will be used to obtain the structure of some molecular ions being investigated by Ben-Ithzak.

Five Selected Publications

1. Toru Morishita and C. D. Lin, "Comprehensive analysis of electron correlations in three-electron atoms," *Phys. Rev. A* **59**, 1835 (1999).
2. Akinori Igarashi and C. D. Lin, "Full ambiguity-free quantum treatment of $D^+ + H(1s)$ charge transfer reactions at low energies." *Phys. Rev. Lett.* **83**, 4041 (1999).
3. T. G. Lee, H. C. Tseng and C. D. Lin, "Evaluation of antiproton impact ionization of He atoms below 40 keV," *Phys. Rev. A* **61**, 062713 (2000),
4. U. Thumm, P. Kürpick, U. Wille, "Size quantization effects in atomic level broadening near thin metallic films," *Phys. Rev.* **B61**, 3067 (2000).
5. P. Zavodszky, G. Toth, S. R. Grabbe, T. Zouros, P. Richard, C. P. Bhalla and J. Tanis, "Forward-backward asymmetry in the elastic scattering of electrons from highly charged ions," *J. Phys.* **B32**, 4425 (1999).

Atomic, Molecular, and Optical Sciences at LBNL

A. Belkacem, H. Gould and M. Prior

Chemical Sciences Division
Lawrence Berkeley National Laboratory
Berkeley, CA 94720
Email: abelkacem@lbl.gov

The goal of the program is to understand the structure and dynamics of atoms and molecules using photons and ions as probes. The current program focussed on studying inner-shell x-ray photo-ionization and photo-excitation of atoms, laser-dressed atoms, and molecules, and on studying molecular orientation effects. The experimental and theoretical efforts are designed to break new ground and to provide basic knowledge that is central to the programmatic goals of the Department of Energy. Unique LBNL facilities such as the Advanced Light Source (ALS), the ECR ion sources at the 88-inch cyclotron, and the National Energy Research Scientific Computing Center (NERSC) are used to perform experimental and computational work. The program makes full use of the unique resources and expertise of the Laboratory in engineering, detector development and computation. The work at the ALS centers on studies of inner-shell photo-ionization and makes use of both synchrotron radiation and the newly constructed 1.5 GeV electron and photon beam line at the ALS booster.

This abstract summarizes progress made in the studies of inner-shell photo-ionization at relativistic energies, x-ray scattering and absorption by atoms and molecules dressed with strong laser fields and measurement of dipole polarizability of cesium. For summaries of other parts of this program refer to the abstracts submitted by M. Prior, "Photon and Heavy Particle Collisions with Aligned Molecules" and by H. Gould, "Slowing, Storing and Cooling Neutral Molecules with Synchrotrons".

I. Photo-ionization and double-ionization at relativistic energies (A. Belkacem and B. Feinberg)

At relativistic energies, the cross section for the atomic photoelectric effect drops off as does the cross section for liberating any bound electron through Compton scattering. However, when the photon energy exceeds twice the rest mass of the electron, ionization may proceed via electron-positron pair creation. We set up a first experiment to study this photo-ionization process, vacuum assisted photo-ionization, at an intense cobalt Source at the Lawrence Berkeley National Laboratory. A beam of 2×10^8 photons/second, and 1.17 MeV and 1.33 MeV energies, is produced through collimation of an intense cobalt source. A signature of vacuum-assisted photo-ionization is given by the simultaneous detection of a K-vacancy and a positron emitted. We measure a ratio of vacuum-assisted photo-ionization to pair production for an Au target to be 2×10^{-3} , a value that is a factor of five larger than the theoretical value. This preliminary number constitutes the first

observation of a new ionization mechanism that is entirely due to the relativistic nature of the photo-ionization process.

We used the same experimental set up to measure the ratio of double K-vacancy to single K-vacancy creation in Au. Using a target dependence measurement technique and extrapolating to very thin targets we obtain a value of $0.5-1 \times 10^{-4}$. This low value is at the limit of sensitivity of this set up and the result should be considered an upper limit. Our experimental value agrees reasonably well with the theoretical values.

In order to study in more detail photo-ionization at higher energies we built a new beam line at the ALS booster ring, branching off the transfer line between the booster and the ALS storage ring. The 7-m long beam line consists of a front-end magnet to extract the 1.5 GeV electron beam, a radiator-target that produces bremsstrahlung photons. We use a high-Z high-density radiator (tungsten) to suppress the emission of low-energy (below 1 MeV) photons through the Landau-Pomeranchuk effect. Downstream from the radiator, a vertical magnet separates the produced photons from the electron beam. The two-beams enter the end-station simultaneously with the electron beam located 5-cm below the photon beam. This configuration allows us to carry electron impact as well as photon impact experiments with the same set up. Both beams are very stable with tunable intensities ranging from 10^3 to 10^{10} electrons/second, 2-3 mm diameter and a repetition rate of 11 Hz. The end-station contains a thin Au target and an electron-positron spectrometer consisting of a permanent magnet and an array of scintillator detectors set in the horizontal plane. The energy of the electrons and positrons is given by the position of the scintillator detector hit. We adjusted the spectrometer to cover the energy range of 10 MeV to 100 MeV, an energy range in which the cross sections of vacuum-assisted photo-ionization, photo-ionization through the Compton effect and photoelectric effect are comparable. A germanium detector, set 2.5 cm from the Au target, is used to detect a K x-ray resulting from the filling of the Au inner-shell vacancy. The first measurement of 1.5 GeV electron impact ionization of Au K-shell yields a value of 25 barns, which is somewhat smaller than the value of 34 barns predicted by theory. However our current beam calibration is not yet reliable to point to a discrepancy theory-experiment. We are currently measuring and analyzing the first data of vacuum-assisted photo-ionization.

II. Laser-synchrotron two-color experiments (T. E. Glover and A. Belkacem)

Multiphoton processes driven by combined synchrotron (x-ray) and laser (optical) radiation provide a basis for novel scientific directions. From a fundamental perspective, synchrotron x-rays can probe unique states of matter formed while a gaseous or solid target is exposed to intense electromagnetic (laser) radiation. We performed a two-color experiment on a Si (111) photo-emission. Experiments are performed at the Advanced Light Source using ~ 700 eV synchrotron light and 800 nm (1 KHz, 100 fs – 40 ps) laser light. The laser intensities were varied from 10^{10} to 10^{14} W/cm². A hemispherical analyzer records x-ray photoelectron spectra (XPS) in the vicinity of the Si 2p photo-emission peak and the arrival time of laser pulses (relative to the x-ray pulses) is varied using an optical delay arm. The ALS is operated in two-bunch mode and electronic gating is used to collect photoelectrons produced by ALS pulses temporally overlapped (or nearly overlapped) with laser pulses. We observe two modifications to the XPS when

pulses are overlapped. First, the Si 2p peak is shifted to lower binding energy (up to 1 eV at high laser intensities). Second, the peak is broadened. These laser-induced modifications are transient. We note two possible mechanisms for the observed effects. First, laser dressing of the continuum can produce a lower amplitude, broader peak (via scattering of laser photons) while also shifting the XPS to lower binding energies (via AC stark shift). A second possibility, the 2p binding energy may be shifted as a result of highly transient excited states of Si created by the laser. Experiments are still in progress to shed some light on the mechanisms involved and possibly distinguish between the two possibilities.

III. Measurements of the dipole polarizability of cesium (H. Gould)

The traditional method of measuring the static dipole polarizabilities of condensable atoms is the E-H gradient balance technique. This balances the deflection due the dipole polarizability, in a transverse electric field gradient. The difficulty of precisely aligning the electric and magnetic field gradients including end effects, and the small deflection, when using thermal beams, limits accuracy.

The longitudinal acceleration of slow cold atoms entering an electric field can be used to measure the dipole polarizability. The energy decrease of the atom exiting the electric field in the atom slowing experiment is given by $\Delta KE = -1/2 \alpha E^2$. Knowledge of the electric field, and the initial and final velocities allows one to determine the polarizability. Since the change in energy of the atom passing through an electric field is path independent, details of the field geometry are much less critical. The feasibility of this method was demonstrated by Maddi, Dinneen and Gould (Phys. Rev. A60, 3882 [1999]). The velocities will be measured, as in the atom slowing experiment, but with careful control of any systematic effects. An accuracy of 0.25% will be attempted for cesium. This would be an improvement of a factor 8 over the best previous measurement which has a 2% accuracy.

To measure the static dipole polarizability of the cesium atom, a new set of precisely machined electric field plates, an accurate voltage supply, and precise timing electronics have been added to the apparatus previously used to measure time-varying electric field gradient slowing and cooling. The electric field plates, made from tungsten coated aluminum, have reached their design electric field of 1×10^7 V/cm with a 0.4-cm gap. Bunches of cold cesium atoms, from the magneto optic trap, launched, by moving molasses, have passed through the plates.

IV. Future plans

Finish the measurements of the cross section of vacuum-assisted photo-ionization for Au and Ag targets. Modify the detection technique for the inner-shell from fluorescence to the detection of Auger electrons to extend the measurement to lower Z-targets. In the next step we plan to use a gas target (Ne, Ar and Xe) and a COLTRIMS to discriminate between the two competing mechanisms (pair creation on the nucleus and pair creation on the electron) that contribute to the vacuum-assisted photo-ionization cross section.

At relativistic energies the transverse fields induced by the electrons on a target are multiplied by the Lorentz factor which in this case is 3×10^3 . Different from the situation at low energies, at relativistic energies, the corresponding magnetic field has the same amplitude as the electric field. Thus the relativistic electron is equivalent to a very intense photon pulse with a duration of 10^{-21} s. We plan to use the COLTRIMS at the 1.5 GeV electron beam line to study the orientation effects in the dissociation of simple molecules by this highly transient and strong transverse field.

We plan to continue the measurements of the modifications of 2p Si photo-electron spectrum as a function of the time delay between the femtosecond laser and the x-ray on the ALS beam line 5.3.1. Parallel to this we will install a gas jet to perform gas phase studies in Argon using the COLTRIMS. These new studies will focus on the modifications of x-ray ionization and x-ray excitation of atoms and molecules dressed with femtosecond high-power laser light.

The measurement of the cesium dipole polarizability will be completed and analyzed. The goal of the experiment is to reach 0.25% accuracy – a factor of eight improvement over the current value. This would test the calculation of the Cs core polarizability to about 10%. Results will be submitted for publication. As this is a sensitive new technique for these measurements, it is expected that other laboratories will pursue the measurement in other trappable atoms. No additional work on atomic dipole polarizabilities is planned at LBNL.

V. Recent publications

- [1] A. Belkacem, D. Dauvergne, B. Feinberg, D. Dauvergne, J. Maddi, and A. Sorensen, “K-shell ionization and double ionization of Au atoms with 1.33 MeV photons”, AIP conference proceedings **506**, “X-ray and inner shell Processes” edited by R. W. Dunford et al, Chicago, Illinois, page 153 (1999).
- [2] J. A. Maddi, T. Dinneen, and H. Gould, “Slowing and Cooling molecules and neutral atoms by time-varying electric-field gradients”, Phys. Rev. A **60**, 3882 (1999).
- [3] D.C. Ionescu, A. Sorensen, and A. Belkacem, “Inner-shell photo-ionization at relativistic energies”, Phys. Rev. A **59**, 3527 (1999).
- [4] D. C. Ionescu and A. Belkacem, “Relativistic collisions of highly charged ions”, Physica Scripta, Vol **80**, 128 (1999)
- [5] A. Belkacem, N. Claytor, T. Dinneen, B. Feinberg, and H. Gould, “Electron capture from pair production by Au⁷⁹⁺ at 10.8 GeV/n”, Phys. Rev. A **58**, 1253 (1998).
- [6] A. Belkacem and A. Sorensen, “Bound-free heavy lepton pair production for photon impact on atomic nuclei”, Phys. Rev. A **57**, 3646 (1998).

Photon and Heavy Particle Collisions with Aligned Molecules

M.H. Prior

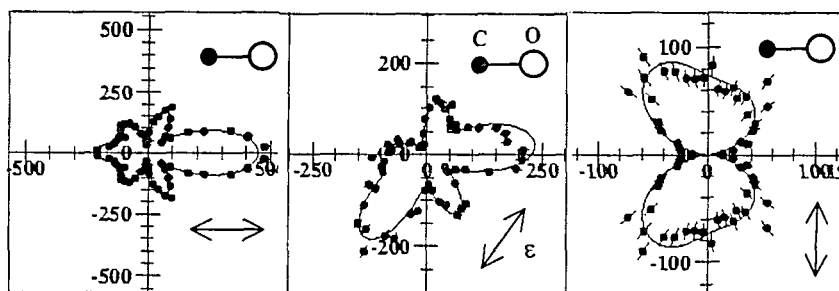
Chemical Sciences Division
MS 88-103
Lawrence Berkeley National Laboratory
Berkeley, CA 94720
E-mail: MHPrior@LBL.GOV

The DOE Atomic, Molecular and Optical Physics program supports studies which "seek to obtain the most accurate and complete fundamental knowledge of the properties and interactions of photons, electrons, atoms, and ions"[†]. This portion of that program performs measurements of unprecedented detail and/or which extend to unexplored species or collision processes. Advanced energy and related technologies, applied plasma environments, planetary and solar atmospheres, involve media wherein many atomic and molecular processes operate simultaneously. Accurate modeling of these environments ultimately must rely upon improved theoretical/computational methods, and the performance of novel and detailed experiments is an essential spur to their development. It is a goal of this program to contribute substantially to that process. A portion of this program is collaborative with colleagues from outside institutions.

[†] Program Descriptions, DOE, ER, BES Summaries of FY 1997 Research in the Chemical Sciences

I. Electron Emission from Core Excited, Fixed in Space CO Molecules

Using the techniques of electron and ion momentum spectroscopy, we have measured the complete emission patterns of core photoelectrons emitted from the C and O atoms for any (and all) relative orientations of the CO molecular axis and the linearly polarization of the incident soft X-ray photons. This has been done for photon energies extending to 30 eV above the K-shell thresholds for both the C and O atoms at beamline 9.3.2 at the LBNL Advanced Light Source. This energy range covers the region of the σ shape resonance in this system, which occurs at about 10 eV photoelectron energy. The emission patterns, when referenced to the molecular frame, show rich structures in their angular variation which reflect the propagation of the photoelectron wave in the two center molecular potential.



Polar plots of carbon K photo-electron emission patterns from oriented CO molecules near the peak of the σ shape resonance (10 eV electron energy). ϵ , is the axis of linear polarization for the photons which propagate normal to the page. The above represent a very small fraction of the results of these measurements, which cover all relative orientations of the molecule and ϵ , and photo electron energies extending to 30 eV; the experiment also made the same measurements for electrons emitted from the O K shell. The scale changes in the panels indicate the prominence of the σ ($\epsilon \parallel$ molecular axis) versus π ($\epsilon \perp$ mol. axis) excitation.

In terms of a multiple scattering view, the intensity at a given angle with respect to the molecular axis is the net result of the addition of a direct wave from the atomic K-shell with waves scattered one or more times from the other atom in the molecule. Our measurements show that the electron emission patterns can be accurately described by a set of real amplitudes and relative phases for excitation of σ and π transitions to electron partial waves with angular momentum ≤ 4 ; the analysis provides the values of these amplitudes and phases. When the analysis is complete, the energy dependence of the amplitudes and phases will be obtained for photoelectron energies up to ~ 30 eV. Accurate and complete knowledge of intramolecular scattering, beyond its intrinsic value as a test of electron wave propagation in multiple centered potentials, can refine the understanding of photoabsorption and electron emission diagnostics of materials and surfaces. The various near edge diagnostic methods used in solid and surface analysis (XAFS; NEXAFS, XANES) are manifestations of the electron wave propagation in a situation with many more scatterers than in a diatomic system such as CO investigated here. The observation of multiple scattering effects in the outgoing propagation of a core photoelectron from one of the atoms in CO thus represents a basic and reduced example of a phenomenon widely applied to materials and surface analysis. Theoretical approaches which successfully deal with the CO system can have application to these important and more complex environments. This work is collaborative with groups from U. Frankfurt, Kansas State Univ. and Western Michigan U.

II. Double Ionization of D₂ in Intense Laser Fields

The behavior of simple molecules exposed to intense femto-second laser pulses includes the dynamics of electron motion in the combined molecular and photon fields and the nuclear motion in the molecular potentials modified ("dressed") by the intense field. Studies of H₂ (or D₂) in high intensity optical fields has revealed interesting phenomena, such as "bond softening", where breakup of the molecule occurs via avoided crossings in the manifold of field dressed molecular potentials. Or the phenomena of enhanced ionization at inter-nuclear separations much outside the equilibrium values. An intense linearly polarized field may also orient the molecule along the polarization axis, yielding highly non-isotropic distributions of ionization products. Nearly all of the experimental studies of double ionization of H₂ (or D₂) molecules in intense laser fields, have been rationalized in terms of a sequential process wherein the molecule is first singly ionized, and then ionized again in a second step as the singly charged molecule, separating on a dissociative curve, passes through inter-nuclear separations where enhanced ionization occurs. Often concentration is upon the second step in the process and, although a neutral molecule is the target, the studies are often labeled as ionization of H₂⁺ (or D₂⁺) ions. This situation contrasts markedly with studies of the double ionization of He, where a direct non-sequential process dominates for all except the highest laser intensities.

We have utilized the technique of coincident momentum spectroscopy to measure, for the first time, the momentum of both D⁺ ions following the double ionization of D₂ by 790 nm 100-200 fs pulses. Our results reveal a new channel for the double ionization of D₂, where the two ions have substantially more energy (5 eV or more each) than seen in the previously observed enhanced ionization process (where the ions have about 2.5 eV each). Furthermore the measurement of the complete distribution of the ion momenta into 4 π solid angle, reveals that this new channel shows a very broad, nearly isotropic, distribution. This contrasts strongly with the more commonly observed distribution from the enhanced ionization mechanism, which is strongly peaked along the laser polarization axis. We have made these observations for laser field intensities ranging from 0.65 to 8.5 x 10¹⁴ Watts/cm². As the field intensity increases, the

energy distribution of the ions in the new channel changes from one with a peak at about 5 eV/ion, to one which is much broader with ion energies ranging up to 10 eV/ion or more. It is important to stress that this new channel, which is substantially weaker than the enhanced ionization channel, could not have been observed without utilization of the high efficiency coincident momentum spectroscopy technique. The mechanism of the new channel is yet to be determined, but may reflect a direct, non-sequential process, or the effects of rescattering of electrons created by single ionization early in the laser pulse. André Staudte (graduate student, U. Frankfurt), C.L. Cocke (on sabbatical leave from KSU), C. Ray (LBNL CSD), H. HW Chong, (LBNL MSD), T.E. Glover (LBNL MSD), R. Schoenlein (LBNL MSD), A. Belkacem (LBNL CSD) and the PI participated in this work.

III. Molecular Alignment Dependence in Slow Charge Transfer Collisions.

The ability to determine the sensitivity of a bi-molecular interaction to the relative orientation of the partners is a level of experimental description rarely achieved but which challenges understanding at the finest scale of detail. In the past we have performed measurements of charge transfer in molecular ion-atom ($\text{HeH}^+ + \text{He}$) and ion-molecule ($\text{He}^{++} + \text{D}_2$) collisions which displayed the dependence of the transfer probability on the momentum transfer and the orientation of the molecular partner. During the last FY we began to explore a molecular ion-molecule collision where the relative orientation of the two molecular axis would be determined. In the system $\text{HeH}^+ + \text{D}_2$, charge transfer from, and ionization of the D_2 yields neutral HeH and two D^+ ions. Detection of the He and H from the rapidly dissociating HeH and the two D^+ ions in 4-fold coincidence on two position sensitive detectors yields the orientation of the two molecules at the time of transfer and ionization. Charge transfer with excitation of the D_2^+ ion to a dissociating state will also reveal the molecular orientations via the three fold coincident He, H and D^+ products. Measurements sensitive to these processes have been made and are in process of analysis. André Staudte, Graduate Student from U. Frankfurt and C.L. Cocke, on sabbatical leave from KSU, and the PI worked on this project.

IV. Future activity

Study of core electron photo emission from oriented molecular systems will continue at the LBNL Advanced Light Source. This will be extended to more complex systems such as acetylene (C_2H_2), ethylene (C_2H_4) and ethane (C_2H_6) to study the effect of increased CC bond length on the C K-photoelectron emission patterns and their variation across a shape resonance in these systems. In calendar 2001, single photon double ionization of He by circularly polarized light will be studied at the elliptically polarized undulator beamline (BL 4.0) at the ALS. This will allow definitive measurements of the circular dichroism in this simple atomic system and resolve conflicts between existing measurements and theoretical predictions. Intense laser field studies will continue along two paths, one will mount a momentum spectrometer assembly at the new femtosecond beamline at the ALS to study K-shell photo emission from targets dressed by synchronous, intense laser fields (This work in collaboration with co PI's A. Belkacem and T.E. Glover, see the abstract of A. Belkacem). Either at the same installation or utilizing a separate laser system, extensions of previous measurements will be made to further describe the new channel observed in the double ionization of D_2 by intense fields. This will include measurement of the electron momenta and the use of circularly polarized laser fields, to modify the strength of electron rescattering collisions processes. Evaluation of oriented molecule collision measurements made on the $\text{HeH}^+ + \text{D}_2$ system will be made to determine the feasibility of continued study of this system and to prepare present results for publication.

V. Recent Publications

- [1] W. Wu, M.H. Prior and H. Bräuning
Orientation-dependent Dissociative Charge Transfer
Physical Review A 57, R5 (1998).
- [2] R. Dörner, H. Bräuning, O. Jagutzki, V. Mergel, M. Achler, R. Moshhammer, J. M. Feagin, T. Osipov, A. Bräuning-Demian, L. Spielberger, J.H. McGuire, M.H. Prior, N. Berrah, J. D. Bozek, C.L. Cocke, and H. Schmidt-Böcking
Double Photoionization of Spatially Aligned D₂
Physical Review Letters 81, 5776 (1998).
- [3] H. Bräuning, R. Dörner, C.L. Cocke, M.H. Prior, B. Krässig, A.S. Kheifets, I. Bray, A. Bräuning-Demian, K. Carnes, S. Dreuil, V. Mergel, P. Richard, J. Ullrich, and H. Schmidt-Böcking.
Absolute Triple Differential Cross Sections for Photo Double Ionization of Helium---
Experiment and Theory
Journal of Physics B: At. Mol. Opt. Phys. 31, 5149 (1998).
- [4] R. Dörner, H. Bräuning, J. M. Feagin, V. Mergel, O. Jagutzki, L. Spielberger, T. Vogt, H. Khemliche, M.H. Prior, J. Ullrich, C.L. Cocke, H. Schmidt-Böcking
Photo Double Ionization of He: Fully Differential and Absolute Electronic and Ionic Momentum Distributions
Physical Review A 57, 1074 (1998).
- [5] R. Dörner, V. Mergel, H. Bräuning, M. Achler, T. Weber, Kh. Khayyat, O. Jagutzki, L. Spielberger, J. Ullrich R. Moshhammer, Y. Azuma, M. H. Prior, C. L. Cocke, and H. Schmidt-Böcking
Recoil ion momentum spectroscopy a 'momentum microscope' to view atomic collision dynamics
AIP Conference Proceedings 443, Issue 1, pp. 334-346 (1998)
- [6] H Schmidt-Böcking, V Mergel, R Dörner, H Bräuning, M Achler, L Spielberger, O Jagutzki, T Weber, K. Khayyat, J. Ullrich, CL Cocke, MH Prior, Y Azuma, Y Awaya, T Kambara,
Cold target helium recoil ion momentum imaging: Understanding correlated electron motion in the double ionisation process.
Australian Journal of Physics, 52, 523 (1999).
- [7] JP Briand, V Le Roux, N Bechu, S Dreuil, G Machicoane, M Prior, Z Xie,
The hollow atoms.
Nuclear Instruments & Methods in Physics Research Section B-Beam Interactions with Materials and Atoms, 154, 166 (1999).

Program Title: **Atomic Physics at the LLNL EBIT**

Principal Investigator(s): **Alex Hamza, Peter Beiersdorfer, and Dieter Schneider**

Mailing Address: Lawrence Livermore National Laboratory
P.O. Box 808, L-414
Livermore, CA 94550

E-mail: Hamza1@LLNL.GOV

- **Program Scope or Definition**

The research on ion/surface interactions with slow (~ 3 keV/amu) highly charged ions (up to Th^{80+}) covers the absolute measurements of enhanced emission yields for sputter ions, formation of hollow atoms and their decay dynamics, energy loss studies, highly charged ion driven emission microscopy, and single ion-induced phase transformations in surfaces. Spectroscopic measurements of the ions in the trap provide data on electron-ion and ion-atom interactions as well as accurate transition energies of lines relevant for understanding QED, nuclear magnetization, and the effects of relativity on complex, state-of-the-art atomic calculations.

- **Recent Progress**

Due to the indirect nature of its band gap, bulk silicon is typically a poor photon emitter upon external excitation. However, as the crystal size approaches nanometer scales, the band gap widens due to quantum confinement and may become direct allowing for more efficient photon emission. Phase transformations induced by intense, ultrafast electronic excitation from slow, highly charged ions have produced nanometer-sized structures in silicon. Beams of highly charged ions of various charge state from 20^+ to 69^+ and various kinetic energies from 5 to 14 keV times charge have been utilized to induce this phase transformation in clean, silicon surfaces. The new phase is characterized by *ex situ* photoluminescence from the irradiated area after excitation with laser wavelengths from 379 - 514 nm. Photoluminescence spectra from the exposed areas show emission centered at ~ 540 nm. This is consistent with emission observed from 1-2 nm silicon nanocrystals. A series of sharp lines at 565, 555, and 548 nm are present in the photoluminescence spectrum from areas exposed to Xe^{44+} which are characteristic of an excitonic series in nanometer-sized material. This is the first observation to the authors' knowledge of excitonic structure in nanometer-sized silicon structures.

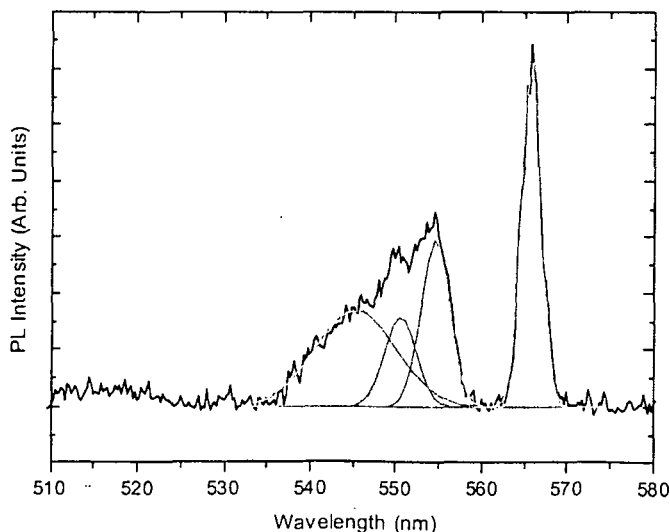


Figure 1. Photoluminescence signal from nanometer-sized silicon features induced via intense ultrafast electronic excitation (Xe^{44+} ion bombardment). Feature at 565 nm and 555 nm wavelength are assigned as the $n=1$ and $n=2$ excitonic states, respectively.

In situ spectroscopy of ion-electron and ion-atom interactions within the trap was carried out for a variety of systems and resulted in dielectronic recombination data involving Ar^{16+} , magnetic sublevel specific electron-impact excitation data for Ti^{20+} , as well as ratios of the triplet to singlet excitation in seven heliumlike ions between Mg^{10+} and Fe^{24+} . Moreover, measurements of the x-ray emission following ion-atom interaction in the trap provided a novel window on charge-exchange processes. The observed spectra revealed the principle quantum number of the captured electron and its angular momentum value. At the low interaction energies studied with our technique (~ 20 eV/amu), statistical assumptions are no longer valid and electrons were shown to be captured in large part into states with angular momentum equal to unity (p states). These states decay directly to the 1s ground state, if a K-shell vacancy is available, as is the case if charge exchange involves a bare or hydrogen-like ion. The resulting x-ray is clearly distinguished in the observed spectrum, as shown in Fig. 2 for the case of Au^{78+} ions interacting with neutral neon atoms. The intensity of this “prompt” x-ray can be compared to theoretical predictions providing a stringent test. Systems studied during the past year extended throughout the entire period table from Ne^{10+} to U^{91+} and revealed surprising deviations from standard predictions.

Our optical spectroscopy of *in situ* ions has yielded the most accurate value of the ground-state transition in a titanium-like ion. Our measurement of W^{52+} was an order of magnitude better than studies carried out by other groups, allowing us to provide a very precise benchmark for theoretical approaches aiming to calculate such a complex ion in the high-Z limit. An effort is now under way to identify and measure the 1s hyperfine transition in hydrogenic thallium. This measurement will provide detailed information on the nuclear structure, especially on how the magnetic fields are distributed within the nucleus.

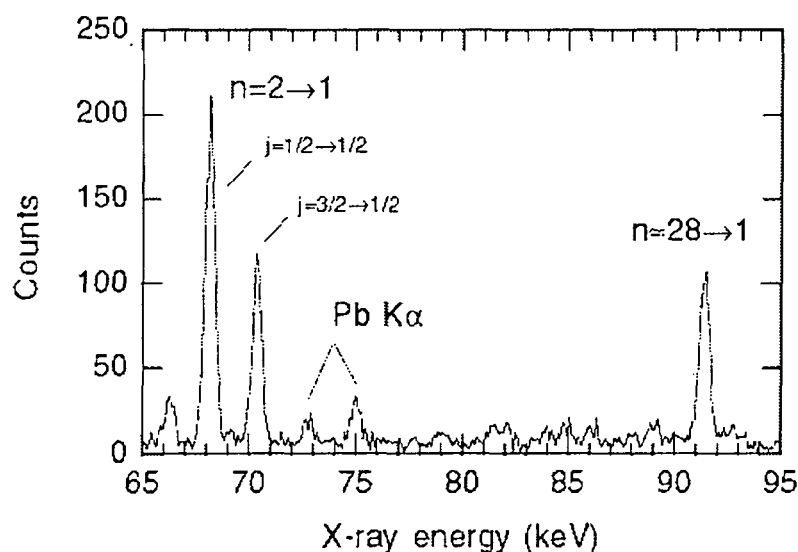


Figure 2. X-ray emission recorded following charge exchange of hydrogen-like Au^{78+} ions with Ne atoms. Prompt deexcitation from the following electron capture into the $n=28$ level as well as $n=2$ to $n=1$ emission is readily discerned. The lead K-shell lines are fluorescent lines and the consequence of the 170 keV electron beam required to make such a high charge state of gold.

• Future Plans

Intense ($>10^{13}$ W/cm²), ultrafast (<10 fs) electronic excitations drive solid surfaces far from equilibrium. The relaxation of the energy imbalance has the capability to transform nanometer-

sized regions to produce novel material properties, i.e. light emitting silicon. We propose to determine the threshold for phase transformation in crystalline, covalent semiconductors due to intense, ultrafast electronic excitation induced by slow, highly charged ions. We further will endeavor to determine the mechanisms for transfer of intense, ultrafast electronic excitation into many-body nuclear motion to form surface structures. The hypothesis that collective electron action (plasmons) mediates the electronic energy transfer will also be probed. A further goal will be to determine the effects of the atomic and electronic structure of the surface on the phenomena (phase transition and secondary particle emission) induced by intense, ultrafast electronic excitation.

The studies of ion-atom interactions will be extended to more complex systems. We will study systems involving ions with an open L-shell and no K-shell vacancy. Our optical measurements will continue to study transitions in complex ions that may enable the development of more accurate calculations. Our focus will remain on the Ti-like isoelectronic sequence, and we intend to complete our measurements of the 1s hyperfine transition in hydrogenic thallium.

- References to publications of DOE OBES sponsored research that have appeared in 1999 and 2000 or that have been accepted for publication.

A. V. Hamza, A. V. Barnes, T. Schenkel, and D. H. Schneider, "Secondary Ion Coincidence in Highly Charged Ion Based Secondary Ion Mass Spectrometry for Process Characterization," *Journal of Vacuum Science and Technology A* **17** (1999) 303.

A. V. Hamza, T. Schenkel, and A. V. Barnes, "Dependence of Cluster Ion Emission from Uranium Oxide Surfaces on the Charge State of the Incident Slow Highly Charged Ion," *European Physical Journal D*, **6** (1999) 83.

A. V. Hamza, A. V. Barnes, E. Magee, T. Schenkel, and D. H. Schneider, "Highly Charged Ion Based Time-of-Flight Emission Microscope," *Reviews of Scientific Instruments*, **71** (2000) 2077.

M. Hattass, T. Schenkel, A. V. Hamza, A. V. Barnes, M. W. Newman, J. W. McDonald, T. Niedermayr, G. Machicoane, and D. H. Schneider, "Charge Equilibration Time in Solids," *Physical Review Letters*, **82** (1999) 4795.

T. Schenkel, A. V. Barnes, T. Niedermayr, M. Hattass, M. W. Newman, G. Machicoane, J. W. McDonald, A. V. Hamza and D. H. Schneider, "Deposition of Potential Energy in Solids by Slow, Highly Charged Ions," *Physical Review Letters*, **83** (1999) 4273.

T. Schenkel, K. J. Wu, H. Li, M. W. Newman, A. V. Barnes, and A. V. Hamza, "Analysis of Sub-Micron Cu-Ta-SiO₂ Structures by Highly Charged Ion SIMS," *Journal of Vacuum Science and Technology, B* **17** (1999) 2331.

T. Schenkel, A. V. Hamza, A. V. Barnes, and D. H. Schneider, "Interaction of Slow, Highly Charged Ions with Surfaces," *Progress in Surface Science* **61** (1999) 23.

T. Schenkel, A. V. Hamza, A. V. Barnes, M. W. Newman, G. Machicoane, T. Niedermayr, J. W. McDonald, D. H. Schneider, K. J. Wu, R. W. Odom, "Surface Analysis by Highly Charged Ion Based Secondary Ion Mass Spectrometry," *Physica Scripta T80* (1999) 73.

- P. Beiersdorfer, G. V. Brown, S. B. Utter, P. Neill, K. J. Reed, A. J. Smith, and R. S. Thoe "Polarization of K-shell X-ray Transitions of Ti^{19+} and Ti^{20+} excited by an Electron Beam," *Physical Review A* **60**, 4156-4159 (1999).
- P. Beiersdorfer, L. Schweikhard, R. Olson, G. V. Brown, S. B. Utter, J. R. Crespo López-Urrutia, and K. Widmann, "X-ray Measurements of Charge Transfer Reaction Involving Cold, Very Highly Charged Ions," *Physica Scripta* **T80**, 121-123 (1999).
- A. S. Shlyaptseva, R. C. Mancini, P. Neill, P. Beiersdorfer, "Polarization Properties of Dielectronic Satellite Lines in the K-shell X-ray Spectra of B-like Fe XXII," *Journal of Physics B* **32**, 1041-1051 (1999).
- A. J. Smith, P. Beiersdorfer, K. J. Reed, A. L. Osterheld, V. Decaux, K. Widmann, and M. H. Chen, "Ratios of $n=3 \rightarrow 1$ Intercombination to Resonance Line Intensities for Heliumlike ions with Intermediate Z-values," *Physical Review A* **62**, 012704 (2000).
- P. Beiersdorfer, G. V. Brown, M.-F. Gu, C. L. Harris, S. M. Kahn, S.-H. Kim, P. A. Neill, D. W. Savin, A. J. Smith, S. B. Utter, and K. L. Wong, "Recent Livermore Excitation and Dielectronic Recombination Measurements for Laboratory and Astrophysical Spectral Modeling," in *Proceedings of the International Seminar on Atomic Processes in Plasmas*, NIFS Proceedings Series No. NIFS-PROC-44 (National Institute for Fusion Studies, Nagoya, Japan 2000), ed. by T. Kato and I. Murakami, p 25-28.
- S. B. Utter, P. Beiersdorfer, and G. V. Brown, "Measurement of an unusual M1 Transition in the Ground State of Ti-like W^{52+} ," *Physical Review A* **61**, 503-506 (2000).
- A. J. Smith, P. Beiersdorfer, K. Widmann, M. H. Chen, and J. H. Scofield, "Measurement of Resonant Strengths for Dielectronic Recombination in Heliumlike Ar^{16+} ," *Physical Review A* (in press).
- P. Beiersdorfer, R. E. Olson, L. Schweikhard, P. Liebisch, G. V. Brown, J. Crespo López-Urrutia, C. L. Harris, P. A. Neill, S. B. Utter, and K. Widmann, "X-Ray Signatures of Charge Transfer Reactions Involving Cold, Very Highly Charged Ions," in "The Physics of Electronic and Atomic Collisions," ed. by Y. Iitkawa et al., AIP Conf. Proc. No. 500 (AIP, New York, 2000), p. 626-635.
- L. Gruber *et al.*, in *Conference on the Application of Accelerators in Research & Industry, Denton, 1998*, edited by J. L. Duggan and I. L. Morgan (AIP Conference Proceedings) **475**, 56 (1999)
- J. Steiger *et al.*, in *Trapped Charged Particles and Fundamental Physics, Asilomar, 1998*, edited by D. H. E. Dubin and D. Schneider (AIP Conference Proceedings) **457**, 284 (1999)
- L. Gruber, J. P. Holder, B. R. Beck, J. Steiger, J. W. McDonald, J. Glassmann, H. DeWitt, D. A. Church, and D. Schneider, "Highly Charged Ion Coulomb Crystallization in Mixed Strongly Coupled Plasmas," accepted to: *Hyperfine Interactions* (1999)
- D. A. Church, D. Schneider, J. Steiger, B. R. Beck, J. P. Holder, G. Weinberg, L. Gruber, D. P. Moehs, and J. McDonald, "Highly-Charged Ions in Traps – Progress and Opportunities," *Physica Scripta*. Vol. **T80**, 148-153 (1999)

ATOMIC AND MOLECULAR PHYSICS AT OAK RIDGE NATIONAL LABORATORY

S. Datz, Head, Atomic Physics
ORNL, Physics Division, P.O. Box 2008
Oak Ridge, TN 37831-6377

Principal Investigators

S. Datz [datzs@ornl.gov]
C. C. Havener [havenercc@ornl.gov]
H. F. Krause [krause@mail.phy.ornl.gov]
J. H. Macek [macek@utk.edu]
F. W. Meyer [meyerfw@ornl.gov]
C. Reinhold-Larsson [reinhold@ornl.gov]
D. R. Schultz [schultzd@ornl.gov]
C. R. Vane [vanecr@ornl.gov]

OVERVIEW

The atomic collision physics research can be broadly characterized in three closely related parts: accelerator-based atomic physics, atomic collisions of low-energy, highly charged ions as supplied by an ECR source, and theoretical atomic collision physics.

The scientific objective of the accelerator-based atomic physics program is development of detailed understanding of the interactions of charged and neutral atoms and molecules with electrons, atoms, surfaces, and solids through investigations employing beams of particles accelerated to high energies. Facilities at ORNL used for the experimental phase of this research include the EN Tandem Van de Graaff and the Holifield Radioactive Ion Beam Facility (HRIBF). Off-site facilities such as the Heavy-Ion Medical Accelerator (HIMAC) in Tokyo and the Super Proton Synchrotron (SPS) at CERN, Geneva, Switzerland, are also used to extend the range of energies examined. Electron-molecular ion interactions at extremely low relative energies are being studied at the CRYRING heavy-ion storage ring in Stockholm, Sweden.

The goal of the ECR-based program is improved understanding of the collisional interactions of low-energy molecular and atomic ions (singly and multicharged) with electrons, atoms, ions, and surfaces. Merged beams are also being used to measure total and state-selective charge exchange and ionization cross sections for multiply charged ions colliding with hydrogen (deuterium) atoms at very low kinetic energies. Analysis of ejected electrons and scattered ions is being performed to study the interaction of low energy multiply charged ions with solid surfaces. The theoretical effort has focused on the dynamics of strongly perturbed systems, such as atoms, ions, solids, surfaces, and nanostructures subject to electromagnetic fields or particle interaction. It also does synergistic support and interchange with our present and future experimental programs.

I. High-Energy Atomic Collisions

Multiple Ionization in Fast Ion-Atom Collisions: Simultaneous Measurement of Recoil

Momentum and Projectile Energy Loss – (M. A. Abdallah, C. R. Vane, C. C. Havener, D. R. Schultz, H. F. Krause, N. Jones, and S. Datz)

Using the ORNL EN Tandem high-resolution Elbek Spectrograph in conjunction with the COLTRIMS technique, we have performed experiments to measure simultaneously the full momentum vector of recoil ions, along with projectile energy loss and scattering angle in ion-atom collisions. We studied multiple ionization in the collisions of 0.83-MeV/u O^{7+} with Ne. Recoil ions (Ne^{q+} , $q = 1-8$) were detected in coincidence with single capture to O^{6+} . The results give the first experimental evidence for the increase of the average electron energy with increasing recoil charge state q . The average ejection angle shows a dramatic decrease with q . Results have been compared with n -electron classical trajectory Monte Carlo (nCTMC) calculations.

These experiments present the first measurements of the average energy and longitudinal momentum of the ejected electrons in multiply ionizing collisions. They also give the first experimental determination of the electron average ejection angle as a function of recoil charge state in such collisions. We have found that the average energy of electrons increases while the average ejection angle decreases with increasing recoil charge state, and therefore decreasing collision impact parameter. In the transverse direction, the role of the ejected electrons in transverse momentum balance is minimum for large recoil charge states (two-body behavior), but important for low charge states as the projectile suffers small deflection (dipole behavior). The measurements represent an advance in determining the full (vector) momentum distribution of all free particles in atomic collisions and therefore provides a rather strenuous test of the theoretical understanding of multiply ionizing collisions, and the validity of the extension of nCTMC calculations to these multi-electron systems. The results of measurements and nCTMC calculations for these specific collisions systems were reported in *Phys. Rev. Lett.* **85**, 278 (2000).

Radiative Electron Capture at Ultrarelativistic Energies: 33-TeV Pb^{82+} Ions

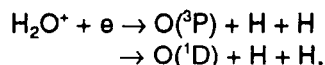
– (C. R. Vane, H. F. Krause, and S. Datz)

Experimental cross sections for radiative electron capture (REC) by 33-TeV Pb^{82+} ions in Be and C targets have been extracted from an analysis of measurements of total electron capture by these ions in Be, C, Al, Cu, Sn, and Au targets. The REC cross sections in the Be and C targets, where REC is significant, were obtained by subtracting measured cross sections for electron capture from pair production (ECP), the only other significant capture process at these energies. The ECP contributions in Be and C were determined from smooth extrapolations of measured cross sections in the heavier targets where the ECP process dominates with suitable accounting for slightly decreased screening effects for the light targets. The measurements represent the highest energy observation of REC by far, and permit unambiguous tests of the process in a regime where magnetic effects dominate over non-relativistic calculations. Whereas radiative recombination cross sections at extremely low energies are found to deviate significantly from theory (with no explanation in sight), we obtain an experimental K-REC cross section of $(0.010 \pm 0.002 \text{ b/electron/Pb K-vacancy})$, which agrees with a calculation of REC made by applying detailed balance to the corresponding process of radiative recombination and using tabulated photoelectric effect cross sections. A comparison is also presented of the present experimental result with other heavy-ion measurements made at lower but still high collision energies, and with very recent results of non-relativistic and relativistic calculations, which differ considerably in this energy regime. The results have been published as a "Rapid Communication" in *Phys. Rev. A* **61**, 10701 (2000).

II. Atomic Processes in Plasmas: Ion-Atom and Molecular-Ion Collisions

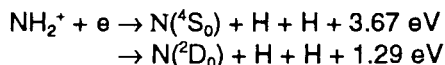
Dynamics of Three-Body Breakup in Dissociative Recombination – (S. Datz)

Work continued on the study of three-body breakup in dissociative recombination. The new modification is the introduction of timing to the detection system that greatly increases the resolution of the experiment. The system under study again was



The CRYRING facility at Stockholm allowed ion storage at 4.5 MeV to relax vibrational excitation and a merged electron beam that gave relative collision energies of ~ 0.001 eV. The three fragments struck an imaging detector consisting of three-stacked microchannel plates and a phosphor screen. The screen is imaged onto a CCD camera and onto a multichannel-photo-multiplier tube. The former records the separation of the fragments and the latter the difference in arrival time. The point is to pick out those events where the plane of the three particles is parallel to the detector plane. This is signaled by the maximum total distance and the minimum time of arrival difference. A resolution of < 800 ps was obtained. Using a 2.5-micron Al filter at the beam center stopped the H atoms, but allowed the identification of O atoms and the problem was reduced to the sum of two two-body systems. The results gave good separation between the $\text{O}({}^3\text{P})$ and $\text{O}({}^1\text{D})$ channels. The results are (1) the ratio of $\text{O}({}^3\text{P})$: $\text{O}({}^1\text{D})$ is $\sim 4:1$; (2) the kinetic energy distribution are randomly distributed indicating a lack of an intermediate (OH^+) state; and (3) the angular distributions show a monotonic rise with decreasing angle with no resemblance to the $\sim 110^\circ$ angle in H_2O^+ and H_2O molecules. This work has been submitted to *Physical Review Letters*.

Using the same technique, the system



was also investigated. Unlike the H_2O^+ case where the most exothermic channel was dominant, the ${}^2\text{D}_0$ channel is dominant in the NH_2^+ DR. The data are presently being analyzed.

The most fundamental case of three-body DR is the $\text{H}_3^+ + e \rightarrow \text{H} + \text{H} + \text{H}$. This channel has $\sim 80\%$ of the total cross section. It is substantially constant up to ~ 0.5 eV ($\sim 6000^\circ\text{K}$) and hence is a contributing factor in the composition of low temperature plasmas.¹ A new technique has been devised which should allow the study of the dynamics of this reaction. An experiment is scheduled for December.

1. S. Datz et al., Phys. Rev. Lett. **74**, 896 (1995).

High-Energy Heavy-Ion Radiation of DNA – (S. Datz, H. F. Krause, and C. R. Vane)

Using Atomic Force Microscopy (AFM), it had been observed by a group at George Washington and Georgetown Universities that electron irradiation of aqueous DNA generally gave single double-strand breaks (DSB) whereas high LET proton radiation gave multiple DSBs with a propensity for the production of small fragments. The latter result indicated a coordinated attack on the DNA. The problem of introducing protons at their Bragg peak energy (~ 150 keV) through a window and into an aqueous sample was partially solved by using neutrons to form proton recoils from collisions with H_2O . Our approach was to use heavy ions at much higher energies but with the same LET as 150-keV protons. This was done using 100-MeV Be ions at the Holographic Radioactive Ion Beam Facility at ORNL and 16-GeV Ar ions from the HIMAC Facility in Japan.

The damage to the DNA is done by secondary electrons either directly or via the free radicals that are formed. Although the LET (dE/dx) for the three different projectiles is the same, the δ -ray spectra are quite different. The total energy loss is due to inelastic collisions with electrons, but the 16-GeV Ar creates fewer electrons, but at higher energy than does the 100-MeV Be, or the 150-keV protons. This means that damage will take place further out from the track. To test the effect of the δ -ray spectrum and hence, e.g., the efficacy of proton versus heavy-ion therapy, we irradiated a matrix of 16 targets using four different doses with four concentrations of free radical quenchers. AFM analysis is presently underway. Initial results look promising.

Development of an Ion Beam Electrostatic Trap for Molecular Ion Physics – (H. F. Krause)

A totally electrostatic (and therefore mass independent) reflecting ion beam trap based on the design of Zajfman et al.¹ has been constructed and tested with beams produced by a Colutron discharge ion source. Automated control and data acquisition systems have been developed and integrated into operation of the trap. Long-term (many seconds) storage of N_2^+ and other ions has been demonstrated in $\sim 10^{-10}$ Torr vacuum by detection of neutrals expelled from the trap. The operating characteristics have been thoroughly explored and lifetimes of numerous atomic and diatomic cations produced by the Colutron have been surveyed with significant trapping efficiency ($\sim 20\%$, and up to 10^5 ions per fill at energies of 1.3 – 3 keV). Lifetimes appear to scale inversely as the charge exchange cross sections (Massey criterion) and trap pressure. Other ion sources that will be needed to produce sufficient intensities of large (interesting) molecular and cluster ions are being investigated. A commercial electron impact source has been purchased.

1. M. Dahan, et al., *Rev. Sci. Instrum.* **69**, 76 (1998).

Ion-Atom Interactions – (C. C. Havener)

Current studies of electron-capture processes are motivated by the fact that they constitute reaction channels of fundamental importance in many environments, e.g., in fusion devices and in the ion implantation process of semiconductors. The ORNL ion-atom merged-beams apparatus is unique in its ability to provide benchmark measurements¹ of electron capture for multi-charged ions and H at eV/u energies. Our recent experimental and theoretical study² of $Cl^{7+} + D$ shows an unexpected decrease in the cross section at low energies, in contradiction to what is expected from a popular simple model and speculation from previous measurements for highly charged ($7+$) ions with multi-electron cores. The observed low energy behavior is interpreted using newly developed couple-channel molecular-orbital hidden-crossing calculations for $N^{7+} + D$. The fact that the cross section for the highly charged multi-electron ion Cl^{7+} does not remain flat toward decreasing energies shows that the actual quasi-molecular structure and associated dynamics remain important. Future efforts will explore other highly charged multi-electron ions with opened and closed shells to determine for which ions, if any, simple models are adequate.

When targets other than atomic H are considered, the presence of more than one electron on the target makes theoretical modeling a challenge that increases the need for benchmark experiments. This last year our gas-cell measurements of $B^{3+} + H_2$ at keV/u energies resolved discrepancies between two coupled-channel molecular-orbital calculations. In collaboration with Okuno's group at the Tokyo Metropolitan University, Japan, electron-capture measurements for $O^{2+} + He$ were performed using an octopole beam guide with O^{2+} ions from a mini-EBIS source. These measurements are being analyzed and will be compared to ion trap rate measurements from the Univ. of Las Vegas, Nevada which suggest that the cross section at eV/u energies is two orders of magnitude too low compared to theory.

The ion-atom merged-beams apparatus is being upgraded to allow measurements with a variety of neutral targets such as Li, S, Fe, Na, O_2 and CH_2 . A negative ion-sputter source has been installed and the demerge section magnet is currently being redesigned to accommodate

heavier neutral beams. A new computer control program has been written which accommodates a variety of beam-chopping schemes that will allow for better signal/noise separation. Collision systems under consideration include $\text{Na} + \text{He}^{2+}$ where strong shape resonances have recently been predicted at eV/u collision energies. Collisions with neutral beams like Fe and S will permit exploration of electron capture from multi-electron systems where accurate, *ab-initio*, coupled-channel calculations are generally not available. For systems like $\text{Ar}^{4+} + \text{Li}$ and $\text{Fe}^{2+} + \text{Fe}$, we will be able to study the competition between single electron capture and simultaneous (or correlated) double-electron capture at low energies. Such detailed measurements will serve as benchmarks for emerging theories.

1. R. A. Phaneuf, C. C. Havener, G. H. Dunn, and A. Muller, *Rep. Prog. Phys.* **62**, 1143 (1999).
2. J. S. Thompson, A. M. Covington, P. S. Krstic, Marc Pieksma, J. L. Shinpaugh, P. C. Stancil, C. C. Havener, "Low Energy Capture by Cl^{7+} D Using Merged Beams", submitted to *Physical Review A* (2000).

III. Particle-Surface/Solid Interactions

Low Energy Multicharged Ion-Surface Interactions – F. W. Meyer, V. A. Morozov, S. Datz, and C. R. Vane)

Low energy ion-surface interactions play major roles in determining the characteristics of edge and divertor plasmas of magnetic fusion devices, are at the core of all plasma processing techniques, and form the basis of most low energy particle detection approaches. Using the recently developed floating surface scattering chamber experiment, we have focused this year on obtaining a more complete picture of the kinds of scattering events leading to projectile neutralization in quasi-binary backscattering collisions from the surface of Au (110). Exploiting the fact that a Au(110) surface has pronounced surface corrugations along the [100] direction, we have made systematic measurements of the charge fractions for low energy Ar ions backscattered from this corrugated surface as function of the azimuthal target orientation for a wide range of incident charge states ($2+ - 13+$). The scattered charge fractions exhibited significant variations with target azimuth, which, moreover, were different for different scattered charge states. Using extensive Monte Carlo trajectory simulations based on the MARLOWE code¹ we were able to deconvolute the observed variations into contributions from different surface collisions. We have found that, at least at the lower energies investigated in the range (i.e. 5 –10 keV), there are significant differences in the neutralization probabilities between backscattering collisions with Au atoms located on the corrugation ridges and those located in the corrugation valleys and side-walls. For example, we found that, while backscattered projectiles are fully neutralized in single collisions with target atoms in the valleys even for initial charge states as high as $11+$, for collisions with ridge atoms, there is more than a 90% probability of surviving in charge state $1+$ or higher. This suggests additional contributions to projectile neutralization from, e.g., nearest neighbors in the surface and/or the electron selvage, the relative importance of which can vary along the corrugation profile. The results of this work have been recently submitted as a Physical Review Letter.²

In addition, we have extended the projectile backscattering measurements to higher energies. At the lower energies initially studied, essentially complete equilibration was still observed, with neutrals being the dominant scattered charge state, even for incident charge states as high as $13+$. In contrast, at the highest energies attainable with the present set-up, i.e., 30–35 keV, the dominant scattered charge states are $2+ - 3+$ for incident Ar^{13+} , and, in general, show significant dependence on incident charge state. Having attained a non-equilibrium regime with these measurements, and having determined the energy dependence of the scattered charge fractions from 2–35 keV, a set of results has now been obtained that is expected to

provide a much more sensitive test of neutralization models and simulations than the previous lower energy data.

In the coming year, analysis of the backscattering data obtained for the Au (110) target will continue. In addition, new measurements will be initiated using an insulator target, in order to study the effect of reduced target electron mobility on projectile neutralization. During the above-surface neutralization phase, electrons pulled from the surface leave a positive surface charge in the case of insulator targets, which is thought to reflect, at eV energies, incompletely neutralized projectiles prior to actual impact on the surface. We will search for this effect using a highly charged incident projectile, by systematic monitoring of scattered charge distributions and energy losses, down to lowest attainable energies, which should show dramatic changes if a transition occurs from backscattering in a binary collision to reflection from an extended repulsive surface charge distribution.

1. M. T. Robinson, *Rad. Eff. Def. Solids* **130**, 3 (1994); *Phys. Rev. B* **40**, 10717 (1989).
2. V. A. Morozov and F. W. Meyer, "Path Dependent Neutralization of Multiply Charged Ar Ions Incident on Au(110)", submitted to *Physical Review Letters* (June, 2000).

Sub-Surface Neutralization of Hollow Atoms and Ultra-Fast Electron Dynamics – (C. R. Vane)

We are developing experimental methods previously used for investigating chemical effects on high-resolution X-ray satellite spectra to measure electron transfer rates of slow, highly charged ions rapidly undergoing neutralization in various dense environments. The energies and intensities of satellite X Rays vary depending on the availability of ligand or other weakly bound electrons to quickly transfer into vacancies of the slow moving ions. Experiments were previously carried out at the ORNL EN tandem measuring electron refilling rates for Ar and Cl implanted in Ni. These are being continued and expanded at the ORNL Holifield Tandem accelerator (HRIBF) to include measurements of X Rays from Ar and Cl in semi-conducting and insulating environments. The goal is to elucidate the mechanisms by which slow, very highly charged ions become completely neutralized in exceedingly short times.

Extensive theoretical and experimental research has been carried out at the ORNL ECR on studies of scattering of slow ions from surfaces, and considerable progress has been achieved in understanding the underlying physics. Less is understood about the sub-surface processes. Most data from ion surface scattering experiments are sums of signals from both the above- and below-surface phenomena. By measuring neutralizing relaxation signals from hollow atoms created in atoms initially located (and always remaining) within dense environments, one can completely isolate the processes occurring below the surface. The intent of the work described here is to complement the on-going ECR-based efforts in understanding these fundamental neutralization processes, and also to use the experimental techniques developed to obtain unique information on the electronic and atomic characteristics of the new materials and structures.

IV. Theoretical Atomic Physics

(Reinhold, Macek, Schultz, Ovchinnikov, and Burgdörfer)

The dynamics of strongly perturbed atomic scale systems, such as atoms, ions, solids, surfaces, and nanostructures subject to electromagnetic fields or particle interactions, form the focus of our theoretical development as does synergistic support and interchange with our experimental programs.

We concluded our development of a quantum transport theory of atomic states through solids. Comparison of classical and quantum simulations for the stripping of light ions showed that the stochastic nature of the interaction destroys most quantum effects. Excitation of highly

charged ions is expected to provide a better test of non-classical transport. Thus, we are currently investigating the transport of atomic states of highly charged ions (Ar^{17+} and Kr^{35+} through carbon foils). These systems provide a unique opportunity to apply our quantum transport theory. The fine structure and the Lamb shift for these ions can be so large (tens of eV) that they should play an important role in the atomic dynamics. Additionally, highly charged ions decay very rapidly, which is expected to affect considerably the dynamics of ions during transport.

We have extended our studies of the kicked Rydberg atom, and we have focused on the classical and quantum stabilization properties of this system for both unidirectional and alternating trains of pulses. For low frequencies, the kicked atom exhibits various classical stable islands within which the atom can be stabilized. These islands disappear, as Rydberg atoms are subject to trains of kicks with a high frequency: i.e. the classical system becomes chaotic. In this case, we have observed clear signatures of quantum localization which were not expected to have any classical analog. Surprisingly, we have shown that the stable quantum states of the system are, in fact, "scarred" wave functions which are localized around the unstable periodic orbits of the system. Since both classical and quantum localization are such that the atom ends up in a well-defined region of phase space, we plan to use this property to tailor well-defined coherent states.

Measurements of slow electrons are a unique capability of the COLTRIMS technique. We have used the hidden crossing theory to identify characteristic features of a top-of-barrier mechanism for producing these slow electrons. We find several such characteristics, including interference of terms with differing symmetry and proportionality with excitation cross sections. To check that these features are indeed characteristic of the proposed mechanism, we have solved a model problem that lacks a top-of-barrier and find that the electron distribution also lacks the characteristic features. Conversely, exact numerical calculations using a model with a potential barrier did show the expected features. We are further developing our capability to compute electron energy and angular distributions in low-energy ion-atom collisions.

We have extended our ability to apply a direct, time-dependent, high-order lattice-function approach to atomic collision problems, treating larger angular momenta in electron-hydrogen scattering than previously, and modeling antiproton helium collisions through a four-dimensional (electronic coordinate) approach. We have initiated work to use these techniques in studying the transport and exciton properties of nanostructures and to support experimental exploration of basic properties of photo-response of nanostructures. Finally, we continue to employ our expertise in few-body atomic rearrangement physics to support, guide, and interact with ongoing experimental (COLTRIMS) investigations of fundamental collision dynamics of interest to applications such as radiation physics.

Some Recent Publications

1. "Multiple Ionization in Fast Ion-Atom Collisions: Simultaneous Measurement of Recoil Momentum and Projectile Energy Loss," M. A. Abdallah, C. R. Vane, C. C. Havener, D. R. Schultz, H. F. Krause, N. Jones, and S. Datz, *Phys. Rev. Lett.* **85**, 278 (2000).
2. "Radiative Electron Capture at Ultrarelativistic Energies: 33-TeV Pb⁸²⁺ Ions," C. R. Vane, H. F. Krause, S. Datz, P. Grafström, H. Knudsen, C. Scheidenberger, and R. H. Schuch, *Phys. Rev. A (Rapid Communications)* **62**, 010701-1 (2000).
3. "Atomic Collision Processes in Solids and Gases at Ultrarelativistic Energies," S. Datz, *Nucl. Instrum. Meth. Phys. Res. B* **164-165**, 1 (2000).
4. "De-excitation X Rays from Resonant Coherently Excited 390-MeV/u Hydrogen-like Ar Ions," T. Ito, Y. Takabayashi, K. Komaki, T. Azuma, Y. Yamazaki, S. Datz, E. Takada, and T. Murakami, *Nucl. Instrum. Meth. Phys. Res. B* **164-165**, 60 (2000).
5. "Dynamics of Three-body Dissociative Recombination: H₃O⁺," S. Datz, R. Thomas, S. Rosén, W. van der Zande, and M Larsson, submitted to *Phys. Rev. Lett.* (2000).
6. "Merged-Beams Experiments," R. A. Phaneuf, C. C. Havener, G. H. Dunn, and A. Muller, *Rep. Prog. Phys.* **62**, 1143 (1999).
7. "Electron Capture in Collisions of C⁺ with H and H⁺ with C", P. C. Stancil, J. -P. Gu, C. C. Havener, P. S. Krstic, D. R. Schultz, M. Kimura, B. Zygelman, G. Hirsch, R. J. Buenker, and M. E. Bannister, *J. Phys. B* **31**, 3647 (1998).
8. "Charge Transfer in Collisions of C⁺ with H and H⁺ with C", P. C. Stancil, C. C. Havener, P. S. Krstic, D. R. Schultz, M. Kimura, J.-P. Gu, G. Hirsch, R. J. Buenker, and B. Zygelman, *Astrophys. J.* **502**, 1006 (1998).
9. "Low-Energy Electron Capture by B⁴⁺ Ions from Hydrogen Atoms", Marc Pieksma and C. C. Havener, *Phys. Rev. A* **57**, 1892 (1998).
10. "Multicharged Ion-surface Measurements at ORNL MIRF Using Decelerated Beams", F. W. Meyer and V. A. Morozov, *Nucl. Instrum. Meth. Physics B* **157**, 297 (1999).
11. "Simultaneous Energy Distribution and Ion Fraction Measurements Using a Linear Time-of-Flight Analyzer with Floatable Drift Tube", V. A. Morozov and F. W. Meyer, *Rev. Sci. Instrum.* **70**, 4515 (1999).
12. "Multicharged ion-surface interactions studies at ORNL with decelerated beams", F. W. Meyer and V.A. Morozov, *Phys. Scripta* **T80**, 226 (1999).
13. "Multi-coincidence studies as a technique for the investigation of ion-surface interactions", V. A. Morozov, F. W. Meyer, P. Roncin, *Phys. Scripta* **T80**, 69 (1999).
14. "Quantum Localization of the Kicked Rydberg Atom," S. Yoshida, C. O. Reinhold, and J. Burgdörfer, *Phys. Rev. Lett.* **84**, 2602 (2000).
15. "Enhanced Population of High-l States Due to the Interplay Between Multiple Scattering and Dynamical Screening in Ion-Solid Collisions," C. O. Reinhold, D. G. Arbo, J. Burgdörfer, B. Gervais, E. Lamour, D. Vernhet, and J. P. Rozet, *J. Phys. B* **33**, L111 (2000).
16. "Influence of Short-Range Interference on Ionization Threshold Law," N. Miyashita, S. Watanabe, M. Mitsuzawa, and J. H. Macek, *Phys. Rev. A* **61**, 014901-1 (1999).
17. "Collisions Near Threshold in Atomic and Molecular Physics," H. R. Sadeghpour, J. L. Bohn, M. J. Cavagnero, B. D. Esry, I. I. Fabrikant, J. H. Macek, and A. R. P. Rau, *J. Phys. B* **33**, R93 (2000).
18. "Time-Dependent Treatment of Electron-Hydrogen Scattering for Higher Angular Momenta ($L > 0$)," D. O. Odero, J. L. Peacher, D. R. Schultz, and D. H. Madison, *J. Phys. B* (2000).

Research Summaries

**(single-PI grants,
alphabetical by PI)**

Molecular Structure and Collisional Dissociation and Ionization

Kurt H. Becker

Department of Physics and Engineering Physics,
Stevens Institute of Technology, Hoboken, NJ 07030

phone: (201) 216-5671; fax: (201) 216-5638; kbecker@stevens-tech.edu

Program Scope:

This program investigates the molecular structure and the collisional dissociation and ionization of selected molecules and free radicals. The work focuses (1) on electron-impact induced ionization studies and (2) on studies of electron-impact induced neutral molecular dissociation processes. Recent and future targets of choice for ionization studies include C_2F_6 , C_2F_5 , SiF_4 , $TiCl_4$, $SiCl_4$ and CCl_4 and its radicals, the molecular halogens Cl_2 , Br_2 , and F_2 , $TiCl_x$ ($x=1-3$), and BCl_3 and its radicals. This choice is motivated on one hand by the relevance of these species in specific current and future etching applications (e.g. poly-Si and amorphous Si, Al and Al-Cu, and WSi_2 and $TiSi_2$ etching and the etching of thin magnetic films) as well as by basic collision physics aspects ($SiCl_x$ and CCl_x are of similar molecular structure as the species studied previously and thus complement the existing data base for these targets; Br_2 , F_2 , and Cl_2 are simple diatomic molecules for which the collisional and spectroscopic data base is extremely scarce). The first targets of choice for the neutral molecular dissociation studies include SiH_4 , $Si(CH_3)_4$ (tetramethylsilane), SiF_4 , and BCl_3 . The fragments to be probed are $Si(^1S)$, $Si(^1D)$, $SiH(X^2\Pi)$, $BCl(X^1\Sigma)$, and $B(^2P^o)$. The scientific objectives of the research program are:

- (1) to provide the atomic and molecular data that are required in efforts to understand the properties of low-temperature processing plasmas on a microscopic scale
- (2) to identify the key species that determine the dominant plasma chemical reaction pathways
- (3) to measure cross sections and reaction rates for the formation of these key species and to attempt to deduce scaling laws
- (4) to establish a broad collisional and spectroscopic data base which serves as input to modeling codes and CAD tools for the description and modeling of existing processes and reactors and for the development and design of novel processes and reactors
- (5) to provide data that are necessary to develop novel plasma diagnostics tools and to analyze more quantitatively the data provided by existing diagnostics techniques

Electron Impact Ionization Studies

We have two experimental techniques at our disposal to study electron impact ionization properties of stable molecules and free radicals and other transient species. The fast-neutral-beam technique is used for the radicals and transient species. Briefly, a dc discharge is ignited in a commercial Colutron ion source which is operated with a positive bias using a suitable feed gas. Primary ions are extracted from the ion source, accelerated to about 3 keV, mass selected in a Wien filter, and sent through a charge-transfer cell filled with a suitably chosen charge-transfer gas for resonant or near-resonant charge transfer. The residual ions in the beam are removed from the neutral target gas beam by electrostatic deflection and most Rydberg species are quenched in a region of high electric field. The fast neutral target beam is subsequently crossed at right angles by a well-characterized electron beam (5 - 200 eV beam energy, 0.5 eV FWHM energy spread, 0.03 - 0.4 mA beam current). The product ions are focused in the entrance plane of an electrostatic hemispherical analyzer which separates ions of different charge-to-mass ratios

(i.e. parent ions from fragment ions). The ions leaving the analyzer are detected by a channel electron multiplier (CEM). Absolute calibration of the relative cross sections can be achieved in two ways. The fast-beam apparatus affords the capability to measure all quantities that determine the absolute cross section directly. The target density is obtained from the energy deposited by the fast target beam into a pyroelectric detector, which is first calibrated relative to a well-characterized ion beam. As an alternative, the well-established Kr or Ar absolute ionization cross sections can be used to calibrate the pyroelectric crystal. The calibrated detector, in turn, is then used to determine the absolute flux of the neutral target beam. The second procedure avoids the frequent and prolonged exposure of the sensitive pyroelectric crystal to fairly intense ion beams.

A time-of-flight mass spectrometer (TOF-MS) is used for the experiments involving stable targets. It consists of two interconnected stainless steel vacuum chambers evacuated to a base pressure of 1×10^{-6} Pa. One chamber contains the electron-impact ion source and the other chamber houses the ion flight tube and the ion detectors. The TOF-MS can be operated either in a linear mode or in a reflection mode. The ion detectors are micro channel plates (MCP) of 40 mm diameter. The ion source chamber is filled with the target gas(es) under study at pressures of about 1×10^{-4} Pa which is measured with a spinning rotor viscosity gauge. The ion efficiency curves (relative partial ionization cross sections) are measured simultaneously for Ar and the target gas under study in a well-defined mixture in an effort to ensure identical operating conditions for all ions and the measured relative partial ionization cross sections are put on an absolute scale by normalization relative to the total Ar ionization cross section at 70 eV. The electron gun is operated using electron pulses of 90 ns width at a repetition rate of 15 kHz. The electron beam has a diameter of about 0.6 mm in the interaction region and the dc-equivalent electron beam current is in the range from 1 - 10 μ A with an energy spread of about 0.5 eV (FWHM). Extraction voltages up to 3 kV with a 10 ns rise time are employed to the repeller roughly 10 ns after the incident electron pulse has passed through the ionization region. After passing through the exit aperture the ions are accelerated by a -3 kV bias voltage applied to the entrance electrode of the flight tube. The ion deflector section consists of two pairs of electrodes for the deflection of the ions in the horizontal (z) and vertical (y) directions. The deflection plates in conjunction with the Einzel lens allow minor corrections of the ion trajectories. The ions are detected by the MCP detector whose output is preamplified and recorded with a 2 GHz multiscaler with a time resolution of 500 ps. Our TOF-MS is operated in such a way that no more than one ion is created during each electron pulse.

C₂F₅: The ionization of C₂F₅ is dominated by the formation of C₂F₅⁺ parent ions and CF₃⁺ fragment ions. The two cross sections are similar in shape except for a slight shift in the appearance energy of the CF₃⁺ partial ionization cross section to higher energies. We determined absolute cross sections at 70 eV of $3.5 \pm 0.6 \times 10^{-16}$ cm² (CF₃⁺) and $1.3 \pm 0.2 \times 10^{-16}$ cm² (C₂F₅⁺). The peak cross sections for the formation of all other singly charged fragment ions and multiply charged ions were less than 0.1×10^{-16} cm². We also determined the appearance energies for the C₂F₅⁺ and CF₃⁺ ions. Our values of 12.5 ± 0.5 eV (C₂F₅⁺) and 14.5 ± 1.0 eV (CF₃⁺) cannot readily be compared with tabulated ionization energies and appearance energies due to the lack of reliable thermochemical data including the ionization energy for the C₂F₅ radical in the literature.

We used the modified additivity rule to calculate also the total single ionization cross sections for the C₂F₅ radical. The agreement between the measured and calculated total single ionization cross section is good only in the regime of low impact energies up to about 50 eV. At higher impact energies the calculated cross section systematically overestimates the measure

cross section and the discrepancy increases with increasing impact energy. We have no simple explanation for this behavior.

TiCl₄; We studied the electron impact ionization of TiCl₄ for electron energies from threshold to 500 eV. Absolute partial cross sections for the formation of all singly charged positive ions and for four doubly charged positive ions were measured using a time-of-flight mass spectrometer (TOF-MS). Dissociative ionization was found to be the dominant process. At lower impact energies up to 40 eV, the ion abundance varies drastically with impact energy, whereas at higher energies, two ionization channels dominate, the formation of the molecular TiCl₃⁺ fragment ion with a maximum cross section of $3.75 \times 10^{-16} \text{ cm}^2$ at 100 eV and the formation of the atomic Cl⁺ fragment ion with a maximum cross section of $4 \times 10^{-16} \text{ cm}^2$ at 70 eV. All fragment ions with the exception of TiCl₃⁺ are formed with excess kinetic energy with the Cl⁺ ion showing the broadest distribution of kinetic energies. The cross section values of the doubly charged ions are about one order of magnitude smaller than those of the singly charged ions. The experimentally determined total single ionization cross section of TiCl₄ is compared with results of semi-empirical calculations and good agreement is found at all impact energies.

Electron Impact Neutral Dissociation Studies

The experimental apparatus for these studies consists of an electron-beam and a gas-beam intersecting at right angles inside a vacuum chamber in conjunction with a tunable laser beam which propagates either parallel or antiparallel to the electron beam in order to maximize the overlap of the three beams. Optical detection of the LIF signal from the interaction region is made perpendicular to both the electron beam and the gas beam. The energy of the electron beam can be varied between 5 eV and 400 eV with typical beam currents of 3 μA at 25 eV and 20 μA at 100 eV and an energy resolution of about 0.5 eV (FWHM). The electron beam is collected in a Faraday cup which consists of three electrically insulated elements which enables us to measure the beam current as well as the beam divergence. The gas beam is an effusive beam emanating from a multi-capillary array of rectangular shape which is positioned about 8 mm above the electron beam axis. The laser system consists of a pulsed Lumonics EX-520 excimer laser operating at 308 nm (XeCl) which is used to pump a Lumonics HD-500 dye laser using Exalite 392A as the dye of choice in the wavelength region under study. The laser system produces 0.0015 nm wide pulses of less than 10 ns duration of up to 3 mJ energy per pulse in the wavelength range from 375- 397 nm. The laser beam enters and exists the vacuum chamber through Brewster-angle windows and the beam intensity passing through the vacuum chamber is monitored by a laser pulse energy meter. The fluorescence from the interaction region is imaged onto the cathode of a thermoelectrically cooled Hamamatsu R1104 photomultiplier tube (PMT). Spectral isolation is achieved by a narrow-band interference filter. The output pulses of the PMT are processed by a gated photon counter whose output, in turn, is directed into a personal computer for data storage and further analysis. Absolute calibration is achieved by comparison with previously determined benchmark cross sections.

SiH₄: Preliminary results were obtained for the formation of final-state specific Si(¹S) atoms following electron impact dissociation of Si₄ for energies from 20 eV to 100 eV. The Si(¹S) ground-state atoms were detected by pumping the Si (3p)² ¹S \rightarrow (3p)(4s) ¹P transition at 390 nm with a tunable dye laser and recording the subsequent Si (3p)(4s) ¹P \rightarrow (3p)² ¹D fluorescence at 288 nm. We found a peak cross section for the formation of Si(¹S) atoms from SiH₄ of $4.5 \times 10^{-17} \text{ cm}^2$ at an impact energy of 60 eV. This leads to a branching ratio of 0.037 for

the formation of Si(¹S) atoms in the electron-impact induced neutral dissociation of SiH₄. Experiments aimed at determining the cross section for the formation of Si(¹D) atoms are underway as are experiments with other Si-bearing molecules such as SiF and Si(CH₃)₄.

Recent publications (since 1998) and manuscripts accepted for publication:

1. "Application of the Modified Additivity Rule for the Calculation of Electron-Impact Ionization Cross Section of Complex Molecules", *J. Phys. Chem.* **102**, 8819-26 (1998), with H. Deutsch, R. Basner, M. Schmidt, and T.D. Märk
2. "Electron-Impact Ionization of the SF₅ and SF₃ Free Radicals", *J. Chem. Phys.* **109**, 6596-600 (1998), with V. Tarnovsky, H. Deutsch, and K.E. Martus
3. "Application of the DM Formalism to the Calculation of Electron-Impact Ionization Cross Sections of Alkali Atoms", *Int. J. Mass Spectrom. Ion Proc.* **185/186/187**, 319-26 (1999), with H. Deutsch and T.D. Märk
4. "Electron Impact Ionization and Dissociation of Molecules Relevant to the Field of Gaseous Dielectrics and its Applications", *Gaseous Dielectrics VIII*, edited by L.G.Christophorou, Plenum Press, New York (1998), p. 3-13, with V. Tarnovsky, H. Deutsch, R. Basner, M. Schmidt, S. Matt, and T.D. Märk
5. "Experimental and Theoretical Determination of Electron Ionization Cross Sections for Atoms, Molecules, and Molecular Ions Relevant to Fusion Edge Plasmas", *Czechoslovak J. Phys.* **48**, 333-8 (1998), with S. Matt, D. Muigg, G. Denifl, M. Sonderegger, T. Fiegele, R. David, V. Grill, P. Scheier, T.D. Märk, H. Deutsch, and A. Stamatovic
6. "Application of the DM Formalism to the Calculation of Cross Sections for the Multiple Ionization of Be, B, C, and O Atoms by Electron Impact", *Int. J. Mass Spectrom.* **192**, 1-8 (1999), with H. Deutsch, G. Senn, S. Matt, and T.D. Märk
7. "Theoretical Determination of the Absolute Electron Impact Ionization Cross Section Function for Silver Clusters Ag_n (n=2-7)", *J. Chem. Phys.* **111**, 1064-71 (1999), with H. Deutsch, J. Pittner, V. Bonacic-Koutecky, S. Matt, and T.D. Märk
8. "Calculated Cross Sections for the Electron Impact Ionization of Metastable Atoms", *J. Phys. B* **32**, 4249-59 (1999), with H. Deutsch, S. Matt, and T.D. Märk
9. "Electron Impact Ionization of the C₂F₅ Free Radical", *J. Phys. B* **32**, L573-7 (1999), with V. Tarnovsky and H. Deutsch
10. "Calculations of Cross Sections for the Electron Impact Ionization of Molecules", *Int. J. Mass Spectrom.* **197**, 37 (2000), with H. Deutsch, S. Matt, and T.D. Märk
11. "Basic Concepts of Plasma Chemistry", in "Encyclopedia of Chemical Physics and Physical Chemistry", edited by J.H. Moore and N.D. Spencer, IOP Publishing, London (2000), in press
12. "Elementary Collision Processes in Plasmas", in "Lectures on Plasma Physics and Plasma Technology", editors; S. Pfau, M. Schmidt, R. Hippler, and K.H. Schoenbach, Wiley-Vieweg Publishing, Weinheim/New York (2000), in press
13. "Calculation of Absolute Electron-Impact Ionization Cross Sections of Dimers and Trimers", *Europ. Phys. J. D* (2000), in press, with H. Deutsch and T.D. Märk
14. "Calculated Cross Sections for the Multiple Ionization of N and Ar Atoms by Electron Impact Using the DM Formalism", *Plasma Phys. Controlled Fusion* (2000), in press, with H. Deutsch and T.D. Märk
15. "Electron-Impact Ionization of TiCl₄", *Thin Solid Films* (2000), in press, with R. Basner, M. Schmidt, V. Tarnovsky, and H. Deutsch

Low-energy ion-surface and ion-molecule collisions

R. L. Champion
Department of Physics
College of William and Mary
Williamsburg, VA 23187-8795
champion@physics.wm.edu

Program Scope The focus of the present experimental research program is upon low-energy, ion-surface and ion-molecule collisions. In the case of the ion-surface studies, the goal has been to examine and understand the effects of adsorbates upon the secondary emission properties of both metallic and semiconductor substrates. Secondary emission is induced by ion (Na^+) impact, the adsorbates studied thus far are oxygen and chlorine, and the substrates have included both crystalline and amorphous samples of Al, Mo W, Ag and Si. The adsorbate coverage is indirectly determined and ranges from none up to a few monolayers. In the ion-molecule studies we have measured absolute cross sections for a number of reactants which are involved in the chemical dynamics of various types of discharges, ranging from CF_4^+ to SF_6^- . Processes examined include charge transfer, electron detachment, collisional decomposition and heavy particle exchange. In both the surface and ion-molecule collision studies, "low energy" implies collision energies ranging from a few up to 500 eV.

Recent Progress

Surface studies. We have completed an initial investigation of the secondary emission of anions from a Si(100) surface upon which resides a known coverage of oxygen. The details of oxygen adsorption to the many facets of silicon have been a subject of numerous theoretical and experimental surface studies. In the case of Si(100), oxygen is thought to chemisorb both in its atomic and molecular form, with the former occurring in the initial stages of oxidation. In particular, it is thought that O_2 molecules initially adsorbed are unstable and dissociate as the surface topology of Si(100) relaxes back to that of a "perfect" surface. [The surface structure of clean Si(100) is not that of the perfect crystal. Every other pair of Si atoms on the surface moves closer together forming what is designated as a 2×1 surface topology. As oxygen is adsorbed on this 'reconstructed' surface, the espoused Si atoms move apart and the surface topology reverts to approximately that of the perfect crystal.] The oxygen atoms that adsorb do so essentially as O^- ; i.e., each adsorbed atom is calculated to gain 0.98 electrons from its neighboring silicon atoms. One of the goals of the present experiments is to see if these ideas about oxygen adsorption might be tested by sputtering experiments carried out at low impact energies.

Shown in figure 1 is a mass spectrum of sputtered anions resulting from 250 eV Na^+ ions impacting a silicon surface which has been exposed to 100 Langmuir of O_2 . [this exposure is thought to correspond to a coverage of about 0.5 monolayer oxygen] The dominant secondary ion is O^- , but there is a surprising amount of, apparently, O_3^- . If this peak centered around 48 amu is, in fact, O_3^- ,

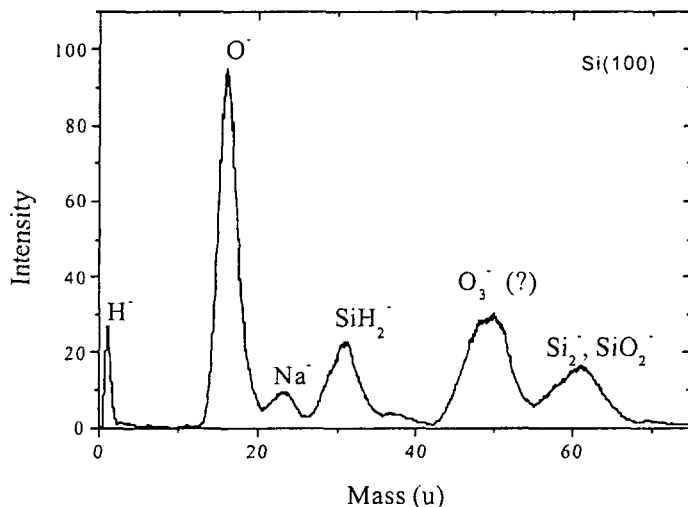


Figure 1 A time-of-flight mass spectrum is shown for Na^+ impacting silicon at 250 eV. The Si(100) has been exposed to 100 Langmuir of O_2 .

initial experiments is the absence (or very low level) of the secondary ion O_2^- . Even if it is somewhat obscured by the SiH_2^- emission, there simply is not much sputtered O_2^- . This observation seems somewhat at odds with previous calculations which indicated primarily molecular (dimer) adsorption of oxygen to silicon. The time of flight spectra in the current experimental arrangement are highly dispersive owing to the fact that the sputtered ions have a fairly large kinetic energy distribution and traverse a rather complicated path in transit from the surface to the detector. In order to confirm the mass assignments given in figure 1, a quadrupole mass spectrometer will be inserted in the place of the energy analyzer. With this improvement the spectrum should be identified without the current ambiguities.

then the coordination between adsorbed atomic and molecular oxygen may be more important than previously imagined. The presence of H^- and SiH_2^- arises from hydrogen delivered to the surface by water vapor, the dominant species in most UHV environments. We are currently making apparatus improvements to lower the partial pressure of H_2O in both the UHV environment and that of the adsorbate gas handling system. Figure 2 shows the absolute probabilities of sputtering the various anions from a Si/O surface as a function of oxygen coverage. The impact energy for those data in figure 2 is 250 eV. Perhaps the most interesting result from these

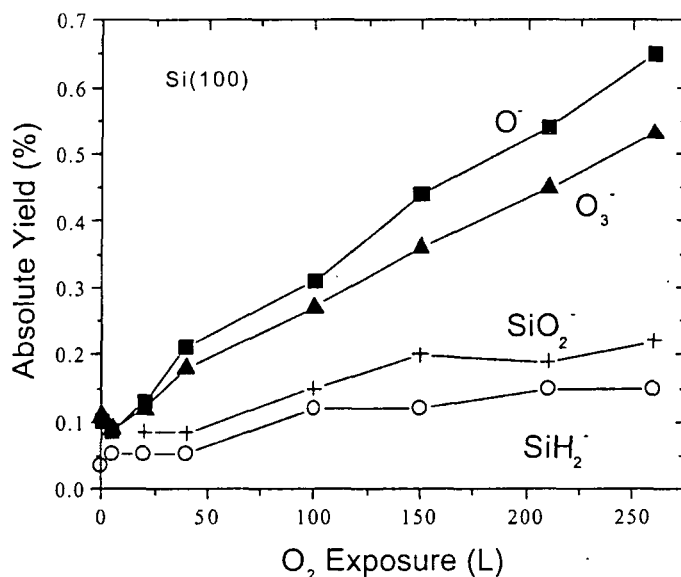


Figure 2 The absolute sputtering probabilities for 250 eV Na^+ impacting a Si(100) surface; as a function of exposure to oxygen.

Gas phase collision studies. We are completing a series of experiments in which cross sections for collisions of SF_6^- with a number of molecular targets are being measured. Cross sections for electron detachment and collisional decomposition are being determined in an attempt to discover the connection between inelastic collisions and dielectric strengths for various gas mixtures which have been proposed for use as gaseous insulators. Shown in figure 3 are the branching ratios for collisional decomposition of SF_6^- into (1) $e^- + SF_6$, (2) $SF_5^- + F^-$, and (3) $SF_5 + F^-$. These branching ratios are simply $R_i = \sigma_i / \sum \sigma_j$, where $i, j = 1 - 3$. For the experiments [panel (b)], the target is N_2 and the abscissa is the relative collision energy, E . The top panel is the result of a calculation which illustrates the way(s) in which SF_6^- will decompose if it is collisionally excited to an internal energy, U , subsequently decomposing in a manner governed by simple statistical considerations. The minimum energy required for the decomposition of SF_6^- is its electron affinity, taken to be 1.0 eV. It is clear that a plausible mapping of $U(E)$ will bring the calculation into reasonable accord with the observed branching ratios. At this point, the experimentally observed cross sections and branching ratios seem to be largely independent of target, suggesting that a two-step process - *viz.*, collisional excitation followed by unimolecular decomposition - may provide a universal description of the collisional dynamics for SF_6^- and targets which are not electronegative.

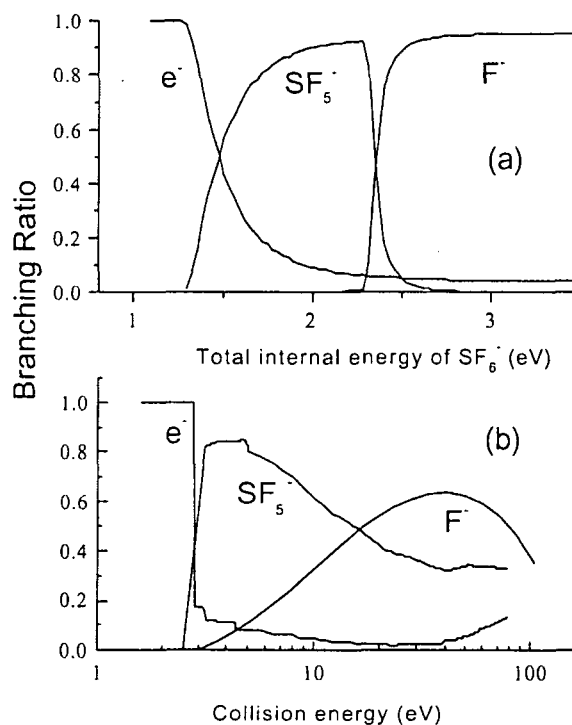


Figure 3 The top panel (a) gives calculated branching ratios for the decomposition of SF_6^- as a function of the internal energy, U , of the molecular anion. The bottom panel shows the same ratios experimentally observed for an N_2 target as a function of relative collision energy, E .

Future Plans Our immediate plans for future investigations include an upgrade to the surface apparatus in which we will install a general purpose ion source to replace the alkali positive ion source currently in place. The new source will utilize three stages of differential pumping (to maintain UHV conditions), and be able to provide both positive and negative, low energy ion beams for surface probes. The discharge ion source will also be capable of producing ion beams of reactive species such as CF_3^+ , which will enable us to perform experiments related to semiconductor etching, etc. In the area of gas phase collisions we will complete the present experiments involving SF_6^- and then turn to examine the ion molecule chemistry for reactants involving SF_5^+ .

Recent Publications(≥ 1998)

Ion-induced secondary electron and negative ion emission from Mo/O.

J. C. Tucek, S. G. Walton, and R. L. Champion
Surf. Sci. 410, 258 (1998).

Negative ion emission from a stainless steel surface due to positive ion collisions.

S. G. Walton, R. L. Champion, and Yicheng Wang
J. Appl. Phys. 84, 1706 (1998).

Collision-induced dissociation, proton abstraction, and charge transfer for low energy collisions involving CH_4^+ .

B. L. Peko, I. V. Dyakov, and R. L. Champion
J. Chem Phys. 109, 5269 (1998).

Photon-Induced anion emission: A mechanism for ion-induced secondary-electron emission from an Al/O surface.

S. G. Walton, B. L. Peko, and R. L. Champion
Phys. Rev. B58, 15430 (1998).

Cross section measurements for various reactions occurring in CF_4 and CHF_3 discharges.

B. L. Peko, I. V. Dyakov, and R. L. Champion
Gaseous Dielectrics VIII, ed by L. Christophorou and J. Olthoff. Plenum Press
New York, 1998, p 45 ff.

Low energy, ion-induced electron and ion emission from stainless steel: The effect of oxygen coverage and the implications for discharge modeling.

S. G. Walton, J. C. Tucek, R. L. Champion and Y Wang.
Journal of Applied Physics 85, 1832 (1999).

Ion-molecule reactions and ion energies in a CF_4 discharge.

B. L. Peko, I. V. Dyakov, R. L. Champion, M.V. Rao and J. K. Olthoff.
Phys. Rev E60, 7449 (1999).

The role of O and Cl adsorbates on the secondary emission properties of tungsten.

W. S. Vogan, S. G. Walton and R. L. Champion
Surface Science 459, 14 (2000).

Amplitude Modulation of Atomic Wavefunctions

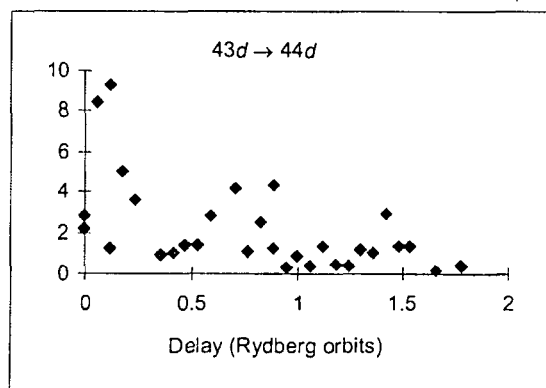
William E. Cooke
Department of Physics
College of William and Mary
Williamsburg, Virginia 23187-8795
DE-FG02-97-ER14800, August 2000

Recent Results

During this past year, we have observed and characterized amplitude modulation in strontium Rydberg wave functions, and we have used our new method of identifying Rydberg state populations to begin characterizing the redistribution of Rydberg states due to an intense unipolar, or half-cycle pulse (HCP).

The basic idea of our wave function modulation technique is to excite and de-excite a core electron with two short laser pulses while a second electron is in a Rydberg state. This type of transition is commonly called an Isolated Core Excitation (ICE) since the laser excitation does not affect the Rydberg electron directly. However, during the short time between the excitation and the de-excitation pulses, the new core electron wave function changes the potential seen by the small r portion of the Rydberg electron. This modulates the Rydberg electron wave function. Our initial studies used barium, but the potential change was too small to accomplish much modulation. We have now shifted one of our studies to strontium, where we have modulated $5snl$ wave functions by driving the transitions $5snl \leftrightarrow 5pnl$ at 412 nm. We expected strontium to show much more modulation because the $5snl$ states are strongly perturbed by the $4d6s$ configuration. When the core electron is excited, this perturbation is removed, so the effective potential changes considerably. We did, in fact, observe considerable redistribution in strontium, as we reported last year. During this past year, we have taken detailed data. Our signal generally consists of two parts: one portion oscillates at the optical frequency and represents our desired separated-step process; a second term varies slowly and represents the interference between the two transitions driven during either of the two core pulses.

The accompanying figure shows typical results following core excitation/de-excitation of the $5s43d$ state resulting in a shake into a $5s44d$ state. Although we simultaneously observe shake into other states, this transition is the strongest. The figure shows how this transfer varies as a function of delay between the two core-laser excitation pulses. This data is the coefficient of only the very fast oscillation (at the optical frequency) to isolate the excitation due to one photon transition during *each* pulse. We are finishing the development of our data fitting routines and expect to have a complete



analysis within three months. Julie Grossen will shortly defend her thesis that describes these measurements in detail. These results will then be submitted to Physical Review A.

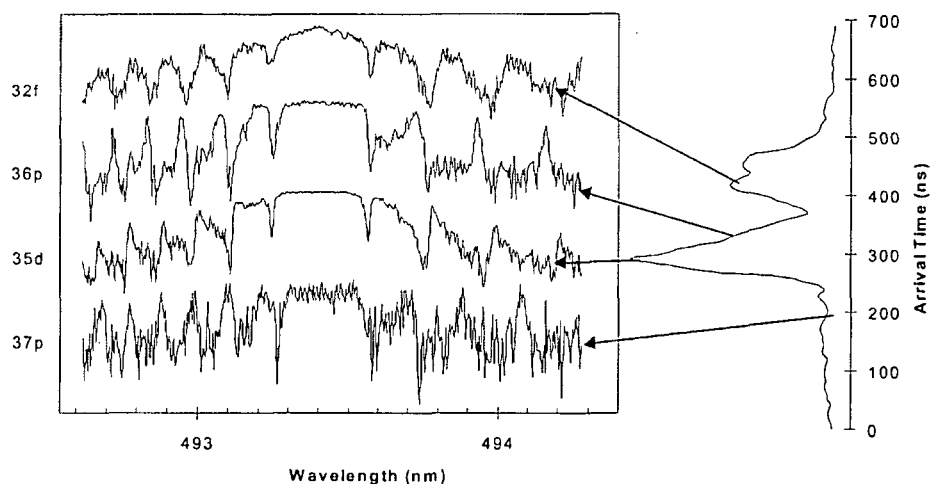
Our current method for detecting Rydberg wave packets is Selective Field Ionization (SFI) which determines the relative population in each Rydberg state. SFI is very simple to implement, one merely applies an increasing electric field to the Rydberg atoms, and collects the ions or electrons after field ionization. The arrival time of the products clearly marks the specific field at which an atom ionized, and consequently determines the atom's Rydberg state. However, field ionization is a slow process (compared to the classical Rydberg orbit time scale) so it can never be used to determine the relative phase between Rydberg states. Since wave function modulation creates phase and amplitude variations to make a coherent wave packet, a different technique (which can respond on a fast time scale) is necessary. We are currently exploring fast electric field redistribution and/or ionization as an alternative scheme.

But, before we can use fast electric field redistribution and/or ionization, it is also necessary to characterize that process on an isolated atom - and even that requires an improvement on the standard SFI Rydberg state detection. SFI has several limitations that are especially troublesome when one needs to characterize a mixture of various values of n and l . First, classical field ionization values ($315/n^4$ MV/cm) only work for low angular momentum states of heavy atoms, while higher l values for all atoms ionize at the more complicated hydrogenic field ionization values. Also, spin couplings between valence electrons can broaden or split the effective field ionization thresholds. Depending on the rate at which the electric field pulse increases, many states show *more than one threshold* as the path to ionization encounters many curve crossings which are neither purely diabatic nor purely adiabatic. The net result is that field ionization must be characterized for *each* state of *each* atom before it can be used for truly comprehensive state analysis. Finally, the state density can be so high for Rydberg states, that even the best SFI detector will not be able to separate adjacent l state thresholds.

In order to study state redistribution by an intense HCP, we have combined SFI and ICE. ICE alone can provide a very specific state determination due to two features in the ICE spectra. Most noticeably, the zeroes in the transition moment (e.g. $6snd \rightarrow 6pnd$ in barium) occur exactly where the effective quantum number of the final state differs by an integer from that of the initial effective quantum number. This affect alone has enabled us to measure the initial effective quantum number to an accuracy of better than 0.1 which clearly separates all the nl states with $l \leq 3$ in barium. Secondly, the positions and the line widths of the autoionizing $6pnl$ states differ significantly with l , showing a rapid monotonic decrease for $l \geq 3$. Finally, the asymmetry near the zero depends on the ratio of the change in quantum defect (with and without core excitation) divided by the line width of the excited, autoionizing resonance. So, the zero position easily determines n , while the shape of the spectra near the zeroes determines l . Of course, this process is complicated considerably if there are many different values of n and l in the any particular mixture of Rydberg states. However, that is precisely where the additional use of SFI allows us to telescope in to just a few values by setting our time gate to monitor only those atoms which ionized at a specific field.

During this past year, we have shown that our combined technique can measure the effects of applying an intense HCP to Rydberg states with $30 < n < 40$. The next figure shows the results of

applying a modest (~ 1.2 KV/cm) HCP to a barium $6s35d$ state. The right-hand panel shows the SFI signature, which had been a single peak at 280 ns in the absence of the HCP. The left-hand panel shows an ICE spectrum taken at each of the time delays designated by the arrows. The wealth of structure allows us to unambiguously identify the myriad of states that are overlapping in their SFI spectra, and the far-left identifies the major component of that spectrum. For example, the clear, sharp peaks in the spectrum at 330 ns identify that as almost entirely due to the $6s35p$ state, even though it is not distinct in the SFI spectra.



Jonathan Curley has developed this method in great detail, and has observed some initial tendencies of the HCP irradiation of Rydberg states. He will defend his thesis before the end of August, and has already prepared a paper describing the combined SFI/ICE technique to submit to Physical Review A.

Recent Publications

“Technique for measuring the linewidth of autoionizing Rydberg states,” Grzegorz Waligorski, Lei Zhou, and W. E. Cooke, Physical Review A **55**, 1544 (1997).

SEMIEMPIRICAL STUDIES OF ATOMIC STRUCTURE

L. J. Curtis

Department of Physics & Astronomy, University of Toledo, Toledo OH 43606

email: ljc@physics.utoledo.edu, URL: <http://www.physics.utoledo.edu/~ljc/sesas.html>

Program Scope and Definition

This project strives to produce a comprehensive and reliable base of accurate atomic structure data for complex many-electron systems. The atomic properties studied involve primary data (wavelengths, frequency intervals, lifetimes, relative intensities, production rates, *etc.*) and derived structural parameters (energy levels, ionization potentials, line strengths, electric polarizabilities, branching fractions, excitation functions, *etc.*). Large blocks of data are systematized and parametrized along isoelectronic, homologous, isoionic, Rydberg, and yrast series. This is accomplished through the use of sensitive data-based mapping reductions, precise experimental measurements, and specialized *ab initio* theoretical computations. Measurements are made primarily through the use of fast ion beam excitation methods, which are combined with available data from laser- and tokamak-produced plasmas, ion trap studies, astrophysical sources, and conventional spectroscopic light sources.

Recent Progress

Earlier studies on this project have demonstrated that high precision interpolative, extrapolative, and statistically smoothed predictions can be made through suitable semiempirical reductions of measured data. By incorporating information from spectroscopic energy level measurements, atomic transition probability data can be presented in an exposition that removes the effects of intermediate coupling, and permits the perturbative effects of configuration interaction, higher order moments, *etc.* to be accurately characterized by a regular and slowly varying parametrization. Thus a small number of precision measurements can be used to generate a large base of reliable and comprehensive data. These methods have been successfully applied to the alkali-metal-like, alkaline-earth-like, and inert-gas-like isoelectronic sequences, and we have summarized the state of knowledge of these systems in a comprehensive review presented as a chapter in a recent monograph [5]. During the past year we have further refined and extended these methods, applying them to many-electron systems of increased complexity and to branched transitions. This has been aided by the increasingly large base of precision data that is becoming available, especially through the utilization of recent measurements of intercombination transitions near the neutral ends of several isoelectronic sequences.

The singlet-triplet mixing angle formulation has been particularly successful by virtue of its ability to combine in a single exposition [5] measurements for both resonance and intercombination lines in either the alkaline-earth-like or the inert-gas-like systems. This allows measurements of resonance transition rates to be used to predict intercombination rates and vice versa. This is quite advantageous because these data tend to have a complementary measurability, with the resonance lifetimes being very short at high Z and the intercombination lifetimes being very long at low Z . New methods (ion traps, *etc.*) yield precision values for intercombination lifetimes near the neutral end of the sequence. This has provided a very sensitive probe of the mixing angle formulation, because the intercombination line strength is dependent on the sine of the mixing angle, which is very small near the neutral end of the sequence (and thus introduces a large correction in the semiempirical parametrization).

An extension of the mixing angle formalism has been made [14] to include the effects of spin-other-orbit interaction as well as differences between singlet and triplet radial wave functions. In the simplest singlet-triplet formulation, the diagonal and off-diagonal magnetic parameters are both set equal to the standard spin-orbit energy. However, already in 1932 Wolfe [Phys. Rev. **41**, 443 (1932)] showed that this formulation can be extended to include the spin-other-orbit interaction energy, since this correction contributes constructively to the diagonal and destructively to the off-diagonal matrix elements. The same effective parametrization with a different phenomenological origin was independently suggested in 1939 by King and Van Vleck [Phys. Rev. **56**, 464 (1939)]. They argued that the radial wave functions may be slightly different for singlet and triplet states within the same configuration, and hence yield different diagonal and off-diagonal spin-orbit integrals. The quality and scope of the data base now available finally permit accurate testing of these early suggestions, and this parametrization has been found to significantly improve the systematization. Since both of the physical mechanisms described above lead to the same expression, the determination of these parameters from measured spectroscopic data can effectively account for both spin-other-orbit interaction and differences between the singlet and triplet radial wave functions, as well as any other contributions that mimic their isoelectronic behavior.

As evidenced in the exposition of Ref. [5], ns - np transitions in alkali-metal-like and ns^2 - $nsnp$ transitions in alkaline-earth-like systems are now well characterized for the entire isoelectronic sequence. However, as pointed out in [5], these methods can presently be applied only to the lowest lying $\Delta n=0$ resonance and intercombination transitions since there the decays are unbranched, allowing line strengths to be deduced directly from lifetime measurements. The regularly and slowly varying isoelectronic behavior exhibited by the line strength does not occur for reciprocal lifetime data for a branched decay, since this involves a sum over many different line strengths, each multiplied by a wavelength factor with a complicated isoelectronic variation. For $\Delta n>0$ transitions, significant branching usually occurs, and the reduction of lifetime measurements to line strength factors requires a knowledge of branching fractions. As indicated in Ref. [5], measurements for these quantities are virtually non-existent in multiply charged ions. The reasons are clear, since the intensity calibration of the detection apparatus using continuum radiation standard lamps poses many problems, and intensity calibration standards based on line radiation in the UV are presently lacking. We have thus undertaken a program of determination of branching fractions of ionic transitions in the UV region.

One portion of this work involved a beam foil study [16] of Sn II, combining a lifetime measurement of the $5s^25p\ ^2D_{1/2}$ level with a measurement of the branching fraction of its decay transitions $5s^25p\ ^2P_{1/2,3/2} - 5s^25p\ ^2D_{1/2}$ at 1400 and 1489 Å. The lifetime measurement utilized the cascade-correlated ANDC method, yielding a value 0.44 ± 0.02 ns. The branching fraction measurement required a calibration of the relative efficiency of our detection apparatus in this wavelength region, which was carried out with NIST-calibrated argon mini-arc secondary standard. The measurement yielded a branching ratio of 0.76 ± 0.04 which combines with the lifetime measurement to give a transition probability for the $\lambda 1400$ Å resonance transition of 1.762 ± 0.084 ns⁻¹.

Another portion of the work involves the development of standards of line radiation in the UV to use in calibrating detection equipment. We have shown earlier [1] that transitions of the form ns^2np^2 - ns^2npn 's in Si I and Ge I are virtually free of configuration interaction, hence their branching fractions can be accurately predicted from intermediate coupling amplitudes deduced from measured spectroscopic energy level data. In this case both the upper and the lower levels are characterized by singlet-triplet mixing angles. Our earlier predictions for Ge I [1] were strikingly confirmed by subsequent branching fraction measurements [Li *et al*, Phys. Rev. A **60**, 198 (1999)]. This motivated the extension of these semiempirical methods to the ions P II, S III, Cl IV and Ar V in the Si sequence [13], to As II, Se III and Br IV in the Ge sequence [13], and to Sb II, Te IV, I IV, Xe V and Cs VI of the Sn sequence.

A similar situation holds for low lying transitions in the Zn, Cd, and Hg isoelectronic sequences. In these cases we have carried out a study [14] predicting branching fractions and relative transition probabilities for the $ns^2\text{-}nsp$ and $nsp\text{-}nsnd$ supermultiplets in Ga II, In II and Tl II. In this work we also applied the extended singlet-triplet mixing angle formalism that incorporates spin-other-orbit interaction and differences between the singlet and triplet radial wave functions. The transition moments between these configurations can also be expressed in terms of the mixing angles and the transition moments in pure spin-orbit coupling, and in the non-relativistic Schrödinger approximation the radial matrix element is the same for all members of a given supermultiplet. In cases for which lifetime measurements are available for the individual values of J for the upper level, it is possible to test whether the J -independence of the supermultiplet radial matrix element, and if that independence is verified, to use these branching fractions to predict lifetimes for the entire supermultiplet given a known lifetime for a single upper level. Using this formalism, we were able to predict the 3D_J lifetimes in Ga II of the $J=1,2$ levels from a measurement for $J=2$ level. In In II all of the sd lifetimes have been measured, so it was possible to predict the individual transition probabilities.

These new results in these ionic systems provide a set of branching fractions that can both specify transition probability rates from lifetime measurements for these ions, and serve as a set of lines of known relative intensities for application to the calibration in the UV region of detection apparatus used in fast ion beam studies.

Future Projects

Because of the success of these semiempirical methods at presenting measured data in a concise and predictive manner, we plan to develop a convenient and user-friendly graphical exposition by which nonspecialist users can obtain the line strength for any desired resonance or intercombination line for any sequence for which an adequate base of isoelectronic data exists. Part of such an exposition already exists in the linearization of the reduced line strengths factors $S_r(\text{Res}) \equiv S(\text{Res})/\cos^2\theta$ and $S_r(\text{Int}) \equiv S(\text{Int})/\sin^2\theta$, but to obtain the physical line strengths, a similar predictive linearization is needed for the mixing angles themselves. A promising formulation in which the quantity $\cot 2\theta$ appears empirically to follow a simple power law dependence in the quantity $1/(Z-C)$ for the Be, Mg, Zn, Cd, and Hg sequences, with this power law being nearly linear for the Zn, Cd, and Hg sequences.

These methods are now being applied in a comprehensive study of the Cd sequence. This is a particularly interesting isoelectronic system, since it begins at a sufficiently high value of Z to possess a very complex core, and yet is low enough in Z to contain many isoelectronic members before reaching the radionuclides (as occurs at the fifth member for the Hg sequence). Thus permits an investigation of the apparent trend of these semiempirical systematizations to be more reliably applicable to complex many electron systems (where *ab initio* calculations are difficult) than they are for simpler systems (where *ab initio* methods are already quite effective). As part of this study we perform *ab initio* calculations over the entire sequence, taking care to maintain a consistent approach for all Z , in efforts to investigate and verify the apparent linearities revealed in the semiempirical studies. Through this theoretical buttressing of the empirical studies we hope to determine the accuracy with which the trends observed for low and intermediate Z can be used to predict values to much higher Z .

A number of projects are also planned utilizing the Argonne ATLAS facility in collaboration with ANL and the University of Notre Dame. For example, we shall explore the use of tilted foils and of magnetized layers to develop a beam of polarized one-electron ions in the metastable $2^2S_{1/2}$ state. Such a beam will permit new types of experiments involving measurement of the angular distribution of decay radiation induced by an external electric field. We also plan to measure state-specific cross sections in the intermediate energy regime for collisions of He-like Ni with various gas targets. These

data would extend the state specific information to a region where relativistic corrections to the energy levels of the projectile ion are more important.

Publications and Submissions of DoE Sponsored Research during 1998, 1999, 2000

1. L.J. Curtis, "Use of Intermediate Coupling Relationships to Test Measured Branching Fraction Data," *J. Phys. B: Atomic, Molec. & Opt. Phys.* **31**, L769-74 (1998).
2. R.M. Schectman, H.S. Povolny, and L.J. Curtis, "Selected Lifetime and Oscillator Strength Measurements in Si II," *Astrophys. J.* **504**, 921-4 (1998).
3. R.E. Irving, M. Henderson, D.G. Ellis, L.J. Curtis, Y. Zou, R. Hellborg and I. Martinson, "Lifetimes of Doubly-Excited $2p^3/$ Levels in Singly Ionized Boron, B II," *Physica Scripta* **57**, 630-3 (1998).
4. A. Vasilyev, E. Jasper, H.G. Berry, A.E. Livingston, L.J. Curtis, S. Cheng, and R.W. Dunford, "Lifetimes of the $3p^2P_{3/2}$ in Sodium-Like Bromine (Br XXV)," *Phys. Rev.* **58**, 732-5 (1998).
5. L.J. Curtis and I. Martinson, "Lifetimes of Excited States in Highly Charged Ions," Chapter 10 of *Atomic Physics with Heavy Ions*, H.F. Beyer and V.P. Shevelko, editors, Springer-Verlag, Berlin/Heidelberg, 1999, pp. 197-218.
6. R. Hellborg, L.J. Curtis, B. Erlandsson, J. Persson, P. Persson, G. Skog and K. Stenström, "Development of Accelerator Mass Spectroscopy at the Lund Pelletron," in *Advances in Nuclear Physics and Related Areas* (Giapouli Publishing, Thessaloniki Greece, 1999) pp. 908-13.
7. R.E. Irving, M. Henderson, L.J. Curtis and I. Martinson, "Accurate Transition Probabilities for the $2s^2^1P_0 - 2s2p^1P_1$ Transition in Be I and B II," *Can. J. Phys.* **77**, 137-43 (1999).
8. M. Henderson, R.E. Irving, L.J. Curtis, and I. Martinson, "Lifetimes of the $5d^96p$ levels in Hg III," *Phys. Rev. A* **59**, 4068-70 (1999).
9. M. Henderson, R.E. Irving, R. Matulioniene, L.J. Curtis, D.G. Ellis, G.M. Wahlgren and T. Brage, "Lifetime Measurements for Ground Term Transitions in Ta II, W II, and Re II," *Astrophys. J.* **520**, 805-10 (1999).
10. H.W. Schäffer, R.W. Dunford, E.P. Kanter, S. Cheng, L.J. Curtis, A.E. Livingston, and P.H. Mokler, "Precision Measurement of the Two-Photon Spectral Distribution from Decay of the $1s2s^1S_0$ Level in Heliumlike Nickel," *Phys. Rev. A* **59**, 245-50 (1999).
11. E. Jasper, A. Vasilyev, K. Kukla, C. Vogel Vogt, H.G. Berry, S. Cheng, L.J. Curtis and R.W. Dunford, "Lifetime Measurements for Allowed and Forbidden Transitions," *Physica Scripta T* **80**, 466-8 (1999).
12. R.W. Dunford, E.P. Kanter, H.W. Schäffer, P.H. Mokler, H.G. Berry, A.E. Livingston, S. Cheng, and L.J. Curtis, "Higher Order Photon Transitions in H-like and He-like Ions," *Physica Scripta T* **80**, 143-4 (1999).
13. L.J. Curtis, "Intermediate Coupling Branching Fractions for UV Transitions for Si and Ge Isoelectronic Sequences," *J. Phys. B: Atomic, Molec. & Opt. Phys.* **33**, L259-63 (2000).
14. L.J. Curtis, "Branching Fractions and Transition Probabilities for Ga II, In II, and Tl II from Measured Lifetime and Energy Level Data," *Physica Scripta* **61**, 31-5 (2000).
15. R. Hellborg, L.J. Curtis, B. Erlandsson, J. Persson, P. Persson, G. Skog, and K. Stenström, "Development of Accelerator Mass Spectroscopy at the Lund Pelletron," *Physica Scripta* **61**, 530-5 (2000).
16. R.M. Schectman, S. Cheng, L.J. Curtis, S.R. Federman, M.C. Fritts, and R.E. Irving, "Lifetime Measurements in Sn II," *Astrophys. J.* **543** (2000) [20 October issue].

High Intensity Laser Interactions with Atomic Clusters

Principal Investigator:

Todd Ditmire

*Laser Science and Technology, Laser Program
Lawrence Livermore National Laboratory*

P. O. Box 808, L-477

Livermore, CA 94550

Phone: 925-422-1349

FAX: 925-422-5537

e-mail: ditmire1@llnl.gov

Program Scope:

The development of ultrashort pulse table top lasers with peak pulse powers in excess of 1 TW has permitted an access to studies of matter subject to unprecedented light intensities. Such interactions have accessed exotic regimes of multiphoton atomic and high energy-density plasma physics. Very recently, the nature of the interactions between these very high intensity laser pulses and atomic clusters of a few hundred to a few thousand atoms has come under study. Such studies have found some rather unexpected results, including the striking finding that these interactions appear to be more energetic than interactions with either single atoms or solid density plasmas. Recent experiments have shown that the explosion of such clusters upon intense irradiation can expel ions from the cluster with energies from a few keV to nearly 1 MeV. This phenomenon has recently been exploited to produce DD fusion neutrons in a gas of exploding deuterium clusters. Under this project, we have undertaken a general study of the intense femtosecond laser cluster interaction. Our goal is to understand the macroscopic and microscopic coupling between the laser and the clusters with the aim of optimizing high flux fusion neutron production from the exploding deuterium clusters or the x-ray yield in the hot plasmas that are produced in this interaction. In particular, we are studying the physics governing the cluster explosions. The interplay between a traditional Coulomb explosion description of the cluster disassembly and a plasma-like hydrodynamic explosion is not entirely understood, particularly for small to medium sized clusters (<1000 atoms) and clusters composed of low-Z atoms. We are focusing on experimental studies of the ion and electron energies resulting from such explosions through various experimental techniques. We are also examining how an intense laser pulse propagates through a dense medium containing these clusters.

Recent Progress

Much of the research undertaken this year has been focused on the interaction of our intense 30 fs pulses with deuterium clusters. This work is motivated by our recent observation of DD fusion in a gas of laser irradiated deuterium clusters. One of the principal goals of this project is to understand the explosion mechanisms of these clusters so that they can be manipulated to enhance the fusion yield. We have also undertaken studies of third harmonic generation from these intense cluster interactions to gain understanding of the electron oscillation dynamics during the interactions. Finally, we have examined hot electron generation from quite large clusters to gain information about how the nature of

the interaction evolves from the sub wavelength scale clusters to clusters of size approaching the laser wavelength (a size scale which may also, ultimately, be interesting for fusion research).

1) Interactions with deuterium clusters

We have conducted a variety of studies on the interaction of 30 fs pulses focused to intensity $>10^{16}$ W/cm² into gases of deuterium clusters. For example, we have conducted deuterium ion time of flight energy spectroscopy. These measurements were conducted from ions escaping the plasma in a high density gas jet (and were consequently not ideal because of space charge problems and ion slowing down in the surrounding gas. Future experiments solve these problems.) This measurement indicated that ions with energy out to 30 keV are produced in the exploding clusters, however, detailed studies of ion energy spectra require an apparatus enabling interactions with a low density cluster beam.

One of the principal diagnostics in these experiments has been the measurement of the 2.45 MeV fusion neutron production. To gain information on the explosion mechanisms, we examined the fusion neutron yield as a function of cluster size (see ref [1]). We find that the fusion yield increases rapidly as the average cluster size increases from 5 to 8 nm. We vary the average cluster size by changing the temperature of the gas jet backing reservoir with liquid helium cooling. The rate of the yield increase with cluster size increase appears to be consistent with a Coulomb explosion model of the ion ejection (In this model, the laser field strips the cluster of its electrons on a time scale much faster than the cluster expansion. The Coulomb forces between ions then drive an explosion. In this simple picture, the ion energies should scale as the square of the cluster size.) In addition, we find that as we increase the average cluster size further to 10 nm, the yield rolls over. We have conducted extensive interferometric probing of the plasmas to gain information on the laser propagation dynamics and now believe that this roll over is the result of increased laser absorption and energy depletion in the front edges of the gas jet. These results are currently under analysis and will be submitted for publication shortly.

2) Two color pump probe experiments

We have also begun pump probe experiments to explore the expansion dynamics of larger, laser heated clusters. In particular, we have constructed an experiment to examine the third harmonic generation of 800 nm pulses in a gas of xenon clusters as the clusters expand from the photoionization and heating of a an initial pump pulse (which has a wavelength of 400 nm). This pump-probe experiment is designed to yield information on the nonlinear oscillation dynamics of the electron cloud in an expanding cluster. This experiment follows on experiments conducted at LLNL two years ago on the linear absorption of a probe laser pulse in xenon clusters as a function of delay after an ionizing pump.

We have conducted initial experiments and have seen some variation of third harmonic signal as delay between the 800 nm and 400 nm pulses. We have not yet reproduced the original absorption measurement (which used 800 nm pulses for both pump and probe) and attribute this to inadequate intensity in the pump pulse to drive the xenon explosion. We have procured appropriate optics to enhance the pump intensity and will begin another round of experiments in the fall.

3) Interactions with large, wavelength scale clusters

Finally, we have conducted a series of experiments on the production of fast electron during the interaction of our intense femtosecond pulses with clusters of diameter approaching that of the laser

wavelength. In these experiments, we produced water clusters with diameter around $1\ \mu\text{m}$ using a special jet developed in a collaboration with Tom Donnelly at Harvey Mudd College. The 30 fs laser pulse was focused to an intensity of nearly $10^{18}\ \text{W}/\text{cm}^2$ into a spray of these small water droplets (whose sizes were characterized by Mie scattering).

The laser produced hot electrons which then produced hard x-rays via bremsstrahlung. We measured the x-ray spectra to gain information about the electron spectra. These measurements indicated that the laser irradiation produced electrons with an effective temperature of around 1 MeV [3]. This result is remarkable because hot electrons produced from a planar target under nearly identical irradiation conditions exhibited a hot electron temperature only half that from the water droplets. We have compared these experimental results with particle-in-cell calculations and have found that this enhancement in hot electron temperature is a result of the laser field distribution around the wavelength scale particle. We are conducting further studies to ascertain the scaling of hot electrons with cluster size.

Future Research Plans

Our future research plans are aimed at an understanding of the interactions between the laser and single clusters to understand in more detail the energy deposition mechanisms. Studies during the previous year have concentrated on interactions of the laser pulse with high density gas jets containing clusters. By using a low density molecular beam of clusters, we intend to undertake a series of studies on single cluster interactions.

To do these future experiments we have constructed a time-of-flight spectrometer coupled to a molecular beam. We have fitted a chamber with a cryogenically cooled gas jet, capable of producing large hydrogen and deuterium clusters with sizes ranging from a 1 to 10 nm. Laser pulses are focused with an aspheric lens into this beam of clusters and fast ejected particles are detected along an axis perpendicular to both the laser and the cluster beam. This spectrometer is designed to yield information on both ion and electron energy spectra. Ion spectra will be characterized both through direct, field free ion time of flight as well as through the use of charged retarding grids. This spectrometer will allow us to examine ions with energy up to 1MeV and will allow charge state differentiation on ions with energy to charge state ratios up to 20 keV/Z. We will also analyze electron spectra, which will be measured by scanning the voltage on the retarding grids.

1) Our first set of experiments will be to examine the ion energy distributions from hydrogen clusters. This is important information in calculating the expected fusion yield from exploding deuterium clusters. We intend to examine these distributions as a function of average cluster size (varied by changing the gas jet temperature) as well as laser intensity, wavelength and pulse width. We will also examine electron energy distributions. This information will be compared to simulations of the laser-hydrogen cluster interactions being developed by Ken Kulander now at LLNL. This round of experiments will essentially examine explosions in the pure Coulomb explosion regime from low Z species. Information derived here will then be used to optimize fusion yield in the high density deuterium gas jet experiments.

2) We then intend to examine spectra from higher Z species (namely N_2 , Ar, Kr and Xe) This will allow us to explore the nature of the cluster explosions as it evolves from a pure Coulomb explosion to a hydrodynamic explosion. Here, electron and ion spectra will be compared with particle dynamics

simulations (i.e. the Kulander model) as well as with hydrodynamic simulations (i.e. the Hyades hydro-code).

3) Additional experiments will follow up on the two color pump probe experiments. While we intend to continue the third harmonic experiments in Xe clusters, we will also begin to look at electron and ion spectra from these two pulse interactions. Once again, we will likely concentrate on deuterium clusters with an eye toward optimizing ion energies for fusion studies.

4) Finally, we will follow up on the micron scale droplet experiments. In particular, we will likely examine the electron spectra directly. We will begin with the electrostatic TOF spectrometer, however, it is likely that we will require a magnetic spectrometer to fully characterize the fast electrons produced in these interactions.

Papers published or submitted on work supported by this grant:

- 1) J. Zweiback, R.A. Smith, T.E. Cowan, G. Hays, K.B. Wharton, and T. Ditmire, "Nuclear Fusion Driven by Coulomb Explosions of Large Deuterium Clusters," *Phys. Rev. Lett.* **84**, 2634 (2000).
- 2) T. Ditmire, J. Zweiback, V. P. Yanovsky, T. E. Cowan, G. Hays, and K. B. Wharton, "Studies of Nuclear Fusion in Gases of Deuterium Clusters Heated by a Femtosecond Laser," *Phys. Plas.* **7**, 1993 (2000).
- 3) T. D. Donnelly, M. Rust, I. Weiner, M. Allen, R. A. Smith, C. A. Steinke, S. Wilks, J. Zweiback, T. E. Cowan, and T. Ditmire, "Hard X-ray Production from Intense Laser Irradiation of Wavelength-Scale Particles" *Phys. Rev. Lett.*, submitted.
- 4) J. Zweiback, T.E. Cowan, J. Hartley, G. Hays, R. Howell R.A. Smith, C. Steinke, and T. Ditmire, "Characterization of Fusion Burn Time in Exploding Deuterium Cluster Plasmas," *Phys. Rev. Lett.* submitted.

Collective Few Body Coulomb Excitations

James M. Feagin

Department of Physics

California State University–Fullerton

Fullerton CA 92834

jfeagin@fullerton.edu

Advances in light source technology have promoted photo double ionization as a fundamental technique for studying the few-body Coulomb problem and especially few-body fragmentation. This project aims to advance our basic understanding of interacting charged particles, in particular, few body Coulomb systems composed of negative electrons and the positive ions they are attached to. In the past ten years, we have seen experiments in helium above and below the double ionization threshold evolve through third and fourth generations. Nevertheless, excitations near threshold on the order of a few eV above or below remain largely unexplored both experimentally and theoretically due to the extremely complicated, likely chaotic, dynamics involved. In recent years there has thus been a shift towards development of first generation photoexcitation experiments with small molecules, because of their experimental accessibility but also because of their intrinsic interest. The few-body fragmentation of these systems also lends itself to fundamental studies of the quantum multiparticle correlations. Peculiarities of quantum entanglement aside, the modern quantum mechanic seeks to exploit these correlations to establish new probes of the quantum and semiclassical excitation amplitudes.

We continue to place strong priority on research relevant to experiment and to maintaining collaborations with experimental groups in this country and in Europe. Our recent efforts in this project have concentrated on: (1) advanced light source ionization of small molecules and understanding the resulting collective excitation; (2) quantum correlations and entanglement with recoil ions as novel probes of few-body fragmentation; and (3) lattice wavepacket simulation of collective excitations relevant to, for example, quantum computing and electron transport in mesoscopic devices. These projects are a continuation of work begun by the principal investigator and supported by the Department of Energy.

Full Photofragmentation of Molecular Hydrogen The coincident measurement of two continuum electrons has been extended to the photo double ionization of molecular hydrogen in the experimentally convenient isotopic form D_2 . Reddish and coworkers¹ in Newcastle and Schmidt and coworkers² in Freiburg have demonstrated a remarkable likeness of D_2 and helium triply differential cross sections (TDCS). L. Cocke along with Dörner and coworkers in Frankfurt have performed at the Advanced Light Source in Berkeley similar experiments but detected instead the

¹ T. J. Reddish, J. P. Wightman, M. A. MacDonald, and S. Cvejanovic, *Phys. Rev. Lett.* **79**, 2438 (1997); J. P. Wightman, S. Cvejanovic and T. J. Reddish, *J. Phys. B* **31**, 1753 (1998).

² N. Scherer, H. Lörch and V. Schmidt, *J. Phys. B* **31**, L817 (1998).

ion pairs in coincidence with the escaping electrons.³ This is a system of fundamental interest since the final state is one with four unbound Coulomb-interacting particles, which introduces several new twists in the physics of double ionization. For example:

- The finite separation of the two nuclei in the initial state and their relative momentum in the final state are new vector quantities that clearly influence the electron angular distributions. The spherical symmetry of the initial state is broken and the electrons in the final state no longer see a point charge.
- The two-center geometry of the nuclear field can give rise to interference effects which can be used to probe the electron-pair continuum correlations in novel ways.
- In atoms, the nucleus acquires at most a small recoil energy of the order of meV, while in molecules the 'Coulomb explosion' of the nuclei results in ionic kinetic energies of several eV, which can be on the order of the final electron energies. The ion pair thus forms a key element of the few-body continuum.

In atoms, the true double-ionization threshold corresponds to the three particles all having zero energy at infinite separations, a highly correlated configuration with all the elements of the three-body problem. In H_2 or D_2 , the corresponding four-body configuration is not directly accessible by photon absorption, since a single photon puts the molecule at an energy corresponding to the Coulomb explosion energy and therefore well above the four-body breakup threshold. The question of the relevance of a threshold analysis for the molecule is nevertheless subtle. The relevant quantities deciding the Coulomb correlation are not the energies of the particles but their relative velocities. In a vertical transition, even when the electrons are ejected with only tens of meV, the ions are still moving slowly with respect to the electrons at the time of breakup. Only later do they begin to move apart under their mutual repulsion. Hence, when all four particles are close together there is likely an influence on the ionic motion by the electronic motion and the formation of a correlated continuum even though the system is far from the true four-body threshold. In the experiments reported so far, where the electrons have 10 eV energy initially, it would seem that they are first ionized and leave the molecular region before the ions have moved significantly.

We have thus been motivated to extend our helium double ionization description to $D_2(\gamma, 2e)$ angular distributions.⁴ At 20 eV above the photo double ionization threshold, one essentially observes a sudden exit of the electron pair followed by a Coulomb explosion of the ion pair along the alignment direction of the molecule at the instant of photoexcitation. Within this 'axial recoil' approximation, we introduce our electron pair excitation amplitude from helium but replace the photon polarization vector by an effective polarization defined by the alignment of the molecular axis. We thus derive a helium-like expression for the electron-pair angular distribution which depends on the orientation of the ion axis at the instant of photoionization.

When integrated over the alignment of an undetected ion axis for comparison with the data of Reddish and of Schmidt, we obtain an expression with two contributions: one identical in

³ R. Dörner et al, Phys. Rev. Lett. **81**, 5776 (1998); R. Dörner and L. Cocke, private communication.

⁴ J. M. Feagin, J. Phys. B **31**, L729 (1998).

form to the helium TDCS, and one with an angular distribution independent of the photon polarization direction and proportional to the square of the difference in amplitudes for parallel and perpendicular molecular excitation. The result is in good agreement with measured ratios of the TDCS in D₂ to that in He and explains observed increases in the ratios where the individual angular distributions vanish due to an exact parity-exchange selection rule.

It has been demonstrated that photo double ionization in helium with circularly polarized photons leads to a circular dichroism in the electron-pair angular distribution.^{5 6} We have thus extended our description of molecular photofragmentation to include dichroism.⁷ Although the phenomenon has a long and rich history in molecular physics, we focus on it as a tool to probe few-body Coulomb dynamics, viz. the transfer of photon chirality to the electron and ion pairs, and provide phase information on excitation amplitudes with a 'look in the mirror'.^{6 7} A new generation of synchrotron experiments is being planned to study this fundamental probe.⁸

Molecular Symmetry of Electron-Pair Atomic States Although resonant states for low-lying double excitations in helium can be classified according to H₂⁺ quantum numbers, it is known that this classification breaks down generally for high-lying resonances. Indeed, calculations show that just below threshold, the underlying classical mechanics is chaotic. Nevertheless, we continue to investigate the general significance of the saddle-inversion label A introduced by Lin, which we have found to be fundamental to the overall classification of electron-pair states above and below threshold.^{9 10}

Quantum Correlations with Recoil Ions We have begun to examine electron and recoil-ion coincidence detection with interferometers following impact ionization. Besides using charged particles—as opposed to photons—to study entanglement and complementarity,¹¹ we find the approach provides new tools for probing scattering amplitudes and few-body Coulomb correlations. For example, we find that the electron detection rate following two-slit interference depends on the product of ionization amplitudes evaluated at the electron momentum corresponding to passage through each slit.¹² Thus, coherent phase information is gained, analogous to the technique of 'quantum phase-space tomography', which is normally lost in conventional scattering experiments.

Diffraction Realizations of Quantum Computing We continue to explore with wavepacket

⁵ J. Berakdar, H. Klar, A. Huetz and P. Selles, *J. Phys.* **B26**, 1463 (1993).

⁶ V. Mergel et al, *Phys. Rev. Lett.* **80**, 5301 (1998).

⁷ T. J. Reddish and J. M. Feagin, *J. Phys.* **B32**, 2473 (1999).

⁸ L. Cocke and R. Dörner, private communication.

⁹ R. Dörner, H. Bräuning, J. M. Feagin et al, *Phys. Rev.* **A57**, 1074 (1998).

¹⁰ J. M. Feagin, M. Walters and J. S. Briggs, *J. Phys. B*, in press (2000).

¹¹ W. K. Wootters and W. H. Zurek, *Phys. Rev.* **D19**, 473 (1979).

¹² J. M. Feagin, Workshop on Many Particle Dynamics (Bad Honnef), invited talk, May (2000); Si-ping Han and J. M. Feagin, in preparation (2000).

simulation how a Grover quantum-computer search¹³ can be realized by diffracting electrons through a mesoscopic junction, and in particular how such a device might be optimized with multiple correlated electrons on atomic length scales. With wavepacket simulation, we have shown that a Grover search can be realized with special spatial filtering within a laser cavity operated in pulsed mode.¹⁴ Much of our research effort has been in looking for ways to implement quantum entanglement into our device, which is widely believed to be a key advantage of quantum over classical computing. We have found, however, that this claim, while accurate by and large, is incomplete: it is possible to obtain quantum speedups using special-purpose devices such as ours that do not necessarily exhibit strong entanglement.¹⁵ We are also investigating electron wave-packet correlation and propagation in various quantum corrals. We find that an electron wavepacket dropped on one focus of an elliptical corral will form a 'whispering-gallery image' at the other focus, simulating an effect which has been spectacularly demonstrated with scanning tunnelling microscopy.¹⁶

Recent Publications

Molecular Symmetries of Electron-Pair Atomic States, J. M. Feagin, M. Walters and J. S. Briggs, *J. Phys. B*, in press (2000).

Photo Double Ionization of Molecular Deuterium, T. J. Reddish and J. M. Feagin, *J. Phys. B* **32**, 2473 (1999).

A Helium-Like Description of Molecular Hydrogen Photo Double Ionization, J. M. Feagin, *J. Phys. B* **31**, L729 (1998).

Photo Double Ionization of Spatially Aligned D₂, R. Dörner et al, *Phys. Rev. Lett.* **81**, 5776 (1998).

Helicity Dependence of the Photon-Induced Three-Body Coulomb Fragmentation of Helium Investigated by Cold Target Recoil Ion Momentum Spectroscopy, V. Mergel et al, *Phys. Rev. Lett.* **80**, 5301 (1998).

Photo Double Ionization of Helium: Fully Differential and Absolute Electronic and Ionic Momentum Distributions, R. Dörner, H. Bräuning, J. M. Feagin et al, *Phys. Rev. A* **57**, 1074 (1998).

¹³ L. K. Grover, *Phys. Rev. Lett.* **79**, 325 (1997); I. L. Chuang et al, *Phys. Rev. Lett.* **80**, 3408 (1998).

¹⁴ A. T. Jurhs, J. Soneson and J. M. Feagin, in preparation (2000).

¹⁵ S. Lloyd, xxx.lanl.gov, quant-ph/9903057 (1999).

¹⁶ H. C. Manoharan et al, *Nature* **403**, 512 (2000); E. Heller, *Nature News and Views* **403**, 489 (2000).

Studies of Autoionizing States Relevant to Dielectronic Recombination

T.F. Gallagher
Department of Physics
University of Virginia
P.O. Box 400714
Charlottesville, VA 22901
tfg@virginia.edu

The scope of this program is slightly broader than the title suggests. We are in fact, investigating problems which exist in two valence electron atoms but not in single valence electron atoms. Our major focus has been on questions directly relevant to dielectronic recombination, but we have also been working on inner electron ionization. Many of the insights derived from the study of two electron atoms have turned out to be applicable to more complex systems, such as molecules.

In the past year we have worked on two topics; dielectronic recombination (DR) from a continuum of finite bandwidth, and multiphoton inner electron ionization.

DR, the recombination of an ion and an electron through an intermediate doubly excited autoionizing state, is the dominant electron-ion recombination mechanism in high temperature plasmas. Such plasmas are found in fusion plasmas and in stars. The Rydberg autoionizing states play a central role in the process, and as a result it is not surprising that small electric fields can have a significant effect.¹ Electric fields mix low angular momentum character into high angular momentum states so that more states contribute to DR, which tends to raise the total DR rate. On the other hand, electric fields also depress the ionization limit, reducing the number of available states, which tends to lower the DR rate. Taking both effects into account, the maximum DR rate for singly charged ions and electrons can be increased by a factor of two by an electric field of ~ 1 V/cm. Several years ago Robischaux and Pindzola suggested that relatively small \bar{B} fields, of approximately 100 G, could increase the DR rates by an analogous mixing of states of different magnetic quantum numbers.²

The enhancements produced by \bar{E} and \bar{B} fields occur at low fields, which are nearly impossible to reach in beam or storage ring measurements of DR. In contrast, it is straightforward to make such measurements even in zero \bar{E} and \bar{B} fields using a continuum of finite bandwidth. During the past year we have published a report of an experiment on DR from a continuum of finite bandwidth, in the presence of combined \bar{E} and \bar{B} fields.³

The experiments are done with Ba, and the continuum of finite bandwidth is the broad Ba $6p_{3/2}11d$ state which straddles the $Ba^+ 6p_{1/2}$ limit. We excite Ba atoms to the continuum of finite bandwidth, the $6p_{3/2}11d$ state, at a well defined energy. The quasi continuous $11d$ electron can be captured into $6p_{1/2}n6$ state, which decays radiatively to the bound $6s_{1/2}n6$ state which we detect by field ionization. Here n , 6 , and m , denote the principal, orbital angular momentum, and azimuthal angular momentum quantum numbers. We have used \bar{E} fields of 0, 0.5, 1.0, and 2.0 V/cm and \bar{B} fields from 0-240 G. We found a clear increase in the DR rate with $\bar{B} \perp \bar{E}$ but no

increase with $\bar{B} \parallel \bar{E}$. There is no increase when $\bar{B} \perp \bar{E}$ because the m quantum number remains good and there is no m mixing. Our experiments suggested that the magnetic field enhancement saturated at 240 G, a finding consistent with that of Bartsch et al., who found that the DR rate declined as \bar{B} (with $\bar{B} \perp \bar{E}$) was raised from 200 to 600 G.⁴

It was clear that it would be useful to raise our magnetic field beyond 240 G, and an apparently equivalent approach is to take advantage of Larmor's theorem and use a rotating, or circularly polarized, electric field. With this thought in mind we have examined DR in the presence of microwave field with linear and circular polarization. An 8 GHz frequency is equivalent to a 5 kG field. To our initial surprise, we could not see any difference between linear and circular polarization. What we did see though is resonant enhancement of DR when the microwave frequency matches the $\Delta n = 1, 2,$ or 3 spacing of the autoionizing Rydberg states. We have verified that the effect is resonant by changing the microwave frequency and observing that the enhancement in DR occurs at the energy for which the Δn spacing matches the microwave frequency. The origin of resonant enhancement is easily understood. When the microwave frequency matches the Δn separation the microwave field couples high l states differing in both l and n by one. In other words, there is a resonant l mixing analogous to that produced by a static electric field. As mentioned earlier, two valence electron atoms exhibit phenomena which can be exploited in other systems, and the resonant enhancement of DR is an excellent example. We expected that an analogous resonant enhancement should occur in ZEKE spectroscopy and have demonstrated that, indeed, it does.

We plan to continue this line of research in two ways in the coming year. First, we plan to explore a wider range of microwave frequencies, to compare more carefully linear and circular polarization, and to examine combined microwave and static fields. Second, we plan to return to the magnetic field enhancement with a stronger magnetic field so that we can map the whole region from 0 to 1000 G.

The second area of research is inner electron ionization. When an alkaline earth Rydberg atom is exposed to a laser pulse of duration shorter than the Kepler orbit time of the Rydberg electron that it is possible to eject the inner electron while leaving the outer electron bound to the atom. The reason for this observation is straightforward. If the pulse is so short, in some of the atoms the outer Rydberg electron does not come near the ion core and can not absorb the photon, while the inner electron easily absorbs the photon and is ionized. The outer electron is thus projected onto the ionic Rydberg states.

The description given above is a time domain description which suggests that if we started from a Rydberg wavepacket we should see the probability of inner electron ionization oscillate as the wavepacket moves radially in and out. We have made wavepackets of Sr and have just observed the expected oscillation in the inner electron ionization.

In the coming year we plan to explore this process more fully. First, we plan to measure not only whether or not inner electron ionization occurs, but also the dependence of the final Sr^+ states distribution on the position of the wavepacket. Second we plan to examine inner electron ionization from Sr Rydberg eigenstates of different l .

References

1. V.L. Jacobs, J. Davis, and P.C. Kepple, Phys. Rev. Lett. 37, 1390 (1976).
2. F. Robicheaux and M.S. Pindzola, Phys. Rev. Lett. 79, 2237 (1997).
3. V. Klimenko, L. Ko, and T.F. Gallagher, Phys. Rev. Lett. 83, 3808 (1999).
4. T. Bartsch, S. Schippers, A. Muller, C. Brandan, G. Gwinner, A.A. Saghir, M. Beutelspader, M. Grieser, D. Schwalm, A. Wolf, H. Danared, and G.H. Dunn, Phys. Rev. Lett. 82, 3779 (1999).

Publications 1998 - 2000

1. B.J. Lyons and T.F. Gallagher, "Mg $3s_{nf}$ - $3s_{ng}$ - $3s_{nh}$ - $3s_{ni}$ intervals and the Mg^+ dipole polarizability," Phys. Rev. A57, 2426 (1998).
2. D.A. Tate and T.F. Gallagher, "Multiphoton ionization dynamics of barium Rydberg states in intense femtosecond pulses," Phys. Rev. A58, 3058 (1998).
3. L. Ko, V. Klimenko, and T.F. Gallagher, "Enhancement of dielectronic recombination by an electric field," Phys. Rev. A59, 2126 (1999).
4. V. Klimenko, L. Ko, and T.F. Gallagher, "Magnetic Field Enhancement of Dielectronic Recombination from a Continuum of Finite Bandwidth," Phys. Rev. Lett. 83, 3808 (1999).

EXPERIMENTS IN MOLECULAR OPTICS

Robert J. Gordon,* Langchi Zhu, and Andreas Schroeder
Department of Chemistry (m/c 111), University of Illinois at Chicago
845 West Taylor Street, Chicago, IL 60607-7061
*email address: rjgordon@uic.edu

1. Program Scope

The objectives of our research are to develop new methods of aligning and deflecting molecules and to study the time-dependent behavior of aligned particles. We are using imaging techniques to observe the alignment and deflection of molecules, ultrafast laser techniques to monitor the time evolution of aligned molecules, and high Rydberg excitation to alter the polarizability of molecules.

The time evolution of aligned molecules is of particular interest for the following reason. If the aligning field is turned off slowly compared with the rotational period of the molecule (e.g., on a nanosecond scale), the molecule returns adiabatically to its unaligned state. But if the field is turned off rapidly (e.g., on a picosecond scale), the molecule may realign periodically after the field is turned off. This long-term coherence of the aligned state could be put to practical use, as, for example, in stereospecific collisions with an aligned target and nanolithography with an aligned projectile.

The motivation for promoting a molecule to a high Rydberg state is that the polarizability of an atom or molecule (and hence its propensity to be aligned or focused) may change dramatically with its electronic state. For example, the static polarizability of an atom varies as its principle quantum number raised to the *seventh* power. A complication is that for highly excited electronic states the polarizability becomes negative, so that particles in such states are repelled, rather than attracted, by a focused laser beam. This phenomenon is of interest in itself, and will be investigated in our molecular optics experiments.

2. Recent Progress

In the process of building our imaging apparatus and setting up the alignment experiment, we discovered an unusual phenomenon in the multiphoton excitation of various molecules. This effect is illustrated in Figures 1 and 2 for iodobenzene (C_6H_5I).^{1,2} At certain wavelengths (e.g., at 266 and 304 nm) the iodine ion image consists of a set of anisotropic rings that are produced by partitioning of the available energy between the various degrees of freedom of the fragments. The rings in Figure 1, for example, are assigned to $n \rightarrow \sigma^*$ and $\pi \rightarrow \pi^*$ transitions of the molecule, producing $I(^2P_{3/2})$ and $I(^2P_{1/2})$ fragments. The available energy is partitioned between vibrational energy of the phenyl ring, spin-orbit energy of the iodine atom, and translational energy of the fragments. In a collaboration with Attila Berces at the

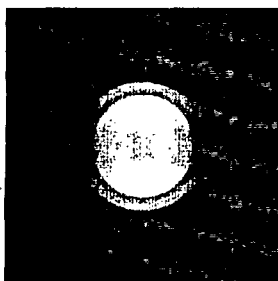


Fig. 1. C_6H_5I (266 nm)

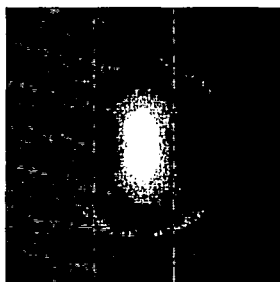


Fig. 2. C_6H_5I (532 nm)

Steacie Institute (NRC, Ottawa), we have performed density functional calculations of iodobenzene which support these assignments. At longer wavelengths (532, 560, 570, 575, 609 nm), however, the image is dominated by what we call an “hourglass” feature. As shown in Figure 2, this feature consists of a continuous distribution of velocities, with an intense spot at zero kinetic energy and a channeling of the recoiling atoms along the polarization direction of the laser beam. We observe a similar feature in CH_3I excitation. Our initial thought was that this effect is caused by alignment of the molecules by the electric field of the focused laser. Further experiments, however, showed that the hourglass effect is insensitive to laser intensity and rotational temperature of the molecule, ruling out a pure alignment mechanism.

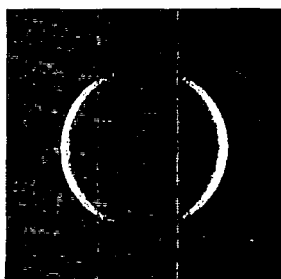


Fig. 3. I_2 (532 nm)

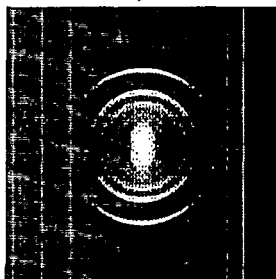


Fig. 4. I_2 (558.8 nm)

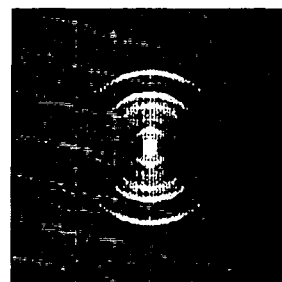


Fig. 5. I_2 (564.4 nm)

Further insight into the origin of the hourglass effect emerges from the photoexcitation of I_2 molecules, as illustrated in Figures 3-5. At 532 nm (Figure 3) we observe an anisotropic ring perpendicular to the direction of the laser polarization, which results from single-photon excitation to the dissociative $A^3\Pi_1$ state. In contrast, at 558.82 nm (Figure 4) the image consists of a set of rings parallel to the polarization vector and a continuous feature sharply peaked at zero velocity. For a diatomic molecule, a continuous energy distribution can result only if a third body carries away the excess energy. Here the third body is an electron, and the hourglass feature is the consequence of dissociative ionization (DI). The detailed mechanism involves a super-excited molecular Rydberg state that simultaneously undergoes dissociation and photoelectron emission. The amount of energy carried off by the electron depends on how far the nuclei have recoiled prior to emission of the electron. It is likely that DI is also responsible for the central spike observed in C_6H_5I and CH_3I , although for molecules as complex as these it is possible that vibrational degrees of freedom also play a role in the energy budget.

The rings in the I_2 image (Figures 4 and 5) have the interesting property that their radii are independent of photon energy, as demonstrated by the nuclear kinetic energy distributions shown in Figure 6. This property is further evidence that the electron carries away a variable amount of energy, in this case leaving the nuclei with the same kinetic energy regardless of the excitation energy. A third property, illustrated in Figures 4 and 5, is that the anisotropy is strongly wavelength dependent. We found evidence that the reduced anisotropy in Figure 4 is caused by a resonance located at an intermediate energy. Together, these effects provide a new understanding of multiphoton dissociative ionization and the role played by three-body interactions.

In another experiment, performed in collaboration with M. Kawasaki at Kyoto University, we demonstrated alignment of CH_3I by a non-resonant focused laser beam.³ We used the fundamental frequency of a pulsed (3 ns) Nd:YAG laser to align the molecule, and a tunable dye laser to photodissociate the molecule and photoionize the iodine fragment. We found that the anisotropy parameter, β , increases from 1.5 to 1.9 as the aligning laser intensity increases from 0 to $1.4 \times 10^{11} \text{ W/cm}^2$.

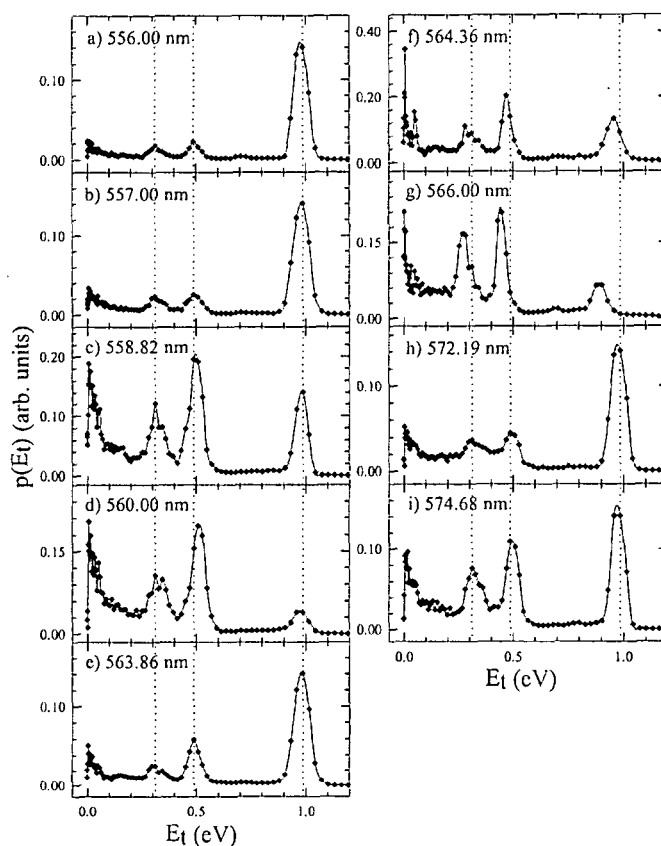


Figure 6. Kinetic energy distributions of the I atom fragments.

3. Future Experiments

We are currently setting up two new experiments which are running concurrently. The goal of the first experiment is to produce rotational recurrences of molecules that have been aligned non-adiabatically with pulses shorter than the rotational period of the molecule. The idea is to produce rotational wave packets that retain their coherence long after the end of the laser pulse. This experiment is being performed in Prof. Schroeder's ultrafast laser laboratory, using Prof. Gordon's imaging apparatus. The ultrafast laser produces pulses of 795, 398, and 265 nm radiation, with a pulse duration ranging from 100 fs to 10 ps, and with repetition rates of up to 1

kHz. Operating the molecular beam nozzle at a rate of 500 Hz, we have produced images of I^+ from I_2 molecules, and I^+ , $^{35}Cl^+$ and $^{37}Cl^+$ images from ICl . Our next step is to use a relatively long (1-10 ps) and weak (10^{12} - 10^{13} W/cm²) pulse to align these molecules and a more intense (150 fs) pulse to dissociatively ionize them after a variable delay. We expect to find a β value that oscillates with the time delay between the pulses.

In the second experiment we will produce molecules in very high Rydberg states and measure their threshold for photoionization by a strong, non-resonant laser field. The objective of this experiment is to determine the conditions for alignment of molecules in high Rydberg, zero electron kinetic energy (ZEKE) states. The idea is that molecules in such states will have greatly enhanced polarizabilities and greatly diminished ionization cross sections. The reason for the latter property is that electrons in ZEKE states have nearly circular orbits and therefore do not interact with the nuclear core. Our plan is to use one or two dye lasers to prepare a molecule such as NO in a high Rydberg state, which will be detected by delayed field ionization. We will next introduce an intense Nd:YAG laser (1.064 μ m or 532 nm, 8 ns duration) in order to measure the intensity threshold for ionization of the ZEKE states. Once the threshold for non-resonant ionization of the ZEKE states has been determined, we will use the Nd:YAG laser to non-destructively focus and deflect the molecular beam.

4. Publications

Two papers on the dissociative ionization of iodine and iodobenzene have been submitted. In addition, the following have been published:

1. R. J. Gordon, L. Zhu, S. Unny, Y. Du, K. Truhins, A. Sugita, M. Mashino, M. Kawasaki, and Y. Matsumi, "Photofragment Imaging Studies of Aligned Molecules," *Imaging Chemical Dynamics*, A. G. Suits and R. E. Continetti, eds, (ACS, Washington, DC, 2000) pp 87-112.
2. R. J. Gordon, General Discussion, Disc. Of the Faraday Society **113**, 87 (1999).
3. A. Sugita, M. Mashino, M. Kawasaki, Y. Matsumi, R. J. Gordon, and R. Bersohn, "Control of Photofragment Velocity Anisotropy by Optical Alignment of CH_3I ," *J. Chem. Phys.* **112**, 2164 (2000).

Quantum Control of Time-Dependent Electron Correlation

Grant #: DEFG02-00ER15053 June 1, 2000 – August 7, 2000

Robert R. Jones, Physics Department, University of Virginia, Charlottesville, VA 22901
rj3c@virginia.edu

Program Scope

We employ intense and/or short laser pulses to investigate and control time-dependent electron correlation within multi-electron atoms. In one line of experiments, coherent pulse sequences are used to generate doubly-excited Rydberg wavepackets in atoms with two valence electrons (i.e. alkaline-earth atoms). By controlling the excitation laser pulse (or pulse sequence), we can manipulate dielectronic dynamics and alter the branching ratio for electron ejection into different energy and angularly resolved continua. In addition, we are developing methods to directly probe the time-dependent electron scattering responsible for configuration interaction in these autoionizing systems. In some cases, strong-field effects are an important aspect of the experiments; e.g. electron-electron interaction during a non-perturbative laser excitation. However, the principal focus of these autoionizing wavepacket experiments is observation and alteration of the field-free evolution of the two-electron system.

In a second line of experiments, we intend to study the role of electron-correlation in strong-field, multiple ionization of atoms. Two-electron ejection via sequential and non-sequential ionization processes will be investigated as a function of the temporal shape of the ionizing laser pulse. Atoms with very different ionization potentials and ratios of single to double ionization potentials will be examined. Laser pulse shaping will also be employed in attempts to optimize the production of ionic Rydberg states formed during the strong-field laser-atom interaction.

Recent Progress

DOE BES support for this project began June 1, 2000 and aided in the completion of an experimental and theoretical project on autoionizing wavepacket manipulation that began earlier in the year. The following paragraphs provide a brief background and summary of the work that was described in two contributed conference presentations in June and a manuscript that was recently submitted to Physical Review Letters [R. van Leeuwen, K. Vijayalakshmi, and R.R. Jones].

Manipulation of Differential Electron Yields via Autoionizing Wavepacket Control

In general, the quantum systems under investigation in studies of laser control are quite complex.[1] As a result, the pulse sequences and quantum dynamics that deliver the highest "yield" in an experiment may not lend themselves to simple interpretation.[2] Nevertheless, taking an intuitive approach to the control of a particular process, by manipulating the spatial distribution of the reactants for example, might be appealing in some cases - even if the result is not precisely optimal.

We have examined the feasibility of "intuitive control" by experimentally addressing the following question: Can fine control over single-electron dynamics be exploited to intuitively manipulate differential decay yields in systems with additional electronic degrees of freedom? Specifically, we used a femtosecond laser pulse to create an angularly localized, $4snL$ Rydberg wavepacket in calcium. In this singly-excited configuration, the $4s$ and nL electrons are essentially independent, and the motion of the angular wavepacket is equivalent to that in a single-electron atom. However, when a second short laser pulse promotes the $4s$ "inner" electron to a $4p$ excited state,[3] the two electrons exchange energy and angular momentum via their mutual Coulomb repulsion. This coherent, time-dependent scattering leads to bound-state configuration mixing and autoionization in addition to the angular motion of the Rydberg wavepacket.

For the particular Ca states of interest, spectroscopic measurements suggested that the lifetime of the autoionizing wavepacket is significantly less than its angular period.[4] Under those conditions, the angular motion of the Rydberg electron is essentially frozen during the autoionization process. Accordingly, we expect that the angular distribution of the autoionized electrons will be highly dependent on the orientation of the wavepacket at the instant of the inner electron's excitation. From a basic physics perspective, freezing the angular distribution of the bound Rydberg electron allows us to examine intra-atomic electron scattering for specific impact angles with minimal change in total cross-section. The experiment proceeds by measuring the angular distribution of electrons ejected into two energetically distinct continua, $4s\epsilon L'$ and $3d\epsilon L'$, as a function of the delay between the laser pulse that creates the wavepacket (the "launch" pulse) and the pulse that drives the isolated-core excitation (the ICE pulse). [3]

Significant modification of the number of electrons ejected at specific angles, without any variation in the total electron yield, is indeed observed. However, the coarse features of the angular distributions are affected less than might be anticipated from the intuitive picture presented above. Nevertheless, the experimental results are in excellent agreement with an R-matrix, quantum defect theory[5-7] calculation that reveals a breakdown of the simple "frozen-wavepacket" picture. Our results have implications for the use of intuitive control in other multi-configurational systems as well as for the feasibility of extracting molecular reaction dynamics from time-resolved, fragment distributions.

Future Plans

We are continuing our studies of time-dependent configuration interaction in Rydberg autoionizing states. Our next project will concentrate on the autoionization of doubly-excited radial wavepackets. First, we will measure the decay of these non-stationary states which is predicted to proceed through a series of short electron ejection bursts, resulting in a "stair-step" decay of the bound wavepacket probability distribution. Second, we will attempt to produce a localized radial wavepacket, from a stationary Rydberg level, using a strong off-resonant ICE laser pulse. The off-resonant excitation should ensure that only that part of the Rydberg wavefunction that is near the ionic core participates in the ICE.[8] We will then probe the decay of the non-stationary

autoionizing state and look for the characteristic radial wavepacket “stair-step” decay. Third, we will explore methods for coherently inhibiting autoionization decay through the interference of two radial Rydberg wavepackets with different mean energies and Kepler periods. By adjusting the launch time and phase of the two component packets, we hope to modify the time-dependent probability for finding the electron near the ion core, and consequently, alter the lifetime of the autoionizing state.

References

1. See, for example, numerous reviews in *Adv. in Chem. Phys.* **101** (1997); J.L. Krause, *Adv. in Quant. Chem.* **35**, 249 (1999); H. Rabitz et al., *Science* **288**, 824 (2000) and references within each.
2. A. Assion et al., *Science* **282**, 919 (1998).
3. W. E. Cooke, T. F. Gallagher, S.A. Edelstein, and R. M. Hill, *Phys. Rev. Lett.* **40**, 178 (1978).
4. R.R. Jones, *Phys. Rev. A* **58**, 2608 (1998); R. van Leeuwen (unpublished).
5. U. Fano, *Phys. Rev. A* **2**, 353 (1970); M. J. Seaton, *Rep. Prog. Phys* **46**, 167 (1983); W.E. Cooke and C.L. Cromer, *Phys. Rev. A* **32**, 2725 (1985).
6. L. Kim and C. H. Greene *Phys. Rev. A* **36**, 4272 (1987); C. H. Greene and L. Kim, *ibid* **36** 2706 (1987); C.H. Greene and M. Aymar, *ibid* **44**, 1773 (1991), and references therein.
7. K-matrices provided by H. van der Hart and C.H. Greene.
8. X. Wang and W.E. Cooke, *Phys. Rev. Lett.* **67**, 976 (1991).

Nonperturbative laser-atom interactions for nonlinear optics

L. Misoguti, S. Backus, I.P. Christov, C. Durfee, H.C. Kapteyn and M.M. Murnane
JILA and Department of Physics, University of Colorado, Boulder, CO 80309-0440
kapteyn@jila.colorado.edu

Project Description

The goal of this project is to study of the interaction of atoms and molecules with intense and very short (< 20 femtosecond) laser pulses, with the goal of developing novel sources of radiation in the VUV and soft x-ray regions of the spectrum. In past work, we demonstrated that ultrashort pulses are ideally suited for generating coherent x-ray high-harmonic radiation, and devised new techniques for phase-matched generation of ultrashort light pulses in the ultraviolet and soft x-ray regions of the spectrum.[1-3] In this project, we are expanding on that research, to investigate new techniques for extending the capabilities of these sources, and to develop theoretical models that allow us to understand in detail the physics of the processes involved.

Recent progress

During the first year of this project we have made very substantial progress, resulting in a number of publications in press and submitted for publication. Two major results from this work are: 1) the first use of temporally-shaped optical pulses for “coherent control” of XUV harmonic emission; and 2) the first demonstration of cascaded four-wave mixing generation of ultrashort VUV pulses.

Coherent control of XUV light emission

The process of high-harmonic generation (HHG) is an extreme example of nonlinear optics. Atoms subjected to an intense short pulse of light emit x-rays as a result of their electric field-induced ionization. The HHG process can be understood in a “recollision” model—after ionization, the newly-freed electron begins to oscillate in the oscillating electric field of the driving laser. If this electron re-encounters its parent ion, it can recombine with it, and release its kinetic energy at impact as a photon in the XUV region of the spectrum. In this picture, repeated ionization and recollision events result in XUV emission in a series of attosecond-duration “bursts,” separated in time by 1/2 optical cycle, or ~1.2 femtoseconds. This periodic emission results in the spectral characteristic of the emission as a series of peak separated in energy by twice the fundamental photon energy.

The XUV emission from each of these bursts can interfere constructively or destructively with emission from subsequent half-cycles; the exact character of this interference determines the spectrum of the HHG emission. In recent work published in Nature,[4] we have shown that by controlling the exact shape of the ~20 fs duration light pulses that drive the HHG process, we can dramatically alter—in a useful way—the spectral characteristics of this emission. The result is in some cases an order-of-magnitude increase in intensity of the selected harmonic.

This work required the development of a laser system capable of controlling the shape of a high-intensity light pulse less than 10 optical cycles in duration. To accomplish this, we took advantage of our past work in ultrashort-pulse laser amplifier systems,[5] and incorporated a new type of pulse-shaping device using a micromachined deformable mirror. This simple type of pulse shaper works by separating the color components of an ultrashort light pulse (which span ~80 nm bandwidth centered on 800 nm), then reflecting them from the deformable mirror.[6] Subsequently, the color components are reassembled back into a pulse. The arrival time of each color component can then be controlled by altering the exact shape of the mirror. Since this mirror has 19 actuators, very precise control of the pulse shape is possible. Although this type of pulse shaper is limited in that it is a “phase-only” shaper and cannot alter the actual spectrum of the driving pulse, this has not proven to be a significant limitation in controlling a highly-nonlinear process such as high-

harmonic generation: color-components that are not wanted can always be moved to early or late times within the pulse where no HHG is taking place.

To demonstrate that precisely-shaped pulses are useful for driving the high-harmonic generation process, we used a two-step procedure. First, we optimized the laser system itself to produce a fourier-transform-limited pulse; i.e. a pulse where all frequency components arrive simultaneously. We do this by performing an optimization of the laser system based on second-harmonic generation. A fraction of the laser output is sent into a second-harmonic crystal. The conversion efficiency of the SHG increases with the peak intensity of the fundamental pulse; thus a transform-limited light pulse should result in the highest possible conversion efficiency. We optimize this pulse using an “evolutionary” algorithm. Starting with a collection of population “members”, each of which corresponds to particular voltages applied to the 19 mirror actuators, the second-harmonic intensity is measured experimentally. Each population member is then ranked for “fitness.” The best solutions are then “mutated” by randomly changing some actuator voltages to create a new “generation.” This computer optimization converges after about 100 generations of about 100 trials each (10,000 total “experiments”). This optimization takes ~10 minutes of real time, and converges very well to a fourier transform-limited pulse.

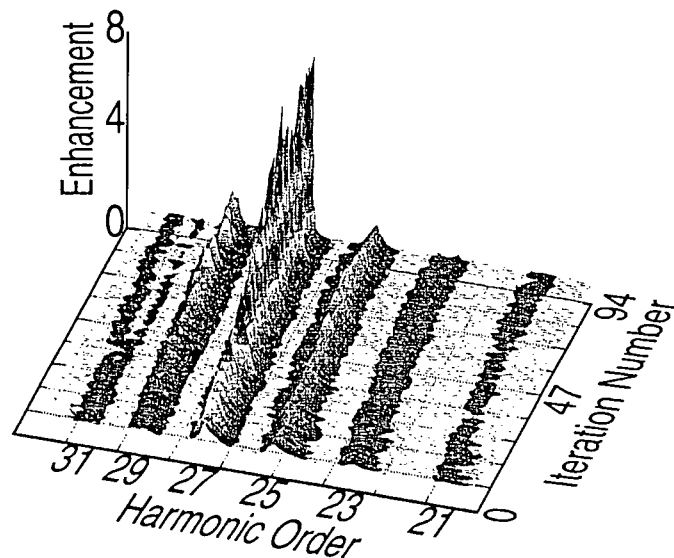


Fig. 1. Optimization of a single (27th) harmonic in argon while suppressing adjacent harmonics. The HHG spectrum for the best pulse of each iteration. The intensity of the 27th order is increased by nearly an order of magnitude, resulting in >75% of the total XUV emission into this harmonic.

This pulse can then be used as the starting point for optimization of high-harmonic generation. In the HHG-optimization setup, we use phase-matched high-harmonic generation in a hollow-core fiber. Harmonics in the range of 21 to 31 are generated, and we observe these harmonics using a grazing-incidence spectrometer and x-ray sensitive CCD camera. We acquire the spectrum obtained with a transform-limited driving pulse, and then apply the evolutionary algorithm to optimize the high-harmonic emission. The simplest fitness criterion to use is simply to observe the peak intensity of a single harmonic order; alternatively, it is possible to optimize to obtain enhancement primarily of only one harmonic order. Figure 1 shows the result of such an optimization. We see that the intensity of the 27th harmonic can be increased by *an order of magnitude* over that which was obtained using a transform-limited pulse. Furthermore, the brightness of other harmonic orders does not increase nearly as much, and the spectral bandwidth of the harmonic order decreases. This is very desirable for application experiments such as time-resolved photoelectron spectroscopy that need monochromatic emission.

This result is remarkable in that we have shown that although second-harmonic emission is optimized using the highest peak-power, transform-limited pulse, *high-harmonic* emission is

optimized with a non-transform limited pulse. This is a manifestation of the fact that HHG is fundamentally a non-perturbative process, and slight changes in pulse shape can “channel” excitation from one harmonic order to another. The optimized pulse shape is actually only slightly different from the transform-limit—21 fs as opposed to the 18 fs fourier-transform limit.

Very recently, we have developed a successful theoretical model of this outcome, and a paper describing this model is in preparation.[7] In the model, we applied the evolutionary algorithm to a numerically-optimized theoretical simulation of HHG emission. This model runs at speeds comparable to the experiment, and finds an optimized pulse shape and emission spectrum that is very similar to experiment—an HHG peak enhancement of $\sim 8x$, and a pulse shape that is slightly longer than the fourier transform limit. The theoretical pulse also has a nonlinear “chirp” that is very similar to that of the experimental optimized pulse shape. Furthermore, this model is a novel theoretical approach that couples a full quantum-mechanical description of the HHG process with a semiclassical picture of the evolution of the ionized electron’s wavefunction. This model clearly illustrates the physics behind the shaped-pulse optimization. The total x-ray signal is the result of coherent interference of the emissions resulting from a number of electron trajectories that emit the correct photon energy on recollision. The number of contributing trajectories is ~ 12 , corresponding to two trajectories every half-cycle of the laser, during the rising edge of the laser pulse (~ 3 optical cycles). In general, for a transform limited pulse the phases of these individual trajectories do not add wholly constructively. On the other hand, the optimized pulse shape clearly shows that the classical trajectories resulting in that harmonic energy are now precisely “in-phase.” The pulse-shaping results in timing adjustments *within the laser pulse* that correspond to coherent control of the wavefunction evolution on the 10 attosecond time scale.

Coherent VUV generation using cascaded nonresonant four-wave mixing

In other work, we demonstrated for the first time a new method for generating coherent light in the vacuum ultraviolet-- using a cascaded four-wave mixing process in a gas. In past work, we demonstrated a new technique which allows us to efficiently up-convert very short (20fs) pulses into the ultraviolet.[2] This technique uses nonlinear four-wave mixing in an atomic gas to generate the UV light, and *phase-matches* the conversion process by using a waveguide structure to alter the propagation velocities of the various colors involved in the interaction. It makes use of a very different regime of laser-atom interaction than that of high-harmonic generation, in that in this case we are not ionizing the nonlinear medium, and we are generating light at wavelengths below the ionization threshold of the gas so that there is no linear absorption of the generated light.

Our original work demonstrated a conversion efficiency of $\sim 20\%$ of the injected light at 400 nm into light at 267 nm. However, subsequent theoretical modeling of this process indicated that we should be able to expect higher efficiencies. Further optimization of the alignment of the waveguide allowed us to obtain conversion efficiencies of up to 40% -- the theoretically predicted amount—and to routinely obtain $>30\%$ efficiency. In this case, the intensity of the signal light in the UV is comparable to the intensity of the pump light. This allows us to drive cascaded processes.[8] For example, if we inject light at 400 nm and 800 nm into the capillary, the first step in the mixing process is $400\text{nm} + 400\text{nm} - 800\text{nm} = 267\text{ nm}$. We can then drive the processes $400\text{nm} + 267\text{nm} - 800\text{ nm} = 200\text{ nm}$, and $267\text{ nm} + 267\text{ nm} - 800\text{ nm} = 160\text{ nm}$. To observe these processes, we set-up a capillary wave-mixing apparatus including differential pumping and a VUV spectrometer. On observing emission from the capillary in the range 80 nm – 267 nm, we see light in a number of wavelength regions, including 267 nm, 200 nm, 160 nm, 133 nm ($400\text{ nm} + 400\text{ nm} + 400\text{ nm} = 133\text{ nm}$), and light at a number of discrete wavelengths in the range of 80-110 nm. This cascaded process has an efficiency on order 10% for 200 nm, $\sim 1\%$ for 160 nm, and $\sim 0.1\%$ for light in the range of 80-130 nm.

Modeling of this nonlinear interaction in the case of cascaded processes complicated by the fact that light can be generated in a large number of waveguide spatial modes. Nevertheless, quite a good correspondence between experiment and theory can be obtained, and this correspondence allows us in many cases to distinguish, for example, a cascaded third-order process from a single-step fifth-

order process and to obtain an estimate of the relative strength of various nonlinear interactions. An example comparing experiment with theory is shown in figure 2.

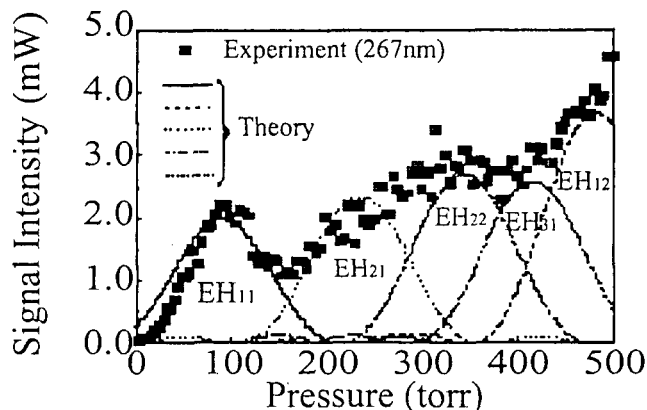


Figure 2: Pressure tuning curve of the 3ω signal at 267nm. Experiment (points) and theory (lines).

Future plans

During the next year, we are planning to expand on our work in a number of areas. In the area of coherent control of high-harmonic generation, this system is a unique testbed for the coherent control of highly nonlinear systems. Learning algorithms such as the evolutionary algorithm have great potential as tools to learn about the quantum system being controlled.[9] Combined theoretical and experimental work will likely yield new insights into this extreme regime of nonlinear light-atom interaction, as well as about the real-world application of learning algorithms to complex systems. We will also continue to parametrize and characterize this system for its use as an ultrashort-pulse short-wavelength light source.

In the area of VUV light generation, the models we have developed are already helping to guide experiments to increase the source brightness. We expect that a number of other improvements will allow us to further optimize the conversion efficiency. Given the highly nonlinear nature of cascaded processes, there is a real possibility of obtaining highly-efficient frequency conversion into the VUV. We are also working to apply the coherent control techniques that have been so successful for high-harmonic generation to this application. We are working on pulse compression of this light, to obtain sub-5 femtosecond pulse durations at very short wavelengths—a light source particularly well-suited for dynamics studies of small molecules and hydrocarbons.

References (Works supported by this grant are highlighted)

- [1] J. Zhou, J. Peatross, M. M. Murnane, H. C. Kapteyn, and I. P. Christov, *Physical Review Letters*, vol. 76, p. 752, 1996.
- [2] C. G. Durfee, S. Backus, M. M. Murnane, and H. C. Kapteyn, *Optics Letters*, vol. 22, p. 1565, 1997.
- [3] A. Rundquist, C. G. Durfee III, S. Backus, C. Herne, Z. Chang, M. M. Murnane, and H. C. Kapteyn, *Science*, vol. 280, p. 1412, 1998.
- [4] R. Bartels, S. Backus, E. Zeek, L. Misoguti, G. Vdovin, I. P. Christov, M. M. Murnane, and H. C. Kapteyn, *Nature*, vol. 406, p. 164, 2000.
- [5] S. Backus, C. Durfee, M. M. Murnane, and H. C. Kapteyn, *Review of Scientific Instruments*, vol. 69, p. 1207, 1998.
- [6] E. Zeek, R. Bartels, M. M. Murnane, H. C. Kapteyn, S. Backus, and G. Vdovin, *Optics Letters*, vol. 25, p. 587, 2000.
- [7] I. P. Christov, R. Bartels, S. Backus, H. C. Kapteyn, and M. M. Murnane, *Physical Review Letters*, vol. Submitted, 2000.
- [8] L. Misoguti, S. Backus, C. G. Durfee, M. M. Murnane, and H. C. Kapteyn, *Physical Review Letters*, vol. Submitted, 2000.
- [9] H. Rabitz, R. de Vivie-Riedle, M. Motzkus, and K. Kompa, *Science*, vol. 288, p. 824, 2000.

High Resolution Spectroscopy of Cluster Ions in Discharges, Clusters in Jets, and Nanoparticles

John W. Keto

Physics Department, The University of Texas at Austin, Austin, TX 78712

keto@physics.utexas.edu

1.0 Introduction

We are using high resolution and time dependent laser spectroscopy to measure the eigenstates and dynamics of clusters and "quasimolecules" of clusters. Spatial or mass selective techniques are combined with laser resolution sufficient to resolve individual quantum states of the clusters. Several experimental technologies are used to produce clusters including high-pressure discharges, supersonic jets, and laser ablation of microspheres (LAM).¹ The latter is capable of producing large quantities of nanoparticles (larger clusters, 1-50 nm dia.) which can be assembled into interesting structures.

Each of these technologies have unique advantages and disadvantages. The discharge and supersonic jet produce smaller clusters than LAM and operate in dilute environments where the clusters have free surfaces and are only weakly perturbed, but experiments must average over a large ensemble of particles (the ensemble is mass specific). In contrast, using clusters manufactured with LAM and deposited onto substrates, we can use near-field scanning optical microscopy (NSOM) which has nanometer scale spatial resolution to measure the laser spectroscopy of a single isolated cluster or assembly of clusters. Though neither technique is free of scientific difficulties, comparison of similar particles with the two techniques should help develop a clear understanding of the quantum states for semiconductor nanocrystals. Time dependent spectroscopy will be used to study the dynamics and reactions of clusters in their environments.

2.0 Single-particle spectra of semiconductor clusters

We have achieved single particle spectra of quantum dot islands using microluminescence, and efforts using NSOM are continuing (DOE publications 3,4,5). The microluminescence instrument uses the spectral separation of the light emitted by the quantum dots to measure the centroid of the diffracted image. Thus the position of the nanoparticle along the slit of the spectrograph can be determined to ± 40 nm, and we can correlate lines in the spectra to a particular dot even though many dots are localized within a distance smaller than the resolution of the microscope. It has been easier to use microluminescence than NSOM for temperatures studies. As the temperature of the cold finger and sample holder change, differential expansivities cause the cluster to move. The larger field of view for microluminescence makes it easier to chase the particle. To solve this problem for NSOM in future experiments, we have designed a sample holder and cold finger which minimize the motion of the particles with temperature.

We have also used microluminescence to examine the spectra of isolated nanocrystals. Initially we found that semiconductor particles produced by LAM were highly chained. We have found that for metal particles chaining is unlikely because photoionization by the laser generates a high state of charge with a resulting coulomb repulsion between nanoparticles. The chaining in semiconductor systems results either from a more rapid recombination of the charge of the cluster, or that a higher charge state is required to prevent chaining of semiconductor clusters as compared to metals. If the particles are collected within 5 cm of the laser ablation region, little chaining occurs. We also found that particles can be collected at larger distances downstream at lower pressures. This is consistent with slower electron-ion recombination at the lower pressures.

¹Hong Cai, Nirmal Chaudhary, Jaemyoung Lee, Michael F. Becker, James R. Brock, and John W. Keto, J. of Aerosol Science 29, 627-636 (1998); US. Patent #5,585,020

High resolution spectra have already been obtained for single, colloiddally grown CdSe nanocrystals.² Interestingly, the spectra exhibited fluorescence blinking; and it was suggested that the blinking results from photoionization of the nanocrystal. For surfactant coated nanocrystals these charges are trapped on the molecule and the exciton experiences a stark shift.³ The single dot lineshape changes with the number and depth of trap states, the temperature of the sample, and the length of time for acquisition of a single dot spectrum. No one has yet succeeded in correlating the single dot fine structure with the size of the particle. Spectral shifts with size have been measured by many groups for ensembles of particles of varying sizes, but these spectral shapes are sufficiently broadened by the dispersion in particle sizes ($\delta\text{dia}/\text{dia} > 5\%$) so that the fine structure cannot be resolved, and spectra cannot be compared with theoretical predictions for energy levels in the cluster.

We have obtained fluorescence spectra from isolated, individual CdSe nanoparticles (see Fig. 1) made by LAM and collected dry on sapphire substrates. Charging and blinking was not observed though we found that only about 70% of the nanoparticles observed by dark field scattering were fluorescent. We have not yet made sequences of spectra over longer time periods, nor have we yet measured spectra at low temperatures. Such studies are planned in the future.

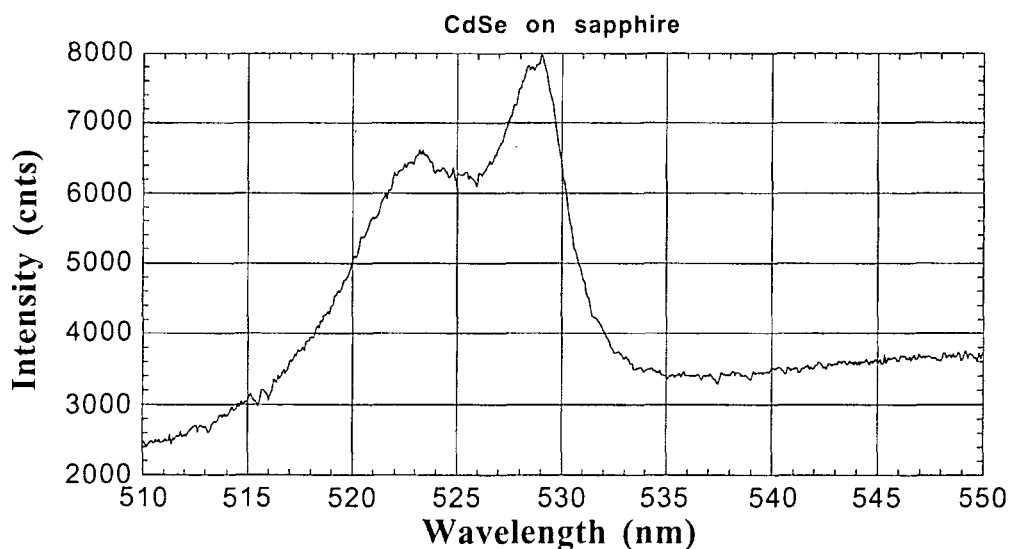


Fig. 1. Microluminescence of a single CdSe nanocrystal made by LAM and collected dry on a sapphire substrate. The spectra shown was taken at room temperature, and the lines are broadened by phonon scattering. The shoulder appearing at longer wavelengths results from sapphire fluorescence.

There has been significant controversy about surface states vs. triplet states as the cause of the Stokes shift (PL shifted from PLE) observed for many of the nanoparticle systems. For CdSe this question seems to have been resolved. Bawendi, and coworkers⁴ concluded that surface states were not involved; the exciton is likely a triplet state. In theoretical calculations for CdSe and InP,

² M. Nirmal, B. O. Dabbousi, M. G. Bawendi, J. J. Macklin, J. K. Trautman, T. D. Harris, and L. E. Brus, *Nature* **383**, 802(1996)

³ S. A. Emmepedocles and M. G. Bawendi, *Science* **278**, 2114(1997)

⁴ Al. L. Efros, M. Rosen, M. Kuno, M. Nirmal, D. J. Norris, and M. Bawendi, *Phys. Rev.* **B54**, 4843(1996)

Zunger⁵ and Whaley⁶ in separate efforts concluded that oxide and dangling bond surface states are not in the band gap. In many experiments with heavily oxidized, silicon nanocrystals, a blue/green fluorescence is observed whose wavelength does not vary with the size of the particle. This fluorescence band is likely from a surface state. Clusters formed by Si⁺ ion implanted SiO₂ which are then annealed in oxygen show a size independent red band. Other experimenters have suggested that this fluorescence results from oxide surface states and is quenched when exposed to atomic H.⁷ In contrast, Brus, *et al.*, obtain stable size-dependent red to green fluorescence (size selective shift from 0.2 to 0.8 eV) from Si particles purposely capped with oxygen.^{8,9} The variety of experimental results, gives only a confusing picture for the structure and states present in Si nanoparticles.

Recently, Liu, *et al.* have calculated the effects of dangling bonds and hydrogen surface states on the energy levels of silicon nanoparticles.¹⁰ Surface defects partly fill the band near the edge of the HOMO, but a clean gap is present. However, if the surface state is allowed to reconstruct, they find the band completely fills because of the resulting strain which distorts the crystal structure throughout the cluster; the particle is essentially a metal. Hydrogen passivation after relaxation preserves this condition, but if the surface is passivated before the nanocrystal relaxes, the bandgap is nearly that of bulk silicon even after relaxation. The use of LAM for synthesis may be a test for this model as the nanocrystals are ejected into the carrier gas at high temperature (~5000 K). If we add hydrogen, passivation may occur before crystal relaxation.

We have attempted experiments to observe fluorescence of Si nanoparticles made by our process collected both on sapphire or Si substrates with stable native oxides; no fluorescence was seen. Fluorescence was quenched either by nonradiative trap states, the gap is filled as suggested by Liu, *et al.*, or the excitation tunnels to the substrate before fluorescence. Experiments by Krauss, *et al.*¹¹ suggest that native oxide on silicon should prevent the tunneling.

Following these initial experiments and as a test of the theory of Liu, *et al.*, we prepared samples of silicon nanoparticles produced by LAM in He/H₂ and pure He carrier gases. In the case of the He/H₂ carrier gas, hot nanoparticles (T~5000K) are ejected into the laser plasma formed in the He/H₂ carrier gas; we had hoped that they would grow a hydride capping layer before surface reconstruction. A second set of samples produced in a pure He carrier gas were exposed to air after collection so that they formed native oxide coatings; a third set of samples were first exposed to H₂ while cold on the collection wafer. No fluorescence was observed for any of the samples. Subsequent high resolution transmission electron micrographs (TEM) and selected area electron diffraction indicate that the silicon nanoparticles are amorphous, while the CdSe were crystalline.

3.0 Future Research

We are now experimenting with different growth conditions to determine if the amorphous character for silicon nanoparticles is dependent upon experimental parameters. We will also

⁵A. Franceschetti, H. Fu, L. W. Wang, and A. Zunger, "Many-body pseudopotential theory of excitons in InP and CdSe quantum dots," *Phys. Rev.* **B60**, 1819(1999).

⁶K. Leung, S. Pokrant, and K. B. Whaley, "Exciton fine structure in CdSe nanoclusters," *Phys. Rev.* **B57**, 12291(1998).

⁷R.R. Lowe-Webb, Lee Hao, J. B. Ewing, S. R. Collins, Yang Weidong, P. C. Sercel, *J. Appl. Phys.* **83**, 2815(1998).

⁸M. I. Freedhoff and A. P. Marchetti, "Quantum Confinement in Semiconductor Nanocrystals," *Handbook of Optical Properties II: Optics of Small Particles, Interfaces, and Surfaces*, CRC Press (New York, 1997), p. 1

⁹L. E. Brus, P. F. Szajowski, W. L. Wilson, T. D. Harris, S. Schuppler, and P. H. Citrin, *J. Am. Chem. Soc.* **117**, 2915(1995)

¹⁰Lei Liu, C. S. Jayanthi, and Shi-Yu Wu, "Factor Responsible for the Stability and the Existence of a Clean Energy Gap of a Silicon Nanocluster," submitted to *Phys. Rev. B*, private comm.

¹¹T. D. Krauss and L. E. Brus, "Charge, Polarizability, and Photoionization of Single Semiconductor Nanocrystals," *Phys. Rev. Lett.*, **83** (23), 4840-4843(1999).

prepare CdSe nanoparticles with different surface capping layers like we have done for Si particles. We will observe the effects on both the structure and fluorescence of the particles.

We are also continuing efforts to obtain high resolution ($\delta\nu \sim 1$ GHz) spectra of nanoparticles with NSOM so that the spectra can be correlated with the size. Our previous low temperature NSOM was run vertically within a Dewar tip submerged in liq He. We had difficulties with unreliability in the approach to the surface at low temperatures. To return to a horizontal motion we designed a unit employing a cold finger for the sample with the NSOM tip penetrating the heat shield through a small hole. This unit offers two advantages: we could more rapidly change fiber tips and we could place a lens (100x objective) so as to image the fluorescence of the sample onto the ccd camera. This unit is then a hybrid of an NSOM apparatus and the microluminescence apparatus.

We will also use LAM to generate a high density (cluster density $>10^{14}$ cm⁻³), flowing, high pressure aerosol of clusters. This aerosol will be expanded through a supersonic jet into vacuum where REMPI will be used to measure the high resolution excitation spectra with mass selective detection. REMPI can observe the spectra of dark states, so that the surface and defect states of even non fluorescent Si clusters can be observed.

4.0 DOE Supported Publications

1. Parminder S. Bhatia, Craig W. McCluskey, and John W. Keto, "Calibration of a computer-controlled precision wavemeter for use with pulsed lasers," *Appl. Optics* **38**, 2486(1999).
2. Parminder S. Bhatia and John W. Keto, "Pressure and power dependence of the optically heterodyne Raman-induced Kerr effect line shape," *Phys. Rev. A* **59**, 4045(1999).
3. H.Htoon, Hongbin Yu, D. Kulik, J. W. Keto, O. Baklenov, A.L.Holmes Jr., B.G. Streetman, and C.K.Shih, "*Quantum dots at the nanometer scale: Interdot carrier shuffling and multiparticle states*," *Phys. Rev. B* **60**, 11026-11029(1999).
4. H. Htoon, J. W. Keto, O. Baklenov, and A. L. Holmes, Jr., C. K. Shih, "Cross-sectional Nano-Photoluminescence Studies of Stark Effects in Self-Assembled Quantum Dots," *Appl. Phys. Lett.* **76**, 700-702(2000).
5. H. Htoon, Hongbin Yu, D. Kulik, J. Keto, C.K. Shih, O.l Baklenov, and A. L. Holmes, "Nano-photoluminescence studies of self-assembled quantum dots," *Self-organized Processes in Semiconductor Alloys-Spontaneous Ordering, Composition Modulation, and 3-D Islanding*, (Material Research Soc., Pittsburg), 2000.
6. James M. Kohel and J. W. Keto, "*Two-photon laser-assisted reactions in Xe and Cl₂ gas mixtures*", to be published, *J. Chem. Phys.*

Spectroscopic Studies of Hydrogen Atom and Molecule Collisions

John Kielkopf

Physics Department, University of Louisville, Louisville KY 40292

john@aurora.physics.louisville.edu

Program Scope

In this project the processes which occur in low energy collisions of excited states of atomic hydrogen with other atoms and ions are being studied with infrared, optical, vacuum ultraviolet, and laser spectroscopy. The purpose of this study is to understand low-energy atom-atom collisions during which light is emitted or absorbed. The transient quasi-molecular state produces radiation far from the unperturbed atomic spectral line. The theory of the line shape is still incomplete, and quantitative experiments are lacking on systems for which the atomic interactions are understood. Thus this work is fundamentally interesting because it allows us to view into the femtosecond duration event during which two or more atoms approach, interact, and separate, and to probe the transient quasi-molecular state. There is a practical side to it as well, since once the spectrum is understood theoretically, it may be used to diagnose the environment under which it is produced, whether that is a chemical reaction, a laser-generated plasma, or the atmosphere of a white-dwarf star.

Because of their fundamental character, radiative collisions with the hydrogen atom play a central role. Some hydrogenic interactions, particularly those for low-lying electronic states, can be calculated very accurately, namely those of H_2 , H_2^+ , H_3 , and H_3^+ , and simpler diatomic radicals such as CH. The interactions become quite complex, even for a diatomic system, with electronic excitation of one of the atoms, because large numbers of molecular states are involved in what appears to be a single asymptotic atomic transition. Furthermore, the radiative transition probability of colliding atoms changes with their separation, an effect which is very significant when the atoms are close and strongly perturbed, and which is only understood well for low-lying diatomic states. In a gas in which there is a large degree of molecular dissociation and ionization of the resulting atoms, the spectrum is also influenced by the presence of several different perturbers, including electrons, interacting simultaneously, and by the effect of the interactions on the statistics of the ensemble. Thus while the basic physics of atomic spectra and atomic collisions is understood, a complete theory for the spectrum from a gas in which radiative collisions are taken into account is not yet available. Experiments in which the diatomic potentials and transition probabilities

for low-lying states are known *a priori*, as is the case for atomic hydrogen, allow us to develop and test the theory without resorting to assumptions about the interactions. The primary difficulty on the experimental side of this program is the development of techniques to observe atomic hydrogen spectra from the mid-wave infrared to the far vacuum ultraviolet at densities high enough for spectral line broadening effects to be detected, and to characterize quantitatively conditions under which the spectra are created.

Recent Progress

Experimental work has been directed in the past year toward studies of plasmas produced by the shock wave that results when a laser is focused into dense H₂ gas targets. With pulses of a few nanoseconds and energies less than a Joule, the energy deposited is sufficient to totally ionize the gas at the focus, and to create a shock front that travels several millimeters outward from the focus and leaves in its wake a bubble of partially ionized atomic hydrogen. The optical and plasma properties of this source are characterized as a function of time after the initiating laser, and as a function of space around the focus. Space- and time-resolved spectroscopy of the source allows us to tune the conditions and select different degrees of ionization, and different densities of atoms and ions. For a pure H₂ target, we can control the relative importance of collisions of excited H with other unexcited H atoms, and with H⁺ and e⁻.

New experiments this year include measurements in sources at initial densities up to 100 atmospheres. A small-volume static high pressure cell was used for these measurements, and spectra were recorded for Lyman α above 1500 Å, and for Balmer α from 6000 to 10,000 Å. The Lyman α profile showed a continuum extending from 1600 Å at the singlet B-X satellite to 2700 Å. This continuum is qualitatively in agreement with the predictions of the line shape theory when the effects of three-body neutral atom collisions are included. For Balmer α , a new near-infrared satellite was found that is due to ion-atom interactions, that is, due to quasimolecular H₂⁺.

The theoretical effort in collaboration with N.F. Allard (Institute of Astrophysics, Paris) has produced profiles for Lyman α , Balmer α , and Lyman β . The major development in the past year has been the systematic inclusion of the dependence of the radiative dipole transition moment on interatomic separation. For spectral regions or gas densities where multiple-perturber effects are not important, this allows us to correctly model collision-induced effects. These turn out to be quite significant, in some cases enhancing spectral satellites that would not otherwise be seen in the far wing of the line. The Lyman α theory includes broadening both by neutral H and by H⁺, all of the excited contributing states from the asymptotic $n = 2$ atomic state, variation of the radiative dipole moment, and trial calculations of velocity averages.

The Lyman α profile also was computed for densities sufficiently high (10^{21} cm^{-3}) to shift the spectrum out of the vacuum ultraviolet to regions above 2000 \AA for comparison with experiments at elevated density.

The theory of Balmer α and Lyman β , both of which access the $n = 3$ atomic state, was developed for collisions with protons. The case of Balmer α is of special interest because it is a strong spectral line in the visible and is accessible for both laboratory plasma diagnostics and ground-based stellar astronomy. The theoretical profiles predict a satellite in the near infrared, that is, structure in the continuum between Balmer α and the Paschen-series limit that is due to radiative collisions of $n = 3$ atomic hydrogen with a proton. Lyman β is somewhat simpler because the lower state is $n = 1$ rather than $n = 2$, but in the vacuum ultraviolet the small perturbations responsible for the far wing of Balmer α map into regions close to the Lyman β line center, while the far wing of Lyman β reveals the effects of very strongly perturbing close collisions.

In 1999-2000 three students completed their M.S. degrees with theses in this program: Kim Edmondson, The Continuous Spectra of Molecular Hydrogen; Taka Tsuchiya, Numerical Modeling of Laser-Produced Blast Waves in Real Gases; and Jeremy Cole, Analysis of Laser-Irradiated H_2 Using a Time-of-Flight Mass Spectrometer.

Future Plans

During the coming budget year, our work will be directed toward understanding the Lyman β profile, and the region between it and Lyman α . This gives access to interactions in the $n = 2$ and $n = 3$ states, in support of the theoretical work on the combined Lyman α and Lyman β system. The experiments require the use of a pulsed gas source, rather than a static cell. The valve we have developed generates a gas column about 1 mm in diameter and 2 mm long with a density of the order of 10^{19} cm^{-3} . The interaction of this target with the laser differs from the static cell in that the shock wave progresses only to the extent of the jet, and there is no subsequent hot gas bubble. However, the hot front in the first 100 ns after the laser pulse produces a highly ionized, dense, hydrogen gas in which the effect of collisions with protons is important. The use of a pulsed valve permits observations of the target with a windowless spectrometer, and gives us access to the spectrum below the MgF_2 cutoff at 1150 \AA which includes the Lyman γ , Lyman β and the blue wing of Lyman α .

Work in collaboration with N.F. Allard on the theory of Lyman β due to collisions with neutral H is underway. Most of the potentials and radiative transition moments which are needed for the work are now available. The computation will include the

neutral and ion collision effects in the Lyman series from the blue wing of Lyman β through the red wing of Lyman α for comparison with experiments. This is a first step toward computing a complete spectrum for a broad range of excited states, rather than for single isolated lines. We also are considering electron collision effects, which are important in the very early emission from the plasma when it is highly ionized. The effect of the interactions on the statistics of the perturber distribution in the vicinity of the radiator is another factor of interest, since we have seen experimental evidence of enhancements in the line wing that are due to the clustering of perturbers around an excited atom to which they are strongly attracted.

Publications 1998-2000

Satellites on the Lyman β line of atomic hydrogen due to H-H⁺ collisions, N. F. Allard, J. Kielkopf and N. Feautrier, *Astron. Astrophysics* **330**, 782-790 (1998).

New study of the quasi-molecular Lyman α satellites due to H-H and H-H⁺ collisions, N. F. Allard, I. Drira, M. Gerbaldi, J. Kielkopf and A. Spielfiedel, *Astron. Astrophysics* **335**, 1124-1129 (1998).

Observation of the far wing of Lyman alpha due to neutral atom and ion collisions in a laser-produced plasma, J. F. Kielkopf and N. F. Allard, *Phys. Rev. A* **58**, 4416-4425 (1998).

Lyman series profiles: from laser-plasmas to white dwarf stars, J.F. Kielkopf and N.F. Allard, invited paper at the 13th International Conference on Spectral Line Shapes, State College, Pennsylvania, July 1998; *Spectral Line Shapes: Volume 10*, AIP Conference Proceedings 467, ISBN 1-56396-754-5, (American Institute of Physics, New York, 1999), pp. 228-239.

The effect of the variation of electric dipole moments on the shape of pressure broadened atomic spectral lines, N. F. Allard, A. Royer, J. F. Kielkopf, N. Feautrier, *Phys. Rev. A* **60**, 1021-1033 (1999).

A collision-induced satellite in the Lyman β profile due to H-H collisions, N.F. Allard, J. Kielkopf, I. Drira and P. Schmelcher. to appear in *European Physical Journal D* (2000).

15 papers presented at conferences 1998-2000.

Project Abstract
DoE Grant DE-FG03-94ER14473
Nonclassical Spectroscopy with Localized Atoms

H. J. Kimble
Norman Bridge Laboratory of Physics 12-33
California Institute of Technology
Pasadena, CA 91125
hjkimble@its.caltech.edu

1 Program Scope

This DoE sponsored research program investigates fundamental atomic radiative processes for single atoms localized on the spatial scale of the optical wavelength. This is a new domain of *strong focussing* in optical physics with optical excitation over an area comparable to the atomic absorption cross-section and with transmitted fields efficiently re-collimated over large solid angle. The scientific objectives of the program of research follow three major thrusts. The first is a continuing investigation of spectroscopy with nonclassical light, now with emphasis on investigations of the alteration of atomic lifetimes and lineshapes for two- and three-state atoms illuminated with squeezed radiation in a domain of *strong focussing*. The second area is a new research effort to explore light scattering for a *quantum aperture*, namely a single atom localized on a wavelength scale and illuminated over a large solid angle. The third area is the coherent manipulation of atomic center-of-mass wavepackets for a single *neutral* atom localized in the *Lamb-Dicke regime* (that is, on a spatial scale much smaller than the optical wavelength).

Within a broader scientific context, spectroscopy with nonclassical sources can lead to improvements in quantitative analysis with enhancements in measurement capabilities beyond the standard quantum limits and offers the potential for new atomic radiative processes relevant to diverse problems in optical physics. The research has the potential to make important contributions to a number of areas of technological significance, including high-density optical storage.

2 Recent Progress

2.1 A New Laboratory

A principal thrust of our DoE sponsored research is the attainment of atomic localization on a scale small compared to the optical wavelength λ in a setting compatible with nonclassical illumination over an area comparable to the radiative cross section ($\frac{3}{2\pi}\lambda^2$). Beyond the capability of *strong focussing* to enable spectroscopy with nonclassical light, such localization and illumination should lead to a new class of radiative interactions. In addition to measuring differential cross sections for the scattered fields, phenomena of interest include the angular distributions of higher order field correlation functions, including those relevant to photon statistics.

In order to achieve these scientific objectives, it has been necessary to make a radical departure from the techniques and tools of our previous experimental program. Hence we have undertaken a major new effort involving the construction of a laboratory with capabilities suitable for trapping, cooling, and localization of a single neutral atom on a spatial scale much smaller than the optical wavelength λ (the Lamb-Dicke regime). This effort is being led by Dr. Ron Legere (who was a graduate student with extensive expertise in laser cooling and trapping in the group of Professor Kurt Gibble at Yale). In building this new apparatus, Dr. Legere has been joined by senior graduate student Mr. David Boozer and first-year student Ms. Andreea Boca and undergraduate Mr. Kaiwen Xu.

This new laboratory is now largely operational, with a source of cold atoms for the experiments consisting of magneto-optical traps (MOT). The so-called “downstairs” MOT-1 is working and collecting roughly 10^7 Cesium atoms. These atoms are next to be cooled with polarization gradients to a few microKelvin, and then transferred with an estimated 10% efficiency to an “upstairs” MOT-2 located in the upper-stage of the UHV chamber with background pressure 10^{-11} Torr. The captured atoms in MOT-2 are then to be cooled to $2\mu\text{K}$ and launched upwards from a position 20cm below a final interaction region. Some few atoms will transit into the focal volume of symmetrically placed high numerical aperture microscope objectives. Here one atom will be trapped within a far-off resonance dipole-force trap (FORT).

Once an atom is localized within the FORT, side-band cooling will commence to achieve a ground-state wavepacket. A project enabling the required Raman transitions with phase-locked diode lasers has recently succeeded and is described in the Senior Thesis of Kaiwen Xu.

2.2 A zero transition-shift FORT

Numerous demonstrations have now been made of atom confinement in optical dipole traps. The typical scheme is to use a trapping laser whose wavelength lies far to the red of any allowed transition from the atomic ground state, so that the AC Stark shift of the ground state is negative and maximized at the points of highest laser intensity. Atoms thus experience an optical dipole force that attracts them to local maxima of the laser field.

For application to our DoE sponsored research, the problem with this simple approach is that excited (as opposed to ground) states generally experience a positive AC Stark shift of comparable magnitude to the negative shift of the ground state. This has at least two unfortunate consequences. First, atoms are *repelled* from the trap when they happen to spend time in an excited state. Second, the effective detuning between an atomic transition and an external exciting field becomes a strong function of the atom’s position within the trap.

It turns out that a clever choice can be made for the wavelength of the trapping laser such that both of these problems are eliminated [as originally conceived by Dr. Christina Hood (of the Caltech Quantum Optics Group) and Dr. Chris Wood (of Research Electro-Optics, Boulder)]. In our experiments with laser-cooled ^{133}Cs atoms, the relevant transition for interactions with nonclassical or other external fields is the $S_{1/2}(F=4, m_F=4) \rightarrow P_{3/2}(F=5, m_F=5)$ transition at $\lambda \simeq 852.359$ nm. When a red-detuned trapping laser is applied to the Cs atom, these levels are both shifted by the AC Stark effect as shown in Figure 1. Here the dotted curve shows the ground state $S_{1/2}(F=4, m_F=4)$ shift, and the solid curve shows the excited state $P_{3/2}(F=5, m_F=5)$ shift, versus wavelength of a circularly-polarized trapping field.

Near the transition resonance at 852 nm, these level shifts allow for trapping of the Cs atom with a traditional dipole-force trap. For small red detunings of the trapping laser (*e.g.* $\lambda \sim 860$ nm), the ground state has a negative energy shift so ground-state atoms will be trapped in local maxima of the laser field. At such wavelengths, however, excited state atoms experience a positive energy shift and will therefore be repelled from the laser field.

Fortunately, the state $P_{3/2}(F=5, m_F=5)$ is also coupled to the $D_{5/2}(F=6, m_F=6)$ state with a transition wavelength ~ 917 nm. Hence, the $P_{3/2}(F=5, m_F=5)$ experiences an additional *negative* AC Stark shift when the trapping laser has a small red detuning from the $P \rightarrow D$ transition. This negative shift and the positive shift from the $S \rightarrow P$ coupling simply add. As a result, it can be seen from Fig. 1 that there is a region of applied wavelengths from ~ 920 nm upward for which Cesium atoms will be trapped in the laser field in both the ground and excited states, since each of these acquires a negative shift in its energy.

In fact, there exists a special wavelength for the trapping laser (near 950 nm for the particular choice of polarizations and levels considered here), for which the S and P states are shifted by an *identical* amount. Hence both the S and P states are trapped in local maxima, and the frequency of the $S \rightarrow P$ transition should be unaffected by the existence of a trapping field at this special wavelength. Stated somewhat differently, such a FORT enables the internal atomic dipole degree of freedom to be decoupled from the external center of mass motion, and should as well lead to greatly increased trap lifetimes.

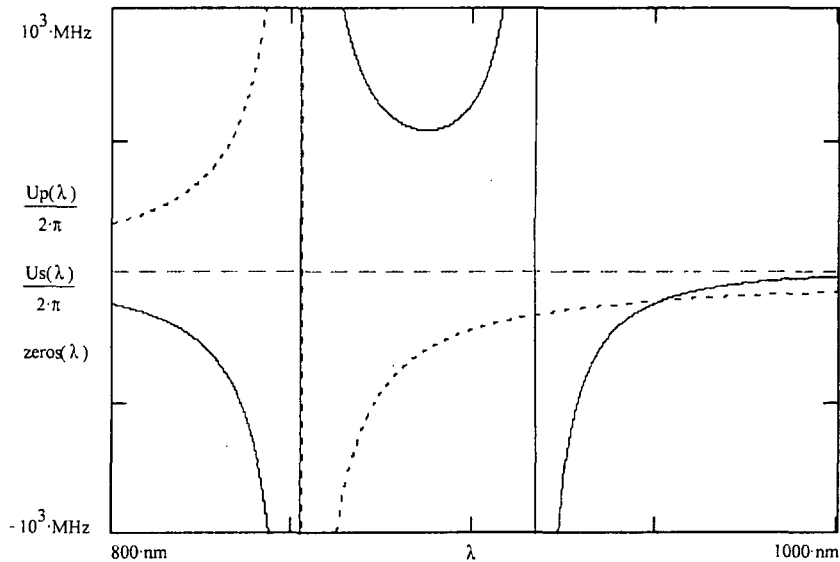


Figure 1: AC Stark shifts for a Cesium atom in a laser field. The dotted curve shows the ground state $S_{1/2}(F = 4, m_F = 4)$ shift $[U_S(\lambda)]$, and the solid curve shows the excited state $P_{3/2}(F = 5, m_F = 5)$ shift $[U_P(\lambda)]$, versus wavelength of a circularly-polarized trapping field.

3 Future Plans

The immediate plan in the laboratory is to load atoms into a strongly focussed, zero-shift FORT of the type described in the preceding section. Atoms trapped and cooled in MOT-1 in the lower chamber are cooled further by polarization gradient cooling and then transferred into a FORT operating around 950nm. A new Ti-Sapphire laser has been acquired, and is now operational for this purpose.

As discussed above, this new design for our FORT should eliminate heating due to intrinsic fluctuations in the dipole force. Hence, our initial efforts are to be devoted to measuring the heating rate in the FORT at various wavelengths to confirm the predictions implicit in Figure 1. The diverse beam switching components have been assembled for this purpose, including the capability for triggered imaging of the FORT. Initial experiments are underway, with as yet no definitive results.

However, given successful trapping and transfer from atoms in MOT-1 into the FORT, we will next move to the full transfer protocol. The plan is to implement a two-stage magneto-optical trap, and then to load atoms into a strongly focussed FORT. Atoms trapped and cooled in MOT-1 in the lower chamber (at 10^{-9} Torr) will be transferred to MOT-2 in the upper chamber (at 10^{-11} Torr). After polarization gradient cooling, the atoms will be transferred into yet a third region in the UHV chamber and thence into a FORT operating around 950nm.

The geometry of the vacuum chamber and optics allows the FORT to have a focal spot near the diffraction limit $\frac{\lambda}{2}$. We will begin with larger trap volumes and atom numbers of roughly 10^2 , moving then systematically toward trapping of a single atom in a FORT of volume $\approx \lambda^3$.

4 Publications and Patents

4.1 Journal Articles Supported by DoE 1998 - 2000

1. "Squeezed Excitation in Cavity QED: Experiment and Theory," Q. A. Turchette, N. Ph. Georgiades, C. J. Hood, H. J. Kimble, and A. S. Parkins, *Phys. Rev. A* **58**, 4056 (1998).
2. "Quantum Interference in Two-Photon Excitation: Part I. Weak-Field Excitation," N. Ph. Georgiades, E.S. Polzik, H.J. Kimble, *Phys. Rev. A* (submitted 1998).
3. "Quantum Interference in Two-Photon Excitation: Part II. Non-Perturbative Solution," N. Ph. Georgiades, E.S. Polzik, H.J. Kimble, *Phys. Rev. A* (submitted 1998).
4. "Quantum Interference in Two-Photon Excitation with Squeezed and Coherent Fields," N. Ph. Georgiades, E.S. Polzik, H.J. Kimble, *Phys. Rev. A* **59**, 676 (1999).
5. "A Single Atom in Free-Space as a Quantum Aperture," S. J. van Enk and H. J. Kimble, *Phys. Rev. A* **61**, 1802 (2000).
6. "Strongly Focused Light Beams Interacting with Single Atoms in Free Space" S. J. van Enk and H. J. Kimble, *Phys. Rev. A* (accepted, 2000).

4.2 DoE Sponsored Patent

"Opto-Electronic Device for Frequency Standard Generation and Terahertz-Range Optical Demodulation Based on Quantum Interference," Nikos P. Georgiades, Eugene S. Polzik, and H. Jeff Kimble, U. S. Patent No. 5,866,896, Issued 2/2/99.

Experimental Study of Interactions of Highly Charged Ions with Atoms at keV Energies

V.O. Kostroun

School of Applied and Engineering Physics, Cornell University, Ithaca, NY 14853

During the past year, we have carried out detailed experiments to investigate interactions of low energy, multiply charged ions with a semiconductor surface. These have led to the unequivocal observation of one electron capture by hyperthermal N^{q+} ($4 \leq q \leq 6$) ions from surface atoms on a clean and oxidized Si(100) surface. The result is significant in that it is the first direct observation and energy gain measurement of one-electron capture by multiply charged ions from a semiconductor surface.

N^{q+} ($4 \leq q \leq 6$) ions were extracted from the Cornell superconducting solenoid, cryogenic electron-beam ion source in the extended pulse mode at $V_{Extr} = 2.3 \text{ kV}$ and charge selected

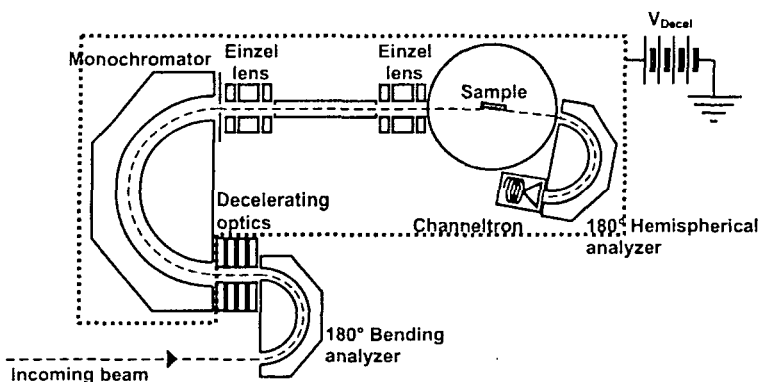


Figure 1. Experimental arrangement to measure energy gain spectra of N^{q+} ($4 \leq q \leq 6$) ions scattered from a silicon surface at grazing angles of incidence.

by a 90° analyzing magnet. The ion beam then entered the scattering chamber where it was decelerated and focused onto a Si(100) sample, figure 1. All components enclosed by the dotted line, including the sample, were at potential V_{Decel} so that the energy of the ion beam incident on the sample was $q(V_{Extr} - V_{Decel})$. The FWHM energy and angular spread of the decelerated beam at 305 qeV was 3.4 qeV and 2° respectively. The sample, an n-

type Si(001) wafer, was mounted on a xyz and rotatable UHV manipulator electrically isolated from ground. The sample was cleaned by flashing up to about 1200°C by direct current heating, and its temperature was measured directly by a chromel-alumel thermocouple attached to the back of the sample. Ions scattered by the one-electron capture process were analyzed by a 180° hemispherical electrostatic analyzer, and individually detected by a channeltron electron multiplier. All experiments were performed using hyperthermal, 305 qeV kinetic energy, N^{q+} ($4 \leq q \leq 6$), multiply charged ion beams.

The incident N^{q+} beam impinged at a 2° grazing angle on a clean and oxidized Si(100) surface. The energy distributions of $N^{(q-1)+}$ ions, N^{q+} ions scattered from the surface following one-electron capture were measured at an angle which gave the maximum number of counts in the angular distribution of the $N^{(q-1)+}$ signal, centered on the peak in the energy distribution.

For N^{5+} ions incident on the sample, figure 2 shows the dependence of the energy gain spectra on sample temperature. The energy gain spectrum (2a) was recorded at room

temperature before the sample was heated. Each of the subsequent spectra, (2b)-(2h) followed a 5 minute heating of the sample at the temperature shown. The sample was then

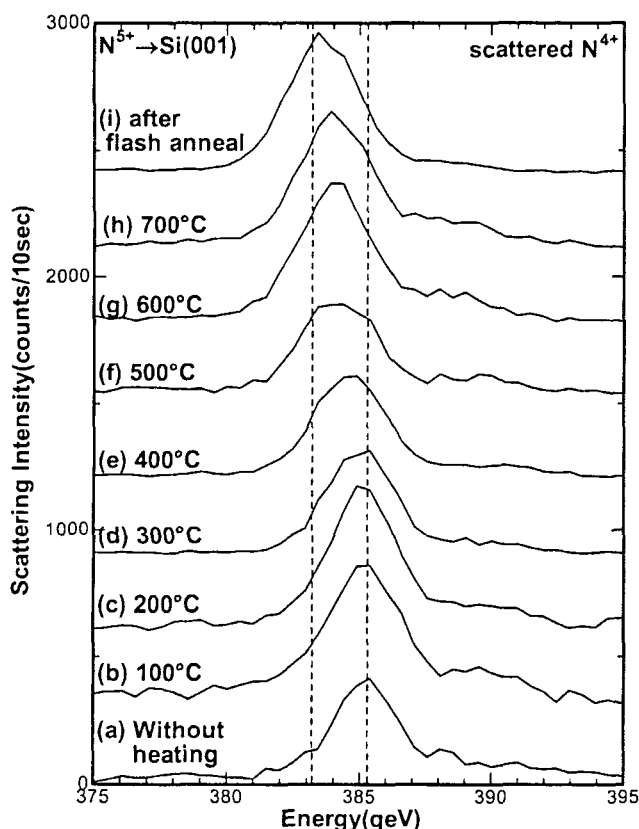


Figure 2. One electron capture energy gain spectra of 305 qeV N^{5+} ions incident on a Si(001) surface at 2° grazing angle and scattered by 2.5° as a function of sample temperature.

allowed to reach room temperature and the spectrum recorded. From figures 2(a)-2(h), we see that the peak in the energy gain spectrum shifts to lower energies as the temperature to which the sample is raised is increased. That is, the peak at 385.4 qeV before the sample was heated progressively shifts to 383.2 qeV as the sample temperature is increased. The overall peak shift of 2.2 qeV or 8.8 eV is due to desorption of the surface oxide layer, and/or desorption of oxygen, carbon, and other surface contaminant atoms with increasing sample temperature. (Observed electron capture from residual gas atoms at 10^{-9} Torr in the scattering chamber is small compared to scattering from the surface.)

The observation of one electron capture would suggest that for N^{5+} ions incident on a Si(100) surface at a 2° grazing angle, it might be possible to determine from the energy gain spectrum the atom or atoms from which the electron was captured.

To this end, energy gain spectra recorded at a scattering angle θ were converted into internal energy changes of the colliding system or Q values. [1] Figure 3(a) shows the energy gain spectrum in figure 2(a). The upper abscissa scale shows the measured kinetic energy of the scattered N^{5+} projectile, now N^{4+} , in qeV, while the lower abscissa scale gives the Q value in eV. Figure 3(b) shows the energy gain spectrum after the sample was flash annealed. Also shown in figure 3 are the Q values calculated for one electron capture by N^{5+} into various (nl) states from free silicon and oxygen atoms. The Q values were determined from total electronic energies calculated using the Hartree-Fock program HF-96. [2] Strictly speaking, the binding energies of electrons in atoms bound to other surface atoms or molecules should be used. Since these are not available, and since in the calculation of Q values only differences of total electronic binding energies appear, the Q values calculated using Hartree-Fock energies for free atoms should give some idea of the Q values.

In figure 3(a), electron capture from free oxygen atoms into $n = 3$ and $n = 4$ states of the projectile occurs at Q values around 23 and 5 eV respectively, while for silicon, capture into $n = 3$, $n = 4$ and $n = 5$ gives Q values around 30, 14 and 7 eV. The Q value spectrum of ions

recorded before the sample was heated shows a broad peak centered at around 20 eV, near the free oxygen Q values. After the sample was heated above 600°C, the Q value spectrum did not change upon reheating, nor did it change after the sample was flash heated to 1200°C. In figure 3(b) after the sample was flash heated, the peak shifted to a lower energy compared to that in 3(a).

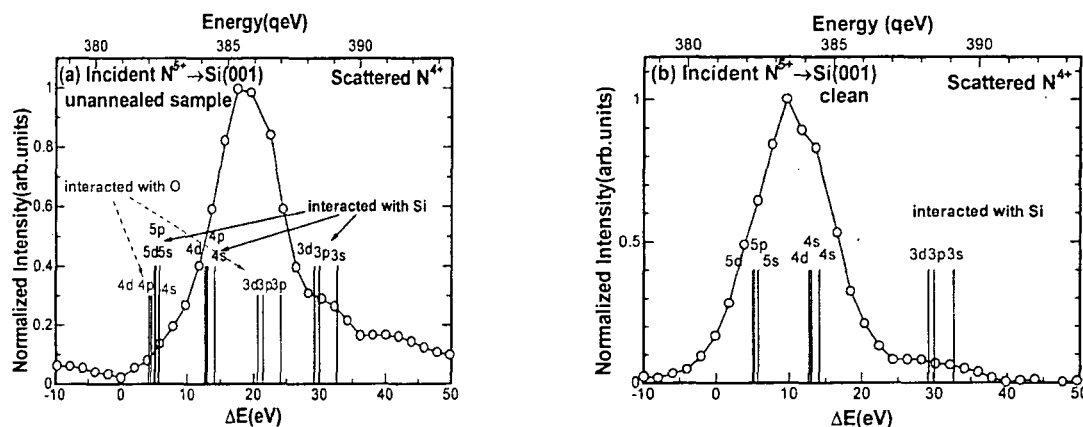


Figure 3. Energy gain spectra and Q values for one electron capture by N^{5+} incident on Si(100) at a grazing angle of 2° , and a scattering angle of 2.5° . (a) Sample not heated and (b) sample heated to 1200°C (clean). Also shown are Q values for one electron capture from free silicon and oxygen atoms into states (nl) of the

According to our interpretation, oxygen (and contaminant) atoms were driven off the Si(100) surface after it was flash heated to 1200°C so that the surface contained mostly Si atoms. Then, mostly capture from silicon into the $n = 4$ and $n = 5$ states of the projectile occurred.

References

- [1] J. Vancura, J.J. Protti, J. Flidr, V.O. Kostroun, *Rev. Sci. Instrum.* **64** (1993) 3139.
- [2] C.F. Fischer, T. Brage, P. Jönsson, *Computational Atomic Structure an MCHF Approach*, (Institute of Physics Publishing, Philadelphia, 1997)

Dynamics of Multielectron Systems Interacting with Light and Matter

Jim McGuire

Department of Physics, Tulane University, New Orleans, LA 70118-5698
mcguire@tulane.edu

Scope: *Multielectron effects in been evaluated and analyzed in cross sections for single and multiple electron transitions in atoms interacting with ions, electrons and photons. In the past year we have begun to probe correlation in time as well as correlation in space between electrons.*

Recent Progress

Understanding *how electrons communicate about time* requires ideas about both correlation and time. The mechanism for electrons to interact is the electron-electron Coulomb interaction, which is the source of spatial electron correlation. Without this spatial correlation the electrons are independent and cannot communicate. Time is often regarded as a parameter common to both the Schrödinger-wave and Newtonian-particle equations. However, the way in which time operates is quite different in the wave and particle limits. In the quantum wave limit of broad delocalized wavepackets, operators for time are difficult to define, as reflected in Pauli's remark that it is "impossible to find a self adjoint (local) time operator conjugate to any Hamiltonian with a bound spectrum (such as an atom)". Fortunately the mathematics of quantum mechanics is straightforward. The concept of time correlation has been used in non-equilibrium statistical quantum mechanics, where it is similar to spatial correlation.

The key conceptual tools needed to study how electrons communicate about time are temporal correlation of the external interactions and spatial correlation between electrons. Both are required for time correlation between electrons. Two examples in which time correlation between electrons plays an observable role in atomic reaction cross sections were studied in detail. The first case is a kinematic peak in a reaction in which electron transfer and ionization both occur. In this case time correlated and time uncorrelated amplitudes add incoherently. The second case is double electron excitation, where coherent reaction pathways interfere. In the second case time correlation between electrons produces a large observable effect on both the shape and intensity of a double excitation resonance.

Time dependence is imposed on a quantum system by an external time dependent interaction, $V_I(t)$. The general expression for the probability amplitude, $a_{fi}(t) = \langle f | U_I(t, t_i) | i \rangle$, for the transition of one or more electrons from $|i\rangle$ at time t_i to $|f\rangle$ at time t may be described most conveniently in the interaction representation using the evolution operator, $U_I(t, t')$, which satisfies,

$$i \partial U_I(t, t') / \partial t = V_I(t) U_I(t, t') \quad , \quad (1)$$

with the initial condition $\lim_{t \rightarrow -\infty} U_I(t, -\infty) = \hat{I}$. The formal solution for the evolution operator may be expressed as a time ordered exponential,

$$\begin{aligned} U_I(t, t_i) &= T \exp \left\{ -i \int_{t_i}^t V_I(t') dt' \right\} \\ &= \sum_{k=0}^{\infty} \frac{(-i)^k}{k!} \int_{t_i}^t \dots \int_{t_i}^t T[V_I(t_1) \dots V_I(t_k)] dt_1 \dots dt_k \quad . \end{aligned} \quad (2)$$

Here T is the Dyson time ordering operator,

$$T[V_I(t_1)V_I(t_2)\dots V_I(t_k)] \equiv \sum_{P(1,2,\dots,k)} \theta(t_1 - t_2)\theta(t_2 - t_3)\dots\theta(t_{k-1} - t_k)V_I(t_1)V_I(t_2)\dots V_I(t_k) , \quad (3)$$

where $\theta(t-t')$ is the Heavyside step function. The sum above is taken over all possible permutations, P , of the parameters $1, 2, \dots, k$. The Dyson time ordering operator, T , imposes ordering of the $V_I(t_j)$ interactions in time to enforce causality in the time evolution of the system. Here $V_I(t) = \sum_j^N V_{Ij}(t)$ is implicitly summed over electrons.

The $V_I(t_j)$'s provide the time dependence to the quantum wave amplitudes, $a_{f_i}(t)$, via Eq.(2). Requiring that correlation in time be independent of the mathematical form of $V_I(t)$, we use the only time dependent term available other than V_I , namely the time ordering operator, T . All time dependence in T arises from the $\theta(t_i - t_j)$ terms in Eq.(3). Thus, time correlation may be removed by replacing all $\theta(t_i - t_j)$ by a constant. Then $T[V_I(t_1)V_I(t_2)\dots V_I(t_k)]$ is a simple product of $V_I(t_j)$ and is therefore uncorrelated in time. Hence there can be no time correlation in U_I . Therefore, we separate the T operator into two terms,

$$T = T_{unc} + (T - T_{unc}) \equiv T_{unc} + T_{cor} . \quad (4)$$

where T_{unc} is the uncorrelated part of T , and $T_{cor} \equiv T - T_{unc}$, acting on $V_I(t_1)\dots V_I(t_k)$, is our time correlation operator. In first order in V_I there is no time correlation. In second order one has,

$$T(V_I(t)V_I(t')) = \theta(t - t')V_I(t)V_I(t') + \theta(t' - t)V_I(t')V_I(t) \quad (5)$$

where,

$$T_{unc}(V_I(t)V_I(t')) = \frac{1}{2}(V_I(t)V_I(t') + V_I(t')V_I(t)) , \quad (6)$$

whence it is easily shown that,

$$T_{cor}(V_I(t)V_I(t')) = \frac{1}{2} \text{sign}(t - t') [V_I(t), V_I(t')] . \quad (7)$$

Calculations using $T \simeq T_{unc}$ correspond to an independent time approximation, where the $V_I(t_j)$ interactions are not correlated in time. In second order a two step process is reduced to two independent one step processes.

In multiple electron transitions correlation in time between electrons generally requires spatial electron-electron correlation in addition to time ordering. Physically this is obvious. In the uncorrelated independent electron approximation without exchange, the probability is represented as a product of single electron probabilities, namely, $P(t) = |a_{f_i}(t)|^2 = \Pi_j | \langle f_j | U_{Ij}(t, t_i) | i_j \rangle |^2 = \Pi_j P_j(t)$. In this limit there is no mechanism for time correlation between transitions of different electrons. Without spatial electron correlation phase information between electrons is lost. Only when spatial electron correlation is included can T_{cor} cause time correlation between different electron transition amplitudes.

Since entanglement is conceptually and mathematically similar to electron correlation, our time correlation operator, T_{cor} , may also be regarded as a time entanglement operator. Observable effects due to T_{cor} occur in both single and multiple electron transitions. However, in our recent work we focused on the effects of time correlation between electrons, i.e. how electrons communicate with one another about time.

About a dozen calculations have been completed to test the effect of time correlation between electrons. We have examined in detail the electron-electron Thomas peak in fast transfer-ionization and double excitation resonances in interactions of fast electrons with helium. In the later reaction T_{cor} changes the resonance intensities by a factor of three and the shapes from a window-type to a nearly asymmetric resonance profile in some cases.

Future Plans

Nano-dynamics. Our methods may be useful for the understanding of sequencing in nanostructures. Most existing studies of nanostructures do not yet include dynamic many-electron effects, including correlation in time between electrons. We note that the Molecular Electronics Company, headed by the chair of electrical engineering at Yale, with a theoretical physicist and two chemists, opened in Chicago in January and is incorporated. Self assembly of nanowires at the molecular level is another example. Our methods open the door for understanding and studying specific methods to *control transmission of quantum information in many-electron systems*. This could be useful in quantum computing, quantum cryptology, fast atomic switching, quantum locks and security, information processing in artificial neural networks, and, in general, control of dynamic sequencing in atoms and molecules. Sequencing and time correlation enable us to understand how electrons communicate about time, and how interfering quantum pathways may be dynamically altered to manipulate the outcome of atomic and molecular reactions. Such control at the atomic level might be achieved, for example, via Pauli blocking, by use of time varying external electromagnetic fields, or use of strong magnetic fields described above. In larger systems, such as molecular fragmentation, time connections between subsystems might be established by extending earlier work on the independent center, independent electron approximation to include time correlation.

Micro-plasmas. Much of the emphasis of our work is on multi-electron transitions, including multiple ionization. It is clear from studies of both strong laser fields and highly charged ions interacting with atomic systems that one may now experimentally access and possibly control regions in which multiple ionization is dominant. It is our view that the transition into the plasma regime occurs sharply as the interaction parameters are changed. A simple argument is that the binomial (or corresponding multinomial) distribution, $\binom{N}{n}P^n(1-P)^{N-n}$, applicable in the strong field limit, changes quickly as the single electron probability P changes. Thus, we expect plasma parameters to be especially sensitive to change in the transition region from single to multiple ionization. The *dynamic formation of plasmas on the nanoscale* has been challenging. We are developing the tools needed to understand this problem. We have estimated that the transition region from single to multiple ionization may be studied using fourth generation synchrotrons where the brightness may be varied from the weak field region well into the strong field region. This basic understanding could be useful in development of more effective and precise etching of computer chips. We note that IBM has recently announced plans to use electrons rather than photons to etch chips. Thus, studies such as ours of multiple ionization in atoms by impact of electron beams could be useful in identifying masking materials and intensity parameters useful for clean, quick etching. The problem of the time evolution of micro plasmas is also basic to the use of intense radiation to treat brain cancer, as is now successfully being done using C^{+12} ion beams at GSI in Darmstadt, Germany.

Arrival times, atomic memory and time symmetry In our approach we have separated the evolution operator into propagation symmetric and antisymmetric in time. Such separation may be useful in resolving basic problems in *sensibly defining quantum operators for arrival times*, dating from work of Aharonov and Bohm. It has recently become clear that different arrival operators lead to different quantum times, including a difference in 'presence time' and 'passage time'. Our techniques provide a method to examine these differences in specific and testable calculations. This is basic to understanding how time is described in quantum systems. Our T_{cor} is necessary for time correlation. Correlation in time is basic to *understanding the role of memory in atomic collisions*.

Neglecting memory is a key condition in statistical Markov processes including master equations, information theory, maximum entropy methods and Fokker Planck. Our methods may be useful in understanding when such statistical methods may or may not be used. With our technique we are able to specifically address the question: are there experimentally testable ways to observe and possibly to control effects of quantum sequencing?

Publications

1. "Thomas peak of the second kind in transfer-ionization", S. Tolmanov and J.H. McGuire, Phys. Rev. A **63**, in press (Oct. 2000).
2. "Exclusive and Inclusive Cross Sections for Compton Scattering from H- and He", J.H. McGuire, S. Itza-Ortiz, A.L. Godunov, D.L. Ederer, J. Wang and J. Burgdoerfer, Phys. Rev. A **62**, 012702 (2000).
3. "Double excitation in helium by impact of fast proton", A.L. Godunov, P.B. Ivanov, V.A. Schipakov, P. Moretto-Capelle, D. Bordenave-Montésquieu and A Bordenave-Montesquieu, J. Phys. B: **33**, 971 (2000).
4. "Time ordering in fast double ionization", J.H. McGuire, A.L. Godunov, S.G. Tolmanov, R. Dreizler, H. Schmidt-Böcking, R. Dörner, V. Mergel and B. Shore, International Journal of Mass Spectroscopy, **192** 65, (1999).
5. "Cross Section Ratio of Double to Single Ionization of Helium by Compton Scattering of 20 keV X-rays", L. Spielberger, H. Bräuning, A. Muthig, J.Z. Tang, J. Wang, Y. Qui, R. Dörner, O. Jagutzki, Th. Tschentscher, V. Honkimäki, J. Burgdörfer, J. McGuire and H. Schmidt-Böcking, Phys. Rev. A **59**, 371 (1999).
6. "Survey of AMO Faculty Positions in US Physics Departments", TAMOC website (1999).
7. "Differential Cross Sections in Antiproton and Proton Helium Collisions", Kh. Khayyat, Th. Wever, R. Dörner, M. Achler, V. Merger, L. Spielberger, O. Jagutzki, U. Meyer, J. Ullrich, R. Moshhammer, H. Knudsen, U. Mikkelsen, P. Aggerholm, S.P. Moeller, R.E. Olson, P. Fainstein, J.H.McGuire, and H. Schmidt-Böcking, Journal of Physics B **32**, L73 - 9, (1999).
8. "Charge and velocity dependence of the ratio of double to single ionization of H^- by Ne^{+q} and Ar^{+q} ", F. Melchert, E. Salzborn, D.B.Utskov, L.P.Presynakov, Catalina Gonzales and J. H. McGuire, Phys. Rev A **59**, 4379 (1999).
9. "Elastic and inelastic scattering of 4d inner shell electrons in $(Y, Gd)_2O_3$ studied by synchrotron radiation excitation", A. Moewes, T.Eskildsen, D.L.Ederer, Jianyi Wang, Jim McGuire and T.A. Calcott, Phys. Rev. **B57**, R8059 (1998).
10. "Double photo ionization of spatially aligned D_2 .", R. Dörner, H.P. Bräunig, O. Jagutzki, V. Mergel, M. Achler, R. Moshhammer, J. Feagin, A. Bräunig-Demian, L. Spielberger, J.H.McGuire, M.H. Proir, N. Berrah, J. Bozek, C.L. Cocke and H. Schmidt-Böcking, Phys. Rev. Lett. **81**, 5780 (1998).
11. "Helicity dependence of the photon-induced three-body Coulomb fragmentation of helium investigated by COLTRIMS", V. Mergel, M. Achler, R. Dörner, Kh. Khyyat, T. Kambara, Y. Awaya, V. Zoran, B. Nyström, L. Spielberger, J.H.McGuire, J. Feagin, J. Berakdar, Y. Azuma and H. Schmidt-Böcking, Phys. Rev. Lett. **80**, 5301 (1998).
12. "Inversion Relations for Exclusive and Inclusive Cross Sections within the Binomial Independent Electron Approximation", M.M.Sant'Anna, E.C.Montenegro and J.H.McGuire, Phys. Rev. **A58**, 2148 (1998).
13. "Ten thousand times faster than a laser, and just as strong", J.H. McGuire and Bruce W. Shore, Physics World, **11**, 25 (1998).
14. "Anti-proton and proton impact excitation-ionization of helium including resonant decay", Jack C. Straton, J.H.McGuire and A.L.Godunov, Nucl. Instru. and Methods in Phys. Research **B 143**, 225 (1998).

Also eight abstracts in refereed conference proceedings were published since 1998.

PROGRESS REPORT
PROJECT: ELECTRON COLLISIONS IN PROCESSING PLASMAS
Investigator: Vincent McKoy

In Year 3, we continued to implement advanced capabilities in our electron-molecule scattering programs and to conduct detailed studies of elastic and inelastic collisions between low-energy electrons and a variety of polyatomic molecules.

Highlights

- Introduced multiconfiguration target states into our programs
- Continued development of efficient strategies for treating target polarization
- Continued to improve computational hardware
- Published two invited review articles and several research papers and presentations

Multiconfiguration Target States

Accurate representations of the ground states of closed-shell systems can usually be obtained from single-configuration, Hartree-Fock-type wavefunctions. Because so many molecules have closed-shell ground states and because a single-configuration description of the target simplifies the construction of the target-plus-projectile trial wavefunction, the original implementation of the Schwinger Multichannel (SMC) method for electron-molecule scattering required that the ground state of the target be described by a single closed-shell Slater determinant.

In recent years, we had relaxed the closed-shell restriction to accommodate doublet ground states, in order to study electron collisions with common radicals. However, the single-configuration requirement had remained, and one of the goals of this research project has been to implement a multiconfiguration description of targets. Multiconfiguration wavefunctions are commonly needed for the accurate description of

- excited states
- ground states undergoing dissociation
- certain ground states at their equilibrium geometry (e.g., that of ozone)

We are now completing development of a multiconfiguration-target implementation of the SMC method and beginning exploratory calculations with it. Our initial application has been to elastic electron scattering by ozone, O₃.

Ozone possesses intrinsic interest and also furnishes a useful test case in that other theoretical [1-6] and experimental [7,8] data are available for comparison. It has long been known that two electronic configurations, $\dots (6a_1)^2(1a_2)^2(2b_1)^0$ and $\dots (6a_1)^2(1a_2)^0(2b_1)^2$, contribute strongly to the ground state of ozone; the occupation numbers of the $1a_2$ and $2b_1$ orbitals are about 1.6 and 0.4, respectively. However, all previous theoretical studies [1-6] of electron-ozone scattering have employed only the $(1a_2)^2$ configuration to describe the molecular wavefunction, although Gianturco *et al.* [6] did conduct a limited study of target correlation effects using density-functional theory. We have now examined the effect of using a two-configuration description of the ground state within the static-exchange approximation for scattering and found it to be surprisingly small: our cross sections agree

closely with static-exchange results obtained using a single-configuration target wavefunction [3]. Presently we are refining this study by including polarization effects. We will then be turning to studies of inelastic collisions employing a multiconfiguration of excited states of the target molecule.

Efficient Treatment of Polarization

In the past few years we have been developing more efficient methods of treating the polarization of the target charge density by the projectile electron during the collision. During the current year, we continued to work on refining those methods while also applying them in their current implementation to problems of practical interest. For example, we have nearly completed a study of elastic scattering by tetrafluoroethene, C_2F_4 , which is of interest both as an analogue of the prototypical and well-studied C_2H_4 molecule and as an important species in plasma etching of semiconductors, either as a primary feed gas or as secondary species produced by the plasma decomposition of other etchants, notably $c-C_4F_8$ (octafluorocyclobutane).

Hardware

During the past year we completed integration of a gigabit ethernet switch into our computational cluster. As anticipated, the addition of high-speed networking removes a communications bottleneck and allows us to run parallel computations at good efficiency on up to 16 processors.

Plans for Coming Year

During the next year we will be completing implementation, testing, and debugging of the enhanced electron-molecule scattering programs. We also expect to apply the new capabilities to study some interesting and significant collision problems. In addition to pursuing our ongoing investigations of fluorocarbon and hydrofluorocarbon etchants used in the semiconductor industry, we will be conducting an intensive study of inelastic electron collisions with N_2 , for which new (as yet unpublished) experimental data have recently been obtained. We expect that employing multiconfiguration descriptions of the excited states of N_2 will make a significant contribution to the accuracy of our results.

We are currently awaiting final word on a further gift of equipment from Intel Corporation in support of our research program. This gift will at least double and possibly quadruple the computational power of our cluster, depending on the precise number of processors and their speed. Over the coming year we will be carrying out setup, configuration, and testing of the new workstations and associated network equipment and putting the upgraded cluster into production use.

Publications and Presentations

Publications and presentations related to this project during the past year:

1. "Collisions of Low-Energy Electrons with CO_2 ," C.-H. Lee, C. Winstead, and V. McKoy, *J. Chem. Phys.* **111**, 5056 (1999).

2. "Electron-Molecule Collisions in Low-Temperature Plasmas: The Role of Theory," C. Winstead and V. McKoy, *Advan. At., Mol., Opt. Phys.* **43**, 111 (2000). (*Special issue, Fundamentals of Plasma Chemistry, M. Inokuti, editor.*)
3. "Collisions of Low-Energy Electrons with C_6H_6 ," M. H. F. Bettega, C. Winstead, and V. McKoy, *J. Chem. Phys.* **112**, 8806 (2000).
4. "Parallel Computational Studies of Electron-Molecule Collisions," C. Winstead and V. McKoy, *Computer Phys. Commun.* **128**, 386 (2000). (*Invited paper for a special issue on "Parallel Computing in Chemical Physics."*)
5. "Electron Scattering by Hexafluorobenzene, C_6F_6 ," C. Winstead, M. H. F. Bettega, and V. McKoy, presented at the Fifty-Second Gaseous Electronics Conference, Norfolk, Virginia, 5-8 October, 1999.

References

- [1] Y. Okamoto and Y. Itikawa, *Chem. Phys. Lett.* **203**, 61 (1993).
- [2] B. K. Sarpal, K. Pfingst, B. M. Nestmann, and S. D. Peyerimhoff, *Chem. Phys. Lett.* **230**, 231 (1994).
- [3] B. K. Sarpal, B. M. Nestmann, and S. D. Peyerimhoff, *J. Phys. B* **31**, 1333 (1998).
- [4] M. T. Lee, S. E. Michelin, T. Kroin, and L. E. Machado, *J. Phys. B* **31**, 1781 (1998).
- [5] M. H. F. Bettega, M. T. do N. Varella, L. G. Ferreira, and M. A. P. Lima, *J. Phys. B* **31**, 4419 (1998).
- [6] R. Curik, F. A. Gianturco, and N. Sanna, *J. Phys. B* **32**, 4567 (1999).
- [7] T. W. Shyn and C. J. Sweeney, *Phys. Rev. A* **47**, 2919 (1993).
- [8] M. Allan, K. R. Asmis, D. B. Popovic, M. Stepanovic, N. J. Mason, and J. A. Davies, *J. Phys. B* **29**, 4727 (1996).

ELECTRON/PHOTON INTERACTIONS WITH ATOMS/IONS

Alfred Z. Msezane, amsezane@ctsps.cau.edu

Department of Physics and CTSPS, Clark Atlanta University, Atlanta, Georgia 30314

During the period covered by this report, we investigated and solved several important problems in electron/photon interactions with atoms/ions with interesting consequences. Many of our research accomplishments have been achieved with national and international collaborators. The elucidation of small-angle electron scattering through innovative theoretical approaches and the solution of the problem of Dispersion Relations when exchange forces are present are examples.

A. EXCHANGE FORCES IN DISPERSION RELATIONS: INVESTIGATION USING CIRCUIT RELATIONS

In order to use Dispersion Relations (DR) to test the validity of measurements in e-Atom experiments, especially when they are conflicting, a clear understanding is necessary of the structure of the left-hand cut discontinuity of the scattering amplitude in the complex energy E plane. In the absence of exchange forces there is no left-hand cut discontinuity for forward scattering. Therefore, the left-hand cut is directly linked to the presence of the *exchange forces*. While the right-hand cut discontinuity (physical) is well understood and corresponds to easily measurable quantities such as the total cross-sections, the left-hand cut discontinuity (unphysical) must be computed theoretically. The importance of the problem is evident from Blum and Burke [1] who stated that "The future of dispersion relations in atomic physics depends critically on a better understanding of the nature of the singularities of the left-hand cut". The application of DR to quantum physics has been a subject of continuing interest, but with no reliable and systematic method to access the unphysical discontinuity until very recently [2, 3]. It has been found [2] that the exact left-hand cut discontinuity for the two-body Schrödinger equation, without exchange forces, can be computed on any finite interval from the Born series stopped at a finite order. Also, a practical approach of including exchange forces in a DR has been discovered [3], thereby resolve the long-standing problem.

In the present work, we have extended the approach of [2] by including in a rigorous way exchange forces in a DR [4] through the novel use of the technique of circuit relations [5]. Our method permits the calculation of the left-hand discontinuity in the complex E plane of the S-matrix element exactly in the presence of exchange forces within the Static Exchange Approximation. The circuit relations are the key elements in our approach, since they carry information from large distances, where perturbation theory applies, to small distances, where the S-matrix is defined through the Jost solutions. Zero energy DR for electron-H scattering have been computed numerically for illustration. The application of external fields could conceivably bring the triple pole closer to the origin thereby enhance its effect on measurable quantities.

B. REGGE TRAJECTORIES FOR SINGULAR POTENTIALS AND REGGE POLE INVESTIGATION OF CHEMICAL REACTIONS

For scattering involving heavy particles such as atoms and molecules, the ordinary partial wave expansion utilizing only non-negative integer values of the angular momentum is often slowly convergent and hardly appropriate for numerical calculation. The complex angular momentum (CAM) representation [6], involving Regge poles calculations, has proved to be the adequate answer. In the case of singular potentials, defined as diverging faster than r^{-2} at the origin, the main difficulty in computing a Regge pole position in the CAM plane, for real positive values of the energy, is that one deals with a singular eigenvalue problem for a non-Hermitian Schrödinger operator.

In the first part of this work, we have developed an accurate and efficient analytical method [7] to augment the relatively few existing methods, which are mostly numerical, for calculating Regge-pole positions. Besides the traditional Regge poles calculations for the singular Lennard-Jones potential, there are other important physical problems that can be treated. The Bose-Einstein condensation and superfluidity of ^4He at extremely low temperatures are such examples. The He-He collision problem, where the possibility of forming dimer resonances exists, has been investigated [8] using the two versions of the Aziz potentials. The problem could be solved only within the framework of the singular potential method. Hence, our interest in this work. In the second part, we have developed [9] a practical procedure for analytically continuing a scattering matrix element into the CAM plane, given its value at the physical angular quantum numbers of 0,1,2---. The procedure first applies a preconditioning function to the scattering matrix element; then the remaining residual function is interpolated using Padé approximations. The method has been illustrated by extracting the leading Regge pole positions and residues for the state selected reactions $\text{Cl} + \text{HCl} (\nu' = 1, j = 5) \rightarrow \text{ClH} (\nu' = 1, j' = 5) + \text{Cl}$ and $\text{I} + \text{HI} (\nu = 0, j' = 0) \rightarrow \text{IH} (\nu' = 0, j' = 2) + \text{I}$, where ν and j are vibrational and rotational quantum numbers, respectively.

C. ELECTRON IMPACT EXCITATION

C.1 Kinematic Representation to Elucidate Small-Angle Electron Scattering

The difficulties of measuring reliably the electron differential cross sections (DCS's) at small scattering angles, including their normalization, are well documented. Even the most recent measurements of the DCS's for H [10] obtained data down to only $\theta = 7^\circ$, and for Li, their limited availability reflects technical problems [11]. We have found that an appropriate representation of the apparent generalized oscillator strength (AGOS) permits the demonstration of its general properties [12]. Only the zero-angle trajectory connects continuously the threshold energy $E = \omega$ and the high energy $E = \infty$, corresponding to the optical oscillator strength limit of the AGOS. Far reaching implications, including the normalization of measured relative DCS's and the identification of their spurious behavior, are discussed and demonstrated using optically allowed transitions in H, Li and Ba [12].

C.2 Electron Impact Excitation at Small-Angles: The Lassetre Limit and Attendant Normalization of Measured Relative DCS's

The recent generalized Lassetre expansion (GLE) [13] employing only a single Regge pole has been used to demonstrate for the first time ever the applicability of the Lassetre limit theorem over the entire electron impact energy without the involvement of the nonphysical region of the AGOS [14]. At forward scattering the GLE yields the unique long-sought after normalization curve to the optical oscillator strength of the measured relative electron DCS's through the AGOS. Optically allowed transitions in H, He, Xe and N_2O have been used to illustrate the normalization procedure, including the identification of spuriously behaved data in the difficult to measure small angular regime.

C.3 Collision Strengths for Transitions Among the $3s^2$, $3s3p$ and $3p^2$ Configuration of Fe XV

Emission lines of Mg-like Fe XV have been observed in the X-ray and EUV (190-350 Å) ranges of the solar spectrum and, therefore, atomic parameters such as radiative rates, collision strengths and excitation rate coefficients are of vital importance for understanding the plasma properties. We have calculated [15] collision strengths for transitions among the energetically lowest 10 fine-structure levels belonging to the $(1s^2 2s^2 2p^6) 3s^2$, $3s3p$ and $3p^2$ configurations of Fe XV using the Dirac atomic R-matrix code of Norrington and Grant. We have compared our results with those recently calculated by Griffin *et al* [16] and Eissner *et al* [17]. Large discrepancies are observed, particularly with those of the former. It is concluded that the values reported by Griffin *et al* are inaccurate for many transitions. Details of the comparisons and the recommendations are found in [15].

C.4. Minima In Generalized Oscillator Strengths for Resonance Transitions in Na and K

The generalized oscillator strength (GOS) is an important property of the atom which manifests directly the atomic wave functions and the dynamics of atomic electrons. We have investigated the GOS's for the Na 3s-3p and K 4s-4p transitions using the spin-polarized technique of the random phase approximation with exchange (RPAE) and the Hartree-Fock approximation (HFA), focusing our attention on the positions of the minima. For the Na 3s-3p transition, inter-shell correlations are found to influence significantly the position of the minimum [18] whose position is predicted by the RPAE at the momentum transfer, K value of 1.258 a.u.. The former value is within the range of values of $K=1.0 - 1.67$ a.u. extracted by us from experimental measurements. The range of K values suggests a careful experimental search for the position of the minimum around the predicted value for confirmation. For the resonance transition in K, both the RPAE and the HFA predict two minima [18]. The first minimum, which is narrower and has never been measured before, is predicted by the RPAE at $K=0.8838$ a.u. while the second is the well-measured one at 2.907 a.u. The positions of the minima are found to be sensitive to inter-shell correlations. This calls for a careful experimental search for the first minimum around the predicted value of K .

D. PHOTON INTERACTIONS WITH ATOMS/IONS

D.1 Relativistic Effects in the Photoionization of Ne-Like Iron

The photoionization of positive ions is of importance in numerous physical situations such as in the understanding and modeling of astrophysical and fusion plasmas. Additionally, the interaction of ionizing radiation with ions is a fundamental process of nature whose detailed systematics are not well understood. We have investigated relativistic effects in the photoionization of Ne-like iron using three sets of calculations [19]. We demonstrated that much similar techniques can reproduce the results of the full Breit-Pauli R-matrix method which includes relativistic effects in photoionization calculations. To allow for the fine-structure splitting of channels in the photoionization of Fe^{16+} , we have performed three sets of calculations. The first combined an *LS* R-matrix calculation with an *LS-JK* frame transformations, using multichannel quantum defect theory. The second used a relativistic random phase approximation based on the Dirac equation. Both methods give resonant photoionization results nearly identical to those from a third calculation using the full Breit-Pauli R-matrix method. An accurate treatment of fine-structure splitting in Fe^{16+} is necessary to realistically include the appropriate resonances which dominate the low-energy photoionization cross section; consequently, in the inverse process of photorecombination, the low-temperature rate coefficient is dominated by those dielectronic recombination resonances.

D.2 Connection Between Drag Currents and Non-Dipole Asymmetry Parameter

For photon energies higher than the ionization potentials of target atoms, the photoionization of the atomic particles, in which the photon momentum is transferred to the ion and the electron after absorption, becomes more important. This insufficiently studied manifestation of electromagnetic radiation pressure upon matter in the gas phase plays an essential role in many natural phenomena such as in the atmospheres of some stars and the upper layers of the Earth's atmosphere, where the intensity of the UV component of the solar radiation is sufficient to cause large flows of charged particles. Expressions for the drag currents which appear under the action of ionizing radiation in atomic gases and their mixtures have been obtained [20]. Also, the connection between the drag currents and one of the non-dipole asymmetry parameters has been established. Experimental investigation of the drag currents for use in precision measurement of the asymmetry parameters has been discussed, particularly for small photoelectron energies where it is difficult to apply the traditional experimental schemes to measure DCS's for photoionization. Non-dipole parameters for Ne 2s, Ne 2p and Ar 1s subshells photoionization have been calculated and compared with measurements and other calculations.

PLANNED / ONGOING RESEARCH ACTIVITIES

Here we list some planned/ongoing research activities involving many of our collaborators.

- Our investigation of exchange forces in dispersion relations using circuit relations will be extended to the multichannel Static Exchange Approximation
- The application of external fields to the e-H scattering problem could conceivably move the triple pole closer to the positive real axis, thereby enhance its effect on measurable quantities.
- Many S-matrices exist for heavy atom- atom reactions. We will investigate possible identification of resonances in atom- atom collisions.
- We will use our present methods to investigate small-angle electron-atom scattering; even the most recent experiments on e- Ne still measure DCS's, down to only 10° .
- Our singular potential method will be used to investigate Bose-Einstein condensation and superfluidity of ^4He at extremely low temperatures as well as the possibility of forming dimer resonances in He -He collisions.
- Collision strengths for transitions among fine-structure levels in ions of importance to astrophysics and fusion plasmas will continue to be investigated, as well as correlation and relativistic effects in photoionization of positive ions.

References And Some Publications

- [1] K. Blum and P. G. Burke, Phys. Rev. **A16**, 163 (1977)
- [2] D. Bessis and A. Temkin, Phys. Rev. **A61**, 032702 (1999)
- [3] A. Temkin and R. J. Drachman, J. Phys. **B33**, L1 (2000)
- [4] D. Vrinceanu, **A. Z. Msezane**, D. Bessis and A. Temkin, Phys. Rev. Lett., Submitted (2000)
- [5] R.G. Newton, *The Complex j -Plane* (Math. Phys. Monograph Series, W.A. Benjamin, Inc., 1964)
- [6] J. N. L. Connor, J. Chem. Soc. Faraday Trans. **86**, 1627 (1990)
- [7] D. Vrinceanu, **A. Z. Msezane** and D. Bessis, Chem. Phys. Lett. **311**, 395 (1999); - Phys. Rev. **A62**, 022719 (2000)
- [8] S. A. Sofianos, S. A. Rakityansky and S. E. Massen, Phys. Rev. **A60**, 337 (1999)
- [9] D. Vrinceanu, **A. Z. Msezane**, D. Bessis, J. N. L. Connor and D. Sokolovski, Chem. Phys. Lett. **324**, 311 (2000)
- [10] M. A. Khakoo et. al., Phys. Rev. Lett. **82**, 3980 (1999); - Phys. Rev. **A61**, 012701 (2000)
- [11] V. Karaganov, I. Bray and P. J. O. Teubner, Phys. Rev. **A59**, 4407 (1999)
- [12] N. B. Avdonina, Z. Felfli, D. Fursa and **A. Z. Msezane**, Phys. Rev. **A62**, 014703 (2000)
- [13] Z. Felfli, **A. Z. Msezane** and D. Bessis, Phys. Rev. Lett. **81**, 963 (1998)
- [14] Z. Felfli, N. Embaye, P. Ozimba and **A. Z. Msezane**, Phys. Rev. **A62**, In Press (2000)
- [15] K. M. Aggarwal, N. C. Deb, F. P. Keenan and **A. Z. Msezane**, J. Phys. **B33**, L391 (2000)
- [16] D. C. Griffin, N. R. Badnell, M. S. Pindzola and J. A. Shaw, J. Phys. **B32**, 2139 (1999)
- [17] W. Eissner, M.E. Galavis, C. Mendoza and C.J. Zeippen, Astron. Astrophys. Suppl. **137**, 165 (1999)
- [18] Zhifan Chen and **A. Z. Msezane**, Phys. Rev. **A61**, 030703 (R) (2000); - J. Phys. **B33**, 2135 (2000)
- [19] N. Haque, H. S. Chakraborty, P. C. Deshmukh, S. T. Manson, **A. Z. Msezane**, N. C. Deb, Z. Felfli and T. W. Gorczyca, Phys. Rev **A60**, 4577 (1999)
- [20] M. Ya. Amusia, A. S. Baltentkov, L. V. Chernysheva, Z. Felfli, **A. Z. Msezane** and J. Norgren, Phys. Rev. A, In Press (2000)

THE STRUCTURE AND DYNAMICS OF NEGATIVE IONS

David J. Pegg

Department of Physics, University of Tennessee, Knoxville, TN 37996
[djpegg@utkux.utk.edu]

Introduction

We have continued investigating the role of electron correlation in atomic structure by experimentally detaching electrons from atomic negative ions. Photodetachment, Heavy Particle Collisional Detachment and Electron Detachment processes were studied. Our results continue to provide sensitive tests of the ability of theory to go beyond the independent electron model.

Photodetachment of K^-

This project was completed during the current grant period. It consisted of two parts. In one experiment the electron affinity of the K atom was measured with a precision that was more than an order of magnitude better than any previous measurement. It is also far more accurate than the best current theoretical value. Details can be found in Ref [1]. In another experiment we studied the rich resonant structure in the photodetachment cross section of K^- in the vicinity of the $K(5^2D, 7^2S, 5^2F)$ thresholds. These resonances are manifestations of the autodetaching decay of highly correlated, doubly excited states of the negative ion. This work is described in detail in Ref [2].

Photodetachment of Li^-

This project was completed in the current grant period. In the experiment we studied doubly excited states of the Li^- ion that appear as resonances in the photodetachment cross section below the $6p$ threshold of Li. This represents the highest level of excitation of any alkali-metal anion so far reported. A complex rotation calculation was used to help identify the strongly correlated, doubly excited states of the quasi-two-electron ion, Li^- . Several members of a strong "+" type series were observed as well as at least one resonance with a "-" type character. Violations of the propensity rules derived from a study of the H^- photodetachment spectrum were observed. The results are described in Ref [3].

Collisional Detachment of Li^- and B^-

We have re-examined our previous measurements of resonant structure in the collisional detachment cross sections for Li^- and B^- projectiles incident on atomic gas targets. In order to eliminate contributions arising from double detachment, we measured the detached electron in coincidence with the residual neutral atom. The single detachment cross sections thus obtained have both a resonant and a non-resonant component. In both the Li^- and B^- spectra a resonance structure appears at threshold, in addition to a higher lying shape resonance. The new resonances are most likely virtual resonances. More details can be found in Ref [4].

Electron Detachment of C_4^-

Heavy ion storage rings have greatly facilitated the investigation of electron-ion interactions. We have used the CRYRING facility in Stockholm, Sweden to measure the cross section for detachment of an electron from the cluster ion, C_4^- . A primary motivation for the experiment was a search for doubly excited resonance states. None were observed.

Future Plans

There are no future plans since the grant has been terminated.

References

- [1]. See RP [1]
- [2]. See RP [2]
- [3]. See RP [3]
- [4]. D.H.Lee, D.J.Pegg and D.Hanstorp, Bull. Am. Phys. Soc. Vol 45, No3, p88 (abstract R9 18). A more complete manuscript is in preparation.

Recent Publications (RP)

- [1]. "A Measurement of the Electron Affinity of K", K.Andersson, J.Sandstroem, I.Kiyan, D.Hanstorp and D.J.Pegg, Phys. Rev A62, 022503(2000).
- [2]. "Spectrum of Doubly Excited States in the K⁻ Ion", I.Kiyan, U.Berzinsh, J.Sandstroem, D.Hanstorp and D.J.Pegg, Phys. Rev. Lett. 84, 5979(2000).
- [3]. "Strongly Correlated States of the Li⁻ Ion", G.Haeffler, I.Kiyan, U.Berzinsh, D.Hanstorp, N.Brandefelt, E.Lindroth and D.J.Pegg, Phys. Rev A (accepted for publication).
- [4]. "Photodetachment of the Ca⁻ Ion at the ³P_{kp} Threshold", D.H.Lee, M.Poston, D.J.Pegg, D.Hanstorp and U.Berzinsh, Phys. Rev A60, 715(1999).
- [5]. "Observation of Resonance Structure in the Na⁻ Photodetachment Cross Section", G.Haeffler, I.Kiyan, D.Hanstorp, B.Davies and D.J.Pegg, Phys Rev. A 59, 3655(1999).

Energetic Photon and Electron Interactions with Positive Ions

Principal Investigator:

Ronald A. Phaneuf
Department of Physics
University of Nevada, Reno
Reno, NV 89557-0058
phaneuf@physics.unr.edu

Program Scope

This experimental research program seeks a deeper understanding of the complex multielectron interactions and resonance phenomena that characterize interactions of positive ions in plasma environments. Examples are thermonuclear fusion, x-ray laser, materials-processing, and stellar plasmas. In addition to precision data on ionic structure, quantitative measurements of photoionization and electron-impact ionization of ions provide critical benchmarks for *ab initio* theoretical studies and data for plasma modeling. Research on photon-ion interactions constitutes the major thrust of this program, and is carried out at the Advanced Light Source, Lawrence Berkeley National Laboratory. The research on electron-ion collisions is conducted at the multicharged ion facility of the University of Nevada, Reno.

Recent Progress

A. Photoionization of Ions

The major emphasis during the past year has been the implementation of a research endstation for quantitative studies of photoionization of positive ions at the Advanced Light Source (ALS). This endstation is permanently installed on undulator beamline 10.0, which provides intense, collimated and highly monochromatic beams of photons in the energy range 17-340 eV. A postdoctoral fellow, Aaron Covington, a Ph.D. student, Alejandro Aguilar, and an undergraduate student, Ian Covington are assigned to this project. Beamline 10.0 is dedicated half-time to high-resolution atomic, molecular and optical physics, for which the principal investigator is a member of the participating research team. The photon-ion end-station is capable of high-resolution absolute photoionization cross-section measurements for both positive and negative ions.

A commercial hot-filament discharge ion source and low-energy accelerator, the Cuernavaca ion gun apparatus (CIGA) from the Centro de Ciencias Físicas in Mexico, produced O^+ and Ne^+ ion beams for the first absolute photoionization measurements using the new end-station. The photo-ion yield data reveal a rich resonance structure superimposed upon the direct photoionization background. A spectral resolving power $E/\Delta E$ of 1,500 is routine with the new apparatus, and measurements of resonances have been performed at resolving powers as high as 35,000, yielding data on resonance widths. In the case of O^+ , significant contributions due to 2P and 2D metastable ions in the primary beam are readily distinguishable, in addition to photoionization from the 4S ground state. The ground-state population fraction in the O^+ ion beam was determined in a separate

attenuation experiment to be 0.43. This permitted comparison of absolute photoionization cross section measurements with ab initio R-matrix theoretical calculations of Nahar [1]. In the case of photoionization of Ne^+ , dual Rydberg series of resonances result from the fine structure in the ground-state configuration. Distinct Rydberg series of resonances are resolved in the photoionization data, with series limits corresponding to the first three excited states of Ne^{2+} . The O^+ and C^+ results are being prepared for publication.

B. Electron-Impact Ionization of Multiply Charged Ions

At the UNR Multicharged Ion Research Facility, absolute cross-section measurements for electron-impact single ionization of Al^{5+} and Al^{6+} were completed using a dynamic crossed-beams apparatus. A postdoctoral fellow, Guillermo Hinojosa is assigned part-time to this project. A high-efficiency electron spectrometer was installed for the next phase of this experiment, whose goal is to provide much more detailed information about indirect ionization mechanisms than has heretofore been possible for ions. The spectrometer consists of a two-stage parallel-plate electrostatic analyzer and a large-area position-sensitive detector. Testing of this spectrometer is in progress, and constitutes the M.S. project of a graduate student, Miao Lu. The results for electron-impact single ionization of Mn^{q+} ($5 \leq q \leq 8$) were submitted and published in *Physical Review A* [2].

Future Plans

A. Photoionization of Ions

To facilitate photoionization studies with multiply charged ions, a permanent-magnet electron-cyclotron-resonance (ECR) ion source is being developed in collaboration with A. Müller and E. Salzborn of Justus Liebig University in Giessen, Germany. The ECR ion source will be assembled and tested at UNR and moved to ALS during the coming year. Negative ion beams will be generated at ALS by electron-capture collisions of positive ions in an alkali vapor cell, or by a sputter negative ion source, although further development related to negative ions is not part of this project. To provide maximum flexibility for experiments, the ECR and negative ion sources will be interchangeable with the CIGA source, and common, reversible power supplies are used on all electrostatic and magnetic beamline components.

During the next period, high-resolution photoionization measurements are planned for Ca^+ , in collaboration with the Giessen group, to be followed by measurements for Sc^{2+} and Ti^{3+} after installation of the ECR source. This is part of a systematic search for broad $3p^5 3d^2 \ ^2F$ resonance features predicted to straddle the ionization thresholds of ions in the K isoelectronic sequence. These resonances were not observable in high-resolution dielectronic recombination experiments. Objectives include the resolution of fine structure and measurement of photoionization resonance lineshapes, which would provide a stringent test of R-matrix theory. To complement the measurements on O^+ and Ne^+ , measurements on S^+ and Ar^+ are also planned. Implementation of the ECR ion source will facilitate systematic studies of the O^{q+} and Fe^{q+} isonuclear sequences, where considerable theoretical work has been done, but no experimental data are available. The photoionization and photofragmentation of molecular ions such as CO^+

is another possibility, for which feasibility using the endstation has already been demonstrated.

B. Electron-Impact Ionization of Multiply Charged Ions

The effort in this part of the program will be devoted to completing the series of absolute electron-impact ionization cross-section measurements for Al^{9+} ions, and implementation of the electron spectrometer and coincidence detection system for ejected electrons. To test the performance of the electron spectrometer and position-sensitive detector, studies of autoionizing states produced by electron capture collisions of multiply charged ions (e.g. Ar^{8+}) with residual gas will precede attempts to detect ejected electrons from electron-ion collisions. Measurements of electrons from metastable autoionizing states of Na-like ions (e.g. Ar^{7+}) produced in the ECR ion source are another possibility for the performance test. These tests will constitute the M.S. thesis of M. Lu.

References

1. S. Nahar, Phys. Rev. A **58**, 3766 (1998).
2. "Electron-impact single ionization of multiply charged manganese ions," R. Rejoub and R.A. Phaneuf, Phys. Rev. A **61**, 032706-1 (2000).
3. "Merged-beams experiments in atomic and molecular physics," R. A. Phaneuf, C. C. Havener, G. H. Dunn and A. Müller, Rep. Prog. Phys. **62**, 1143 (1999).
4. "Studies of the photoionization of Ne^+ ," A.M. Covington, I.R. Covington, G. Hinojosa, R.A. Phaneuf, I Alvarez, C. Cisneros, B.M. McLaughlin, M.M. Sant'Anna and A.S. Schlachter, Bull. Am. Phys. Soc. **45**, No. 3, 113 (2000).
5. Photoionization of the O^+ ($2s^2 2p^3 \text{}^3\text{P}$ and ^2D) metastable states, A. Aguilar, A.M. Covington, I.R. Covington, G. Hinojosa, R.A. Phaneuf, I Alvarez, C. Cisneros, B.M. McLaughlin, S. Nahar, M.M. Sant'Anna and A.S. Schlachter, Bull. Am. Phys. Soc. **45**, No. 3, 113 (2000).
6. "Development of a collinear apparatus for photon-ion interaction studies," A. Aguilar, A.M. Covington, R.A. Phaneuf, I. Alvarez, C. Cisneros, J. de Urquijo, N. Berrah, J.D. Bozek, I. Dominguez, A.S. Schlachter, M. Lubbell, T.J. Morgan, A. Müller and E. Salzborn, Bull. Am. Phys. Soc. **43**, 1335 (1998).
7. Studies of photon-ion interactions at ALS," A.M. Covington, A. Aguilar, I Alvarez, N. Berrah, J. Bozek, C. Cisneros, I.R. Covington, I. Dominguez, G. Hinojosa, M.M. Sant'Anna, A.S. Schlachter and R.A. Phaneuf, ALS Annual Users Meeting, Compendium of Abstracts, 1999.
8. "Electron-impact ionization of multicharged manganese ions", R. Rejoub and R.A. Phaneuf, Proc. APS Topical Conference on Atomic Processes in Plasmas, Auburn, AL, March 23-26, 1998.

9. "Electron-impact ionization of multicharged manganese ions", R. Rejoub and R.A. Phaneuf, Bull. Am. Phys. Soc. 43, 1339 (1998).

X-ray Spectroscopy of $n=3\rightarrow$, $4\rightarrow$, and $5\rightarrow 1$ Transitions in Heliumlike Ar, Ti, and Cr.

Progress Report June, 1999 - May, 2000

A. J. Smith¹

¹*Department of Physics, Morehouse College, Atlanta GA 30314.*

asmith@morehouse.edu

Unfunded Liaison/Collaborator: P. Beiersdorfer

Lawrence Livermore National Laboratory, Livermore, CA 94550

August 4, 2000

1. Scope of work

During this second project year June 1999-May 2000, we continued to focus our efforts on measurements on heliumlike ions. We used the LLNL EBIT, and the EBIT high resolution spectrometers to accurately measure line positions and intensities, and we have compared the measured values to theoretical predictions. Our paper: "Ratios of $n = 3 - 1$ Intercombination to Resonance Line Intensities for Heliumlike ions with Intermediate Z-values", has been accepted for publication in PRA after minor changes. Similarly our paper: "Measurement of Resonant Strengths for Dielectronic Recombination in Heliumlike Ar¹⁶⁺", has received favorable referee comments, and is expected to be published soon [1-3]. We describe below the measurements and data analyses that were carried out.

2. Recent progress

A. Dielectronic Recombination in heliumlike Cr^{22+}

We have completed measurements and data analyses on the resonance strengths for dielectronic recombination in heliumlike chromium, similar to our measurements for heliumlike argon. We used the LLNL EBIT and an Iqlet x-ray detector to study the KLM, KLN, KLO, and KLP resonances. In each case we measured the two branches of the resonance: Thus we obtained resonance strengths for the $n = 2 - 1$ transitions i. e. KLM, KLN, KLO, and KLP of $K\alpha$, as well as the $n = 3 - 1$ transition in KLM of $K\beta$, the $n = 4 - 1$ transition in KLN of $K\gamma$, and the $n = 5 - 1$ transition in KLO of $K\delta$. Although these measurements essentially extend the argon measurements, they were different in the sense that we swept the electron beam current in addition to sweeping the beam voltage. The current sweep ensures a constant beam-ion overlap. These results are being prepared for publication [2].

B. Lifetime of argon ions

We have extended our lifetime measurements to obtain the lifetimes of coronal lines in F-like Ar X, B-like Ar XIV, and Be-like Ar XV using the LLNL EBIT. The levels involved undergo a magnetic dipole (M1) decay to the ground state for the lines at 4412.4 Å in boronlike Ar^{13+} and 5533.4 Å in fluorine like Ar^{9+} . The bereliumlike line at 5943.73 Å involves an excited 2s2p level. The electron beam in EBIT is first turned on for 0.13 ms to ionize and excite argon+ ions. The beam is then turned off, leaving the excited ions in a Penning trap in a magnetic trapping mode. X-ray photons are monitored as the trapped ions decay. Very accurate lifetimes which differ significantly from earlier measurements are obtained in these studies. The results have been submitted for publication in *Astrophysical Journal*. [4]

C. Polarization of K-shell x-ray transitions of Ti^{19+} and Ti^{20+} excited by an electron beam

We have used a pair of polarization-sensitive spectrometers to measure spectra of heliumlike and lithiumlike titanium excited by the nearly monoenergetic electron beam of EBIT. The measurements allow us to deduce values for the polarization of the He-like resonance line w, the intercombination lines x and y, the forbidden line z, and the Li-like resonance line q which agree well with a relativistic distorted-wave calculation [5].

3. Future plans

During project year June 2000 - May 2001, we will continue to carry out measurements on heliumlike ions of intermediate-Z atoms which are important for high temperature plasma diagnostics. We will continue to use the clean environment provided by an electron beam ion trap (EBIT) to provide atomic data that can be used to put together improved spectral models for high temperature, high density plasmas.

A. Maxwellian plasmas from an electron beam ion trap

In recent measurements at the LLNL EBIT, the electron beam energy was swept in such a way that it produces a Maxwell-Boltzmann distribution of electron beam energy. This technique has is used to simulate Maxwellian type plasmas. We shall use the technique to study $K\beta$ and $K\gamma$ line emissions in argon, titanium, and chromium.

B. High-n Satellites to $K\beta$ lines of heliumlike Cr^{22+}

As a follow-up to our measurements on high-n DR contributions to the $K\beta$ ($n = 3 \rightarrow 1$) resonance line in heliumlike Ar^{16+} , in which we explored the $1/n^3$ scaling law for DR satellite intensities, we will extend these measurements to $Cr(Z=24)$.

4. Publications List

- [1] "Ratios of $n = 3 - 1$ Intercombination to Resonance Line Intensities for Heliumlike ions with Intermediate Z-values," A. J. Smith, P. Beiersdorfer, K. J. Reed, A. L. Osterheld, V. Decaux, K. Widmann, and M. Chen, Accepted for publication, *Phys. Rev. A* (2000).
- [2] "Measurement of Resonant Strengths for Dielectronic Recombination in Heliumlike Ar^{16+} ," A. J. Smith, P. Beiersdorfer, K. Widmann, M. Chen, and J. H. Scofield, To be published, *Phys. Rev. A* (2000).
- [3] "Recent Livermore Excitation and Dielectronic Recombination Measurements for Laboratory and Astrophysical Spectral Modeling," P. Beiersdorfer, G. V. Brown, M. -F. Gu, C. L. Harris, S. M. Kahn, S. -H. Kim, P. A. Neill, D. W. Savin, A. J. Smith, S. B. Utter, and K. L. Wong, Conference contribution for the "Int. Seminar on Atomic Processes", Tokyo, Japan; To be published as a NIFS proceeding.
- [4] "Experimental M1 Transition Rates of Coronal Lines from Ar X, Ar XIV, and Ar XV", E. Traebert, S. B. Utter, P. Beiersdorfer, G. V. Brown, H. Chen, C. Harris, P. Neill, D. W. Savin, A. J. Smith, submitted to *Astrophysical Journal*, 2000.
- [5] "Polarization of K-shell x-ray transitions of Ti^{19+} and Ti^{20+} excited by an electron beam", P. Beiersdorfer, G. Brown, S. Utter, P. Neill, K. J. Reed, A. J. Smith, and R. S. Thoe, *Phys. Rev. A* **60**, 4156 (1999),

DYNAMICS OF FEW-BODY ATOMIC PROCESSES

Anthony F. Starace, P.I

*Department of Physics and Astronomy
The University of Nebraska
116 Brace Laboratory
Lincoln, NE 68588-0111
Email: astarace1@unl.edu*

I. PROGRAM SCOPE

Most generally, this program is concerned with elucidating the role of many-body (specifically, electron-correlation) effects on atomic processes. The main emphasis of this program recently has been on benchmark studies of negative ion photodetachment processes in the energy region of highly-excited two-electron resonances. Our goals have been: (i) to search for photodetachment propensity rules and to compare and contrast them with those for the fundamental three-body Coulomb system, H^- ; (ii) to examine the role of the non-Coulomb core in permitting the population of propensity-rule forbidden two-electron resonances; and (iii) to identify the calculated photodetachment cross section structures with particular correlated, two-electron states. At the present time we are studying higher-order photon processes, both in the perturbative (i.e., multiphoton) regime and in the non-perturbative (i.e., intense laser) regime.

II. RECENT PROGRESS

A. Photodetachment of He^- in the Vicinity of the He^* ($n=3, 4,$ and 5) Thresholds

[C.-N. Liu and A. F. Starace, *Phys. Rev. A* **60**, 4647-4666 (1999)]

The motivations for this comprehensive study were the existence of new experimental data in a few selected energy regions and for a few partial photodetachment cross sections as well as the spotty agreement of the new data with prior theoretical predictions, i.e., poor agreement for the weakest intensity cross section and reasonably good agreement only for the most intense cross sections. Our results agree with the experimental data in all cases. Furthermore we predict two $^4D^e$ resonances near the He ($n=3$) threshold that have never been observed or predicted before, and we present results showing their effects on partial cross sections and photoelectron angular distributions. Near the He ($n=4$ and 5) thresholds, we predict about 30 quartet Feshbach resonances and 4 quartet shape resonances which have not been observed or predicted before. In addition, in this energy region our results are in excellent agreement with the few available experimental results for particular partial cross sections; we also provide for the first time an identification of all resonance features observed experimentally. We also prove analytically that resonances having a Fano-Cooper ρ parameter equal to unity will mimick each other in all partial cross sections.

B. Two-Photon Detachment Cross Sections and Dynamic Polarizability of H^- Using a Variationally Stable, Coupled-Channel Hyperspherical Approach [M. Masili and A. F. Starace, *Phys. Rev. A* (in press)]

The motivation for this work is that there has been no theoretical consensus on the shape or magnitude of the two-photon detachment cross section for the H^- ion, a fundamental three-body Coulomb system. The problem is the extreme sensitivity of multiphoton detachment processes to the value of the electron affinity as well as the important role that electron correlations play. Our aim in this work is to present a benchmark calculation that employs a variationally stable approach developed in my group with prior DOE support and a coupled-channel hyperspherical approach, which is known to provide an excellent representation of fundamental three-body Coulomb systems. Our results give excellent agreement for the first time with one other detailed calculation, the B-spline results of H. van der Hart [*Phys. Rev. A* **50**, 2508 (1994)]. Thus for the first time a theoretical consensus for this fundamental process is achieved. The paper compares our results with all other theoretical results and also presents results for the dynamic polarizability and the one-photon detachment cross section as a way of allowing others to judge the reliability of our approach since these other processes have already achieved a consensus on what are the correct results.

C. Mirroring and Mimicking of Partial Cross Sections in the Vicinity of a Resonance [C.-N. Liu and A. F. Starace, *Physics Essays* (in press)]

Our recent analytical findings that resonance profiles in alternative partial cross sections precisely mirror each other in the case that the Fano and Cooper correlation index, ρ^2 , tends to zero is applied in this paper to recent experimental observations of unusual resonance profile behaviors. Our analytical work is consistent with the following: (i) recent experimental measurements of Li photoionization, in which the resonance profiles of the $2s^22p$ triply excited state in the single and double partial cross sections exhibit opposite asymmetries [R. Wehlitz et al., *Phys. Rev. A* **60**, R17 (1999)]; (ii) high resolution measurements of the low-energy photoionization spectrum of Ar by N. Berrah's group in which two (weak) resonances in the $Ar^+ 3p^5$ ($J=3/2, 1/2$) partial cross sections exhibit mirroring profiles, resulting in complete cancellation in the total photoionization cross sections [S. E. Canton-Rogan et al., *Phys. Rev. Lett.* (in press)]; and (iii) experimental findings that Auger line shapes in partial cross sections show asymmetric line profiles, with the differences effectively compensating each other in the summed (total) cross section to produce the expected Lorentzian line shape [R. Camilloni et al., *Phys. Rev. Lett.* **77**, 2646 (1996)].

D. Non-Perturbative, Time-Dependent, Two-Active Electron Approach to Photodetachment by Li^- by an Ultrashort Laser Pulse [G. Lagmago Kamta and A.F. Starace]

We have modified an eigenchannel R-matrix code for two active electron systems so as to solve directly the time-dependent Schrödinger equation for the case of a short, intense laser pulse. The advantage of this approach is that electron correlation effects are treated accurately. Already we have obtained above-threshold-detachment (ATD) results for Li^- which show clear evidence of

electron correlation effects. We are presently characterizing these effects and examining their influence on each ATD photoelectron peak.

III. FUTURE PLANS

Our primary efforts in the coming year focus on the direct solution of the two-electron, time-dependent, three-dimensional Schrödinger equation. These large-scale calculations take full account of few-body (i.e., Coulomb) correlations. Our goals are to obtain the first double ionization cross sections for Li^- ; to obtain results for ejected electron angular distributions, both in ATD processes and in double ionization processes; and to obtain evidence for the influence of doubly-excited electron resonances on intense laser detachment processes.

IV. REFERENCES

1. A.F. Starace, NOVEL DOUBLY EXCITED STATES PRODUCED IN NEGATIVE ION PHOTODETACHMENT, in *The Physics of Electronic and Atomic Collisions: XX International Conference*, Ed. F. Aumayr and H.P. Winter (World Scientific, Singapore, 1998).
2. C.N. Liu and A.F. Starace, ANALYSIS OF DOUBLY-EXCITED STATE RESONANCES BELOW THE $\text{Li}(5p)$ THRESHOLD IN Li^- PHOTODETACHMENT, *Phys. Rev. A* **58**, 4997 (1998).
3. C.-N. Liu and A.F. Starace, MIRRORING BEHAVIOR OF PARTIAL PHOTODETACHMENT AND PHOTOIONIZATION CROSS SECTIONS IN THE NEIGHBORHOOD OF A RESONANCE, *Phys. Rev. A* **59**, R1731 (1999).
4. C.-N. Liu and A.F. Starace, PHOTODETACHMENT OF Na^- , *Phys. Rev. A* **59**, 3643 (1999).
5. C.-N. Liu and A.F. Starace, PHOTODETACHMENT OF He^- IN THE VICINITY OF THE $\text{He}^*(n=3, 4, \text{ and } 5)$ THRESHOLDS, *Phys. Rev. A* **60**, 4647 (1999).
6. M. Masilli and A.F. Starace, ONE- AND TWO-PHOTON DETACHMENT CROSS SECTIONS AND DYNAMIC POLARIZABILITY OF H^- USING A VARIATIONALLY STABLE, COUPLED-CHANNEL HYPERSPHERICAL APPROACH, *Phys. Rev. A* (in press).
7. C.-N. Liu and A.F. Starace, MIRRORING AND MIMICKING OF PARTIAL CROSS SECTIONS IN THE VICINITY OF A RESONANCE, *Physics Essays* (in press).

CORRELATED CHARGE-CHANGING ION-ATOM COLLISIONS

J. A. Tanis

Department of Physics, Western Michigan University

Kalamazoo, MI 49008-5151

email: tanis@wmich.edu

I. PROGRAM SCOPE

This research involves the experimental investigation of atomic processes occurring mainly in collisions of fully-stripped and few-electron projectiles with neutral gas targets. Additionally, studies of photon interactions with matter have recently been undertaken as well. Major emphases are the study the electron-electron interaction in various collision phenomena, and the investigation of connections to photoinduced processes. Much of this work involves the use of atomic lithium and Li-like systems because of their unique and relatively simple structure. Results are of interest from both fundamental and applied points of view and are relevant to the understanding of correlations in atomic structure and collision dynamics, including highly-excited atomic systems.

II. RECENT PROGRESS

1. One- and Two-K-shell Vacancy Production in Li by 95 MeV/u Ar¹⁸⁺

A comprehensive study of single K-shell excitation and double-K-shell-vacancy production in atomic Li induced by 95 MeV/u Ar¹⁸⁺ projectiles was recently completed. The measurements were conducted at GANIL (Caen, France), and the work was done in collaboration with the group of Dr. N. Stolterfoht, Berlin. At this high velocity ($v/c = 0.42$), excitation and ionization should be well described by perturbation theories, and connections to photoinduced processes are expected. High-resolution spectra for Auger-electron emission, resulting from the deexcitation of singly- or doubly-excited states, were measured for various electron emission angles. Both single-K-shell excitation and double-K-shell vacancy production show strong dependences on the electron emission angle. Single-K-shell excitation results mainly from dipole-like transitions, showing that the fast ions can be considered a source of virtual photons. Experimental anisotropy parameters for the $(1s2snp)$ ²P states resulting from single-K-shell excitation were found to be in good agreement with predictions of the Born approximation.

In the case of double-K-shell-vacancy (i.e., hollow atom) production, the two K vacancies come about mainly by ionization plus excitation of the atomic Li target, giving rise to excited states in Li⁺. Strong line intensities from the $2s^2$ ¹S and $2s3s$ ³S excited states are explained in terms of *shake* processes, providing direct spectral identification for the electron-electron (*e-e*) interaction in producing the doubly vacant K-shell configurations. Production of the $2s3s$ ³S state, with intensity greater than that of the $2s^2$ ¹S state, is attributed to a correlated *double-shake* process that involves a dynamical manifestation of the Pauli exclusion principle. Production of the $2s2p$ ³P state is attributed largely to the *dielelectronic* manifestation of the *e-e* interaction, resulting from

slow electron emission, in which the mutual binary scattering of the two electrons causes a transition. These results thus show that the shake and dielectronic contributions to the $e-e$ interaction can be separately identified from specific spectral features alone.

2. Formation of 2l2l' Autoionizing States in $F^{8+} + Ne$ Collisions

Here we are concerned with two-electron transfer (capture) processes in intermediate-velocity collisions between highly-charged ions and neutral target atoms. By isolating the specific states associated with these two-electron transitions, insight into the nature of these transitions, as well as the mechanisms responsible for producing them, can be gained. We have investigated the formation of projectile autoionizing 2l2l' states for 0.5 – 1.75 MeV/u (4.5-8.4 a.u.) F^{8+} projectiles colliding with neon targets. These measurements were done at Western Michigan University using the tandem Van de Graaff. Results for 0.75 MeV/u $F^{8+} + Ne$ are shown in Fig. 1. Based on auxiliary measurements for a He target (not shown), we can infer that for the Ne target two-electron transfer occurs either by double capture from the K shell, or from combined capture from the K shell and the L shell. For the velocity range investigated, the relative probability for K-shell capture from Ne is expected to increase with projectile velocity.

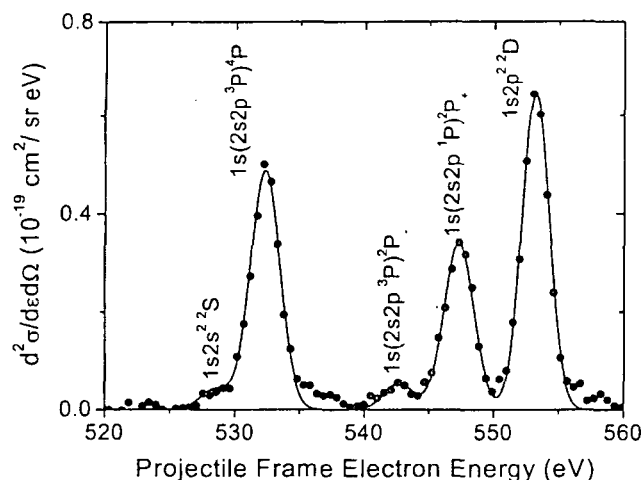


Fig. 1. Projectile autoionizing 2l2l' states formed in 0.75 MeV/u $F^{8+} + Ne$ collisions, plotted as a function of the electron energy in the projectile frame of reference.

Particularly noteworthy in the spectrum is the relatively small intensity of the $1s(2s2p^3P)^2P$ line, for which the captured electrons have their spins aligned. Based on the large $1s(2s2p^3P)^4P$ intensity, for which the captured electron spins are also aligned, the $1s(2s2p^3P)^2P$ intensity might be expected to be greater than the $1s(2s2p^1P)^2P$ intensity, if the transfer of the two electrons involved independent events. This is apparently not the case, however. The strong suppression of the 2P line suggests that quantum mechanical interference effects, resulting from state mixing, play a significant role in the two-electron transfer process.

3. Double-K-Shell Vacancy Production in Li-like Ions Colliding with Helium

In work related to that described above for the production of hollow states in Li, double-K-shell-vacancy production is being investigated for Li-like C^{3+} ions colliding with helium, but at intermediate ($v \leq 10$ a.u.) velocities. The focus of this work is to determine the mechanisms responsible for producing these hollow states, and the role of the electron-electron ($e-e$) interaction in their formation. To date, measurements have been conducted for 0.5-1.7 MeV/u

C^{3+} ions colliding with He. This work is being done at Western Michigan University using the tandem Van de Graaff accelerator.

A high-resolution Auger emission spectrum for 1 MeV/u $C^{3+} + He$ is shown in Fig. 2. In addition to several single-K-shell excitation lines, the double-K-shell vacancy states that can be identified from this spectrum are the two-electron states $2s2p^3P$, $2s2p^1P$, and $2p^2^1D$ and the three-electron state $2s2p^2^2S$, for which two decay branches are observed (at ~ 285 eV and 293 eV). Contrary to the results for atomic Li described above, no $2l3l'$ configurations can be positively identified, while it is interesting to note that the three-electron double-K-shell vacancy state $2s2p^2^2S$, corresponding to double-K-shell excitation, is observed. The mechanisms leading to the formation of these double-K-shell states are currently being investigated.

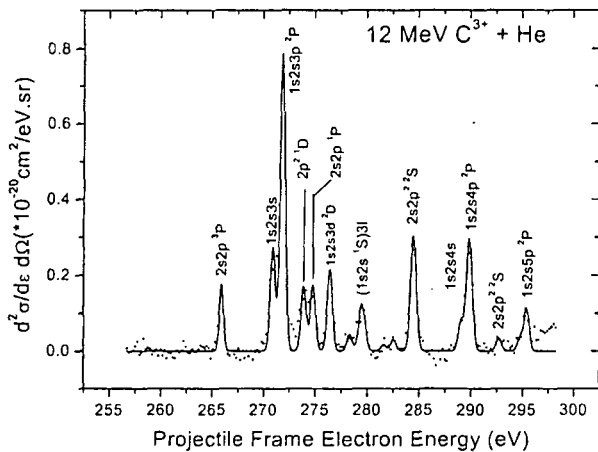


Fig. 2. Projectile $1s2l1l'$ and $2l2l'$ autoionizing states formed in 1 MeV/u $C^{3+} + He$ collisions. The electron energy region corresponding to the strong $1s2s2l$ lines formed via single K-shell excitation is not shown.

4. Multi-particle Continuum States from the Photoionization of Atoms and Molecules

A collaborative research effort to explore the dynamics of photoionization in atoms and molecules is in progress. This work is being done at the Lawrence Berkeley Laboratory Advanced Light Source (ALS) in collaboration with the Frankfurt (Germany) group of Prof. H. Schmidt-Böcking, the Kansas State group of Prof. C. L. Cocke, and M. Prior at Berkeley. The experiments are made possible by the bright beams of ultraviolet light generated at the ALS and an imaging technique used to simultaneously measure the momentum vectors of all outgoing particles following photoionization. The kinematically complete final populations of the multi-particle continuum states produced in the double ionization of D_2 and Ne were determined. Since D_2 (chemically identical to H_2) is the simplest molecular species found in nature, these studies allow a probe of the most fundamental interactions between radiation and matter. Measurements of K-shell photoionization of heavier molecules such as CO provide insights into the nature of electron scattering in molecular potentials.

II. FUTURE PLANS

The primary emphasis of our research is the study of multielectron processes occurring in atomic collisions. In particular, the nature and importance of the electron-electron ($e-e$) interaction in giving rise to various collision phenomena are explored, as are connections to photoinduced processes. New work will be conducted at WMU, and in collaborative efforts with researchers at other universities and laboratories, thereby enabling us to carry out a comprehensive and

complementary set of investigations of fundamental and applied processes occurring in atomic collisions. Specific planned projects include: (1) production of hollow (i.e., doubly-K-shell vacant) states in Li and other three-electron systems, (2) quantum-mechanical interference effects in two-electron transfer processes for highly-charged ions colliding with neutral targets, and (3) interference from intramolecular scattering in the photoionization of C₂H₂ molecules. In addition to the work that will be done at WMU, studies will be conducted at Kansas State, the ALS in Berkeley, and at GANIL (Caen, France).

IV. PAPERS PUBLISHED DURING 1998, 1999, AND 2000

"Target Ionization and Projectile Charge Changing in 0.5-8 MeV/q Li^{q+} + He (q=1,2,3) Collisions," O. Voitke, P.A. Závodszky, S.M. Ferguson, J.H. Houck, and J.A. Tanis, *Phys. Rev. A* **57**, 2692 (1998).

"Double K-shell Excitation of Li by 10.6 MeV/nucleon N⁷⁺ Projectiles," J.A. Tanis, J.-Y. Chesnel, F. Frémont, M. Grether, B. Skogvall, B. Sulik, M. Tschersich, and N. Stolterfoht, *Phys. Rev. A* **57**, R3154 (1998).

"Two- and Three-Body Effects in Single Ionization of Li by 95 MeV/u Ar¹⁸⁺ Ions: Analogies with Photoionization," N. Stolterfoht, J.-Y. Chesnel, M. Grether, B. Skogvall, F. Frémont, D. Lecler, D. Hennecart, X. Husson, J.P. Grandin, B. Sulik, L. Gulyás, and J.A. Tanis, *Phys. Rev. Lett.* **80**, 4649 (1998).

"Dielectronic Recombination in Li⁺," P.A. Závodszky, J.H. Houck, J.A. Tanis, W.G. Graham, E. Jasper, J.R. Mowat, W.W. Jacobs, and T. Rinckel, *Phys. Rev. A* **58**, 2001 (1998).

"Two- and Three-Body Effects in Single Ionization of Li by 95 MeV/u Ar¹⁸⁺ Projectiles: Analogies with Photoionization," N. Stolterfoht, J.-Y. Chesnel, M. Grether, J.A. Tanis, B. Skogvall, F. Frémont, D. Lecler, D. Hennecart, X. Husson, J.P. Grandin, Cs. Koncz, L. Gulyás, and B. Sulik, *Phys. Rev. A* **59**, 1262 (1999).

"Excitation of Li by Fast (> 10 MeV/u) N⁷⁺ and Ar¹⁸⁺ Projectiles," J.A. Tanis, J.-Y. Chesnel, F. Frémont, D. Hennecart, X. Husson, D. Lecler, A. Cassimi, J.P. Grandin, B. Skogvall, M. Tschersich, B. Sulik, J.-H. Bremer, M. Grether, and N. Stolterfoht, *Physica Scripta T* **80**, 381 (1999).

"Production of Hollow Lithium by Multi-Electron Correlation in 95 MeV/nucleon Ar¹⁸⁺ + Li Collisions," J.A. Tanis, J.-Y. Chesnel, F. Frémont, D. Hennecart, X. Husson, A. Cassimi, J.P. Grandin, B. Skogvall, B. Sulik, J.-H. Bremer, and N. Stolterfoht, *Phys. Rev. Lett.* **83**, 1131 (1999).

"Forward-Backward Asymmetry in the Inelastic Scattering of Electrons from Highly-Charged Ions", P.A. Závodszky, G. Tóth, S.R. Grabbe, T.J.M. Zouros, P. Richard, C.P. Bhalla, and J.A. Tanis, *J. Phys. B: At. Mol. Phys.* **32**, 4425 (1999).

"Dielectronic Recombination of Ground-State and Metastable Li⁺ Ions", A.A. Saghir, J. Linkemann, M. Schmitt, D. Schwalm, A. Wolf, T. Bartsch, A. Hoffknecht, A. Müller, W.G. Graham, A.D. Price, N.R. Badnell, T.W. Gorczyca, and J.A. Tanis, *Phys. Rev. A* **60**, R3350, (1999), Rapid Communication.

"Two- and Three-body Effects in Fast Ion-Atom Collisions: Analogies between Photon and Charged Particle Impact," N. Stolterfoht, B. Sulik, J.A. Tanis, J.-Y. Chesnel, L. Gulyás, F. Frémont, D. Lecler, D. Hennecart, X. Husson, J.P. Grandin, M. Grether, Cs. Koncz, and B. Skogvall, X-ray and Inner-Shell Processes, 18th International Conference, AIP Conference Proceedings 506, (AIP, New York, 2000), pp. 427-443.

"One- and Two-K-Shell Vacancy Production in Atomic Li by 95 MeV/u Ar¹⁸⁺ Projectiles," J.A. Tanis, J.-Y. Chesnel, F. Frémont, D. Hennecart, X. Husson, D. Lecler, A. Cassimi, J.P. Grandin, J. Rangama, B. Skogvall, B. Sulik, J.-H. Bremer, and N. Stolterfoht, *Phys. Rev. A* **62**, in press.

PRECISION MEASUREMENTS OF ATOMIC LIFETIMES IN ALKALI-LIKE SYSTEMS

Carol E. Tanner

University of Notre Dame
College of Science
Department of Physics
225 Nieuwland Science Hall
Notre Dame, IN 46556, USA
carol.e.tanner.1@nd.edu

INTRODUCTION

Precision measurements in atomic systems are important to the analysis of data in many areas of physics and provide fundamental information about atomic structure. Scientists in the fields of astrophysics, geophysics, and plasma fusion all depend on oscillator strengths to determine the relative elemental compositions. Often, relative values of oscillator strengths are measured precisely. However, accurate atomic lifetimes are needed to obtain absolute values. In addition, the interpretation of parity nonconservation (PNC) experiments requires accurate knowledge of transition matrix elements. Many of these scientific needs are addressed theoretically with sophisticated many-electron calculations of atomic structure. The measurements addressed in this research program fulfill some of these needs experimentally with a precision that surpasses current theoretical accuracy. Precision measurements play the important roles of assessing the accuracy of many-electron atomic-structure calculations and guiding further theoretical development. Alkali-like atoms, with a single electron outside of a closed shell, provide the simplest open shell systems for detailed comparisons between theory and experiment.

This research program employs a variety of techniques for making precision lifetime measurements in neutral and ionic systems. One highly developed technique is laser excitation of a fast atomic beam. We use this approach in both ionic and neutral systems with short decay lifetimes of order tens of nanoseconds. In the pursuit of these and other goals, the Experimental Atomic Physics Group at Notre Dame has established an Atomic Physics Accelerator Laboratory at Notre Dame (APALaND). We have also developed a second technique that employs delayed-photon coincidence counting with pulsed-laser excitation. We apply this technique for states with lifetimes that range from 0.1 to 1 microsecond.

FAST BEAM LIFETIME MEASUREMENTS

We perform our fast beam laser work in our newly established accelerator laboratory that includes a Danfysik accelerator with a hollow-cathode universal ion source. The accelerator is capable of producing ion beams with energies that range from 20 to 200 keV. The beam line also includes a charge exchange cell for the production of neutral atoms and other charge states. A variety of laser systems are also in place: a Ti-sapphire laser pumped by an Ar-ion laser covers the near IR wavelength region, a stabilized ring dye laser with frequency doubling covers the visible spectrum and the near UV, and diode lasers are used to excite specific near IR transitions. The design of the target chamber allows both longitudinal and transverse excitation.

During the past year, we published a paper on our fast-beam laser lifetime work performed on the $^{133}\text{Cs } 6p \ ^2P_{1/2, 3/2}$ states [1]. This paper includes a detailed comparison of our results with atomic theory as well as theoretical and experimental analyses of the beam divergence effect. Understanding this effect is important in fast beam measurements where a measurement uncertainty of less than 0.3% is desired. This paper also contains a detailed description of our beam velocity measurements. We measured the fast beam velocity by observing the Doppler shift of the

$6s\ ^2S_{1/2} \rightarrow 6p\ ^2P_{3/2}$ resonance with a counter propagating laser beam. We used diode lasers for both perpendicular and parallel excitation of the fast atomic beam. The diode laser systems is of our own design, the details of which have been submitted for publication [2]. The system includes an air-tight housing, a temperature controller, and a stable current source.

We are presently pursuing lifetime measurements of the cesium $7p\ ^2P_{1/2, 3/2}$ states. High precision measurements of these lifetimes are important to the interpretation of fundamental experiments and will demonstrate the capabilities of our new apparatus (shown in Figure 1). We expect to substantially reduce the uncertainty present in our $6p\ ^2P_{1/2, 3/2}$ results. The new apparatus incorporates many improvements. A new fiber optic system collects light in a 360° annular ring centered on the beam axis. The flexibility of the fibers allows the collection system to translate over a range of 10 cm along the atomic beam direction. The annular configuration improves our collection efficiency, and the cylindrical symmetry about the beam axis minimizes uncertainties due to misalignments between the translation stage and the atomic beam axis. We have also constructed a vacuum feedthrough comprised of 70,000 optical fibers that allows light to pass continuously through the vacuum wall and into our cooled photomultiplier housings. The new fiber-bundle feedthrough improves the coupling efficiency of photons to the detector. Additional changes include a fiber bundle collection system before the laser interaction region to provide a continuous monitor of the atomic beam background and a continuous laser power monitor. In reference [3], we discuss the details of incorporating these additional signals into our data acquisition system.

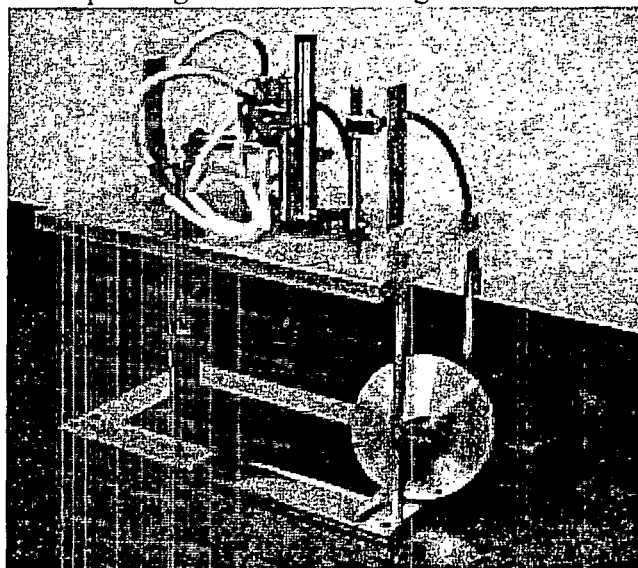


Figure 1. Photograph of the lifetime apparatus in used at APALaND. As shown, the atomic beam passes from right to left through the apparatus.

One of the primary advantages of our fast-beam technique is the precise time scale obtained by direct measurement of the beam velocity. We have recently demonstrated an improved velocity measurement using a calibrated etalon in conjunction with our wavemeter. In the past, our wavemeter resolution limited our uncertainty in the velocity to 0.14%, which had been the single largest contribution to the uncertainty of 0.27% in our current measurements [1]. We have demonstrated the advantages of our etalon technique with investigations of the $\text{Li } 2p\ ^2P_{1/2, 3/2}$ lifetimes. For these measurements, a dye laser was used to excite the $2s\ ^2S_{1/2} \rightarrow 2p\ ^2P_{3/2}$ transition along the atomic beam direction. The Doppler shift of the resonance was determined using a calibrated solid etalon with a 6.8 GHz free spectral range. We improved our wavelength resolution by a factor of 5 resulting in a velocity uncertainty of about 0.03% [4].

The versatility of the fast beam laser technique allows us to measure atomic lifetimes in both neutral and charged atomic systems. Since the capability of measuring lifetimes with an uncertainty below 0.3% has been well documented for neutral systems, we are expanding our

project to include the measurement of lifetimes in alkali-like ionic systems. Measurements along an isoelectronic sequence can reveal the importance of relativistic, spin-orbit, and electron correlation effects. In addition, allowed lifetimes are sensitive to radial matrix elements that depend on the electron wave function far from the nucleus. Core correlation and polarization effects also have an influence on such lifetimes. Thus, precision measurements of lifetimes can guide theoretical development by providing a means for testing theoretical wave functions at large radial distances. These interests motivate our proposed measurements of atomic lifetimes in the singly ionized alkali-like systems. Our laser wavelength capabilities cover the low-lying ns-np transitions in Ca⁺, Sr⁺, and Ba⁺. With intra-cavity frequency doubling, our dye laser wavelength range can be extended to include similar transitions in Be⁺ and Mg⁺.

PULSED LASER LIFETIME MEASUREMENTS

The technique of delayed-photon coincidence counting represents a new direction for our program of precision measurements. With this technique, we have measured the cesium $5d\ ^2D_{3/2, 5/2}$ and $11s\ ^2S_{1/2}$ state lifetimes. These investigations were motivated by a reported discrepancy between many-body perturbation theory calculations by Dzuba, *et al.* and a lifetime measurement by other authors. With lifetimes of order 1 μ s, these states are not well suited for measurement by our fast-beam technique. These measurements were performed in collaboration with Prof. Andrew Sieradzan of Central Michigan University using a YAG-pumped pulsed dye laser. The high intensity of this laser allows excitation of the $5d\ ^2D_{3/2, 5/2}$ states from the $6s\ ^2S_{1/2}$ ground state via the weak quadrupole transition. The $5d\ ^2D_{3/2, 5/2}$ state lifetimes were obtained by observing the delayed emission of decay photons in coincidence with the excitation pulses [5]. These investigations also motivated us to develop a pulsed diode laser system in our laboratory. The system involves rapidly shuttering a diode laser with an acousto-optic modulator. The single-mode diode laser permits narrow band selective excitation of the excited state, unlike the YAG-pumped dye laser. Our diode-laser expertise has also led to a collaboration with a condensed-matter group at Notre Dame. The rapidly shuttered diode laser system was successfully used to investigate the response time of superconducting optical detectors. Laser light with a 30 ns rise time was directed at thin-film high-temperature superconducting detectors with repetition rates ranging from 1 Hz to 100 kHz. The investigations succeeded in clearly discriminating between different frequency-related mechanisms in the observed responsivity at the selected laser wavelength. This work was published in reference [6]

HYPERFINE ENERGY SPLITTINGS

A natural direction to take with our fast beam experiments is the investigation of hyperfine energy splittings in ionic systems. Since the hyperfine interaction between the electrons and the nucleus is small, it can be treated as a perturbation to the fine structure of an atom and can be expressed through a series of multi-pole moments. The largest term describes the magnetic dipole moment interaction between the nucleus and the electrons, the second term describes the electric quadrupole interaction, and the third describes the magnetic octupole interaction. Thus measurements of hyperfine energy splittings can provide important nuclear structure information. The series can be continued to include higher order multi-poles, but the strengths of the terms decrease rapidly; in fact even the third term is often ignored. However, with the precision that can now be achieved with laser spectroscopy, one might be able to determine the nuclear magnetic-octupole moment of some atomic species. In particular, with a diode-laser frequency resolution of about 1 kHz, we expect to determine the magnetic-octupole moment of the cesium nucleus.

We also propose measurements of hyperfine energy splittings in ionic systems for the purpose of testing atomic and nuclear structure theory. The hyperfine structure of ionic systems has not been as thoroughly studied as that of many neutral alkalis. We have demonstrated the capability of observing hyperfine energy splittings with our fast beam apparatus during our velocity measurement in cesium [1]. The hyperfine structure of ionic systems can be similarly resolved in our accelerator because of the velocity compression that occurs during the acceleration

process. These measurements can be performed in parallel with our lifetime measurements, employing the same laser and detection technology.

CONCLUSION

In summary, precision measurements of lifetimes and hyperfine energy splittings provide important atomic and nuclear structure information. These measurements also test atomic and nuclear theories and are necessary for the interpretation of fundamental investigations in a variety of scientific areas. In particular, cesium is the subject of a recent PNC experiment and interpretation of this results in terms of weak interaction coupling constants requires the precision measurements provided by this research program.

Support of this work is acknowledged from the Fundamental Interactions Branch, Division of Chemical Sciences, Office of Basic Energy Sciences, U. S. Department of Energy.

REFERENCES

1. R. J. Rafac, C. E. Tanner, A. E. Livingston, H. G. Berry, "Fast Beam-Laser Lifetime Measurements of the Cesium $6p\ ^2P_{1/2, 3/2}$ States", *Phys. Rev. A* **60**, 3648-3662 (1999).
2. V. Gerginov, D. DiBerardino, R.J. Rafac, S. T. Ruggiero, and C.E. Tanner, "Diode Lasers for Fast-beam Laser Experiments," submitted for publication, 2000.
3. C. E. Tanner, "Laser Excitation of Fast Atomic Beams for Precision Lifetime Measurements," in *Accelerator Based Atomic Physics Techniques and Applications*, ed. by S. M. Shafroth and J. C. Austin, AIP Press: New York, 1997.
4. D. DiBerardino, R. J. Rafac, D. M. Glantz, C. E. Tanner, "Laser Doppler Velocimetry of a Fast Beam with a Temperature Stabilized Solid Etalon", *Opt. Comm.* **143**, 118-124 (1997).
5. D. DiBerardino, C. E. Tanner, A. Sieradzan, "Precision Lifetime Measurements of the Cesium $5d\ ^2D$ and $11s\ ^2S_{1/2}$ States using Pulsed Laser Excitation", *Phys. Rev. A* **57**, 4204-4211 (1998).
6. S.T. Ruggiero, M.P. Mischke, C.E. Tanner, A.J. Wilson, L.R. Vale, and D.A. Rudman, "Wavelength Dependent Photoresponse in YBCO Thin-Film Systems," *IEEE Trans. Appl. Superconductivity* **9**, 3182-3185 (1999).

Laser-Produced Coherent X-Ray Sources

Donald Umstadter, P.I.
University of Michigan, Ann Arbor (dpu@umich.edu)

I. PROGRAM SCOPE:

With the development of ultrashort-duration optical probes just over a decade ago, the subject of ultrafast phenomena has blossomed into a mature field, having yielded important discoveries about dynamics in the fields of biology, chemistry, materials science and physics. However, the long-wavelength of optical light has limited the spatial resolution of direct ultrashort time-domain measurements to the micron-size scale. (Furthermore, optical wavelengths are unable to penetrate into the bulk of most materials.) Conversely, while shorter wavelength and more penetrating x-ray sources have enabled important discoveries in studies of phenomena that occur on the ultra-small size scale, they have not, until recently, had the ultrashort pulse durations of their optical counterparts. But now with the development of table-top high-peak-power optical laser systems, it has become feasible to generate—for the first time—ultrashort-pulse-duration x-ray probes. By extending the energy of ultrafast strobes from the eV- to the keV-energy range, they enable a marriage between observations on the ultrafast with those on the ultra-small scales, giving scientists novel and exciting research capabilities.

Ultrafast x-rays can be applied with advantage to most any problem that is currently studied with longer pulse-duration light sources, such as synchrotrons and free-electron lasers. Processes that occur on the subpicosecond time-scale are particularly suitable, including photosynthesis and conformational changes in ultrafast biology and chemistry, inner-shell electronic processes in atomic systems, and phase transitions in materials science.

The most obvious advantage of laser-produced x-ray sources is their compact size (table-top) and affordability (<\$500k), features which potentially permit their operation at university, industrial and hospital labs. Ultrafast laser-driven x-ray sources are also particularly advantageous in the study of photo-initiated processes, since in this case the optical pump and x-ray probe are absolutely synchronized to each other, being derived from the same laser. Also, in cases where there is significant absorption of the x-ray probe pulse (such as in-vitro imaging of live biological cells), the sample is often destroyed by the probe due to radiation damage. Thus, in order to acquire an image before the occurrence of blurring from heat-induced motion, a single-shot pump-probe measurement with ultrashort-duration and high-peak-power x-rays is required. Low-repetition rate, laser-produced x-ray sources are also best suited for studies of systems that

are slow to relax or that involve irreversible processes, in which the sample must be moved between shots due to damage by the pump.

It follows that there is currently a need for bright sources that have keV-energy (within, or shorter wavelength than, the “water window”), femtosecond pulse-duration, high peak-power, high spatial coherence and that sit on a table-top. In order better understand the physics of such light sources, we are currently studying relativistic harmonic generation.

II. RECENT PROGRESS:

A. Relativistic nonlinear Thomson scattering

Ultra-high-peak-power lasers now make it possible to create a sufficient photon density to study Thomson scattering in the relativistic regime. With increasing light intensity, electrons quiver during the scattering process with increasing velocities, approaching the speed of light when the laser intensity approaches 10^{18} W/cm². In this limit, the effect of light’s magnetic field on electron motion should become comparable to that of its electric field, and the electron mass should increase because of the relativistic correction. Consequently, electrons in such high fields are predicted to quiver nonlinearly, moving in figure-eight patterns, rather than in straight lines, and thus to radiate photons at harmonics of the frequency of the incident laser light, with each harmonic having its own unique angular distribution. This is referred to as nonlinear Thomson scattering or relativistic Thomson scattering.

Previously, we observed the generation of the second and third harmonics, with their unique angular patterning, originating from this process [1]. Nonlinear Thomson scattering itself is not suitable as a x-ray source, because of its incoherence, uncollimation, and low efficiency. However, coherent harmonic generation—utilizing nonlinear Thomson scattering and collective plasma motion—may be a feasible way to generate x-rays. With this in mind, we more recently observed—for the first time—phase-matched relativistic harmonic generation in plasmas [7]. Third harmonic light was detected and discriminated spectrally and angularly from the harmonics generated from competing processes. Its angular pattern is a narrow forward-directed cone, which is consistent with phase-matching of a high-order transverse mode in a plasma. The signal level is found to be

on the same order of magnitude for a circularly polarized pump pulse as for a linearly polarized pump pulse.

In this experiment, we used a Ti:sapphire-Nd:glass laser system based on chirped-pulse amplification that produces ≤ 2 -J, 400-fs pulses at 1.053- μm wavelength. The 50-mm-diameter laser beam was beamsplit into two beams. The first beam was sent to a type-II KDP crystal to produce a second-harmonic pulse which was then focused by an $f/3$ off-axis parabolic mirror into the center of a gas jet (hydrogen or helium, with a flat top of 750 μm in length and a gradient of 250 μm) to pre-ionize the gas into a plasma (i.e., used as a prepulse). The second beam, the pump pulse, was sent through a delay line to vary its temporal delay and then through a half-wave waveplate and a thin-film polarizer to vary its energy. After that, it was focused by an $f/3.3$ lens onto the same gas jet with its focus overlapping with, and its direction collinearly counter-propagating with respect to, that of the second-harmonic prepulse. The prepulse has a focal spot of 12 μm FWHM (full width at half maximum), and the pump pulse has a focal spot of 14 μm . In this experiment, the prepulse energy was fixed at ~ 90 mJ, corresponding to a peak vacuum intensity of 2×10^{17} W/cm^2 , which is three orders of magnitude higher than the ionization threshold of hydrogen, enough to produce a plasma column of > 50 - μm diameter. The pump-pulse intensity was varied by adjusting the half-wave waveplate and the maximum was about 2×10^{17} W/cm^2 , which corresponds to a normalized vector potential $a_0 = 8.5 \times 10^{-10} \lambda [\mu\text{m}] I^{1/2} [\text{W}/\text{cm}^2] = 0.4$. The polarization of the prepulse was set to be linearly polarized, and that of the pump pulse was controlled to be either linearly polarized or circularly polarized by use of a quarter-wave waveplate located before the focusing lens. For the data presented below, the pump pulse was linearly polarized.

The third harmonic light generated by the pump pulse and emitted in the forward direction was collected by the focusing parabolic mirror of the prepulse and was then separated from the prepulse and the pump pulse by passing through a 527-nm-wavelength and a 1053-nm-wavelength high-reflection dielectric mirrors. It was then diagnosed with an imaging grating spectrometer and a beam-pattern imaging system. The use of a prepulse at the second harmonic is to make sure that it cannot produce harmonics at the wavelength of third harmonic of the pump pulse. The delay of the pump pulse was set such that the pump pulse entered the plasma 7 ps after the prepulse passing through the gas jet, avoiding the mixing of the prepulse and the pump pulse in the plasma to generate the third harmonic but not allowing enough time for recombination. No significant change in the third harmonic signal was observed when the delay was varied from 5 ps to 20 ps.

The forward-propagating third harmonic beam was

collimated by the parabolic mirror, which converted the angular pattern of this emission into the transverse intensity pattern of the collimated beam. Therefore, by imaging the latter with a CCD (charge-coupled device) camera and matching narrow bandpass filters, we obtained the angular profile of the third harmonic. Fig. 1 shows the angular pattern of the narrow unshifted third harmonic signal for a hydrogen gas density of 1.5×10^{19} cm^{-3} and a pump laser intensity of 1.7×10^{17} W/cm^2 with the prepulse [7]. It shows a cone with a radius (cone angle) of 5.62° and a ring width of $< 0.44^\circ$. The narrow angular width ($< 0.44^\circ$) of the cone is strong evidence for good coherence (phase matching) of this third harmonic beam, as compared to the broad angular width ($> 30^\circ$) of the angular pattern of incoherent harmonic emission from single-particle relativistic Thomson scattering [1].

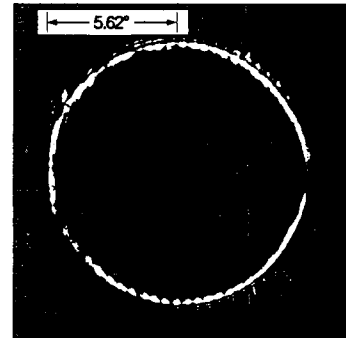


FIG. 1. Angular pattern of the third harmonic generated for a plasma density of 3×10^{19} cm^{-3} and a pump laser intensity of 1.7×10^{17} W/cm^2 , when a prepulse is used.

III. FUTURE PLANS:

A. Symmetry-Breaking

We will investigate and identify the mechanism that breaks the symmetry and thus permits the observation of harmonics with circular polarization. Several possibilities are the excitation of a plasma wave or the existence of a channel. The relative role of these two possibilities will be investigated by varying the time delay and intensity of a prepulse.

B. High-order Harmonic Generation

We are in the process of studying the conversion efficiency into the various harmonics as a function of harmonic order. A Seya-Namioka mount ultraviolet spectrometer will permit us to measure out to the thirtieth harmonic. A Hettrick mount XUV spectrometer will permit us to measure out to the 200th harmonic. In either case a multichannel-plate detector will be used.

C. Phase-Matching

In the direction of propagation of the laser beam, the harmonics produced from individual electrons are added coherently, leading to high conversion efficiency and good coherence. However, because of the mismatch between the phase velocity of the laser beam and that of the generated harmonics in a plasma, the harmonic pulse become 180° out of phase with the pump laser pulse after propagating a certain distance (the detuning length λ_c). This results in the occurrence of the opposite process, i.e., the conversion of energy from the harmonic pulse back to the pump laser pulse. The process reverses again after another detuning length, i.e., when the harmonic pulse is in phase with the pump pulse. As a result, the intensity of the harmonic pulse as a function of the interaction length just oscillates between zero and the maximum (the saturation intensity I_{sat}) with a period of $2\lambda_c$, as illustrated in Fig. 2(a). This leads to a serious problem that the increase of the interaction length cannot increase the conversion efficiency. Furthermore, the maximum intensity of the harmonic pulse and the detuning length decrease with higher harmonic number, making the generation of x-ray pulses ineffective.

The same problem occurs for harmonic generation in crystals. However, two methods has been used to satisfy the phase matching conditions: one is to use the birefringence of crystals, and the other is quasi-phase-matching. The former method can not be used for nonlinear Thomson scattering because the polarization of the harmonics are the same as the pump laser pulse and the plasma is isotropic without strong external fields. The latter method requires the creation of a longitudinal plasma grating (periodically interlacing layers of plasma and vacuum in the direction of beam propagation) with a period equaling two detuning lengths (each layer one detuning length). In the layer of plasma, the harmonic pulse grows. In the next layer (vacuum), although the harmonic pulse is 180° out of phase, its intensity stays the same because there is no plasma to convert the energy. After this layer, the harmonic pulse is in phase with the pump laser pulse again, and its grows in the following layer of plasma. In this way, the harmonics can grow with increasing interaction length and a high conversion efficiency can be obtained for a long gain medium.

It is difficult to create such a perfect plasma grating; however, a good approximation such as a sinusoidal density perturbation of plasma or just electrons can be produced relatively easy. For instance, a slow-phase-velocity (quasi-stationary) ion acoustic wave may be excited through modulational instability. In addition, a standing electron plasma wave can be driven by the ponderomotive force of a laser standing wave produced from the collision of two counter-propagating laser beams, as illustrated in Fig. 2(c). Another method is to

drive an electron plasma wave with a laser beat wave produced by collinear co-propagation of two laser pulses with different wavelengths ($\lambda_0, \lambda_0 + \Delta\lambda_0$). The direction of propagation of the laser beat wave should be opposite to the relativistic-intensity pump pulse. The quasi-phase-matching condition is satisfied when the wavelength of the electron plasma wave, which is determined by $\lambda \simeq \lambda_0 (\lambda_0 + \Delta\lambda_0) / \Delta\lambda_0$, is equal to $4\lambda_c$.

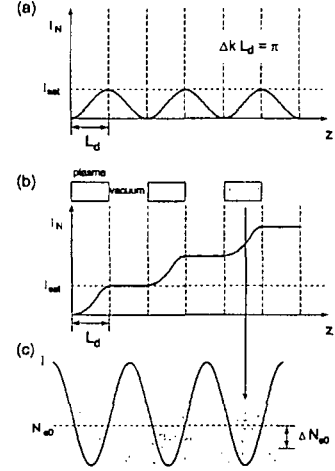


FIG. 2. Quasi-phase-matching scheme for increasing the conversion efficiency of harmonics generated through nonlinear Thomson scattering: (a) The mismatch of the phase velocities of the pump pulse and the harmonics results in the saturation of the intensities of the harmonics in one detuning length. (b) Quasi-phase-matching can be obtained by the use of periodically interlacing layers of plasma and vacuum. (c) Such a plasma-vacuum interlacing structure can be created approximately by laser beat waves driving an electron standing wave through laser ponderomotive force.

The detuning length λ_c is a function of both plasma density and pump laser intensity when the pump intensity is relativistic, i.e.,

$$\lambda_c = \frac{\lambda_0}{2\pi \left[\sqrt{1 - \frac{\omega_p^2}{\gamma(n\omega_0)^2}} - \sqrt{1 - \frac{\omega_p^2}{\gamma\omega_0^2}} \right]},$$

where n is the harmonic number (note that only odd-number harmonics can be generated by coherent nonlinear Thomson scattering in the forward direction), λ_0 is the vacuum wavelength of the pump pulse, ω_p is the plasma frequency which is linearly proportional to plasma density, $\gamma = \sqrt{1 + a_0^2/2}$, $a_0 = 8.5 \times 10^{-10} \lambda_0 [\mu\text{m}] I^{1/2} [\text{W}/\text{cm}^2]$, and I is the pump laser intensity. As a result, the choice of the specific harmonic that is quasi-phase-matched can be made by changing plasma density and/or laser intensity, as shown in Fig. 3. Take the case in which the plasma standing wave is created by beating of two counter-propagating $0.8\text{-}\mu\text{m}$ -wavelength long pulses as an example. The period of the

plasma standing wave is equal to $0.4 \mu\text{m}$. At a plasma density of $5 \times 10^{19} \text{ cm}^{-3}$ ($5 \times 10^{18} \text{ cm}^{-3}$), the 154th (1550th) harmonic is quasi-phase-matched for $1 \times 10^{18} \text{ W/cm}^2$ pump intensity, and the 255th (2560th) harmonic is quasi-phase-matched for $1 \times 10^{19} \text{ W/cm}^2$ pump intensity. When the quasi-phase-matching condition is met, the intensity of this specific harmonic can be increased by a factor of $(L/2\lambda_c)^2$, which is seven orders of magnitude for a plasma length of $600 \mu\text{m}$ in this case.

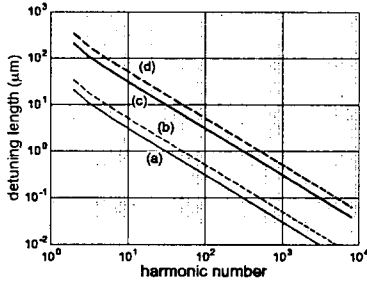


FIG. 3. The detuning length of harmonic generation as a function of the harmonic number for various plasma densities and pump laser intensities: (a) $5 \times 10^{19} \text{ cm}^{-3}$, $1 \times 10^{18} \text{ W/cm}^2$, (b) $5 \times 10^{19} \text{ cm}^{-3}$, $1 \times 10^{19} \text{ W/cm}^2$, (c) $5 \times 10^{18} \text{ cm}^{-3}$, $1 \times 10^{18} \text{ W/cm}^2$, and (d) $5 \times 10^{18} \text{ cm}^{-3}$, $1 \times 10^{19} \text{ W/cm}^2$.

Without (quasi-)phase-matching, coherent (or partially coherent) harmonics may be generated and emitted in a cone of a specific cone angle θ_0 . One example of such coherent third-harmonic cone is shown in Fig. 1. A simple model shows good agreement with the observed emission [7]. For the parameters of the experiment, $N_e = 10^{19} \text{ cm}^{-3}$ ($\lambda_p = 11 \mu\text{m}$) and $r_0 = 12 \mu\text{m}$, we find $\theta = 5.3^\circ$ and $\Delta\theta = 0.42^\circ$, which are in approximate agreement with the measured values ($\theta = 5.62^\circ$ and $\delta\theta = 0.44^\circ$).

D. Advantages of Plasma Harmonics

Generation of x-ray pulses through coherent nonlinear Thomson scattering has several advantages. First, the duration of the harmonic pulse is roughly equal to the duration of the pump laser pulse. That is, femtosecond x-ray pulses can be produced if femtosecond pump laser pulses are used. Second, x-ray production via high harmonic generation of a laser beam can have great spatial and temporal coherence. Also, the dispersion due to the free-electron component does not limit the conversion efficiency as it does in the case of harmonics from electrons initially bound to atoms. Lastly, the conversion efficiency can be increased if the interaction length is increased by using, e.g., plasma waveguides.

- [1] S. Y. Chen, A. Maksimchuk and D. Umstadter, "Experimental observation of nonlinear Thomson scattering," *Nature*, **396**, 653 (1998).
- [2] M. Nantel, J. Itatani, A. D. Tien, J. Faure, D. Kaplan, M. Bouvier, T. Buma, P. Van Rompay, J. Nees, P. P. Pronko, D. Umstadter and G. Mourou, "Temporal Contrast in Ti:Sapphire Lasers: Characterization and Control," *IEEE J. Selected Topics Quant. Electron.* **4**, 449-458 (1998).
- [3] M. Nantel, G. Ma, S. Gu, J. Itatani, and D. Umstadter, "Pressure ionization and line-merging in strongly-coupled plasmas produced by 100-fs laser pulses," *Phys. Rev. Lett.* **80**, 4442 (1998).
- [4] G. S. Sarkisov, V. Yu. Bychenkov, V. N. Novikov, V. T. Tikhonchuk, A. Maksimchuk, S. Y. Chen, R. Wagner, G. Mourou and D. Umstadter, "Self-focusing, channel formation and high-energy ion generation in the interaction of an intense short laser pulse with a He jet," *Phys. Rev. E* **59** 7042 (1999).
- [5] F. Faenov et al., "High-Resolved X-Ray Spectra of Hollow Atoms in a Femtosecond Laser-Produced Solid Plasma" *Physica Scripta*, **T80**, 536—538 (1999).
- [6] D. Umstadter, S.-Y. Chen, G. Ma, A. Maksimchuk, G. Mourou, M. Nantel, S. Pikuz, G. Sarkisov and R. Wagner, "Dense and Relativistic Plasmas Produced by Compact High-Intensity Lasers," *Astrophysical Journal Supplement Series*, **127** 513-518, (2000).
- [7] S.-Y. Chen, A. Maksimchuk, E. Esarey and D. Umstadter, "Observation of Phase-Matched Relativistic Harmonic Generation," *Phys. Rev. Lett.* **84**, 5528 (2000).
- [8] A. Maksimchuk, S. Gu, K. Flippo, D. Umstadter and V. Yu. Bychenkov, "Forward Ion Acceleration in Thin Films Driven by a High-Intensity Laser," *Phys. Rev. Lett.* **84**, 4108 (2000).
- [9] A. Maksimchuk, M. Nantel, G. Ma, S. Gu, C. Y. Cote, D. Umstadter, S. A. Pikuz, I. Yu. Skobelev, A. Ya. Faenov, "X-Ray Radiation from Matter in Extreme Conditions," *J. Quant. Spectrosc. Radiat. Transfer* **65**, 367 (2000).